

Università degli Studi di Milano

**Doctorate School of Chemical Sciences and
Technologies**

Department of Chemistry

PhD Course in Chemical Sciences- XXXIII cycle



**Palladium Catalyzed Reactions: Reductive Cyclization of
Nitroarenes, and Oxidative Carbonylation of Aniline**

PhD thesis of:

Doaa Reda Mohamed Ramadan

Matr. n. R11990

Advisor: Prof. Fabio Ragaini

Coordinator: Prof. Emanuela Licandro

Academic year 2020/2021

to my family

Acknowledgement

First and foremost, praises and thanks to God, the Almighty Allah, for his grace and blessings throughout my work to complete this research successfully.

I would like to express my deep gratitude and appreciation to my supervisor **Prof. Fabio Ragaini** for the suggestion of the research point and for his continuous support during my PhD studies. His guidance helped me finish this project and I am sincerely thankful for his immense knowledge, encouragement, insightful comments and mostly for devoting much of his time and efforts in the supervision of the thesis.

My sincere thanks go to **Dr. Francesco Ferretti**, for his great support and guidance through the course of this study. His dynamism, vision, and motivation have deeply inspired me, and I am extremely grateful for his help during the experimental work and for his valuable ideas, thoughts, and comments during the writing of this thesis. I would also like to thank him for providing advice and friendship to me during my presence in Italy.

I would like to thank **all my fellow lab colleagues**, for their support, for the stimulating discussions that we had and for all the fun we had during my time in Italy. My special thanks to my friend **Manar Abdellatif** for the valuable conversations we had about science, research, and life and for the sleepless nights we were working together before deadlines, and for all the help she gave me during the last months of my PhD.

Finally, my heartfelt thanks go to **my parents**, for their love, prayers, and sacrifices for educating and preparing me for my future. Their faith, sacrifice, and confidence in my abilities, allowed me to accomplish this work in the present standard. I would also like to thank **my sister and my brother**, for their continuous support to complete this research work. I am very thankful for **my late grandmother** for always believing in me even if she is no longer here, her encouragement and unconditional love still inspire me.

For all my friends and family, your encouragement when the times got rough is much appreciated.

Table of contents

Chapter I: Reductive cyclization of nitroarenes	7
1. Introduction	7
1.1. Nitrogen-heterocycles.....	7
1.2. Carbazoles.....	7
1.3. Methods of carbazole formation.....	9
1.3.1. Methods involving formation of benzene ring (A).....	9
1.3.2. Methods involving formation of pyrrole ring (B).....	11
1.3.3. Methods involving both rings of the carbazole.....	23
2. Results and discussion	24
2.1. Optimization of the catalytic system.....	24
2.2. Preparation of nitrobiaryls substrates.....	35
2.3. Investigating the scope of the reaction.....	38
2.4. Kinetic study of the thermal cyclization of 2-nitrosobiphenyl.....	44
3. Conclusions	46
4. Experimental work	47
4.1. General consideration.....	47
4.2. General analysis method.....	47
4.3. Kinetic studies.....	48
4.4. General protocol for optimization trials conducted in a pressure tube.....	48
4.5. Procedure for catalytic reactions conducted in an autoclave.....	49
4.6. Procedure for a 15-fold large scale synthesis of carbazole 79	49
4.7. Preparation of phenylformate.....	50
4.8. Synthesis of palladium catalysts.....	50
4.9. Preparation of <i>o</i> -aminophenyl 103	51
4.10. Preparation of <i>o</i> -nitrosobiphenyl 104	52

4.11. Preparation of 2-nitrobiaryls through Suzuki-Miyaura cross-coupling.....	52
4.12. Preparation of 2-nitrobiaryls through Ullmann cross-coupling.....	61
4.13. Preparation of 2-nitrobiaryls through simple organic transformations.....	62
4.14. General procedure for nitrobiaryls cyclization to carbazoles.....	64
Chapter II: Oxidative carbonylation of anilines.....	75
1. Introduction.....	75
2. Results and discussion.....	77
2.1. Role of iodide.....	77
2.2. Effect of iron-containing promoters.....	78
2.3. The effect of different I/Fe and Cl/Fe ratios.....	84
2.4. Reactions under milder conditions.....	86
2.5. Reaction byproducts.....	88
3. Conclusions.....	93
4. Experimental work.....	95
4.1. Materials and general procedures.....	95
4.2. Catalytic reactions.....	95
4.3. Quantitative analysis methods for catalytic reactions.....	96
References.....	98
Appendix.....	104
1. NMR spectra.....	104
2. Short resume of the PhD candidate	165

List of abbreviations

HIV	human immunodeficiency virus.
SPhos	2-Dicyclohexylphosphino-2',6'-dimethoxybiphenyl.
DCE	Dichloroethane.
DME	Dimethoxyethane.
DMF	<i>N,N</i> -dimethylformamide.
DMSO	Dimethylsulfoxide
THF	Tetrahydrofuran.
Me-THF	2-Methyltetrahydrofuran.
TDI	Toluene diisocyanate
DBU	1,8-Diazabicyclo[5.4.0]undec-7-ene.
Phen	10-Phenanthroline.
TMPhen	3,4,7,8-Tetramethyl-1,10- phenanthroline.
Ar-BIAN	Bis(aryl)acenaphthenequinonediimine.
PPN Chloride	Bis(triphenylphosphine)iminium chloride.
PPN Acetate	Bis(triphenylphosphine)iminium chloride.
TLC	Thin layer chromatography.
GC	Gas chromatography.
SAR	structure activity relationship.
GC-MS	Gas chromatography- mass spectrometry.
HPLC	High pressure liquid chromatography.
HPLC-MS	High pressure liquid chromatography- mass spectrometry
EI	Electron ionization
CFL	compact fluorescent lamp.
TOF	turnover frequencies.
ICP	Inductively coupled plasma.

Chapter I: Reductive cyclization of nitroarenes.

1. Introduction.

1.1. Nitrogen-heterocycles.

The wide class of nitrogen-containing aromatic compounds contains some of the most important building blocks for the synthesis of more complex molecules. In particular nitro compounds and anilines occupy a prominent role in organic synthesis owing to their use as starting materials for a plethora of nitrogen-heterocycles with a wide range of applications as dyes,^[1-2] explosives^[3-4] and pharmaceutical materials.^[5] Different N-heterocycles are predominant functional scaffolds in many natural compounds, which make them essential for the chemical reactions that occur in all living organisms. For many decades, medicinal chemists have been constructing N-heterocycles scaffolds for their biologically active properties.^[6-7] It is thus not surprising that the interest in developing new and improved methodologies to synthesize N-heterocycles has steadily been growing. Nitroarenes are considered one of the most common entry point for the preparation of almost all N-heterocycles.^[8] Thus, any transformation that involves using them directly to prepare N-heterocycles in one pot is highly desirable since it saves one or more synthetic step.^[9]

For many years now, our research group have been developing accessible methods for the preparation of various N-heterocycles through reductive cyclization of the appropriate nitroarene precursor.^[10-18] In the next paragraphs, we will focus specifically on reporting and discussing the previous techniques used to prepare carbazoles since part of the practical work of this thesis deals with optimizing a novel catalytic procedure for Pd-catalyzed reductive cyclization of 2-nitrobiphenyl to produce carbazoles.

1.2. Carbazoles.

The tricyclic carbazole ring system (**Figure 1**) is an essential component of many biologically active natural compounds^[19-23] (e.g., alkaloids) and synthetic drugs^[24-28] (**Figure 2**). In synthetic materials, carbazoles are valuable π -extended building blocks for both small-molecule and polymeric opto-/thermo-electronic materials because of their desirable electronic and charge transport characteristics, as well as their high thermal stability.^[29] To tune the carbazole's properties and incorporate them into more complex compounds either the chemical functionalization of the parent carbazole moiety or the construction of the tricyclic scaffold from simple, readily available molecules is required. Due to its electron-rich nature, carbazole (**Figure 1**) are considered a moderate nucleophile that can be functionalized with a variety of electrophiles (acyl, tertiary alkyl, nitro, halogen, etc.).^[30] The most reactive positions for electrophilic substitution are the “*para*” positions to the nitrogen atom (position 3 and 6). However, alternative syntheses are required when functionalization of the 2, 4, 5, or 7 ring positions is needed, or when mono and/or unsymmetrical substitution patterns are desired or for functional groups that cannot readily be introduced by electrophilic substitution.^[31-33]

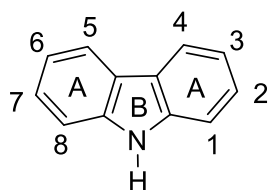


Figure 1. Structure of carbazole ring system.

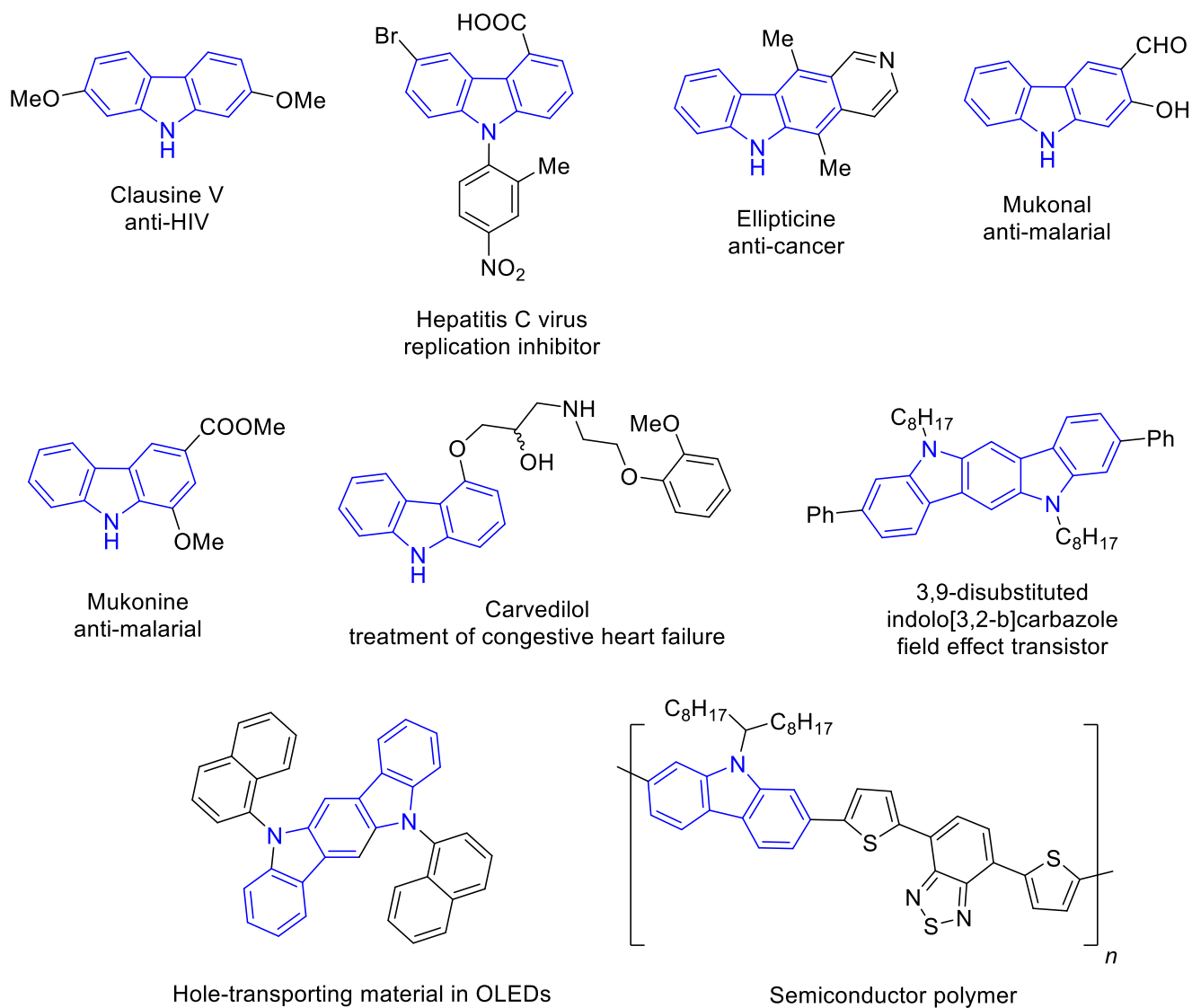


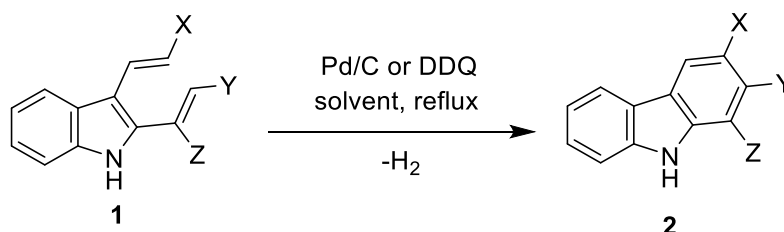
Figure 2. The carbazole structure motif in biologically active natural compounds, synthetic drugs, and advanced synthetic materials.

1.3. Methods for carbazole formation.

Given the tremendous demand on functionalized carbazoles and their derivatives across many fields, carbazoles have received considerable attention in the literature, particularly in terms of their synthetic methodology. In the past decades, a considerable number of improved or novel methods for carbazole synthesis have been reported. The reported methods were classified based on whether they lead to generation of the benzene (A) ring or pyrrole (B) ring or both rings of the carbazole in tandem.^[34]

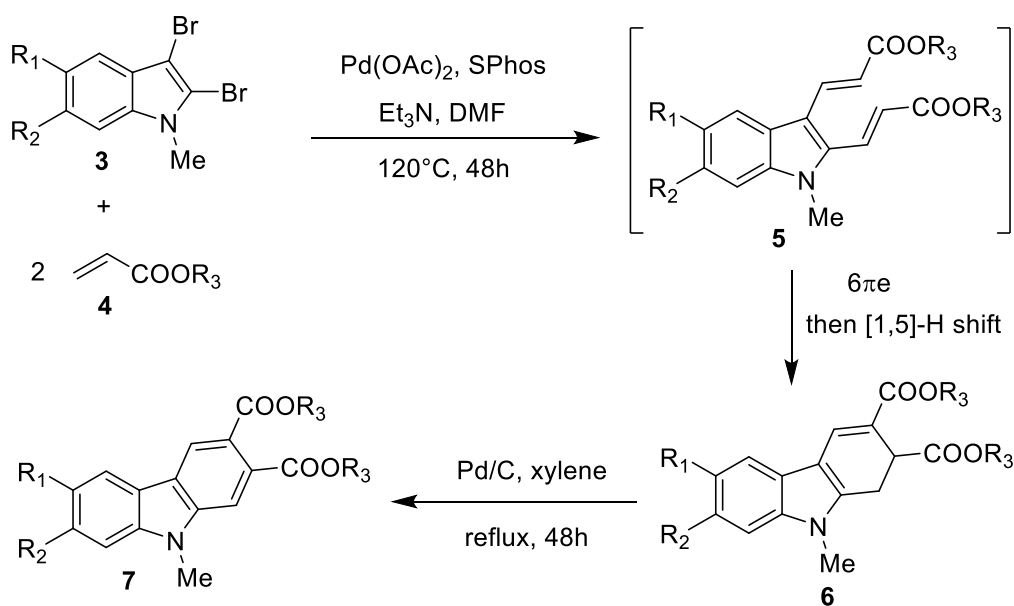
1.3.1. Methods involving formation of benzene ring (A).

Numerous methods involving a 6π electrocyclic reaction have been developed to construct the carbazole A (benzene) ring from indoles modified with unsaturated moieties on the C2 and C3. An efficient protocol for the synthesis of a broad range of carbazole derivatives is the electrocyclic reaction of 2,3-divinylindoles **1** to functionalized carbazoles **2**. Usually, this reaction is carried out at high temperatures in the presence of dehydrogenating agents such as palladium on activated carbon or 2,3-dichloro-5,6-dicyano-1,4-benzoquinone (DDQ) (**Scheme 1**).^[35-36] Some recent developments will be discussed below.



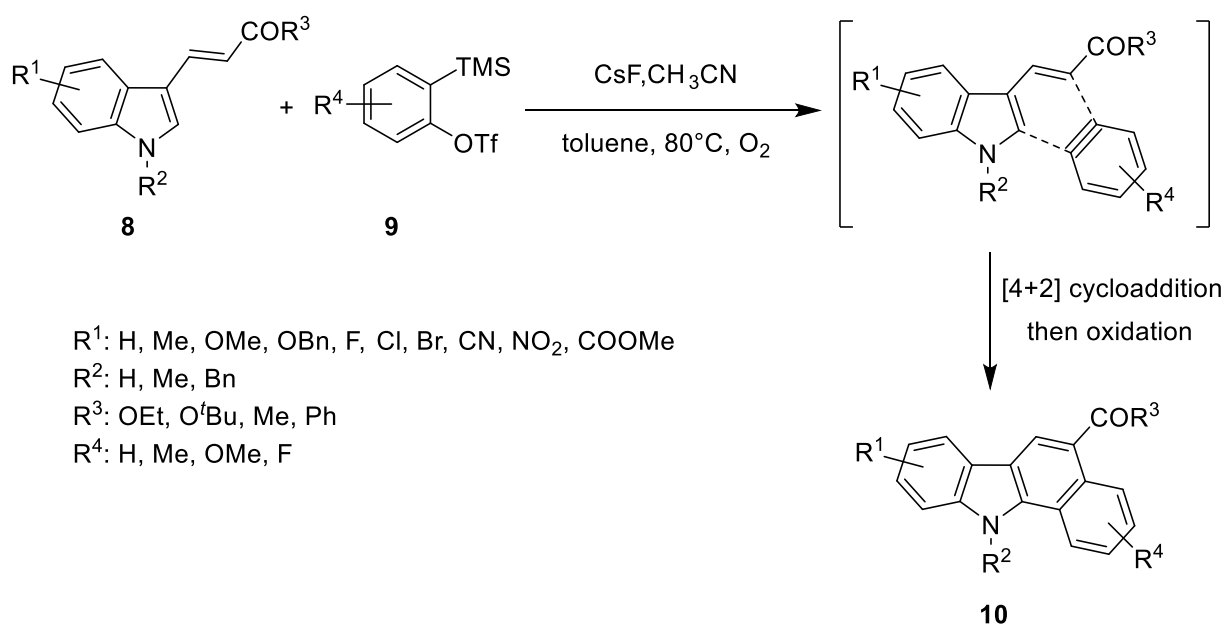
Scheme 1. 6π electrocyclic reaction for carbazole formation.^[35-36]

A synthetic procedure for carbazoles was developed by Langer and co-workers starting from N-methyl-2,3-dibromoindoles **3**. These are used as starting material for a double-Heck coupling reaction with acrylic esters **4** in tandem with 6π -electrocyclization (**Scheme 2**). During the cyclization, the aromaticity of the indole moiety is maintained by a [1,5]-H shift leading to the intermediate **5**. Aromatization of the new six-membered ring to the final carbazole 9-methyl-2,9-dihydro-1H-carbazole **7** is achieved by dehydrogenation using with Pd/C in refluxing xylene.^[37] Although, this method affords carbazoles in good yields, the need for synthesising brominated indoles as the starting point and the limited variations of substituents in the product (only ester group) are the main drawbacks.



Scheme 2. Langer's method for carbazole formation.^[37]

[4+2] Cycloadditions are a widely used class of reactions for the construction of six-membered ring systems in organic synthesis. Their value is especially due to the usually high regioselectivity, with respect to other reactions, in the formation of substituted six membered rings. Thus, these approaches have been reported for the synthesis of the A (benzene) ring of carbazoles. Tao et al. developed a procedure for synthesis of benzo [a]carbazoles that starts with a [4+2] cycloaddition between 3-alkenylindoles **8** and a benzyne generated *in-situ* from 2-trimethylsilylphenyl triflate **9** in the presence of caesium fluoride in acetonitrile-toluene. The reaction was performed under dioxygen atmosphere thus the intermediately formed Diels–Alder cycloadduct is eventually oxidized to yield the carbazole scaffold **10** (Scheme 3).^[38]

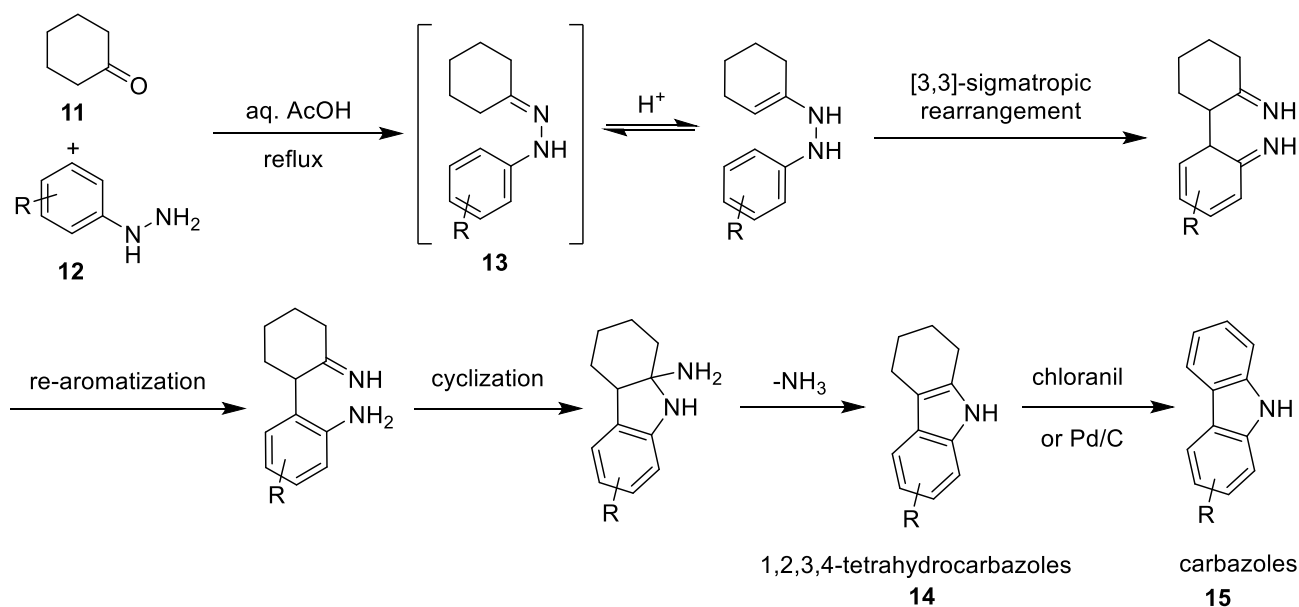


Scheme 3. Tao et al. synthesis of benzo[a]carbazoles.^[38]

One advantage of this procedure over Langer's method is that it does not require an extra dehydrogenation step since the aromatization of the cycloadduct is achieved directly under dioxygen atmosphere. However, preparation of the indole precursor remains an obstacle.

1.3.2. Methods involving formation of pyrrole ring (B).

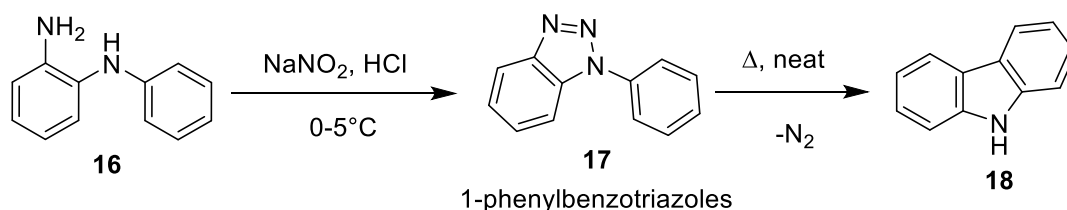
Fischer indole synthesis, first proposed in 1883, is one of the oldest reactions in organic chemistry, but it still remains an essential reaction for the formation of the five-membered ring in indoles.^[39] The procedure involves the reaction of a phenylhydrazine with a carbonyl compound (aldehyde or ketone) under acidic conditions. The Borsche–Drechsel modification of the Fischer synthesis, some years later, allowed the preparation of carbazoles in an analogous way. The synthetic pathway involves the condensation of cyclohexanones **11** with phenylhydrazines **12** to produce arylhydrazones **13**, which undergo an acid-promoted isomerization followed by a [3,3]-sigmatropic rearrangement to produce the five-membered ring. The so formed animal then eliminates ammonia to affords 1,2,3,4-tetrahydrocarbazoles **14** (**Scheme 4**).^[40-43] Finally, carbazoles **15** can be obtained by dehydrogenation using palladium on activated carbon or chloranil.



Scheme 4. Key steps for the Borsche–Drechsel carbazole synthesis.^[39-43]

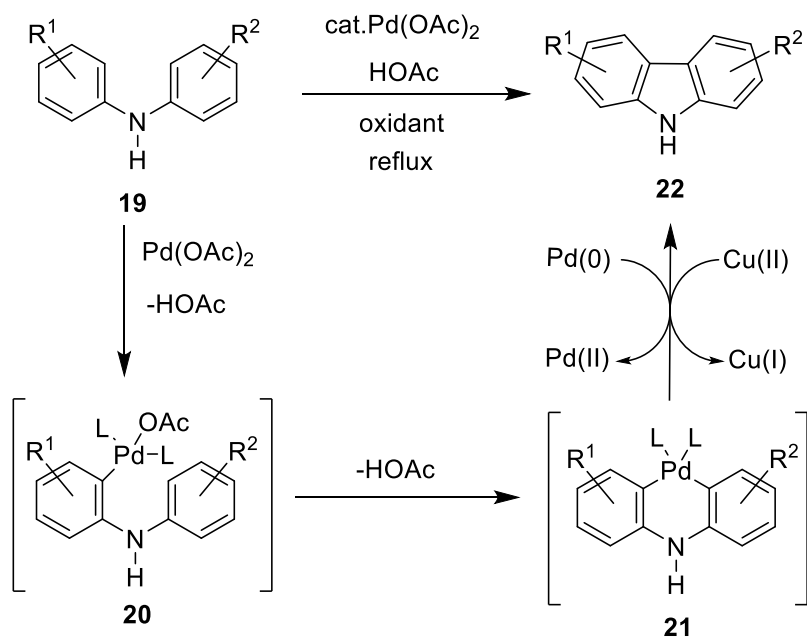
Another classical method to obtain carbazole **18** is through the thermal reaction of 1-phenylbenzotriazole which is known as the Graebe–Ullmann synthesis (**Scheme 5**).^[44] The starting material, 1-phenylbenzotriazole **17**, can be obtained by diazotization of N-(2-aminophenyl)aniline **16**.^[45-46] Despite the fact that this reaction proceeds almost quantitatively with unsubstituted 1-phenylbenzotriazole, it is very sensitive to the presence and nature of substituents. Few information is

known about the mechanism of this reaction, but most likely it involves a diradical intermediate in the thermolysis of the triazole.^[47]



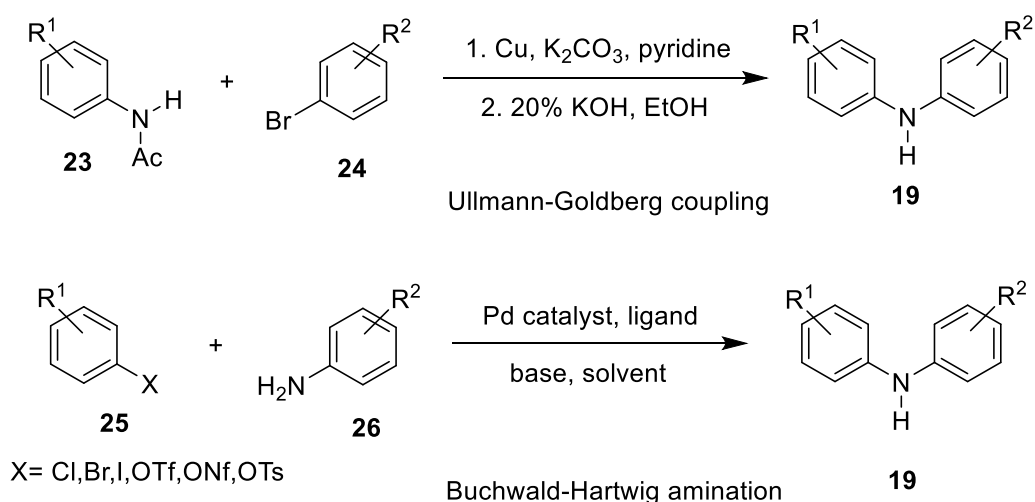
Scheme 5. Graebe-Ullmann synthesis of carbazoles.^[45-46]

In 1975, Åkermark and co-workers reported a palladium (II)-catalyzed oxidative cyclization of *N,N*-diarylamines **19** to carbazoles **22** (**Scheme 6**).^[48] The reaction proceeded through an initial direct palladation of the C-H of one aromatic ring of the amine to form the intermediate **20**. Palladation of the second aromatic ring leads to the formation of palladacycle **21**, which in turn undergoes reductive elimination forming the central carbon-carbon bond of the carbazole skeleton. This method represents one of the pioneering works on the synthesis of the five-membered ring of carbazoles by direct C-H activation. Although the procedure showed a general applicability owing to the tolerance of a wide range of substituents, it requires stoichiometric amounts of palladium(II) acetate, thus limiting its interest for preparative purposes.^[48] More recently, Knölker and co-workers reported a catalytic version of the reaction. In this modification, catalytic amounts of palladium can become effective by re-oxidation of palladium(0) to palladium(II) using copper(II) acetate as stoichiometric oxidant.^[49-58] Since then, numerous alternative oxidants (e.g., tert-butyl hydroperoxide, benzoquinone, and catalytic tin(II) acetate in combination with oxygen, oxygen, and air, respectively) have been reported (**Scheme 6**).^[59-69] Recently, Knölker and co-workers have also isolated and characterized by X-ray crystallography a palladacycle of the type **21**.^[70] This key intermediate, proposed by Åkermark 37 years before,^[48] was trapped by using pivaloyloxy and acetyl groups for directed palladation.^[70]



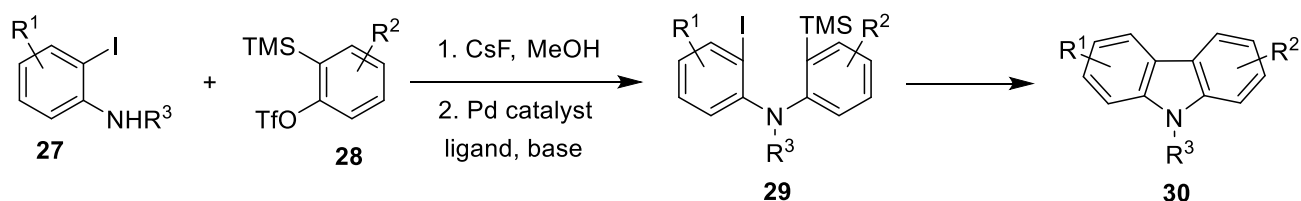
Scheme 6. Palladium (II) mediated oxidative cyclization of *N,N*-diarylamines to carbazoles.^[48-58]

The traditional method for the preparation of the required diarylamines **19** is the copper mediated Ullmann-Goldberg coupling of acetanilides **23** with bromobenzenes **24** followed by alkaline hydrolysis of the generated acetamide moiety (**Scheme 7**).^[71-74] Nowadays, the preferred method for the synthesis of diarylamines is the palladium(0)-catalyzed Buchwald-Hartwig amination (**Scheme 7**).^[75-80] The advantages of this protocol over the Ullmann-Goldberg one are that it requires only catalytic amounts of the transition metal and can be performed under milder reaction conditions.



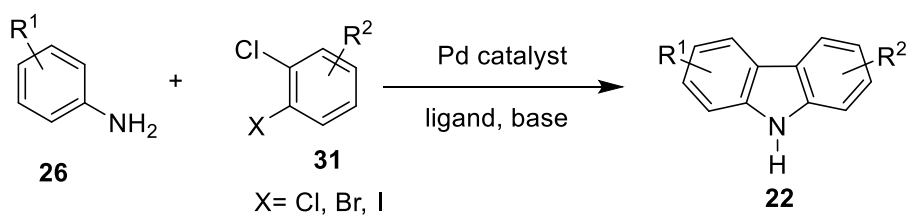
Scheme 7. Traditional methods for synthesis of diarylamines.^[71-80]

A one-pot, two-step method for the synthesis of carbazoles was reported by Larock and co-workers in 2004.^[81] The method involves cross-coupling of 2-iodoanilines **27** with silylaryl triflates **28** in the presence of cesium fluoride. The reaction is believed to proceed through an aryne intermediate followed by palladium(0)-catalyzed cyclization of the afforded biarylamine to produce carbazoles **30** (**Scheme 8**).^[81-82] The advantage of this method is the use of a palladium(0) species as the active catalyst for the cyclization reaction, this allows for lower catalyst loadings and oxidizing reaction conditions are not needed. A drawback of that methodology is the fact that the starting materials (halogenated arylamines) are not as easily accessible as the non-halogenated arylamines that are used in the palladium(II)-catalyzed Åkermark process discussed before (**Scheme 6**).



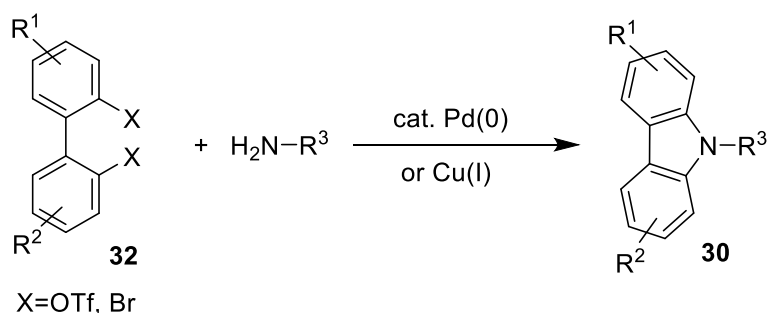
Scheme 8. Larock synthesis of carbazoles.^[81-82]

Recently, Ackermann and Althammer reported a modification of Larock method. The modification involves a palladium-catalyzed one-pot domino N–H/C–H bond activation that leads to the formation of carbazoles **22**.^[83-84] Through this procedure, a range of carbazoles were synthesized by coupling of different anilines **26** with 1,2-dihaloarenes **31** (**Scheme 9**).



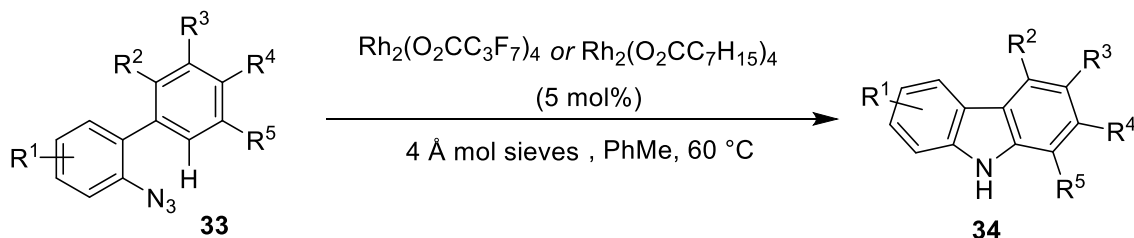
Scheme 9. Ackermann and Althammers synthesis of carbazoles.^[83-84]

Although less atom-economical, a similar approach is the synthesis of carbazoles **30** through double palladium(0)-catalyzed Buchwald–Hartwig coupling of 2,2-dihalo-biphenyls or biphenyl-1,2,2'-diyl bistriflates **32** with primary amines or ammonia (**Scheme 10**).^[85-88] The starting material can be prepared by Suzuki-Miyaura cross coupling of the appropriate coupling partners.

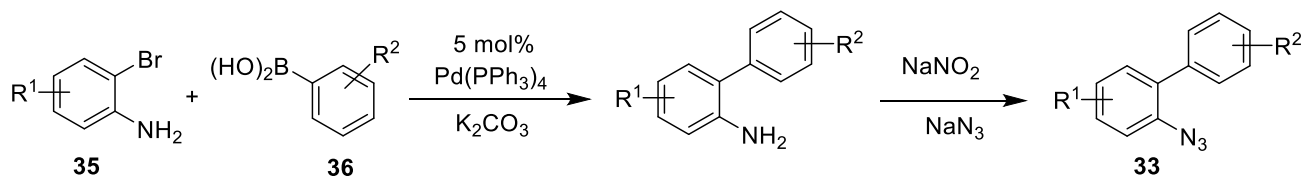


Scheme 10. Synthesis of carbazoles via two-fold Buchwald-Hartwig coupling.^[85-88]

Stokes and co-workers reported a procedure for synthesis of substituted carbazoles **34** from readily available biaryl azides **33** using a Rh₂(II) carboxylate catalyst (**Scheme 11**).^[89] A drawback of this method is the strong dependence of carbazole formation on the electronic and steric nature of the R², R³, or R⁴ substituents. Electron withdrawing groups on R² (e.g., F and Cl) result in higher yields, whereas lower conversion and yield were observed when R² is an electron donating group (e.g. Me).^[89-90] The starting biaryl azides **33** were synthesized through Suzuki cross-coupling reaction of 2-bromoanilines **35** and phenyl boronic acids **36** followed by a diazotization/azidation sequence (**Scheme 12**).^[89] The method is more environmentally friendly than the previously described double Buchwald-Hartwig coupling, since it only produces N₂ as side product. However, arylazides are less stable and less abundant on the market than arylhalides and their preparation is not always straightforward.

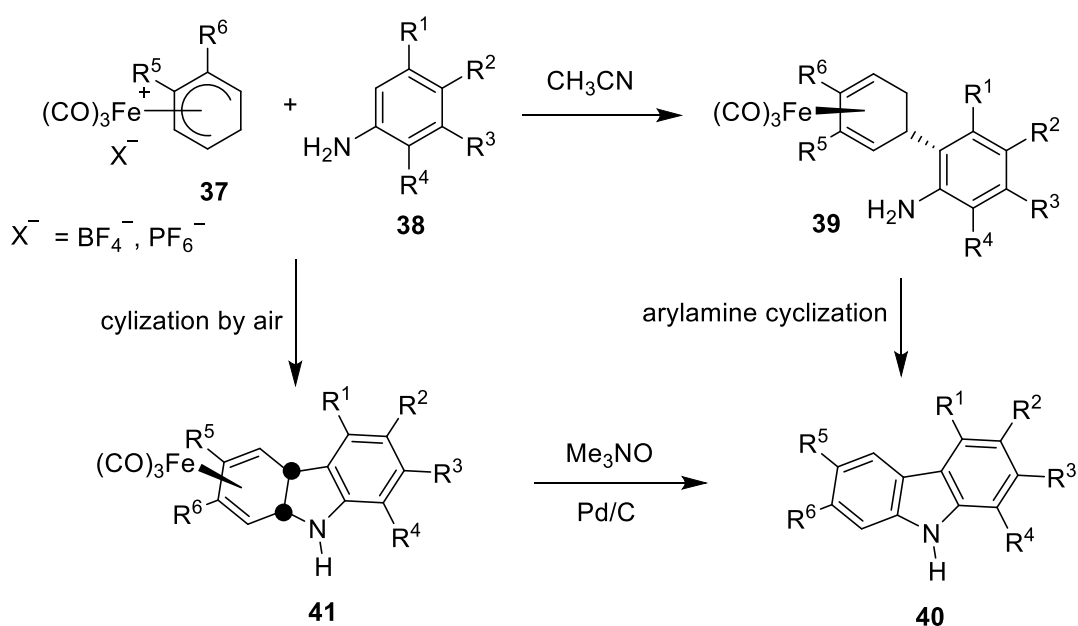


Scheme 11. Synthetic method for substituted carbazoles from biaryl azides.^[89]



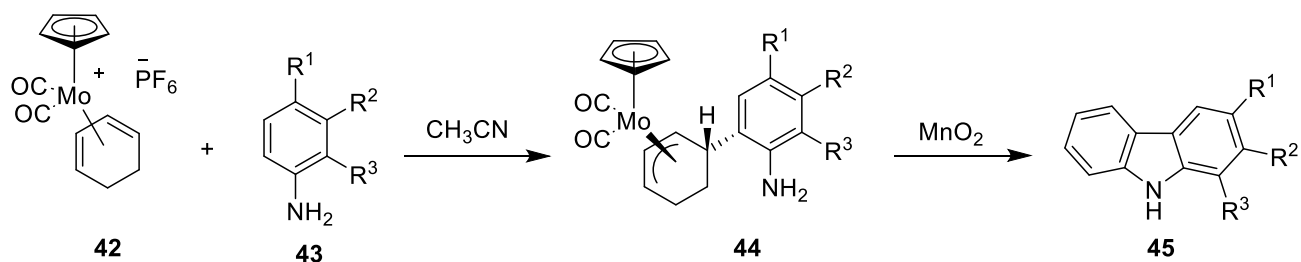
Scheme 12. Synthesis of biaryl azides through Suzuki cross-coupling then diazotization followed by azidation.^[89]

An advantageous method for the synthesis of highly substituted carbazoles is achieved through the electrophilic aromatic substitution of electron-rich arylamine **38** with tricarbonyl(η^4 -cyclohexa-1,3-dienylium)iron complex salts **37**.^[91-93] These cations efficiently give electrophilic aromatic substitution on arylamines. Oxidative cyclization of the resulting iron-arylamine complexes **39** leads directly to carbazoles **40** (**Scheme 13**). The sequence of those two reactions represents a highly convergent pathway to many carbazoles. The reaction involves consecutive iron-mediated C-C and C-N bond formations followed by aromatization. Alternatively, reaction of the arylamines **38** with the tricarbonyl iron-coordinated cyclohexadienylium ions **37** in air leads to direct formation of the tricarbonyl iron-coordinated *4a,9a*-dihydrocarbazoles **41**. Afterwards, demetallation of the complexes **41** to the corresponding free ligands and subsequent aromatization afford the carbazoles **40**.



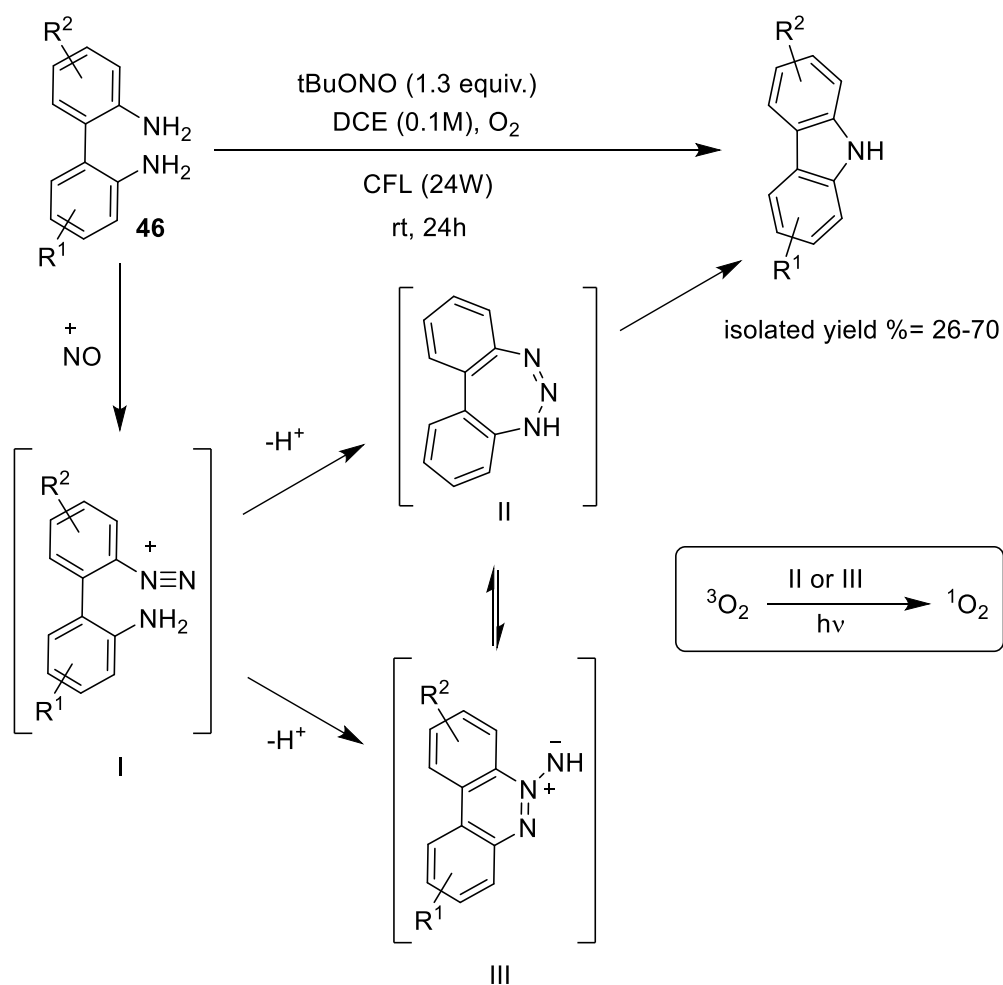
Scheme 13. Iron-mediated synthesis of carbazoles.^[91-93]

Knölker and co-workers have developed an approach analogous to the iron-mediated carbazole synthesis discussed above (**Scheme 13**) employing a molybdenum-mediated reaction instead. The reaction begins with formation of regio- and stereoselective molybdenum complex **44** via electrophilic aromatic substitution of electron-rich arylamines **43** with the cationic molybdenum complex **42**. Oxidative cyclization of **44** with simultaneous aromatization and demetallation using activated manganese dioxide affords the carbazoles **45** (**Scheme 14**).^[94]



Scheme 14. Knölker molybdenum-mediated carbazole synthesis.^[94]

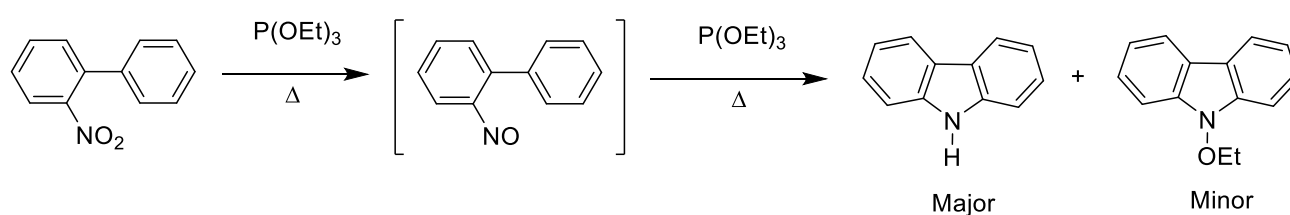
Recently, Cho et al showed that N-H carbazoles can be accessed through a visible-light-induced reaction of 2,2'-diaminobiaryls **46** in the presence of *tert*-butyl nitrite without the need of external photosensitizer (**Scheme 15**).^[95] This method proceeds through an *in-situ* formation of a visible-light-absorbing photosensitizing intermediate, benzocinnoline *N*-imide (III), and it only requires *t*-BuONO, molecular oxygen and natural resources such as visible light to afford NH carbazoles in moderate yields (25-70 %). The transformation of triplet molecular oxygen to singlet oxygen that, in turn, promotes the synthesis of carbazole is activated by benzocinnoline *N*-imide (III) intermediate. These claims were supported by experimental and computational studies.



Scheme 15. A visible-light-induced synthesis of N-H carbazoles from 2,2'-diaminobiaryls.^[95]

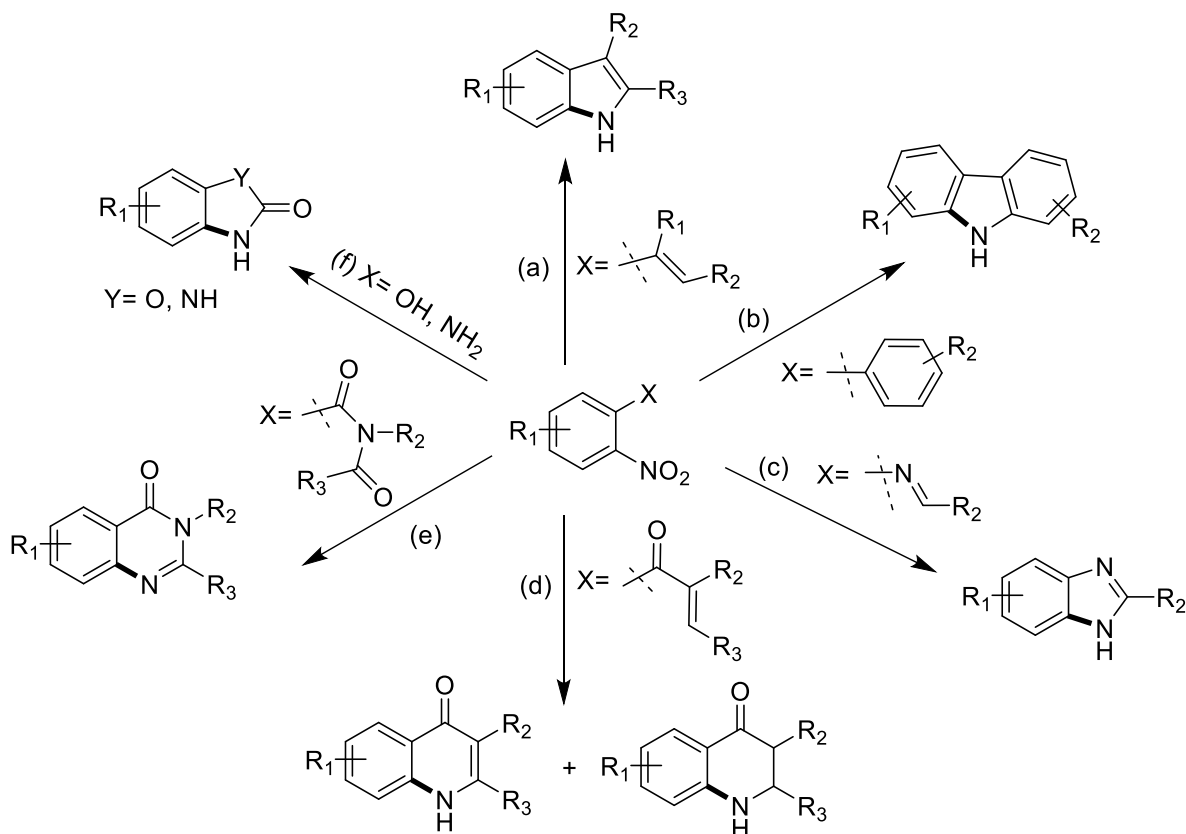
One of the most widely employed methods for carbazole synthesis involves the deoxygenative cyclization of *o*-nitrobiphenyl derivatives in the presence of suitable organophosphorus reagents. This method is commonly referred to as the Cadogan cyclization (**Scheme 16**).^[96-99] The most important advantages of this method are the increased substrate scope, higher substituent tolerance, and a more precise regiocontrol of functional group placement within the product (determined by relative position in the biphenyl starting material). A variety of functionalized carbazoles has been prepared by this procedure. The widely accepted mechanism for this transformation involves exhaustive deoxygenation to a singlet nitrene that later undergoes a C-H insertion, although evidence has also been provided that the cyclization may occur at the nitrosoarene stage.

The reaction is commonly conducted by refluxing in an excess of triethyl phosphite, as both the reductant and the reaction solvent. While generally successful, this procedure exhibits considerable substrate dependence, both in terms of the reaction time and product distribution. In addition, the desired carbazole is often contaminated by the *N*-ethoxy derivative, which results from alkyl transfer to the product either directly from solvent or, more likely, from the triethyl phosphate by-product of the reaction.^[100-101] This side reaction is particularly dominant in case of long reaction times or with substrates bearing electron-donating substituents.



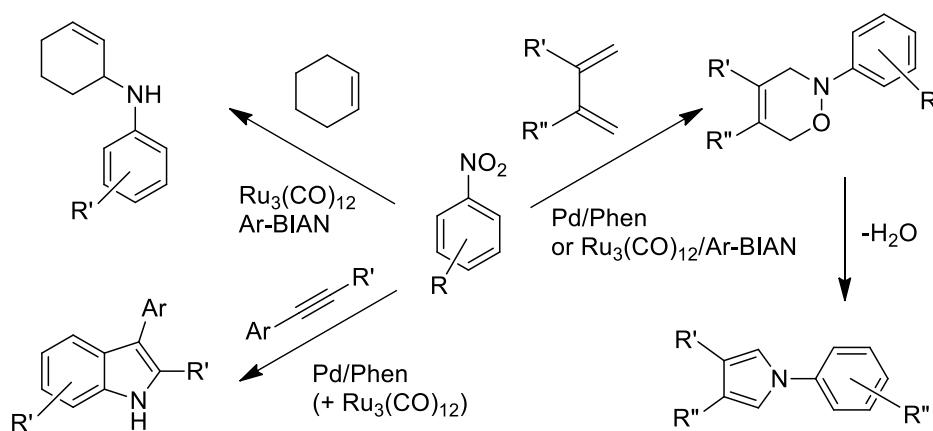
Scheme 16. Cadogan synthesis of carbazole.^[96-99]

Furthermore, the undesired alkylated impurity is usually difficult to remove, requiring careful, tedious chromatographic purification, which complicates the large-scale syntheses required for industrial applications. Attempts have been made to solve the problem of unwanted alkylation by the reagent or by-product by using triphenylphosphine which offered the possibility to remove the by-product, triphenylphosphine oxide, by a number of methods including precipitation, or chromatography, thus simplifying purification.^[102] However, the generation of a large amount of phosphorus waste detracts from this approach. Apart from the low sustainability in terms of atom economy, another main drawback of this method is the relatively high cost derived from using a stoichiometric reductant based on phosphorus. As a more environmentally friendly alternative to Cadogan reaction, five-membered ring heterocycles have been carried out more effectively through transition metal catalyzed reductive cyclization reactions of nitroarenes with CO as the stoichiometric reductant.^[103-108] Indeed, a large variety of bulk^[109-112] and fine^[11, 15, 113-114] chemicals have been prepared often with high efficiency with these systems. A plethora of nitrogen-containing heterocycles have been prepared by *intra*-molecular cyclization of suitably *ortho*-substituted nitroarenes using CO as a stoichiometric reductant (**Scheme 17**).



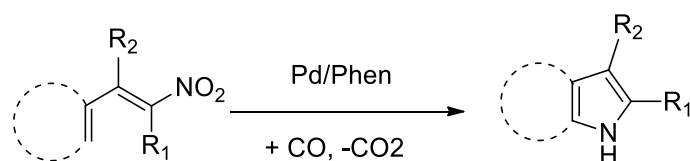
Scheme 17. *Intra*-molecular cyclization reactions of nitroarenes.

Although less studied than *intra*-molecular cyclizations, examples of *inter*-molecular cyclization reactions have been also reported. In the latter reactions, the unsaturated group is on a separate molecule with respect to the nitroarene (**Scheme 18**).^[10, 12, 115-116] This makes the *inter*-molecular reactions a valuable alternative to reactions in **Scheme 13** because reagents are often commercially available, whereas most of the reagents for the reactions in **Scheme 17** need to be synthesized in one or more steps.



Scheme 18. *Inter*-molecular nitroarene cyclization reactions.^[10, 12, 115-116]

More recently, β -nitroolefins have also been employed as substrates, to give indoles, thienopyrroles or pyrroles (**Scheme 19**).^[13-14, 16, 117]

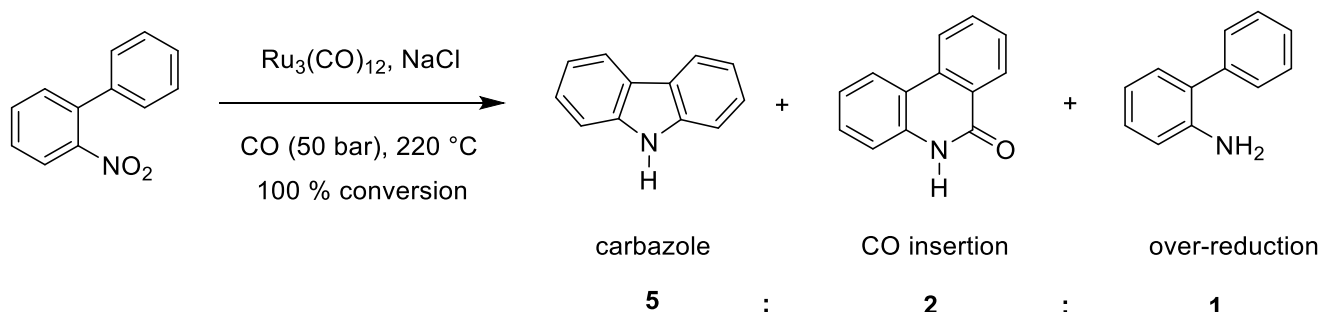


Scheme 19. Cyclization of β -nitrostyrenes and nitrodienes.^[13-14, 16, 117]

The reactions shown in **Scheme 17** can be catalyzed by low-valent complexes of ruthenium^[116, 118-119], rhodium^[120-121] or palladium^[10, 33, 122-124] and, in a few cases, even iron complexes have been demonstrated to be competent catalysts.^[125-126]

Palladium/phosphine catalysts are effective for the reductive cyclization of *o*-nitrostyrenes to indoles but fail when applied to biaryl substrates.^[103] It should be noted that the use of phosphite and phosphine as a ligand is not advisable for a long-term use of the catalyst. Specifically, phosphines have been observed to be converted quantitatively into the corresponding phosphine oxides under similar conditions.^[127-128] Thus, the catalyst loses activity and stability as triphenylphosphine is oxidized and, moreover, removal of the phosphine oxide from the product by crystallization causes unacceptably large product losses in most cases.^[127] Therefore, in the last decade, the most studied and the most active and selective systems reported are based on the use of palladium/phenanthroline complexes.

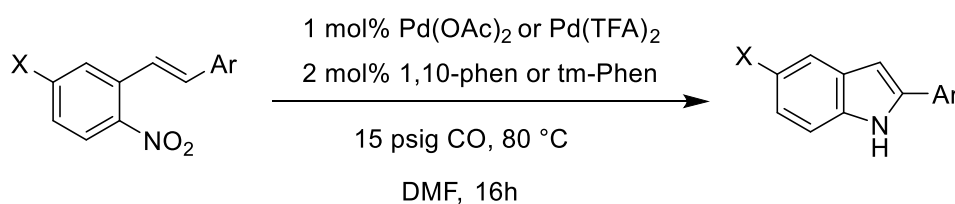
The first reports on transition metal catalyzed reductive cyclization of nitrobiaryls to produce carbazoles employed $\text{Ru}_3(\text{CO})_{12}$ as the catalyst under relatively harsh conditions such as 220 °C and 50 bar of CO (**Scheme 20**).^[129-130] The forcing conditions and the moderate yields of carbazoles obtained due to competitive formation of products from CO insertion and over-reduction, significantly limit the synthetic utility of this system.



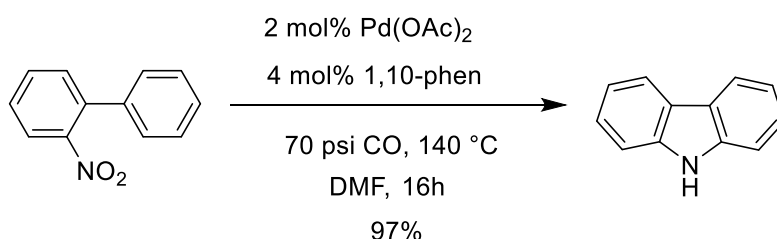
Scheme 20. Ruthenium-catalyzed reductive cyclization of nitrobiphenyls.^[129-130]

Milder conditions were investigated by Davies and co-workers for the synthesis of indoles (**Scheme 21**)^[127] and carbazoles (**Scheme 22**)^[33] starting from *o*-nitrostyrenes and 2-nitrobiphenyls,

respectively. Treatment of *ortho*-nitrostyrenes with palladium (II) and 1,10-phenanthroline or 3,4,7,8-tetramethyl-1,10-phenanthroline (TMPhen) in DMF at 1 bar of CO and 80 °C afforded indoles in good to excellent yields. The synthesis of indoles by this strategy was considered more convenient since it employs cheap carbon monoxide as the stoichiometric reductant with low catalyst loading and CO₂ is the only stoichiometric by-product, which offers significant economic and environmental advantages over the standard triethylphosphite deoxygenation procedure. The synthesis of carbazoles from *o*-nitrobiphenyl required much harsher conditions, higher catalyst and ligand loadings at higher pressure and temperature (**Scheme 18**). In addition, only a relatively narrow substrate scope was reported including few functionalized carbazoles in many cases in moderate yields.^[33]



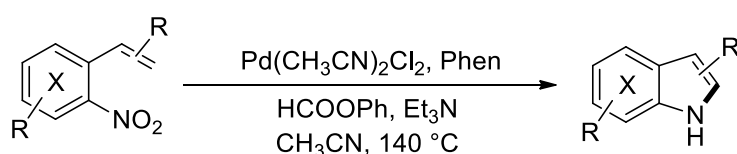
Scheme 21. Davies' mild conditions for palladium-catalyzed reductive cyclization of 2-nitrostyrenes.^[127]



Scheme 22. Davies' mild conditions for palladium-catalyzed reductive cyclization of 2-nitrobiphenyl.^[33]

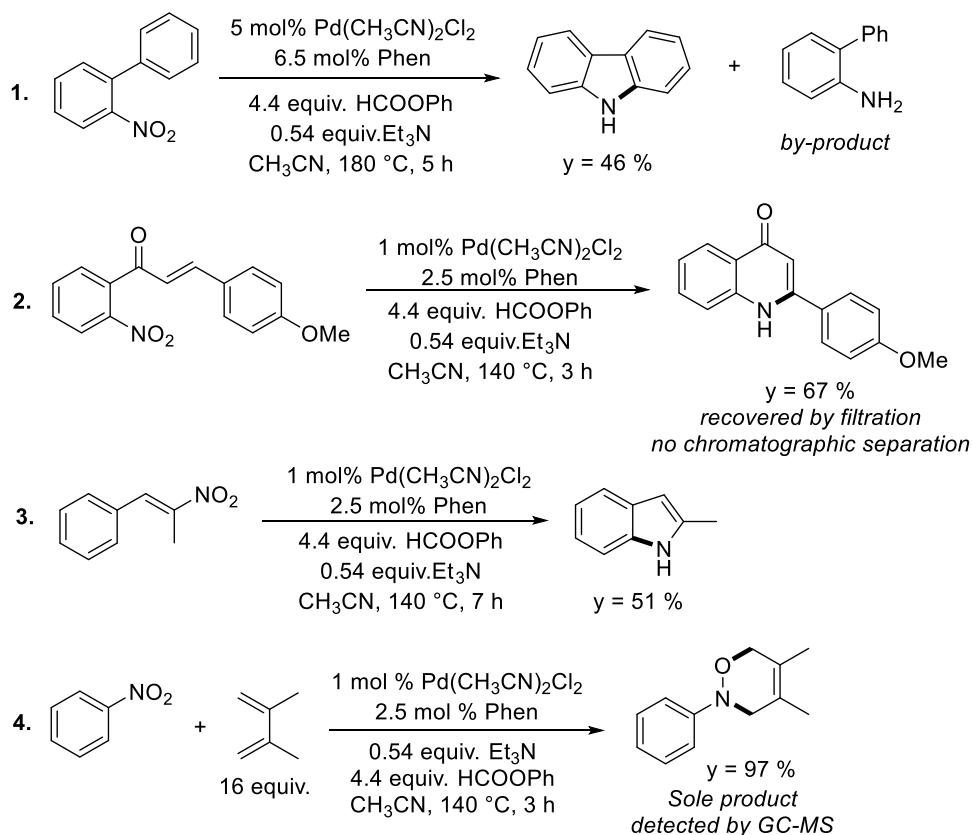
Despite the high efficiency of several of these reactions, their use has not spread outside the limited number of groups that reported them. This is most likely because they generally involve the use of pressurized CO, requiring safety measures and pressure equipment that are not available in most synthetic organic laboratories. This issue is common to other carbonylation reactions and in recent years many reagents have been studied that are able to release CO *in situ* in order to overcome the problem.^[131-132] However, some of these reagents are toxic (for example Mo(CO)₆) or not commercially available. Moreover, in several cases the decomposition of the CO-releasing molecule and the actual catalytic reaction need to be performed in two separate reactors connected to each other. Since the reactors should be able to withstand at least a moderate pressure (a few bars) these facts limit the scale of the reaction to available reactors.

Our group at Milano University has developed a synthetic method based on the use of formate esters as suitable CO releasing substances in the preparation of indoles from *o*-nitrostyrenes.^[18] Formate esters are convenient because of their commercial availability, low cost and low toxicity. Phenyl formate was found to be more effective than alkyl formates, allowing lower temperatures to be employed and higher selectivities to be achieved. Moreover, phenyl formate can be activated by weak organic bases, whereas alkyl formates require the use of strong bases or the addition of a ruthenium catalyst, which makes the catalytic system more complex. The reactions could be operated in a single glass pressure tube. This equipment is cheap and available in different sizes. A steel autoclave can also be used, but without the need for pressurized CO. The best catalytic system optimized for the synthesis of indoles is based on the use of Pd(CH₃CN)₂Cl₂ as pre-catalyst and 1,10-phenanthroline as ligand, phenyl formate as the CO releasing agent and triethylamine as the base to activate it, in acetonitrile at 140 °C (**Scheme 19**).



Scheme 23. Ragaini's optimized catalytic system for indole synthesis.^[18]

The developed protocol was also tested in other reactions, such as the synthesis of oxazines from nitroarenes and dienes, the cyclization of *o*-nitrobiphenyl to give carbazole, the synthesis of quinolones from chalcones and the cyclization of β -nitrostyrenes to give indoles (**Scheme 24**).^[18]



Scheme 24. Synthesis of other N-heterocycles (yields of isolated products are reported).^[18]

The protocol worked in all cases even though experimental conditions were not optimized for these specific reactions. Wide margins for improvement clearly existed, but the oxazine yield was already higher than that previously obtained using pressurized CO.

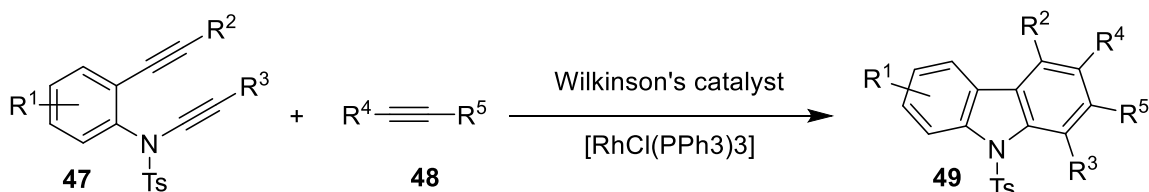
Since the single experiment for the synthesis of an oxazine by the palladium/phenanthroline catalyzed reaction of nitrobenzene and 2,3-dimethylbutadiene using phenyl formate as a CO source (4th reaction in **Scheme 24**) had given an excellent yield (97%), the scope and limitation of the reaction were afterwards studied. Many functional groups were well tolerated, and yields were higher than those obtained by any previously reported method.^[17] Instead, the unoptimized synthesis of carbazole (1st reaction in **Scheme 24**) gave only a low yield (<50%), thus leaving room for improvement. One aim of this work is to investigate several modifications of the reported catalytic system to make it suitable for the synthesis of carbazoles.

Part of the work of this thesis focused on the optimization of the previously reported catalytic protocol for the synthesis of carbazoles from *o*-nitrobiaryls as well as investigating the scope and mechanism of the reaction. The large difference on the optimized conditions and the catalyst behavior with respect to those optimized for indoles synthesis, suggests important differences between the mechanism of the two reactions and stability of the involved intermediates.

1.3.3. Methods involving both rings of the carbazole.

Besides the synthetic strategies that leads to the formation of either ring A or B of the carbazole ring discussed above, there are several synthetic procedures in which both rings A and B are formed in one step. However, the starting compound in almost all cases is an aromatic ring bearing an alkyne group *ortho* to a N-alkynyl amino group. A representative example is discussed below.

An important example on methods constructing both the benzene (A) ring and the pyrrole (B) ring of the carbazole in tandem is the Vollhardt-type cyclotrimerization of diynes **47** and alkynes **48** developed by Witulski and Alayrac.^[133] This method uses catalytic amounts of Wilkinson's catalyst [RhCl(PPh₃)₃] for the preparation of substituted carbazoles **49** (**Scheme 25**).^[133] However, the decreased availability of the precursors is usually a drawback for these reactions.



Scheme 25. Witulski and Alayrac tandem formation of both the benzene (A) ring and the pyrrole (B) ring of the carbazole system.^[133]

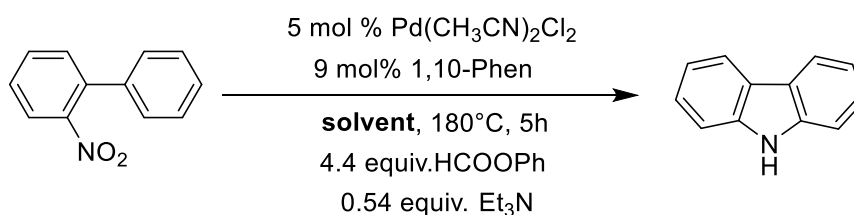
2. Results and discussion.

Our aim is to take advantage of the previously described preliminary experiment (1st reaction in **Scheme 24**) using our phenyl formate catalytic procedure and applying several modifications to make it suitable for carbazole synthesis. Taking into account Davies conditions for Pd(OAc)₂ catalyzed reductive cyclization using CO gas (**Scheme 22**).

2.1. Optimization of the catalytic system.

At first the reaction was investigated employing the commercially available *o*-nitrobiphenyl as the model substrate to determine the optimum conditions for the synthesis of carbazole. We started our investigation by re-testing our previously developed protocol.

Table 1. Pd-catalyzed reductive cyclization of 2-nitrobiphenyl: solvent effect.^(a)



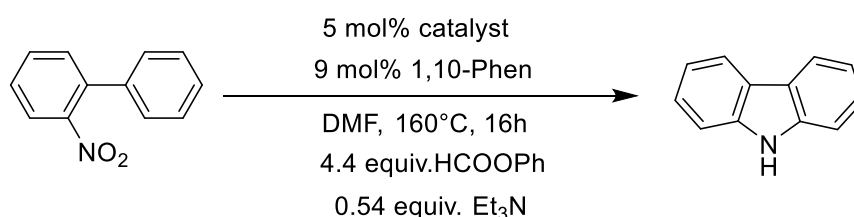
Entry	solvent	% conversion	% carbazole selectivity	% amine selectivity
1	CH ₃ CN	94.7	35.3	29.8
2	DMF	99.7	66.0	20.1

(a) Experimental conditions: *o*-nitrobiphenyl (107.6 mg, 0.54 mmol), Pd(CH₃CN)₂Cl₂ 5 mol%, Phen 9 mol%, HCOOPh (260 μL, 2.38 mmol, 4.4 equiv.), Et₃N (40 μL, 0.28 mmol, 0.54 equiv.), solvent (10 mL), 180 °C, time=5h. Reactions were performed in a pressure tube. The reagent conversion and product selectivity were measured by gas chromatography using biphenyl as the internal standard.

The reductive cyclization reactions of *ortho*-functionalized nitroarenes using carbon monoxide as the reductant and Pd complexes as the catalyst works well in polar solvents. In the preliminary experiments on *ortho*-nitrobiphenyl reported by the group,^[18] acetonitrile was used as the solvent. Methanol or other protic solvents are not compatible with the transformation since they will lead to a faster reduction of the nitro to amine and its subsequent carbonylation to form carbamates and ureas. DMF is often a good solvent for these reactions,^[33] thus we tested it before screening other conditions. Noticeably, its use almost doubled the selectivity in carbazole and allowed to reach nearly complete conversion (>99%). For this reason, it was selected instead of acetonitrile for the rest of the optimization.

Smitrovich and Davies performed a comprehensive screening conditions employing Pd(OAc)₂ and phenanthroline as the catalyst for the synthesis of carbazoles from *o*-nitrobiphenyls. By changing the precatalyst to palladium(II) trifluoroacetate they noticed a lack of activity thus concluding that an important factor was the presence of a coordinating anion.^[33] Since, during the cyclization, a series of proton transfer are involved in the synthesis of the final product, it is possible that acetate acts as a bifunctional catalyst in promoting these transfers and make the reaction irreversible.^[9] Prompted by these results, we performed some experiments using either Pd(OAc)₂ as the catalyst (entry 3, Table 2) or Pd(CH₃CN)₂Cl₂ in presence of a source of acetate (entry 2, Table 2). The temperature was lowered by 20 °C with respect to the experiments in Table 1 in order to better distinguish the effect of variations. The absence of acetate anion had no effect on the reaction (compare entries 1 and 2, Table 2), in fact Pd(CH₃CN)₂Cl₂ gave much better conversion than Pd(OAc)₂ (compare entries 1 and 3, Table 2), while, the addition of chloride source enhanced the conversion even when Pd(OAc)₂ is used as the catalyst (compare entries 3 and 4, Table 2). Thus, our initial hypothesis was not confirmed by these initial results. Therefore, we decided to use Pd(CH₃CN)₂Cl₂ as the catalyst for the rest of the optimization.

Table 2. Pd-catalyzed reductive cyclization of 2-nitrobiphenyl: effect of acetate and chloride ions.

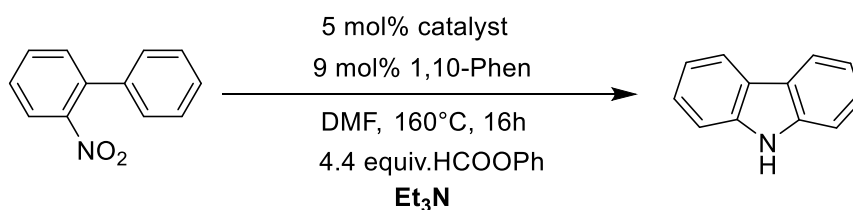


Entry	catalyst	additive (mol%)	% conversion	% carbazole selectivity	% amine selectivity
1 ^(a)	Pd(CH ₃ CN) ₂ Cl ₂	-----	99.7	55.5	24.8
2 ^(a)	Pd(CH ₃ CN) ₂ Cl ₂	PPN acetate (5)	99.6	54.5	25.2
3 ^(a)	Pd(OAc) ₂	-----	74.2	44.3	11.3
4 ^(a)	Pd(OAc) ₂	PPN chloride (5)	99.8	54.5	14.6
5 ^(b)	Pd(OAc) ₂	-----	100	82.1	2.0
6 ^(b, c)	Pd(OAc) ₂	-----	100	85.4	4.6
7 ^(b, d)	Pd(OAc) ₂	-----	98.9	24.6	25.3
8 ^(b, e)	Pd(OAc) ₂	-----	97.5	39.9	17.9

(a) Experimental conditions: *o*-nitrobiphenyl (107.6 mg, 0.54 mmol), Pd-catalyst 5 mol%, Phen 9 mol%, HCOOPh (260 μL, 2.38 mmol, 4.4 equiv.), Et₃N (40 μL, 0.28 mmol, 0.54 equiv.), DMF (10 mL), 160 °C, time=16h. Reactions were performed in a pressure tube. The reagent conversion and product selectivity were measured by gas chromatography using biphenyl as the internal standard. (b) The reaction was performed in a glass liner that was later inserted in a steel autoclave and charged with CO (6 bar) adapting the procedure reported in ref.^[33] see the experimental part for details. (c) phenol (4.4 equivalent) was added. (d) Et₃N (0.54 equivalent) was added. (e) phenol (4.4 equivalent) and Et₃N (0.54 equivalent) were added.

The use of CH₃CN as the solvent already allowed us to reach full conversion of the starting reagent (entry 1, Table 2) but only a moderate selectivity in carbazole due to amine formation. In our attempt to understand what causes the amine formation and thereby decreases the selectivity in carbazole, we run several reactions under conditions similar to those employed by Davis (we cannot add CO continuously to keep pressure constant, so we applied a higher initial CO pressure) that use CO gas as the stoichiometric reductant and tested the effect of phenol and Et₃N separately as well as both together (entries 5-8, Table 2). We found out that phenol had little effect on the reaction (compare entries 5 and 6, Table 2) while Et₃N (entry 7, Table 2) increased the selectivity in the amine side product and greatly decreased the selectivity in carbazole. Addition of both phenol and Et₃N (entry 8, Table 2) had a lesser negative effect on the reaction, possibly because hydrogen bonded Et₃N is less noxious to the reaction. Thus, we decided to study the effect of the identity and the amount of base in more depth. First, the effect of base amount in our phenyl formate protocol was studied (Table 3). Halving the amount of the base increased the selectivity in carbazole and decreased it in amine (entries 2, 4). It appears that Et₃N plays a relevant role in the over-reduction of *o*-nitrobiphenyl to *o*-aminobiphenyl side product. Hence, we decided to investigate the effect of the type of base as well. In fact, replacing Et₃N with K₂CO₃ (entry 4, Table 3) gave full conversion, even with the use of Pd(OAc)₂ pre-catalyst and in absence of any chloride ion, with concomitant increase of the selectivity in carbazole to 72%. Thus, we decided to test several different bases including organic and inorganic ones for the reaction (Table 4).

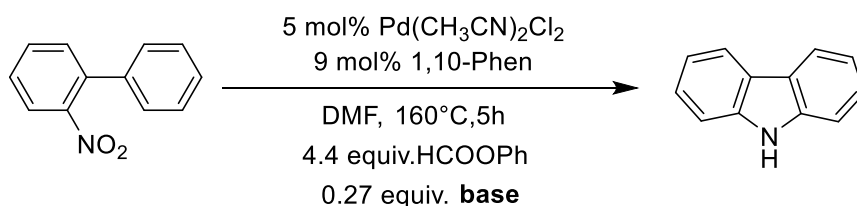
Table 3. Effect of base amount on the reaction.^(a)



Entry	catalyst	amount of base	% conversion	% carbazole selectivity	% amine selectivity
1	Pd(CH ₃ CN) ₂ Cl ₂	0.54 equiv.	99.7	55.5	24.8
2	Pd(CH ₃ CN) ₂ Cl ₂	0.27 equiv.	99.6	60.4	15.6
3	Pd(OAc) ₂	0.54 equiv.	74.2	44.3	11.3
4	Pd(OAc) ₂	0.27 equiv.	79.2	53.2	8.9
5 ^(b)	Pd(OAc) ₂	0.27 equiv.	100.0	72.0	12.2

(a) Experimental conditions: *o*-nitrobiphenyl (107.6 mg, 0.54 mmol), Pd-catalyst 5 mol%, Phen 9 mol%, HCOOPh (260 μL, 2.38 mmol, 4.4 equiv.), Et₃N, DMF (10 mL), 160 °C, time=16h. Reactions were performed in a pressure tube. The reagent conversion and product selectivity were measured by gas chromatography using biphenyl as the internal standard.

(b) K₂CO₃ was used instead of Et₃N as the base.

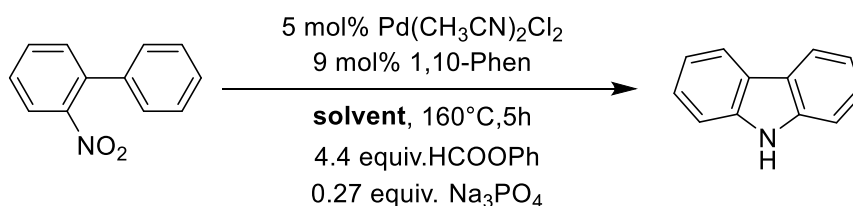
Table 4. Screening of bases.^(a)

Entry	base	% conversion	% carbazole selectivity	% amine selectivity
1	Et ₃ N	99.2	55.2	19.0
2	DBU	100.0	57.2	30.0
3	Li ₂ CO ₃	100.0	84.7	5.8
4	Na ₂ CO ₃	100.0	87.6	3.8
5	K ₂ CO ₃	100.0	81.3	6.7
6	Cs ₂ CO ₃	95.3	68.5	9.4
7	KH ₂ PO ₄	85.0	49.1	31.1
8	K ₂ HPO ₄	99.9	81.3	8.3
9	K ₃ PO ₄ ·H ₂ O	99.9	86.4	4.4
10	K ₃ PO ₄	100.0	87.1	4.1
11	Na ₂ HPO ₄	87.1	62.9	24.3
12	Na ₃ PO ₄	100.0	89.0	2.4

(a) Experimental conditions: *o*-nitrobiphenyl (107.6 mg, 0.54 mmol), Pd(CH₃CN)₂Cl₂ 5 mol%, Phen 9 mol%, HCOOPh (260 μL, 2.38 mmol, 4.4 equiv.), base (0.27 equiv.), DMF (10 mL), 160 °C, time=5h. Reactions were performed in a pressure tube. The reagent conversion and product selectivity were measured by gas chromatography using biphenyl as the internal standard.

Most of the inorganic bases gave better results than organic ones. Although the reason has still not been elucidated, *N*-based organic bases increased selectivity in *o*-aminobiphenyl (entries 1 and 2, Table 4). As shown before in (entry 5, Table 3) replacing Et₃N with K₂CO₃ in one experiment greatly improved both the conversion and selectivity of the reaction. When comparing the use of K₂CO₃ with K₃PO₄ (entries 5 and 10, Table 4) and the use of Na₂CO₃ with Na₃PO₄ (entries 4 and 12, Table 4), it appears that phosphates gave better selectivity in carbazole than carbonates.

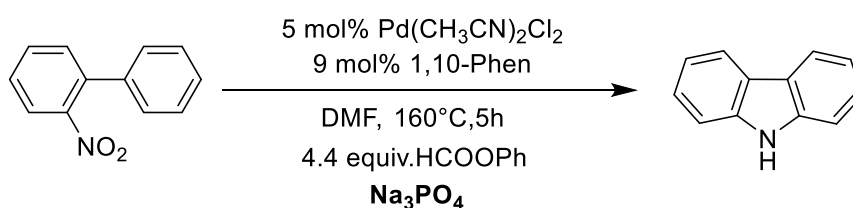
Conversion decreased in case of KH₂PO₄ and Na₂HPO₄ (entries 7, 11, Table 4, respectively). This can be attributed to lower solubility in DMF. Moreover, those bases can act as a hydrogen source which explains the increase of the selectivity in aminobiphenyl. Small differences between sodium and potassium salts for example in the tribasic salt can also be attributed to small differences in solubility. Among the carbonates (entries 3-6, Table 4), Na₂CO₃ gave the best results. Therefore, we tested Na₃PO₄ and it gave the best selectivity in carbazole (entry 12, Table 4). Thus, it was chosen as the base for the rest of the optimization due to the much better yield (89%) at a lower temperature (160 °C) and a lower base amount (0.27 equiv.) compared to our starting point (yield=~66%, entry 2, Table 1). Settled on Na₃PO₄ as the base of choice, we re-investigated the possibility to change the solvent (Table 5). However, DMF remained the best solvent for our conditions. A possible explanation for this behaviour is the low solubility of the inorganic base in the other solvents.

Table 5. Re-investigation of the effect of different solvents using an inorganic base.^(a)

Entry	solvent	% conversion	% carbazole selectivity	% amine selectivity
1	DMF	100.0	89.0	2.4
2	DME	39.0	25.6	16.6
3	CH ₃ CN	94.8	73.0	8.7
4	Me-THF	21.5	33.0	10.5

(a) Experimental conditions: *o*-nitrobiphenyl (107.6 mg, 0.54 mmol), Pd(CH₃CN)₂Cl₂ 5 mol%, Phen 9 mol%, HCOOPh (260 μL, 2.38 mmol, 4.4 equiv.), Na₃PO₄ (24 mg, 0.146 mmol, 0.27 equiv.), solvent (10 mL), 160 °C, time=5h. Reactions were performed in a pressure tube. The reagent conversion and product selectivity were measured by gas chromatography using biphenyl as the internal standard.

Since the identity and the amount of the base plays such an important role in our conditions, a re-optimization of the amount of base was performed in the aim of further reducing it. We were pleased to find out that the amount of base can be lowered down to 0.135 equiv. (~12 mg) without affecting the conversion and still maintaining an excellent selectivity (entry 3, Table 6). The reaction could be performed even using a lower amount of base (only 0.0675 equiv.) with only a slight decrease in the selectivity (entry 4, Table 6). To avoid potential experimental error in weighing such little amount (~6 mg), 0.135 equiv. of the base was used in the following optimization.

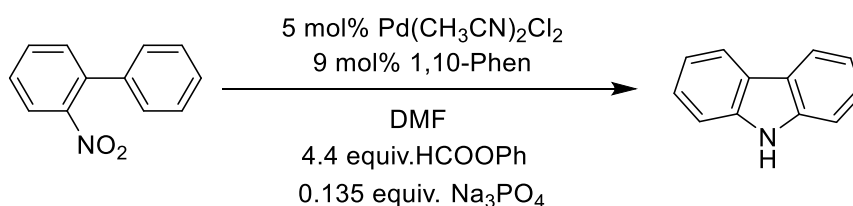
Table 6. Optimization of the amount of the base.^(a)

Entry	amount of Na ₃ PO ₄	% conversion	% carbazole selectivity	% amine selectivity
1	0.54 equiv.	100	87.3	2.5
2	0.27 equiv.	100	89.0	2.4
3	0.135 equiv.	100	89.6	2.8
4	0.0675 equiv.	100	87.7	4.1

(a) Experimental conditions: *o*-nitrobiphenyl (107.6 mg, 0.54 mmol), Pd(CH₃CN)₂Cl₂ 5 mol%, Phen 9 mol%, HCOOPh (260 μL, 2.38 mmol, 4.4 equiv.), Na₃PO₄, DMF (10 mL), 160 °C, time=5h. Reactions were performed in a pressure tube. The reagent conversion and product selectivity were measured by gas chromatography using biphenyl as the internal standard.

Several experiments were performed to determine the optimum temperature and time for our procedure. The reaction can be performed at a lower temperature (entry 3, Table 7) but the selectivity in aminobiphenyl slightly increased. Also, performing the reaction at 170 °C (entry 4, Table 7) gave a better result than 160 °C (entry 3, Table 6) and the best selectivity in carbazole so far. Comparing entries 2 and 3 in Table 7, it can be noted that besides the increase in conversion with time, there is also an increase of carbazole selectivity with time which is indirect indication that some reaction intermediate is accumulating. Most likely the intermediate *o*-nitrosobiphenyl is more stable than other nitroso intermediate involved in reductive cyclizations (e.g., *o*-nitrostyrene). Its cyclization into the carbazole is not a so fast reaction even at relatively high temperatures, this made us reconsider our assumption that the initial electron transfer from palladium to the nitrobiphenyl is the rate determining step. To avoid incomplete conversion or accumulating intermediates while applying the devised protocol for substituted nitrobiaryls, the reaction was performed at 170 °C. The reaction was also carried out for longer time for the same reason, although in most cases is likely that full conversion is reached after 1h (entry 4-5, Table 7).

Table 7. Optimization of reaction temperature and time.^(a)



Entry	temperature (°C)	time (h)	% conversion	% carbazole selectivity	% amine selectivity
1	120	2	51.8	69.3	6.6
2	140	2	78.0	84.4	4.0
3	140	5	100	89.4	4.1
4	170	1	100	92.3	2.8
5	170	2	100	92.0	2.6
6	180	1	100	90.5	2.3

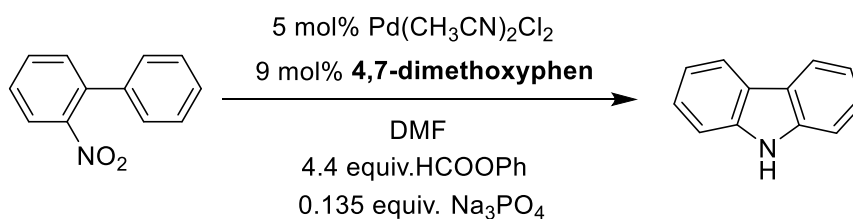
(a) Experimental conditions: *o*-nitrobiphenyl (107.6 mg, 0.54 mmol), Pd(CH₃CN)₂Cl₂ 5 mol%, Phen 9 mol%, HCOOPh (260 μL, 2.38 mmol, 4.4 equiv.), Na₃PO₄ (12 mg, 0.073 mmol, 0.135 equiv.), DMF (10 mL). Reactions were performed in a pressure tube. The reagent conversion and product selectivity were measured by gas chromatography using biphenyl as the internal standard.

Phenanthroline has proven to be of general applicability in the field of reduction and carbonylation reactions of nitroarenes.^[134-135] However, it is not necessarily the best ligand of this class for all reactions. In a recent paper,^[14] Ragaini and coworkers investigated the use of a series of substituted phenanthrolines in a synthesis of thienopyrroles related to the reaction in **Scheme 19** and showed that 4,7-dimethoxyphenanthroline was more effective than other phenanthrolines. Most likely, the more

electron donating character of this ligand with respect to unsubstituted phenanthroline favors the initial electron transfer from the palladium complex to the nitroarene. The same beneficial effect could occur even for the reaction of nitrobiaryl and may allow to improve the performance of the catalytic system for those reactions in which the results are only moderate or good. Thus, we repeated some experiments that initially gave lower conversion and selectivity using 4,7-dimethoxyphenanthroline to check if the reaction can be further improved under milder conditions (Table 8).

The use of 4,7-dimethoxyphenanthroline had a negative effect on the selectivity in carbazole (compare entry 1, Table 8 to entry 3, Table 7), while the conversion is slightly increased in some cases (see entry 1, Table 7 and entry 2, Table 8). These results are a further indication that the initial electron transfer from the palladium complex to the nitroarene is not the rate determining step in case of the reductive cyclization of *o*-nitrobiphenyls. It appears that the relatively high stability of *o*-nitrosobiphenyl makes the rate of cyclization step at least comparable to that of the reduction of the nitro group.

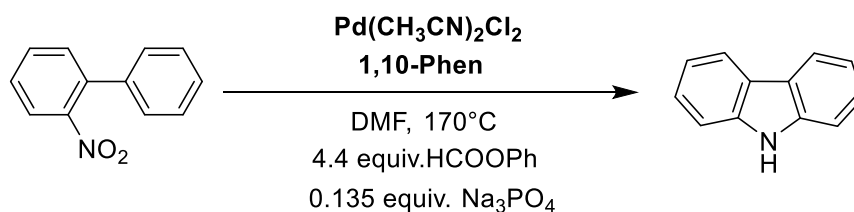
Table 8. Use of 4,7-dimethoxy-1,10-phenanthroline as the ligand.^(a)



Entry	temperature (°C)	time (h)	% conversion	% carbazole selectivity	% amine selectivity
1	140	5	94.4	75	16.3
2	120	2	67.1	61.1	16.8

(a) Experimental conditions: *o*-nitrobiphenyl (107.6 mg, 0.54 mmol), Pd(CH₃CN)₂Cl₂ 5 mol%, 4,7-dimethoxyphen 9 mol%, HCOOPh (260 μL, 2.38 mmol, 4.4 equiv.), Na₃PO₄ (12 mg, 0.073 mmol, 0.135 equiv.), DMF (10 mL). Reactions were performed in a pressure tube. The reagent conversion and product selectivity were measured by gas chromatography using biphenyl as the internal standard.

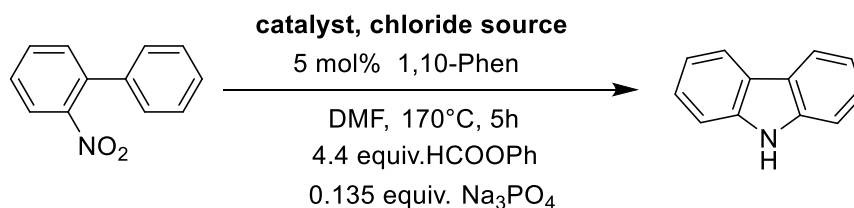
It is thus interesting to establish the rate determining step in order to further improve the catalytic reaction. Besides the possible mechanistic progresses of the work, since the use of 4,7-dimethoxyphenanthroline did not impart any significant improvement to the reaction, 1,10-phenanthroline was employed for the rest of the optimization.

Table 9. Optimization of the catalyst and ligand amounts.^(a)

Entry	catalyst (mol%)	ligand (mol%)	time (h)	% conversion	% carbazole selectivity	% amine selectivity
1	2	9	1	97.4	86.9	2.9
2	2	5	1	93.2	89.3	1.7
3	2	5	2	96.8	92.8	1.6
4	2	5	3	98.7	90.8	1.7
5	1	5	1	86.6	86.2	1.8
6	1	5	2	94.5	90.8	1.7
7	1	5	3	96.2	90.0	2.0
8	1	5	5	97.8	90.8	2.2
9	0.1	5	16	94.2	85.3	5.0

(a) Experimental conditions: *o*-nitrobiphenyl (107.6 mg, 0.54 mmol), Pd(CH₃CN)₂Cl₂, Phen, HCOOPh (260 μL, 2.38 mmol, 4.4 equiv.), Na₃PO₄ (12 mg, 0.073 mmol, 0.135 equiv.), DMF (10 mL), 170 °C, time=5h. Reactions were performed in a pressure tube. The reagent conversion and product selectivity were measured by gas chromatography using biphenyl as the internal standard.

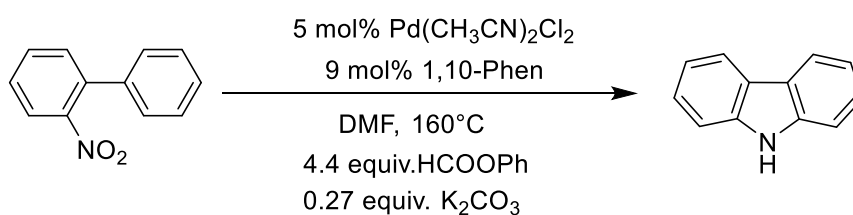
Given the relatively high amount of ligand and metal precursor employed, we aimed at reducing both. At first, the catalyst loading was lowered from 5 mol% to 2 mol% while keeping the same amount of ligand (entry 1, Table 9), then the amount of ligand was also lowered to 5 mol% (entry 2). In both cases, good yield was obtained but a little decrease in the conversion was observed. The conversion and selectivity only slightly enhance with increasing the time of the reaction (entries 2-4, 5-8, Table 9). Interestingly the catalyst loading can be decreased down to 0.1 mol% prolonging the reaction time up to 16 h (entry 9, Table 9), although a little decrease in the carbazole selectivity was observed. It is important to mention that in entries 2-8, Pd-black was detected in the early stage of the reaction (already forming after 30 minutes) indicating a decrease in the stability of the catalyst at lower ligand concentrations. As explained before, presence of chlorides impart stability to the system. Therefore, 1 mol% of the catalyst and 5 mol% of the ligand were employed in combination with a chloride source to the reaction, in order to prevent an early deactivation of the catalyst.

Table 10. Testing different sources of chloride.^(a)

Entry	catalyst	additive	time	% conversion	% carbazole selectivity	% amine selectivity
1	1 mol % Pd(CH ₃ CN) ₂ Cl ₂	5 mol% NaCl	2 h	93.2	88.2	1.7
2	2 mol % Pd(CH ₃ CN) ₂ Cl ₂	10 mol% NaCl	1 h	91.6	90.3	1.9
3	2 mol % Pd(CH ₃ CN) ₂ Cl ₂	5 mol% PPN chloride	1 h	99.3	91.0	2.1
4	0.1 mol % Pd(CH ₃ CN) ₂ Cl ₂	5 mol% PPN chloride	16 h	80.5	84.6	6.7
5	0.1 mol % Pd(CH ₃ CN) ₂ Cl ₂	0.5 mol% PPN chloride	16 h	60.5	79.5	6.0
6	1 mol % Na ₂ [PdCl ₄]	-----	2 h	99.8	91.3	1.4
7	1 mol % Na ₂ [PdCl ₄]	-----	3 h	99.8	91.0	1.5
8	1 mol % Na ₂ [PdCl ₄]	-----	5 h	99.9	95.0	1.7
9	2 mol % Na ₂ [PdCl ₄]	-----	2 h	100.0	90.0	1.5

(a) Experimental conditions: *o*-nitrobiphenyl (107.6 mg, 0.54 mmol), Pd-catalyst, Phen 5 mol%, HCOOPh (260 μ L, 2.38 mmol, 4.4 equiv.), Na₃PO₄ (12 mg, 0.073 mmol, 0.135 equiv.), DMF (10 mL), 170 °C, time=5h. Reactions were performed in a pressure tube. The reagent conversion and product selectivity were measured by gas chromatography using biphenyl as the internal standard.

The addition of NaCl to the reaction (entries 1 and 2, Table 10) did not have a positive effect (compare with entries 6 and 2 in Table 9) most likely due to the low solubility of the salt in DMF. Addition of an organic source of chloride such as PPN chloride slightly improved conversion and selectivity (compare entry 3 in Table 10 to entry 2 in Table 9). However, it seems that its effect is highly dependent on the concentration of the catalyst (entries 4 and 5 in table 10) and at a low catalyst loading the addition of PPN chloride has a negative effect. To avoid the presence of organic counterions and to ensure a precise Pd/chloride ratio without the need of weighing very small amounts of salts, we tested Na₂[PdCl₄] as a catalyst. Thus, the concentration of chloride in the reaction medium was double compared to Pd(CH₃CN)₂Cl₂, this had a positive effect on both the conversion and the selectivity of the reaction (entry 8 in Table 10). In addition, formation of metallic palladium at an early stage of the reaction was not observed.

Table 11. Control experiments and limitations of catalytic system.^(a)

Entry	% conversion	% carbazole selectivity	% amine selectivity
1 ^(b, d)	12.7	59.8	0.0
2 ^(b, e)	80.6	70.0	12.9
3 ^(c)	100.0	72.0	8.6
4 ^(c, f)	100.0	75.0	11.7
5 ^(c, g)	100.0	76.1	13.0

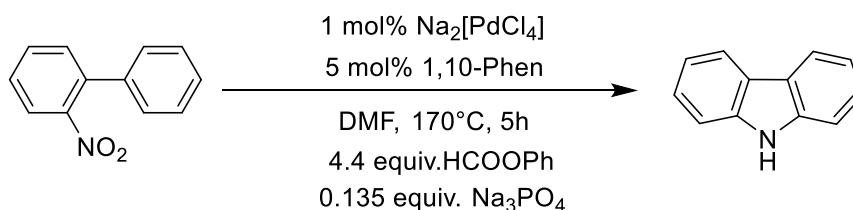
(a) Experimental conditions: *o*-nitrobiphenyl (107.6 mg, 0.54 mmol), Pd(CH₃CN)₂Cl₂ 5 mol%, Phen 9 mol%, HCOOPh (260 μ L, 2.38 mmol, 4.4 equiv.), K₂CO₃ (20.2 mg, 0.146 mmol, 0.27 equiv.), DMF (10 mL), 160 °C. Reactions were performed in a pressure tube. The reagent conversion and product selectivity were measured by gas chromatography using biphenyl as the internal standard. (b) time=5h. (c) time=16. (d) reaction was performed in absence of HCOOPh. (e) PdCl₂ was used instead of Pd(CH₃CN)₂Cl₂. (f) 5 μ L of H₂O were added. (g) 50 μ L of H₂O were added.

A control experiment was carried out to check the actual role of formate. A reaction was thus performed in the absence of phenyl formate (entry 1, Table 11) to test if DMF can act as a source of CO. In fact, DMF is known to decompose to give CO and dimethylamine on heating. Only ~7 mg of carbazole were detected corresponding to a GC yield of 7.6 %. Further experiments were performed to test the limitation of the devised protocol. The use of PdCl₂ (entry 2, Table 11) was tested since it is a cheaper pre-catalyst: the reaction proceeded giving relatively good initial results, although a pre-formation of the active complex by stirring PdCl₂ and the ligand might be necessary to get better yields. It was not worth it to investigate the use of that catalyst in more depth since Na₂[PdCl₄] was selected as the best precursor, that is also cheap and easily obtainable from PdCl₂. Some reactions were performed to check the effect of water by adding few microliters on purpose (5 μ L, 50 μ L) (entries 4 and 5 in Table 11, respectively). In both cases water had a positive effect on the carbazole selectivity (compare with entry 3, Table 11) while also the amine selectivity increases. Water, in conjunction with CO, is known to reduce nitroarenes to anilines efficiently. It was initially our concern whether moisture present in any reagent or solvent may be the cause for the low selectivity in the first attempts to get carbazole. However, these experiments clearly show that trace amounts of water cannot be held responsible for the formation of large amounts of amine.

Finally, some experiments were performed to test the sensitivity of the devised protocol and see if it can be applied in less demanding mediums and hence increase the availability of the reaction for synthetic chemistry. To our surprise, assembling the components of the reaction in air did not quench the reaction (entry 2, Table 12) and the starting nitrobiphenyl was fully converted while keeping a high selectivity. This indicates the high stability of our protocol which utilize Na₂[PdCl₄] as the catalyst. When assembling the reaction under O₂ (entry 3, Table 12), the reaction slowed down indicating that excess of O₂ has a negative effect on the activity, however the selectivity in carbazole was relatively

high. The result indicates a partial catalyst deactivation probably due to the formation of stable inactive complexes.^[136] No metallic palladium precipitation was anyway noticed. In addition, assembling the reaction in air using undistilled commercial DMF gave ~ 94% yield (entry 4, Table 12). The reaction was also performed in the absence of 1,10-phenanthroline (entry 5, Table 12) to verify if the catalyst Na₂[PdCl₄] is stable enough for the reaction to proceed without adding a ligand. No conversion of nitrobiphenyl was detected indicating the essential role of phenanthroline as the ligand.

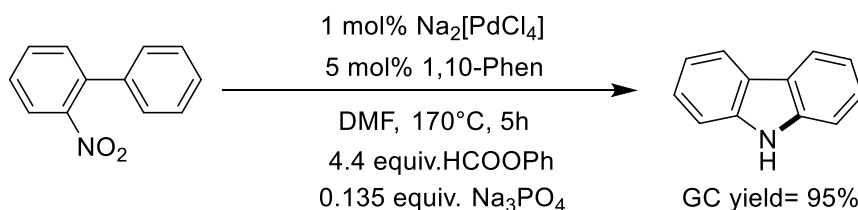
Table 12. Limitations of the optimized catalytic system.^(a)



Entry	% conversion	% carbazole selectivity	% amine selectivity	initial gas phase
1	99.9	95.0	1.7	N₂
2	100.0	97.0	1.2	air
3	30.0	91.3	3.3	O₂
4^(b)	100.0	93.5	1.4	air
5^(c)	0.0	0.0	0.0	N₂

(a) Experimental conditions: *o*-nitrobiphenyl (107.6 mg, 0.54 mmol), Na₂[PdCl₄] 1 mol%, Phen 5 mol%, HCOOPh (260 μL, 2.38 mmol, 4.4 equiv.), Na₃PO₄ (12 mg, 0.073 mmol, 0.135 equiv.), DMF (10 mL), 170 °C, time=5h. Reactions were performed in a pressure tube. The reagent conversion and product selectivity were measured by gas chromatography using biphenyl as the internal standard. (b) Reaction was assembled using undistilled commercial DMF. (c) reaction was performed in the absence of Phen.

As a proof of the robustness and applicability of the devised procedure, a 15-fold large-scale synthesis was performed using a lower catalyst loading (0.5 mol%) and decreasing the solvent amount to one third of the required volume in order to facilitate the work-up. The reaction was also assembled in the air. Very nicely the product was separated in 85% yield using a work-up that did not involve a chromatographic separation (see experimental section) making the procedure even more accessible, valuable for preparative purposes and economically advantageous. Hence, herein we report a highly stable protocol for carbazole synthesis (**Scheme 26**) that can tolerate air and moisture, uses phenyl formate as a CO surrogate and can be performed using commercial DMF. Overall, this makes our strategy for carbazole preparation a very convenient method for the synthetic chemist.

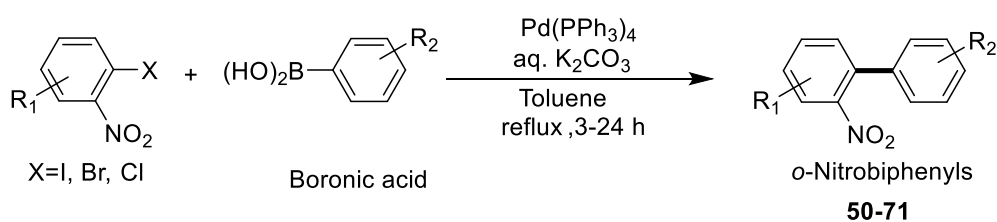


Scheme 26. Optimized conditions for reductive cyclization of 2-nitrobiphenyls.

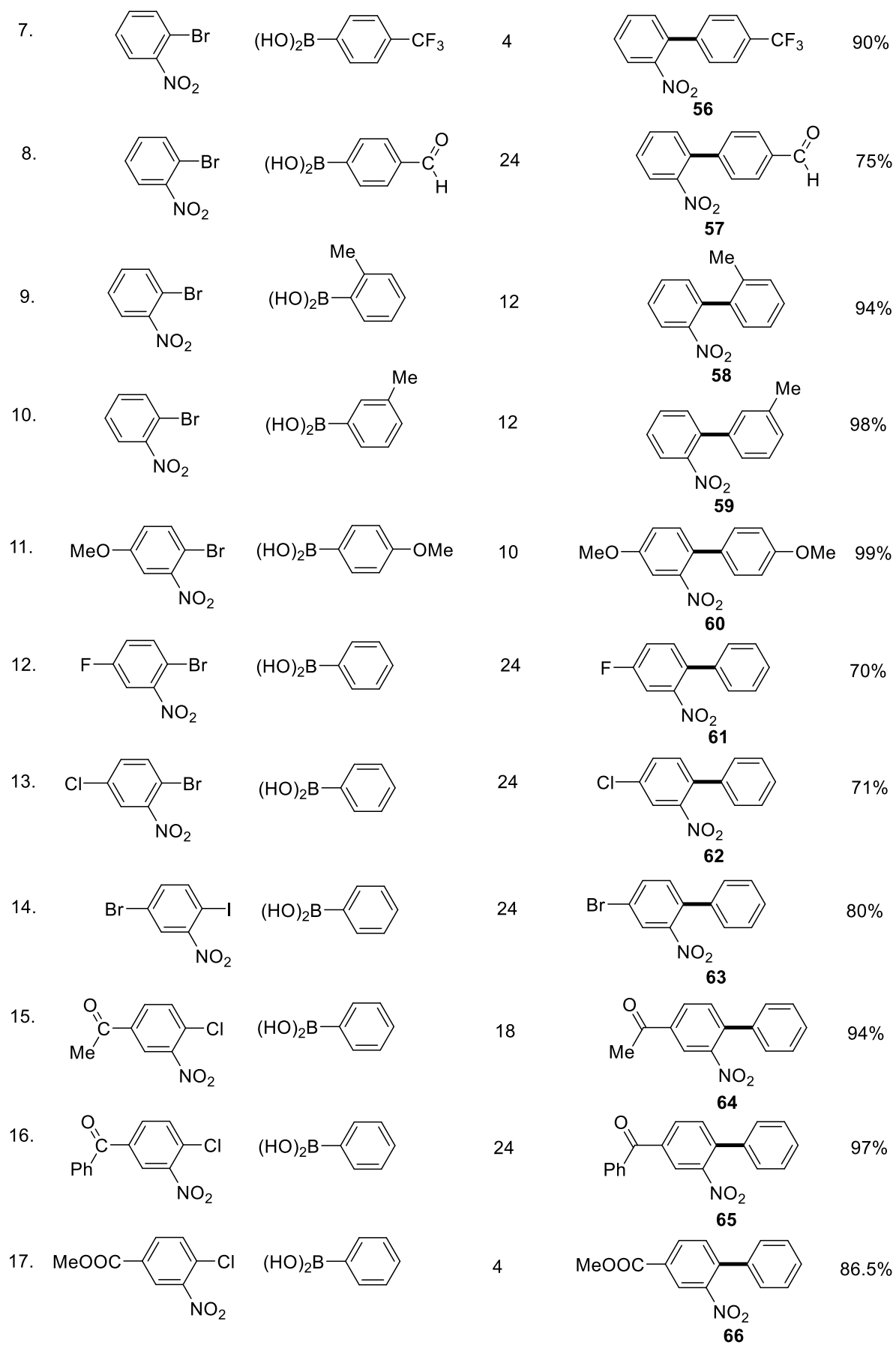
2.2. Preparation of nitrobiaryl substrates

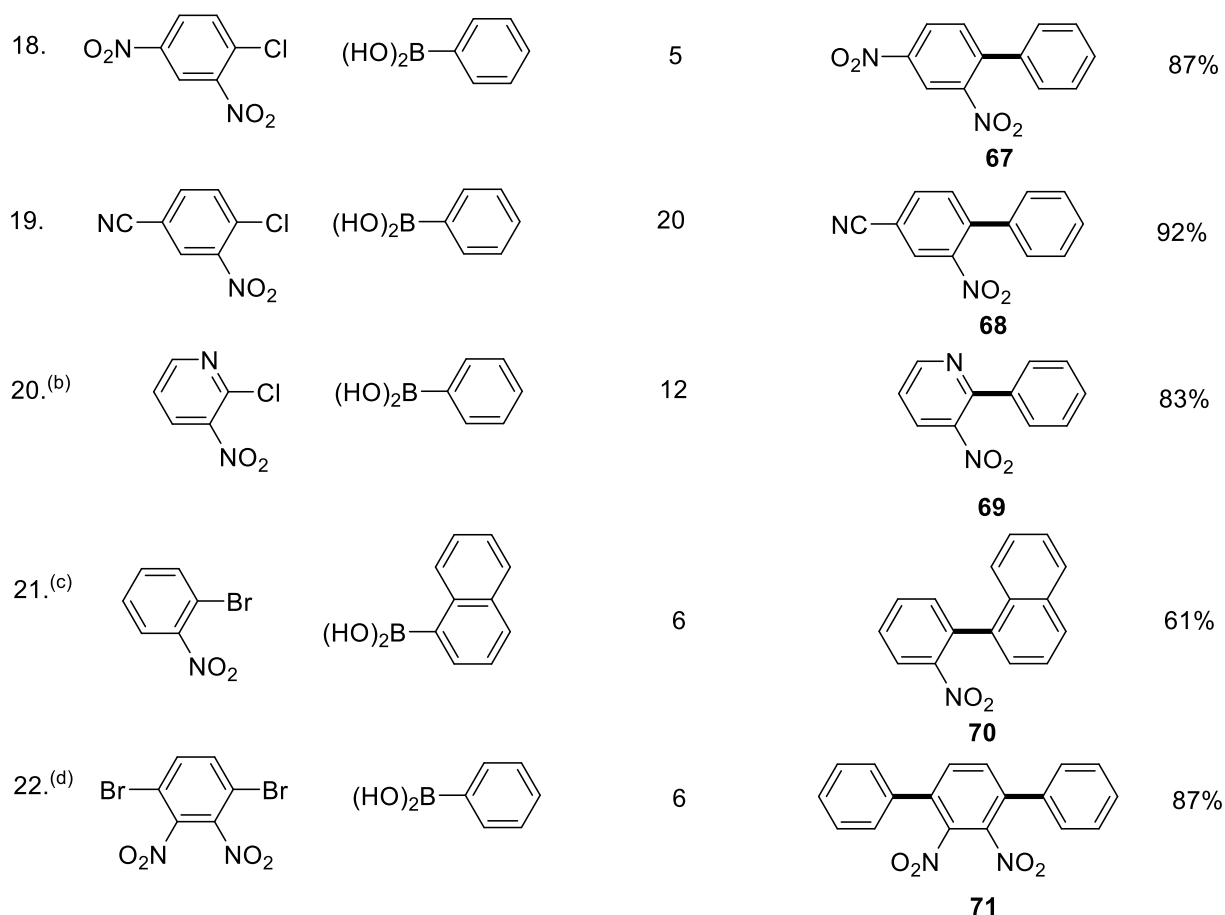
Once we determined the ideal conditions for the reaction, the scope and limitations of the catalytic system were investigated by running the reaction on different substrates of the same class. Thus, part of this thesis regarded the preparation of *o*-nitrobiaryls, mostly by either the Suzuki-Miyaura cross coupling^[102] (Table 13) or the Ullmann cross coupling^[137-138] (**Scheme 27**) of the suitable coupling partners. Some substrates were prepared by nitration of the biphenyl precursor^[102] (**Scheme 28**), or by simple organic transformation of another substrate such as hydrolysis^[102] (**Scheme 29**), demethylation^[102] (**Scheme 30**) or reduction^[139] (**Scheme 31**).

Table 13. Nitrobiaryls prepared through Suzuki-coupling.^(a)

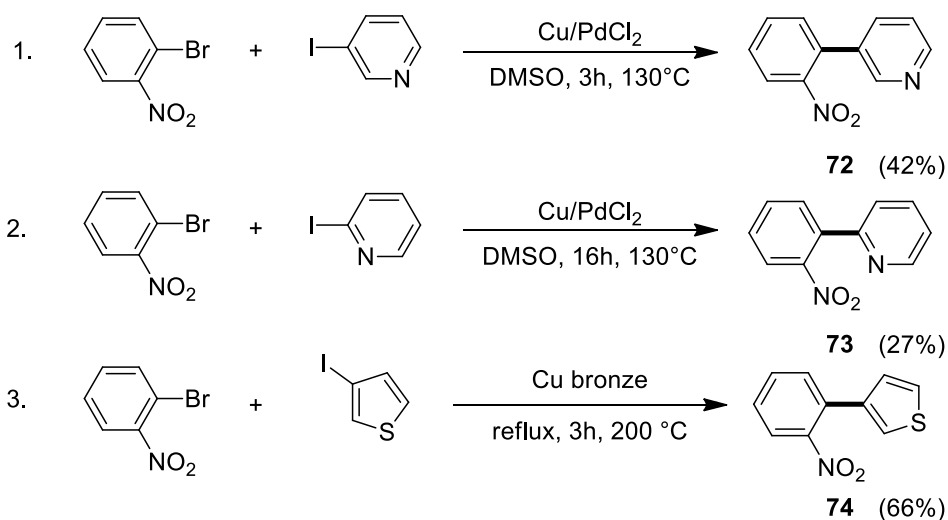


Entry	halonitrobenzene	boronic acid	time (h)	<i>o</i> -Nitrobiaryls	isolated yield
1.			16		95%
				50	
2.			18		96%
				51	
3.			5		82%
				52	
4.			24		89%
				53	
5.			6		93%
				54	
6.			20		97%
				55	

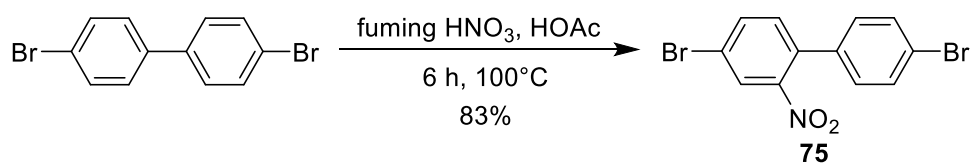




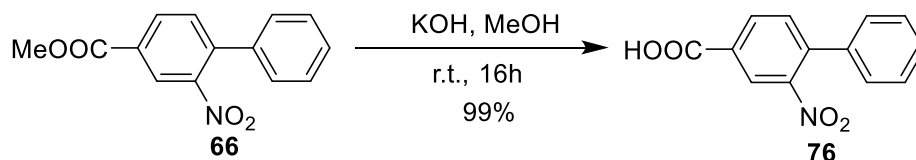
(a) Experimental conditions: halonitrobenzene (5 mmol), boronic acid (5.5 mmol, 1.1 equiv.), K_2CO_3 (1.38 g, 10 mmol, 2 equiv.), $Pd(PPh_3)_4$ (58 mg, 0.05 mmol, 1 mol%), toluene (8 mL), water (5 mL); (b) 2-chloro-3-nitropyridine (5.4 mmol), phenylboronic acid (7 mmol), K_2CO_3 (13 mmol), $Pd(PPh_3)_4$ (0.1 mmol, 2 mol%), 1,2-dimethoxyethane (8 mL), water (3 mL); (c) DMF (15 mL) was used instead of the toluene/water mixture; (d) 1,4-dibromo-2,3-dinitrobenzene (1.63 g, 5 mmol), phenylboronic acid (1.83 g, 15 mmol, 3 equiv.), K_2CO_3 (2.76 g, 20 mmol, 4 equiv.), $Pd(PPh_3)_4$ (116 mg, 0.1 mmol, 2 mol%), toluene (10 mL), water (10 mL).



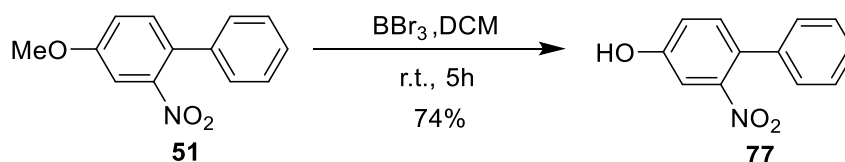
Scheme 27. Nitrobiphenyls prepared through Ullmann cross-coupling.



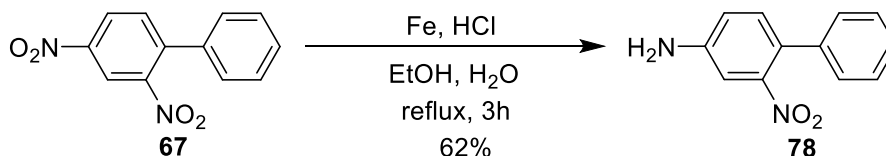
Scheme 28. Preparation of 4,4'-dibromo-2-nitrobiphenyl by nitration of 4,4'-dibromobiphenyl.



Scheme 29. Preparation of 2-nitrobiphenyl-4-carboxylic acid by hydrolysis of 4-carbomethoxy-2-nitrobiphenyl.



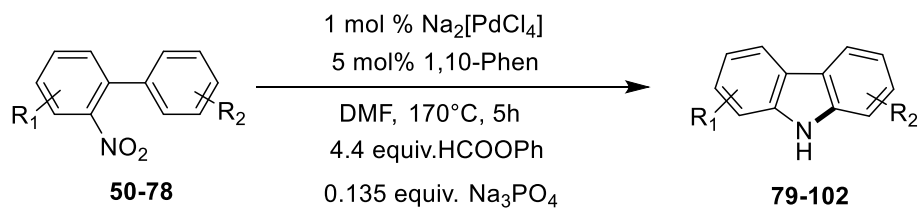
Scheme 30. Preparation of 4-hydroxy-2-nitrobiphenyl by demethylation of 4-methoxy-2-nitrobiphenyl.

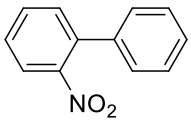
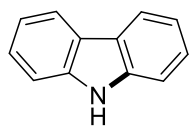
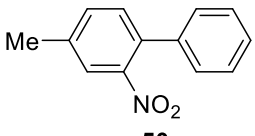
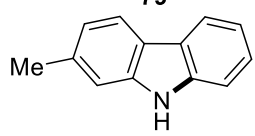
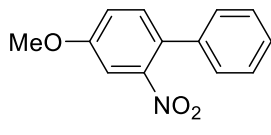
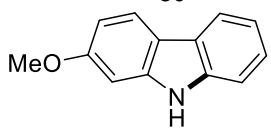
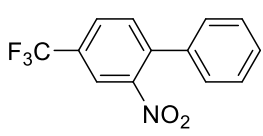
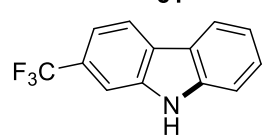
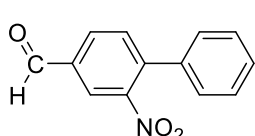
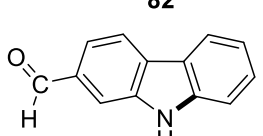
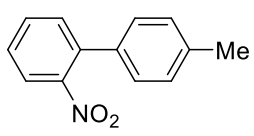
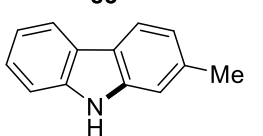
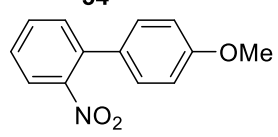
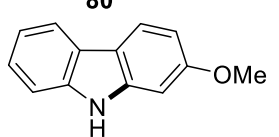
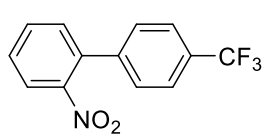
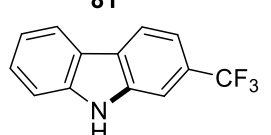
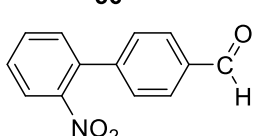
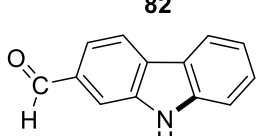


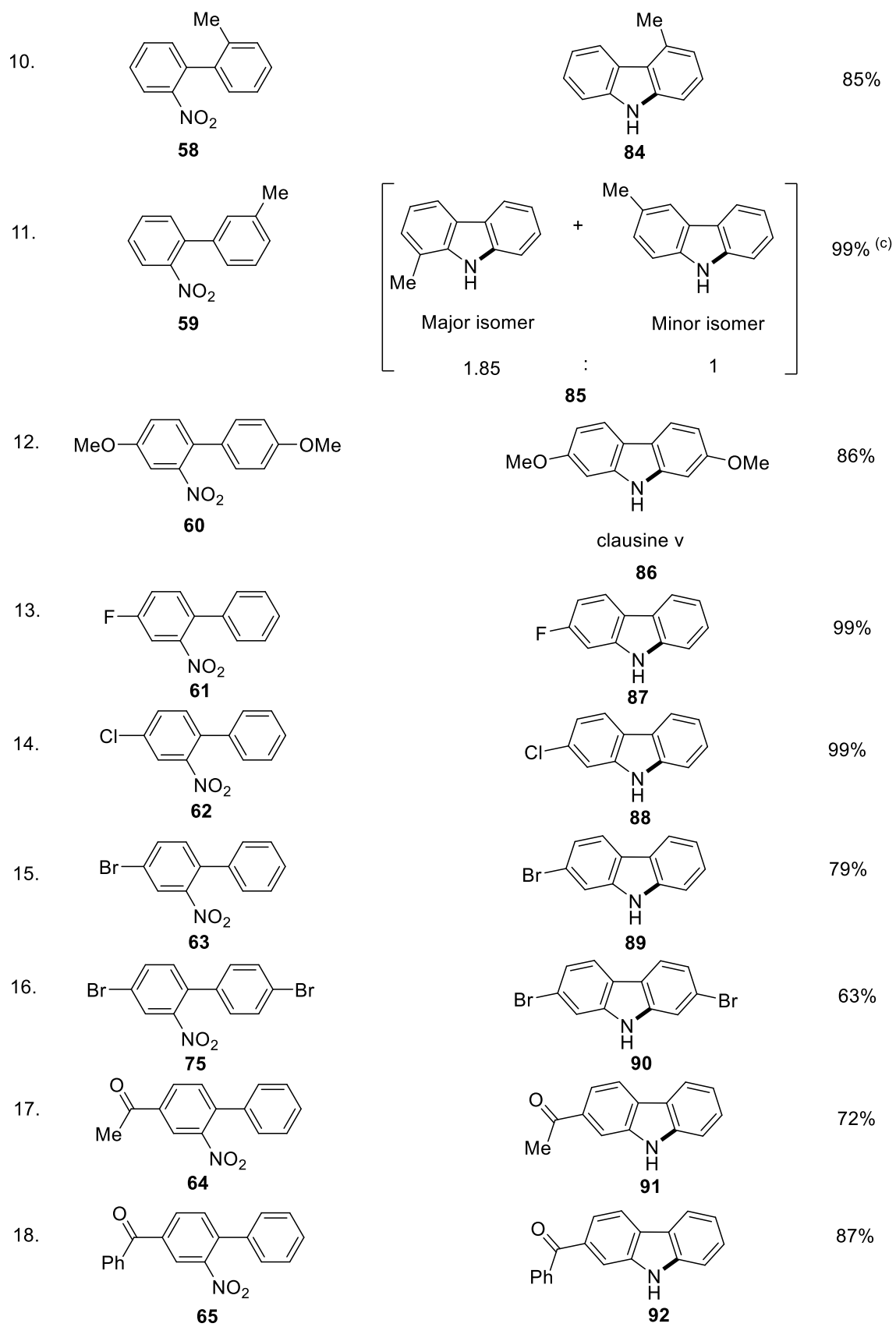
Scheme 31. Preparation of 4-amino-2-nitrobiphenyl by reduction of 2,4-dinitrobiphenyl.

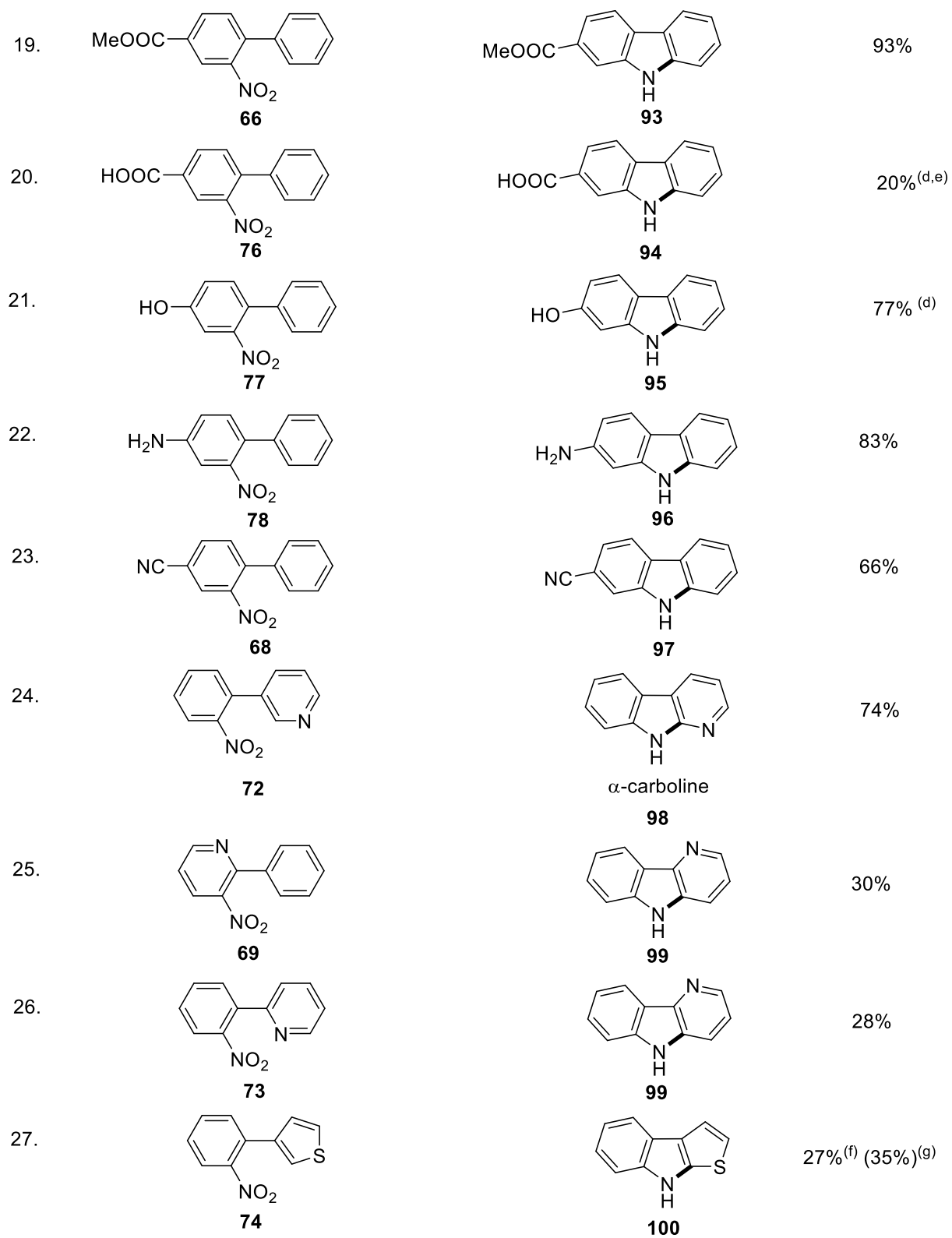
2.3. Investigating the scope of the reaction.

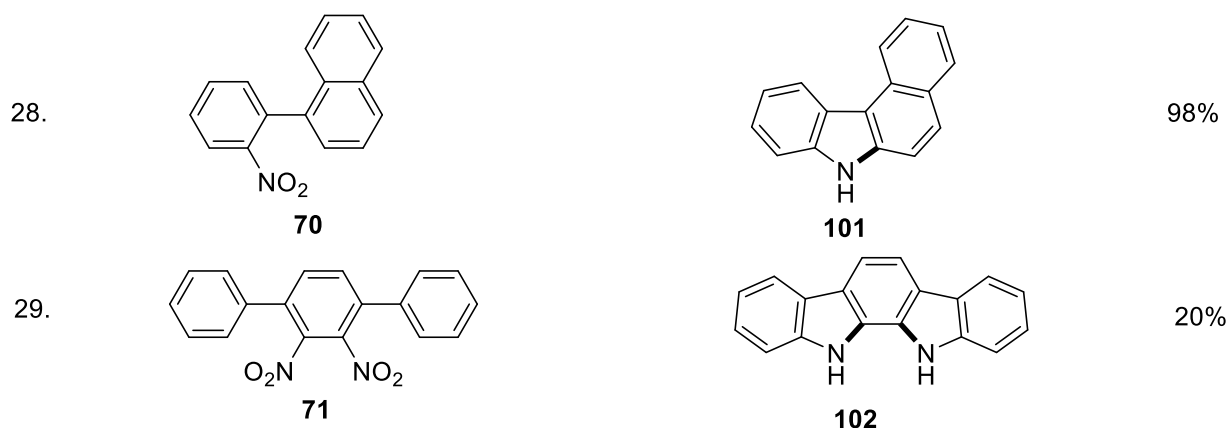
Having the optimized conditions in our hands and the prepared 2-nitrobiaryls, we proceeded with the exploration of the reaction scope (Table 14).

Table 14. Substrate Scope.^(a)

Entry	nitrobiphenyl	carbazole	yield
1.	 50	 79	93% ^(b)
2.	 51	 80	98%
3.	 52	 81	88%
4.	 53	 82	89%
5.	 54	 83	92%
6.	 55	 80	97%
7.	 56	 81	89%
8.	 57	 82	80%
9.	 58	 83	92%







(a) Experimental conditions: *o*-nitrobiphenyl (0.54 mmol), Na₂[PdCl₄] 1 mol%, Ph_{en} 5 mol%, HCOOPh (260 μL, 2.38 mmol, 4.4 equiv.), Na₃PO₄ (12 mg, 0.073 mmol, 0.135 equiv.), DMF (10 mL), 170 °C, time=5h. Reactions were performed in pressure tube. Isolated yields are reported. (b) GC yield=95%. (c) isomer ratio from GC chromatogram is 1.85:1. (d) reaction mixture was acidified before separation. (e) an alternative pathway to obtain the product is hydrolysis of the corresponding ester **97** which proceed with a yield 95%. (f) Na₂[PdCl₄] 2 mol % and Ph_{en} 5 mol% . were used, time= 16 h. (g) Na₂[PdCl₄] 2 mol % and 4,7-dimethoxyphenanthroline 5 mol% . were used, time= 16 h.

Generally, our optimized catalytic procedure shows significant substituent-tolerance affording substituted carbazoles in good to excellent yields. Compounds **80-83** were prepared in two different approaches from nitrobiphenyls where the substituent is either on the ring bearing the nitro group or on the unsubstituted phenyl. Apart from compound **83**, both ways afforded the cyclized product in almost the same yield which means that both electron donating and electron withdrawing groups are well tolerated on either ring of the nitrobiphenyl. Regarding 2-trifluoromethylcarbazole **83**, the small decrease in yield (9%) can be explained by the electron withdrawing effect of CF₃ group. In fact, the initial reduction of the nitro group, leads to the intermediate formation of a nitrosobiphenyl. The electrophilic nitroso group is then responsible for the cyclization. However, an electron withdrawing group on the other aromatic ring, could slow down the cyclization step leading to a partial accumulation of the nitroso intermediate and thus to the possible formation of side products. However, this effect is not observed with the other substrates and this is most likely because the reaction is performed under relatively robust conditions and at complete conversions, thus differences in conversion could not be appreciated.

We continued to explore the applicability of our catalytic system for the reductive cyclization of other substituted nitrobiphenyls focusing on obtaining carbazoles with significant pharmaceutical value. We were pleased to find out that carbazoles bearing strong electron donating group such as methoxy group can be obtained in a very good yield (compound **81**, entry 7, Table 14). Clausine V **86**, a common anti-HIV drug bearing two methoxy groups was prepared in 86% yield (entry 12, Table 14).

The position of the substituent on the nitrobiphenyl did not have a major effect on the yield of the product. For instance, nitrobiphenyls bearing methyl group on *o*-, *m*-, or *p*- position with respect to the C-C bond between the two phenyl rings were all well tolerated affording methylcarbazole in 85%, 99%, 97% yield, respectively (entries 10, 11, 6, Table 14, respectively).

The reductive cyclization of 3'-methyl-2-nitrobiphenyl (entry 11, Table 14) afforded two isomers with a ratio of 1.85:1 that was identified through GC analysis before the chromatographic separation. Unfortunately, only the major isomer could be separated in a pure form the column (see experimental part). The ^1H NMR spectrum of the major fraction corresponds to 1-methylcarbazole indicating that the cyclization is favoured on the *ortho*-position with respect to the methyl group.

Halogenated carbazoles were also prepared in very good yields (entries 13-16, Table 14). The lower yields in case of bromide substituent (entries 15, 16, Table 14) can be attributed to an activation of C-Br bond by palladium catalyst resulting in side-reactions that decreases the selectivity in the required product. This also explain why the yield of the dibromocarbazole **90** is lower than the mono-bromocarbazole **89**. However, the yield of dibromocarbazole **90** which is a valuable precursor for phosphorescent devices^[140-142] is still satisfactory (63%, entry 16, Table 14). Carbazoles bearing acetyl group and benzoyl group were also prepared in very good yields (entries 17 and 18, respectively, Table 14).

Revising the literature reporting biologically valuable carbazoles and their structure activity relationship (SAR),^[143] it can be clearly noted that substituents such as COOMe, COOH, OH, OMe, and CHO impart some biological activity to the carbazole scaffold (see Figure 2). The aldehyde group was well tolerated with a yield of 92% (entries 5, 9 in Table 14). The reductive cyclization of 4-carbomethoxy-2-nitrobiphenyl proceeded smoothly affording the corresponding carbazole in 93% yield (entry 19, Table 14). On the other hand, 2-nitrobiphenyl-4-carboxylic acid afforded the corresponding carbazole only in a poor yield (20%, entry 20, Table 14). Taking into account that some of the product may be present as a sodium salt, the reaction mixture was acidified before the chromatographic separation, however the main loss of the product is probably due to the fact that the COOH group may cling to the OH groups of the silica causing the product to not elute entirely. A more convenient pathway to obtain carbazole-2-carboxylic acid **94** is the hydrolysis of 2-carbomethoxycarbazole **93** that proceed smoothly with a 95% yield. Moreover, 2-hydroxycarbazole **95** was synthesized in 77% yield (entry 21, Table 14) which offer the possibility of further functionalization of the hydroxyl group. It is also worth mentioning that reductive cyclization of hydroxy-2-nitrobiphenyl was reported to be either very difficult reaction^[144-145] or to not work at all.^[102]

We were pleased to obtain the 2-aminocarbazole **96** in a very good yield of 83% (entry 22, Table 14) which contradicts our previous expectation regarding the effect of such a strongly electron donating substituent on the reductive cyclization of nitroarenes. At this stage, it became clear to us that the reductive cyclization of 2-nitrobiphenyl follows a different mechanism from that of 2-nitrostyrenes. The relative rates of the steps in the catalytic cycle of the reaction are clearly different and most probably the higher stability of the intermediate makes the cyclization step acquire more importance on the overall rate of the reaction.

Reductive cyclization of 4-cyano-2-nitrobiphenyl affords the corresponding carbazole **97** in only 66% yield (entry 23, Table 14). From previous experiences on this kind of reactions, the reductive cyclization of nitroarenes bearing nitrile group is usually complicated by side product formation thus the result in this case is still surprisingly good.

The biologically important natural alkaloid α -carboline **98** was synthesized in 74% yield (entry 24, Table 14). However, the reductive cyclization of 3-nitro-2-phenylpyridine **69** and 2-(2-nitrophenyl)pyridine **73** proceeded in poor yields (entries 25 and 26, respectively, Table 14). When the reaction was applied to 2-(2-nitrophenyl)thiophene (entry 27, Table 14) under optimized condition, unconverted substrate was recovered. Repeating the reaction with higher catalyst loading (2 mol%) and prolonging the time to 16 hours resulted in formation of the product **100** in 27% yield, although the conversion was still not complete. As mentioned above, in a recent article our group reported that 4,7-dimethoxy-1,10-phenanthroline had a strong positive effect on the reductive cyclization of 2- and 3-(2-nitrovinyl)-thiophenes to thienopyrroles^[14] which somewhat resembles the reductive cyclization of 2-(2-nitrophenyl)thiophene. Thus, we decided to test the use of 4,7-dimethoxy-1,10-phenanthroline for that reaction obtaining an increased yield of 35%. This improvement suggests that further optimization of the reaction may enhance the yields of those carbazoles with an extra heteroatom that proved to be problematic substrates. The low yield in those cases indicate that either the reduction of the nitro group is more difficult or that the formed intermediate is highly stable.

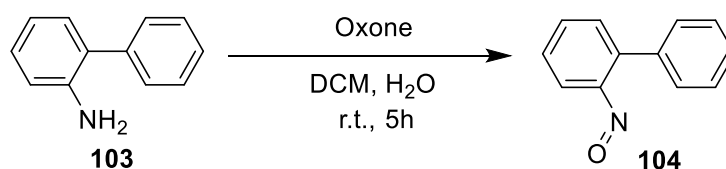
A carbazole with an extra fused aromatic ring was also obtained in an excellent yield (98%, entry 28, Table 14). An initial test on the possibility of performing a double reductive cyclization of 2,3-dinitro-1,1'-terphenyl (entry 29, Table 14) succeeded affording the double cyclized product in 20 % yield. Considering the challenging nature of the substrate structure with two adjacent NO₂ groups which sterically hinder the reaction and the fact that the catalyst and ligand amounts were not doubled, that initial result is quite promising and clearly there is room for improvement in the near future.

2.4. Kinetic study of the thermal cyclization of 2-nitrosobiphenyl.

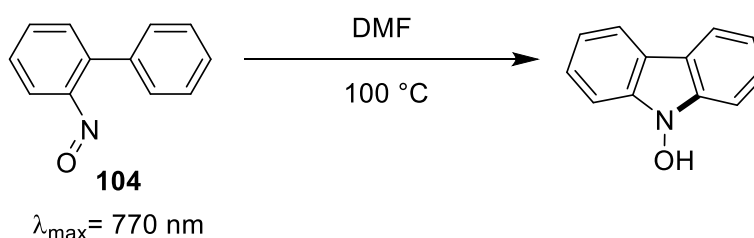
Owing to the indirect evidence found during the optimization indicating that the cyclization of *o*-nitrosobiphenyl intermediates is a determinant step in the reductive cyclization of *o*-nitrobiphenyls, a deeper study on the thermal cyclization of *o*-nitrosobiphenyl **104** in DMF was started. Surprisingly, studies on this reaction have not been reported so far in the literature although 2-nitrosobiphenyl is a bench-stable compound. First, *o*-nitrosobiphenyl **104** was prepared through selective oxidation of *o*-aminobiphenyl **103** using Oxone (KHSO₅. ½ KHSO₄. ½ K₂SO₄) as the oxidizing agent (**Scheme 32**).

A kinetic study of the thermal cyclization of 2-nitrosobiphenyl **104** in DMF at 100 °C was performed. The progress of the reaction was followed by UV spectroscopy (**Scheme 33**) since 2-nitrosobiphenyl has a strong absorption band at 770 nm. The cyclization reaction was found to be first order in *o*-nitrosobiphenyl (**Figure 3**). When a base is added, in this case triethylamine, the rate of the reaction is also first order in the base, with a non-zero intercept, up to a point (10 equiv. with respect to nitrosobiphenyl) where a plateau is reached (**Figure 4**). The effect of inorganic bases on the rate of the reaction could not be studied due to their low solubility in organic solvents at 100 °C which will not ensure the accuracy of the reported concentrations and will complicate the recording of the UV spectra. The results obtained using triethylamine anyway indicate that the role of the base is not confined to the activation of phenylformate. The base is also involved in the cyclization step and accelerates it. A previous theoretical studies on the cyclization reaction reported by Davies^[146] propose that a reversible 1,5-hydrogen migration is involved in the 1,5-electrocyclization of nitrosobiphenyl. We thus propose

that this H-migration is indeed facilitated by bases and shifting the reversible process towards N-oxygenated intermediate that, under catalytic conditions in the presence of Pd and CO, is irreversibly reduced to carbazole (Scheme 34).



Scheme 32. Synthesis of 2-nitrosobiphenyl.



Scheme 33. Uncatalyzed cyclization of 2-nitrosobiphenyl.

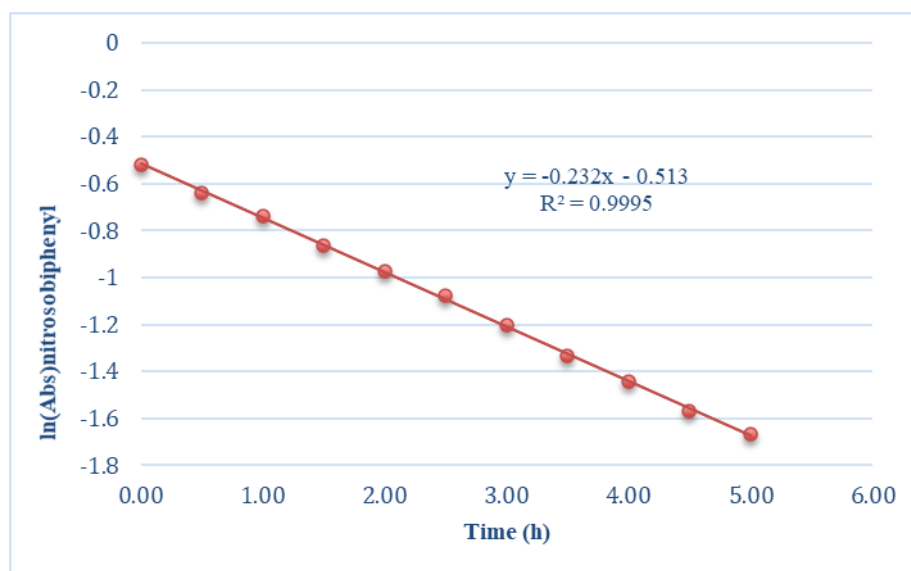


Figure 3. linear relation between ln (Abs) and time. 2-nitrosobiphenyl (conc. 2mg/mL, 0.055 mmol, 10 mg), DMF (5 mL), 100 °C, absorbance was recorded by UV-spectroscopy at 770 nm.

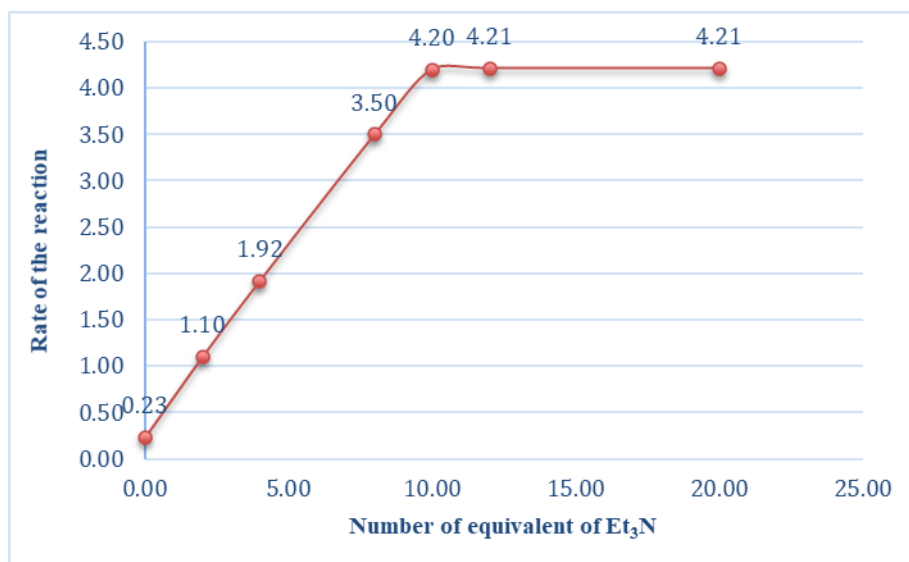
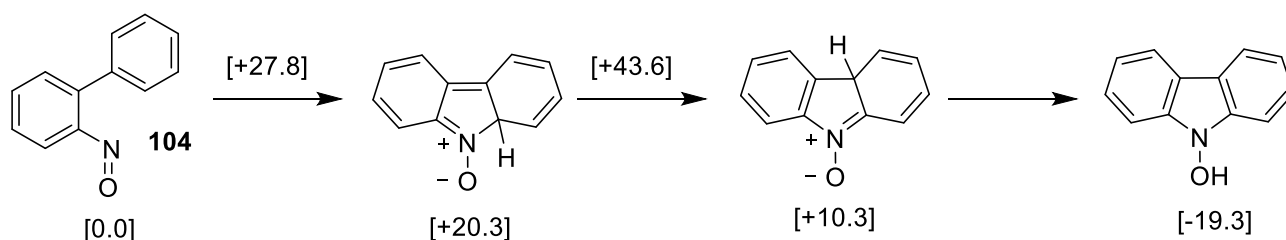


Figure 4. Effect of Et₃N on rate of the reaction. 2-nitrosobiphenyl (conc. 2mg/mL, 0.055 mmol, 10 mg), appropriate amount of the base with respect to 2-nitrosobiphenyl was added, DMF (5 mL), 100 °C, absorbance was recorded by UV-spectroscopy at 770 nm.



Scheme 34. B3LYP/6-31+G*-optimized geometries and energies for the 1,5-electrocyclization of 2-nitrosobiphenyl. Energies are given in kcal/mol relative to reactants.

3. Conclusions.

In conclusion, we have developed a highly stable protocol for carbazole synthesis (**Scheme 26**) that can tolerate both air and moisture and can be performed using commercial DMF without distilling it. Strength of the protocol is that it avoids handling pressurized CO lines since the reaction employs phenyl formate as a CO surrogate which enable the synthetic chemist to perform the reaction in a pressure tube, a cheap and readily available tool for any laboratory. Moreover, the reported catalytic system can tolerate a wide range of substituents, including both electron donating and electron withdrawing groups regardless of their position on the substrate. The practical value of the method was demonstrated by synthesizing several carbazoles with pharmaceutical or thermo/electrical applications in good to excellent yields. Besides the robustness and stability of our procedure, the reaction can also be easily scaled-up affording carbazole in a very good yield (85%) even under more challenging conditions and using a work-up that did not involve column chromatography, making our procedure even more accessible, valuable for preparative purposes and economically advantageous.

4. Experimental work.

4.1. General consideration.

Unless otherwise stated, all reactions and manipulations were performed under a dinitrogen atmosphere using standard Schlenk apparatus. All glassware and magnetic stirring bars were kept in an oven at 120 °C for at least two hours and let to cool under vacuum before use. Solvents were dried and distilled by standard procedures and stored under dinitrogen atmosphere. Et₃N and DBU were distilled from CaH₂. Inorganic bases were dried by heating at 180 °C for 8 h under vacuum, then left to cool down under vacuum and were stored under dinitrogen. They were weighed in the air but stored under dinitrogen atmosphere to avoid water uptake. Phenyl formate was prepared following a procedure reported in the literature (see below). Deuterated solvents were purchased by Sigma-Aldrich: DMSO-*d*₆ (commercially available in 0.75 mL vials under dinitrogen atmosphere) was used as purchased while CDCl₃ was filtered on basic alumina, degassed with three freeze-pump-thaw cycles, and stored under dinitrogen over 4 Å molecular sieves. 1,10-Phenanthroline (Phen) was purchased as hydrate (Sigma-Aldrich). Before use, it was dissolved in CH₂Cl₂, dried over Na₂SO₄ followed by filtration under dinitrogen atmosphere and evaporation of the solvent in vacuum. Phen was weighed in the air but stored under dinitrogen atmosphere to avoid water uptake. All the palladium precursors employed in this work were prepared starting from commercially available PdCl₂ (see below). Unless otherwise stated commercially available reagents were used as received.

4.2. General analysis methods.

¹H-NMR and ¹³C-NMR spectra were recorded at frequencies of 300 or 400 MHz for the proton and 75 or 101 MHz for the carbon on Bruker Avance 300/400 spectrometers. Chemical shifts are reported in ppm relative to TMS; the data are reported as follows: proton multiplicities (s=singlet, d=doublet, t=triplet, q=quartet, dd= doublet of doublet, td= triplet of doublet, ddd= doublet of doublet of doublet, m=multiplet and br.=broad), coupling constants and integration.

Elemental analyses were performed on a Perkin Elmer 2400 CHN elemental analyser.

GC quantitative analyses were performed on a DANI 86.10 gas chromatograph equipped with a FID detector using a SUPELCO Analytical SLBTM-5ms column (Fused Silica Capillary Column 30 m x 0.32 mm x 0.5 µm film thickness). A standard analysis involves the preparation of a sample solution in CH₂Cl₂ of conc. 0.1 mg/mL calculated with respect to the amount of biphenyl used as an internal standard. A complete list of the instrumental parameters employed is showed in Table 15. A calibration curve was made using biphenyl as the internal standard. The compounds used as standards were obtained as follow: aminobiphenyl **103** was prepared as previously reported^[147] (see below), carbazole was recrystallized from ethanol, and commercial *o*-nitrobiphenyl was purchased from Fluorochem and used without further purification. The purity of all the standards used for calibration was checked by ¹HNMR and elemental analysis.

Table 15. Instrumental parameters for Gas-chromatographic analyses for **DANI 86.10 HT.**^(a)

COLUMN PROGRAM		
rate (°C/min)	temperature (°C)	time (min)
-	60	6
20	120	1
7	160	0
15	270	20.34

INJECTOR PROGRAM		
rate (°C/min)	temperature(°C)	time (min)
-	50	0
700	120	0
200	275	42

(a) Injection volume: **1.0 µL**, carrier gas: **He**, carrier gas pressure: **1.2 bar**, air pressure at the detector: **0.7 bar**, hydrogen pressure at the detector: **0.7 bar**, auxiliary gas: **N₂**, auxiliary gas pressure: **1.3 bar**, detector temperature: **300 °C**, total time= **43.02 min**.

4.3. Kinetic studies:

Kinetic studies of the thermal cyclization reaction of 2-nitrosobiphenyl **104** were performed following the reactant conversion by UV spectrophotometry. The absorbance was recorded on a single beam UV-visible spectrophotometer at 770 nm (the λ_{max} of 2-nitrosobiphenyl). Reactions were performed under N₂ in a Schlenk glassware consisting of a 10 mL chamber connected to a glass cuvette, so that the progress of the reaction can be followed without the need to transfer the reaction content into an external cuvette. Before starting the reaction, 5 mL of DMF was added into the apparatus under nitrogen and the blank was recorded. The solvent was then discarded, and the apparatus was cleaned. Then, 1 ml of 2-nitrosobiphenyl stock solution was added using a pipette (10 mg, 0.055 mmol, prepared by dissolving 100 mg of 2-nitrosobiphenyl in 10 mL DMF). In case of reactions carried out in presence of Et₃N, the appropriate amount of the base with respect to 2-nitrosobiphenyl was added at this stage. DMF was added to reach an overall volume of 5 mL and then the first absorbance at time=0 was recorded. After that the reaction was heated at 100 °C by immersing the 10 mL chamber of the glassware in a preheated oil bath. The absorbance was recorded at selected time interval after fast cooling of the reaction mixture in a water bath.

4.4. General protocol for optimization trials conducted in a pressure tube.

The reaction was performed under dinitrogen atmosphere placing the pressure tubes in a large mouth Schlenk tube. All the palladium catalysts were added to the reaction through stock solutions prepared

in the appropriate solvent. Every catalyst was weighed and stored in the air except for Pd(OAc)₂ that was stored under dinitrogen. All the solutions were prepared under dinitrogen atmosphere using distilled solvents. For catalytic runs that required an amount of Phen less than 10 mg, a stock solution was prepared to avoid large weighing errors.

In a typical catalytic reaction, the substrate was weighed in the air and placed in a heavy-wall glass pressure tube. Stock solutions of the catalysts and Phen were added. An amount of solvent required to reach a total volume of 10 mL was added and the reaction mixture was stirred for 10 min. Finally, phenyl formate and the base were added in this order. The pressure tube was plugged with a screw cap and immersed in a preheated oil bath at the appropriate temperature. At the end of the reaction, the pressure tube was lifted from the oil and let to cool to room temperature. Then, the screw cap was carefully removed, the excess of CO was vented, and the content were analyzed by GC or subjected to column chromatography. (Caution: evolution of dissolved CO from the solution may continue for some minutes, keep the tube under a hood).

4.5. Procedure for catalytic reactions conducted in an autoclave.

For entries 5-8 in Table 2, the method was adapted from Davies article.^[33]

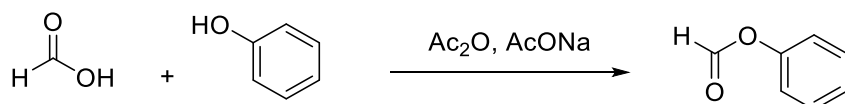
2-Nitrobiphenyl (117 mg, 0.589 mmol) was weighed in the air in a glass liner and then placed inside a Schlenk tube with a wide mouth under a dinitrogen atmosphere. Then a stock solution of the catalyst and ligand, prepared by dissolving Pd(OAc)₂ (80.0 mg, 0.356 mmol, 2 mol%) and 1,10-phenanthroline (128 mg, 0.710 mmol, 5mol%) in DMF (50 mL), and DMF (3.35 mL) were added. When specified in the footnote to the tables, additives (phenol and Et₃N) were added at this stage. The liner was closed with a screw cap having a glass wool-filled open mouth which allows gaseous reagents to exchange. The Schlenk tube was immersed in liquid nitrogen until the solvent froze and evacuated and filled with dinitrogen three times. The liner was rapidly transferred to a 200 mL stainless steel autoclave and this was then evacuated and filled with dinitrogen three times. The system was pressurized with CO (6 bar) and subsequently immersed in a pre-heated oil bath at 140 °C for 16 h. At the end of the reaction, the autoclave was quickly cooled with an ice bath and vented. The reagent conversion and product selectivity were measured by gas chromatography using biphenyl as the internal standard.

4.6. Procedure for a 15-fold large scale synthesis of carbazole 79.

In a 250 mL Fisher-Porter bottle 2-nitrobiphenyl (1.614 g, 8.1 mmol), Phen (73 mg, 0.405 mmol, 5 mol%), Na₂[PdCl₄] (23.8 mg, 0.081 mmol, 1 mol%) and DMF (50 mL) were added in the air and the reaction was stirred for 10 min at rt. Phenyl formate (3.9 mL, 35.64 mmol, 4.4 equiv.) and Na₃PO₄ (179.5 mg, 1.095 mmol, 0.135 equiv.) were added. The bottle was closed and transferred to an oil bath preheated at 170 °C. The reaction mixture was heated with continuous stirring for 16 hours. Then the reactor was lifted from the oil bath and allowed to cool to room temperature. The reaction was filtered to remove Pd-black, then poured into water (100 mL) containing 1 mL of HCl (to get rid of Phen and

any amine impurity), a precipitate formed. The reaction mixture was filtered, and the precipitate was washed with aq. NaHCO_3 solution to get rid of phenol. The solid was then dissolved in CH_2Cl_2 (30 mL), dried over Na_2SO_4 . After filtration, evaporation of the solvent under reduced pressure afforded the pure carbazole **79** (1.15 g, 85%).

4.7. Preparation of phenyl formate.



The synthesis was performed following a procedure reported in the literature.^[148]

Under a dinitrogen atmosphere, formic acid (38 mL, 1 mol) was added to acetic anhydride (76 mL, 0.8 mol) in a 250 mL Schlenk flask. The mixture was stirred at 60 °C for 1 h and then let to cool to room temperature. This mixture was transferred using a cannula into a 500 mL flask containing phenol (18.8 g, 200 mmol) and sodium acetate (16.4 g, 200 mmol) keeping the flask into a water/ice cooling bath during the addition. (Attention: the reaction is rather exothermic.) The reaction was stirred for 3 h at room temperature and then diluted with toluene (150 mL). The solution was washed with water (3×100 mL) and the organic phase was dried over MgSO_4 . After filtration, evaporation of toluene under reduced pressure at room temperature afforded phenyl formate as a pale-yellow liquid (yield 65%).

Figure 5: ^1H NMR (400 MHz, CDCl_3) δ 8.33 (s, 1H), 7.47 - 7.41 (m, 2H), 7.30 (t, $J = 7.5$ Hz, 1H), 7.18 ppm (m, 2H). **Figure 6:** ^{13}C NMR (101 MHz, CDCl_3) δ 159.33, 149.98, 129.73, 126.39, 121.16 ppm.

4.8. Synthesis of palladium catalysts.

a) Synthesis of $\text{Pd}(\text{CH}_3\text{CN})_2\text{Cl}_2$.

The synthesis was performed following a procedure reported in the literature.^[149]

PdCl_2 (1.011 g, 5.70 mmol) was suspended into 70 mL of CH_3CN and refluxed for 2 h. In order to remove undissolved material, the hot reaction mixture was filtered through filtering paper by using a Teflon cannula. The solution was cooled to 0 °C to promote the precipitation of the desired complex. The so-formed orange-yellow solid was filtered through a Buchner funnel. (1.470 g, 99.5 % yield).

Elemental analysis for $\text{C}_4\text{H}_6\text{Cl}_2\text{N}_2\text{Pd}$. Calc.: C 18.52; H 2.33; N 10.80. Found: C 18.80; H 2.28; N 10.80.

b) Synthesis of $\text{Pd}(\text{OAc})_2$.

The synthesis was performed following a procedure reported in the literature.^[150]

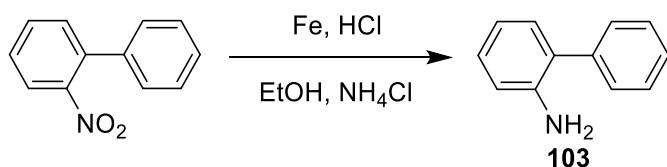
PdCl₂ (1 g, 5.72 mmol) was suspended into 100 mL of water. HCOONa (1.6 g, 23.4 mmol) and NaOH (2 g, 50 mmol) were subsequently added. After 30 min metallic Pd in the form of finely divided powder appeared. Water was removed and the obtained solid washed with water (3 × 30 mL). The solid was suspended in 40 mL of glacial acetic acid and 0.6 mL of concentrated nitric acid was slowly added under stirring. The mixture was refluxed for 30 min while nitrogen was bubbled inside the reaction solution to remove NO₂ from the reaction mixture. The volume of the reaction mixture was reduced to one third using gentle heating. After allowing to cool to room temperature an orange powder precipitated. It was collected by filtration on a Buchner funnel affording the desired compound (0.86 g, 86 % yield).

Elemental analysis for C₄H₆O₄Pd. Calc.: C 21.40; H 2.69. Found: C 21.54; H 2.67.

c) Synthesis of Na₂[PdCl₄]

The synthesis was adapted from a synthetic procedure for Li₂[PdCl₄] reported in the literature.^[151] PdCl₂ (0.50 g, 2.8 mmol) was suspended in distilled water (3 mL) and NaCl (0.33 g, 5.6 mmol) was added. The reaction was heated at 70 °C for 1 h until complete dissolution of PdCl₂. The obtained brown-red solution was allowed to cool to room temperature and filtered on filter paper by canula. Water was then evaporated under vacuum affording a brown solid that was smashed into powder and kept under vacuum at 80 °C for 8 h (until constant weight).

4.9. Preparation of *o*-aminobiphenyl (103)^[152]



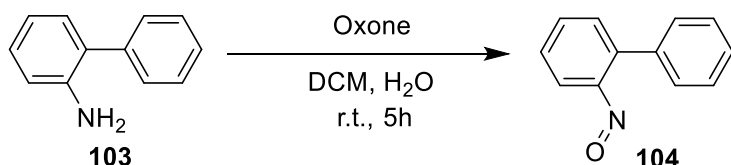
The synthesis was performed following the general procedure reported in the literature.^[147]

In a 2-necked 250 mL round-bottomed flask was charged with ethanol (40 mL). Iron powder (7 g, 125 mmol) was added in portions under efficient stirring, followed by concentrated HCl (1.1 mL, 12.5 mmol). The suspension was stirred at 65 °C for 2 h and was then cooled to 55 – 60 °C over a period of 10 min. Then 25% aqueous ammonium chloride solution (20 mL) was added. *o*-Nitrobiphenyl (4.98 g, 25 mmol) was added in portions (exothermic) while maintaining the internal temperature at 65 – 80 °C. The reaction mixture was stirred at 55–65 °C for an additional 3 h and was then cooled to 40 °C. Ethanol (50 mL) and Celite (10 g) were added subsequently. The reaction mixture was filtered over a pad of Celite (10 g) with suction. The filter cake was washed with EtOH (100 mL), and the filtrate was concentrated under reduced pressure. To the residue, ethyl acetate (60 mL) and saturated aqueous NaHCO₃ (25 mL) were added. The biphasic mixture was stirred at 20–25 °C, and the organic layer was separated. The organic layer was washed with brine (2×30 mL) and dried over sodium sulfate. The solvent was removed under reduced pressure to afford the product as a light brown solid (3.24 g, 65 % yield). The product was analytically pure and was used without further purification.

Figure 7: ^1H NMR (400 MHz, CDCl_3) δ 7.52 -7.42 (m, 4H), 7.41 - 7.32 (m, 1H), 7.23 - 7.10 (m, 2H), 6.86 (t, $J = 7.4$ Hz, 1H), 6.80 (d, $J = 7.9$ Hz, 1H), 3.83 ppm (br. s, 2H). **Figure 8:** ^{13}C NMR (101 MHz, CDCl_3) δ 143.35, 139.55, 130.58, 129.21, 128.93, 128.61, 127.88, 127.30, 118.93, 115.85.

Elemental analysis for $\text{C}_{12}\text{H}_{11}\text{N}$. Calc.: C 85.17; H 6.55; N 8.28. Found: C 84.80; H 6.66; N 8.18.

4.10. Preparation of *o*-nitrosobiphenyl (104)^[153]



The synthesis was performed following the general procedure reported in the literature.^[154]

In a 250 mL Schlenk flask, *o*-aminobiphenyl (1.7 g, 10 mmole) was dissolved in CH_2Cl_2 (15 mL). To this solution, Oxone (KHSO_5 , $\frac{1}{2}$ KHSO_4 , $\frac{1}{2}$ K_2SO_4 - 12.3 g, 40 mmole, 4 equiv.) and 65 mL of water were added. The reaction was stirred under dinitrogen at room temperature and the progress of the reaction was followed by TLC until completion (5h). At the end of the reaction, the two layers were separated, and the aqueous layer was extracted with CH_2Cl_2 (2×50 mL), the combined organic layers were washed with 1 N HCl (2×50 mL), saturated NaHCO_3 solution (2×50 mL), water (2×50 mL), brine (2×50 mL) and dried over MgSO_4 . Then, it was filtered, the solvent was evaporated under reduced pressure. The compound was further purified by recrystallization from ethanol affording the pure product as white crystals (1.185 g, 56% yield). The NMR was concentration dependent due to dimerization of 2-nitrosobiphenyl in solution.^[153] Thus, the sum of the signals of monomer and dimer are overlapped in the reported NMR spectra. A doublet at 5.61 is due to dimer while that at 6.24 is due to monomer (**Figure 9**).

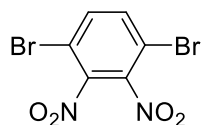
Figure 9: ^1H NMR (400 MHz, $\text{DMSO}-d_6$) δ 8.00 - 7.84 (m), 7.72 - 7.39 (m), 7.34 (d, $J = 6.7$ Hz), 7.17 (dd, $J = 6.0, 2.7$ Hz), 7.06 (t, $J = 8.2$ Hz), 6.90 (d, $J = 7.9$ Hz), 6.24 (d, $J = 8.0$ Hz), 5.61 ppm (d, $J = 7.8$ Hz). **Figure 10:** ^{13}C NMR (101 MHz, $\text{DMSO}-d_6$) ^{13}C NMR (101 MHz, $\text{DMSO}-d_6$) δ 163.45, 145.56, 139.90, 139.38, 137.03, 136.78, 136.56, 136.41, 135.86, 134.73, 132.44, 131.92, 131.62, 131.36, 130.53, 129.90, 129.22, 129.17, 128.91, 128.57, 128.42, 128.34, 128.28, 128.14, 127.97, 127.76, 125.10, 123.54, 105.63 ppm.

Elemental analysis for $\text{C}_{12}\text{H}_9\text{NO}$. Calc.: C 78.67; H 4.95; N 7.65. Found: C 78.98; H 5.0; N 7.80.

4.11. Preparation of 2-nitrobiaryls through Suzuki-Miyaura cross-coupling.

All the 2-halonitrobenzenes and boronic acids employed in the Suzuki-Miyaura couplings were obtained from commercial sources. The only exception is 1,4-dibromo-2,3-dinitrobenzene whose synthesis is reported below.

1,4-dibromo-2,3-dinitrobenzene



A first attempt to get the double nitration of 1,4-dibromobenzene was performed in a 1:1 mixture of HNO₃ (65 wt %) and H₂SO₄ (96 wt %) at 95 °C for 5 h. However only mono-nitrated compound was recovered in almost quantitative yield.

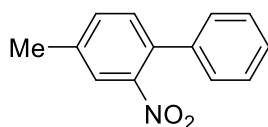
The 2-nitro-1,4-dibromobenzene obtained was thus nitrated following the indication of Hammond *et al.*^[155] In a 250 mL round bottom flask, 2-nitro-1,4-dibromobenzene (21.7 g, 77.2 mmol) and sodium nitrate (32.7 g, 385 mmol) were suspended in 100 mL H₂SO₄ (88 wt %) at 0°C. The flask was immediately immersed in a preheated oil-bath. The mixture was heated at 100 °C for five hours and then poured into crushed ice (~500 mL). The crude solid was collected by filtration on a Buchner funnel and thoroughly washed with water affording 22.4 g of a yellow solid mainly containing the three isomers: 2,3-, 2,5- and 2,6-dinitro-1,4-dibromobenzene. The three isomers can be separated following the procedure reported by Sunde *et al.*^[156] In particular, 3 g (9.3 mmol) of crystalline pale yellow 2,3-dinitro-1,4-bromobenzene were isolated by recrystallizing the crude from acetic acid (29 mL). Yield 12 %. **Figure 11:** ¹H NMR (400 MHz, CDCl₃) δ 7.75 ppm (s, 2H). **Figure 12:** ¹³C NMR (101 MHz, CDCl₃) δ 182.95, 136.99, 114.47 ppm.

Elemental analysis for C₆H₂Br₂N₂O₂. Calc.: C 22.11; H 0.62; N 8.60. Found: C 21.83; H 0.70; N 8.33.

General procedure for synthesis of 2-nitrobiphenyls through Suzuki-Miyaura cross-coupling.^[102]

In a 50 mL 2-neck flask, a mixture of the desired 2-halonitrobenzene (5 mmol), boronic acid (5.5 mmol, 1.1 equiv.), K₂CO₃ (1.38 g, 10 mmol, 2 equiv.) and Pd(PPh₃)₄ (58 mg, 0.05 mmol, 1 mol%) were added under nitrogen. The flask was then evacuated and filled with dinitrogen three times. Water (5 mL) and toluene (8 mL) were added then the flask was closed and heated to reflux. The reaction was followed by TLC and upon complete consumption of the starting material (2-24 h), the reaction was cooled, filtered over a pad of celite, and washed with Et₂O (50 mL). The organic mixture was washed with H₂O (2 × 50 mL) and brine, dried over MgSO₄, and concentrated *in vacuo*. Column chromatography of the residue (hexane: ethyl acetate) gave the pure product.

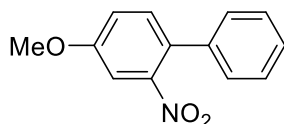
4-Methyl-2-nitrobiphenyl (50)^[33]



Prepared according to general synthesis from 4-bromo-3-nitrotoluene (1.08 g, 5 mmol) and phenylboronic acid (0.67 g, 5.5 mmol). Column chromatography (95:5 hexane: EtOAc) gave the product as a yellow oil (1.013 g, 95% yield). **Figure 13:** ^1H NMR (400 MHz, CDCl_3) δ 7.67 (s, 1H), 7.46 -7.37 (m, 4H), 7.34 -7.30 (m, 3H), 2.47 ppm (s, 3H). **Figure 14:** ^{13}C NMR (101 MHz, CDCl_3) δ 149.26, 138.80, 137.56, 133.61, 133.13, 131.85, 128.74, 128.12, 128.06, 124.49, 20.96 ppm.

Elemental analysis for $\text{C}_{13}\text{H}_{11}\text{NO}_2$. Calc.: C 73.23; H 5.20; N 6.57. Found: C 72.95; H 5.42; N 6.90.

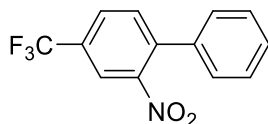
4-Methoxy-2-nitrobiphenyl (51)^[102]



Prepared according to general synthesis from 4-bromo-3-nitroanisole (1.16 g, 5 mmol) and phenylboronic acid (0.67 g, 5.5 mmol). Column chromatography (95:5 hexane: EtOAc) gave the product as a yellow solid (1.10 g, 96% yield). **Figure 15:** ^1H NMR (400 MHz, CDCl_3) δ 7.44 -7.32 (m, 5H), 7.31-7.21 (m, 2H), 7.15 (dd, $J = 8.6, 2.6$ Hz, 1H), 3.90 ppm (s, 3H). **Figure 16:** ^{13}C NMR (101 MHz, CDCl_3) δ 159.28, 149.84, 137.46, 132.94, 128.84, 128.77, 128.19, 128.00, 118.83, 109.18, 56.08 ppm.

Elemental analysis for $\text{C}_{13}\text{H}_{11}\text{NO}_3$. Calc.: C 68.11; H 4.84; N 6.11. Found: C 68.41; H 5.04; N 6.27.

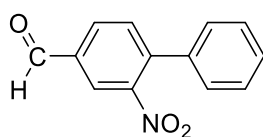
4-Trifluoromethyl-2-nitrobiphenyl (52)^[102]



Prepared according to general synthesis from 4-bromo-3-nitrobenzotrifluoride (1.35 g, 5 mmol) and phenylboronic acid (0.67 g, 5.5 mmol). Column chromatography (90:10 hexane: EtOAc) gave the product as a yellow solid (1.1 g, 82% yield). **Figure 17:** ^1H NMR (300 MHz, CDCl_3) δ 8.13 (s, 1H), 7.88 (d, $J = 8.0$ Hz, 1H), 7.62 (d, $J = 8.0$ Hz, 1H), 7.52 -7.39 (m, 3H), 7.38 -7.27 ppm (m, 2H). **Figure 18:** ^{13}C NMR (75 MHz, CDCl_3) δ 149.30, 139.95, 136.09, 133.01, 130.92 (q, $J = 34.5$ Hz), 129.17, 129.09, 128.93 (q, $J = 3.3$ Hz), 127.89, 123.00 (q, $J = 271.5$), 121.60 (q, $J = 3.7$ Hz) ppm. **Figure 19:** ^{19}F (376 MHz, CDCl_3) δ -62.72 ppm (s, 3F).

Elemental analysis for $\text{C}_{13}\text{H}_8\text{F}_3\text{NO}_2$. Calc.: C 58.44; H 3.02; N 5.24. Found: C 58.41; H 3.20; N 5.30.

4-Formyl-2-nitrobiphenyl (53)^[102]

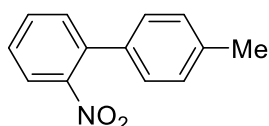


Prepared according to general synthesis from 4-chloro-3-nitrobenzaldehyde (0.928 g, 5 mmol) and phenylboronic acid (0.67 g, 5.5 mmol). Column chromatography (40:60 hexane: EtOAc) gave the

product as a yellow solid (1.01 g, 89% yield). **Figure 20:** ^1H NMR (300 MHz, CDCl_3) δ 10.10 (s, 1H), 8.33 (d, $J = 1.5$ Hz, 1H), 8.12 (dd, $J = 7.9, 1.6$ Hz, 1H), 7.65 (d, $J = 7.9$ Hz, 1H), 7.51-7.40 (m, 3H), 7.40-7.28 ppm (m, 2H). **Figure 21:** ^{13}C NMR (75 MHz, CDCl_3) δ 189.55, 149.92, 141.76, 136.26, 136.07, 133.10, 132.35, 129.27, 129.07, 127.84, 125.19 ppm.

Elemental analysis for $\text{C}_{13}\text{H}_9\text{NO}_3$. Calc.: C 68.72; H 3.99; N 6.16. Found: C 68.77; H 4.31; N 6.25.

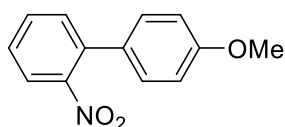
4'-Methyl-2-nitrobiphenyl (54)^[157]



Prepared according to general synthesis from 1-bromo-2-nitrobenzene (1.01 g, 5 mmol) and 4-tolylboronic acid (0.75 g, 5.5 mmol). Column chromatography (90:10 hexane: EtOAc) gave the product as a yellow oil (0.992 g, 93% yield). **Figure 22:** ^1H NMR (400 MHz, CDCl_3) δ 7.83 (d, $J = 8.1$ Hz, 1H), 7.61 (td, $J = 7.6, 1.3$ Hz, 1H), 7.51 -7.40 (m, 2H), 7.29 - 7.19 (m, 4H), 2.42 ppm (s, 3H). **Figure 23:** ^{13}C NMR (101 MHz, CDCl_3) δ 149.49, 138.24, 136.33, 134.49, 132.28, 132.01, 129.54, 128.01, 127.84, 124.08, 21.31 ppm.

Elemental analysis for $\text{C}_{13}\text{H}_{11}\text{NO}_2$. Calc.: C 73.23; H 5.20; N 6.57. Found: C 73.08; H 5.12; N 6.49.

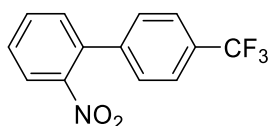
4'-Methoxy-2-nitrobiphenyl (55)^[158]



Prepared according to general synthesis from 1-bromo-2-nitrobenzene (1.01 g, 5 mmol) and 4-methoxyphenylboronic acid (0.835 g, 5.5 mmol). Column chromatography (90:10 hexane: EtOAc) gave the product as a yellow solid (1.112 g, 97% yield). **Figure 24:** ^1H NMR (400 MHz, CDCl_3) δ 7.80 (d, $J = 8.4$ Hz, 1H), 7.59 (t, $J = 8.2$ Hz, 1H), 7.44 (t, $J = 7.5$ Hz, 2H), 7.26 (d, $J = 8.8$ Hz, 2H), 6.96 (d, $J = 8.8$ Hz, 2H), 3.84 ppm (s, 3H). **Figure 25:** ^{13}C NMR (101 MHz, CDCl_3) δ 159.82, 149.54, 135.97, 132.26, 132.04, 129.61, 129.25, 127.85, 124.12, 114.34, 55.42 ppm.

Elemental analysis for $\text{C}_{13}\text{H}_{11}\text{NO}_3$. Calc.: C 68.11; H 4.84; N 6.11. Found: C 67.76; H 4.99; N 6.20.

4'-Trifluoromethyl-2-nitrobiphenyl (56)^[158]

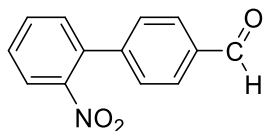


Prepared according to general synthesis from 1-bromo-2-nitrobenzene (1.01 g, 5 mmol) and 4-(trifluoromethyl)phenylboronic acid (1.045 g, 5.5 mmol). Column chromatography (90:10 hexane: EtOAc) gave the product as a yellow solid (1.21 g, 90% yield). **Figure 26:** ^1H NMR (400 MHz, CDCl_3) δ 7.95 (dd, $J = 8.1, 1.1$ Hz, 1H), 7.75 - 7.61 (m, 3H), 7.56 (td, $J = 7.9, 1.4$ Hz, 1H), 7.50 - 7.36 ppm (m, 3H). **Figure 27:** ^{13}C NMR (101 MHz, CDCl_3) δ 149.00, 141.47,

135.24, 132.84, 131.94, 130.40 (q, $J = 33.3$ Hz), 129.14, 128.50, 125.70 (q, $J = 3.7$ Hz), 124.52, 124.18 (q, $J = 273.71$ Hz) ppm. **Figure 28:** ^{19}F NMR (376 MHz, CDCl_3) δ -62.55 (s, 3F) ppm.

Elemental analysis for $\text{C}_{13}\text{H}_8\text{F}_3\text{NO}_2$. Calc.: C 58.44; H 3.02; N 5.24. Found: C 58.33; H 3.15; N 5.22.

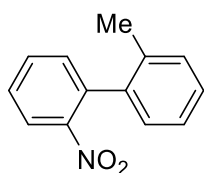
4'-Formyl-2-nitrobiphenyl (57)^[159]



Prepared according to general synthesis from 2-bromonitrobenzene (1.01 g, 5 mmol) and 4-formylboronic acid (0.83 g, 5.5 mmol). Column chromatography (90:10 hexane: EtOAc) gave the product as pale-yellow crystals (0.854 g, 75% yield). **Figure 29:** ^1H NMR (300 MHz, CDCl_3) δ 10.07 (s, 1H), 8.01 - 7.87 (m, 3H), 7.68 (td, $J = 7.5, 1.2$ Hz, 1H), 7.56 (td, $J = 7.9, 1.4$ Hz, 1H), 7.52 - 7.39 ppm (m, 3H). **Figure 30:** ^{13}C NMR (75 MHz, CDCl_3) δ 191.78, 149.98, 143.91, 136.02, 135.51, 132.86, 131.85, 130.09, 129.24, 128.84, 124.64 ppm.

Elemental analysis for $\text{C}_{13}\text{H}_9\text{NO}_3$. Calc.: C 68.72; H 3.99; N 6.16. Found: C 69.08; H 4.24; N 6.24.

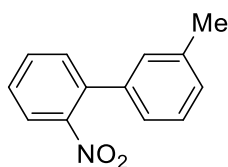
2'-Methyl-2-nitrobiphenyl (58)^[158, 160]



Prepared according to general synthesis from 2-bromonitrobenzene (1.01 g, 5 mmol) and 2-tolylboronic acid (0.75 g, 5.5 mmol). Column chromatography (95:05 hexane: EtOAc) gave the product as a yellow oil (1.002 g, 94% yield). **Figure 31:** ^1H NMR (400 MHz, CDCl_3) δ 8.00 (d, $J = 8.2$ Hz, 1H), 7.64 (td, $J = 7.5, 1.2$ Hz, 1H), 7.52 (t, $J = 8.5$ Hz, 1H), 7.38 - 7.18 (m, 4H), 7.10 (d, $J = 7.5$ Hz, 1H), 2.11 ppm (s, 3H). **Figure 32:** ^{13}C NMR (101 MHz, CDCl_3) δ 149.24, 137.58, 136.66, 135.74, 132.67, 132.31, 130.11, 128.40, 128.32, 125.88, 124.23, 20.01 ppm.

Elemental analysis for $\text{C}_{13}\text{H}_{11}\text{NO}_2$. Calc.: C 73.23; H 5.20; N 6.57. Found: C 73.12; H 5.36; N 6.53.

3'-Methyl-2-nitrobiphenyl (59)^[161]

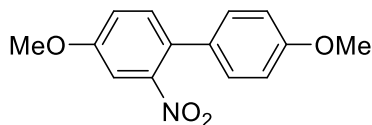


Prepared according to general synthesis from 2-bromonitrobenzene (1.01 g, 5 mmol) and 3-tolyl boronic acid (0.75 g, 5.5 mmol). Column chromatography (95:05 hexane: EtOAc) gave the product as a yellow oil (1.043 g, 98% yield). **Figure 33:** ^1H NMR (300 MHz, CDCl_3) δ 7.85 (dd, $J = 8.0, 0.8$ Hz, 1H), 7.61 (td, $J = 7.5, 1.3$ Hz, 1H), 7.53 - 7.39 (m, 2H), 7.33 (t, $J = 7.5$ Hz, 1H), 7.23 (d, $J = 7.6$ Hz,

1H), 7.14 (d, $J = 9.9$ Hz, 2H), 2.41 ppm (s, 3H). **Figure 34:** ^{13}C NMR (75 MHz, CDCl_3) δ 149.45, 138.47, 137.42, 136.53, 132.27, 132.03, 129.11, 128.66, 128.62, 128.12, 125.06, 124.07, 21.50 ppm.

Elemental analysis for $\text{C}_{13}\text{H}_{11}\text{NO}_2$. Calc.: C 73.23; H 5.20; N 6.57. Found: C 73.23; H 5.36; N 6.56.

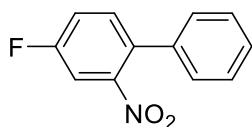
4,4'-Dimethoxy-2-nitrobiphenyl (60)^[158]



Prepared according to general synthesis from 4-bromo-3-nitroanisole (1.16 g, 5 mmol) and 4-methoxyphenylboronic acid (0.835 g, 5.5 mmol). Column chromatography (80:20 hexane: EtOAc) gave the product as a yellow solid (1.28 g, 99% yield). **Figure 35:** ^1H NMR (400 MHz, CDCl_3) δ 7.35-7.29 (m, 2H), 7.25 - 7.18 (m, 2H), 7.13 (dd, $J = 8.6, 2.7$ Hz, 1H), 6.97 - 6.89 (m, 2H), 3.88 (s, 3H), 3.83 ppm (s, 3H). **Figure 36:** ^{13}C NMR (101 MHz, CDCl_3) δ 159.43, 158.87, 149.73, 132.85, 129.50, 129.26, 128.24, 118.67, 114.19, 109.00, 55.96, 55.35 ppm.

Elemental analysis for $\text{C}_{14}\text{H}_{13}\text{NO}_4$. Calc.: C 64.86; H 5.05; N 5.40. Found: C 64.70; H 5.19; N 5.26.

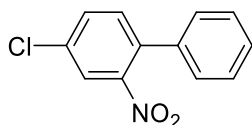
4-Fluoro-2-nitrobiphenyl (61)^[102, 162]



Prepared according to general synthesis from 2-bromo-5-fluoronitrobenzene (1.1 g, 5 mmol) and phenylboronic acid (0.67 g, 5.5 mmol). Column chromatography (90:10 hexane: EtOAc) gave the product as a yellow solid (0.76 g, 70% yield). **Figure 37:** ^1H NMR (300 MHz, CDCl_3) δ 7.61 (dd, $J = 8.0, 2.5$ Hz, 1H), 7.50 - 7.27 ppm (m, 7H). **Figure 38:** ^{13}C NMR (75 MHz, CDCl_3) δ 161.38 (d, $J = 249.75$ Hz), 149.53 (d, $J = 7.5$ Hz), 136.61, 133.62 (d, $J = 7.8$ Hz), 132.73 (d, $J = 3.57$ Hz), 128.90, 128.52, 128.09, 119.75 (d, $J = 21.0$ Hz), 111.93 (d, $J = 26.5$ Hz) ppm. **Figure 39:** ^{19}F NMR (376 MHz, CDCl_3) δ -111.25 (dd, $J = 13.2, 7.7$ Hz, 1F).

Elemental analysis for $\text{C}_{12}\text{H}_8\text{FNO}_2$. Calc.: C 66.36; H 3.71; N 6.45. Found: C 66.65; H 4.08; N 6.32.

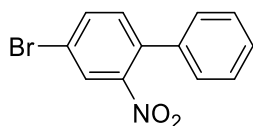
4-Chloro-2-nitrobiphenyl (62)^[159]



Prepared according to general synthesis from 2-bromo-5-chloronitrobenzene (1.18 g, 5 mmol) and phenylboronic acid (0.67 g, 5.5 mmol). Column chromatography (90:10 hexane: EtOAc) gave the product as a yellow oil that slowly crystallized (0.83 g, 71% yield). **Figure 40:** ^1H NMR (400 MHz, CDCl_3) δ 7.86 (d, $J = 2.1$ Hz, 1H), 7.60 (dd, $J = 8.3, 2.2$ Hz, 1H), 7.48 - 7.36 (m, 4H), 7.34 - 7.27 ppm (m, 2H). **Figure 41:** ^{13}C NMR (75 MHz, CDCl_3) δ 149.59, 136.40, 134.92, 134.08, 133.16, 132.50, 128.93, 128.70, 127.96, 124.34 ppm.

Elemental analysis for C₁₂H₈ClNO₂. Calc.: C 61.69; H 3.45; N 5.99. Found: C 61.73; H 3.74; N 5.78.

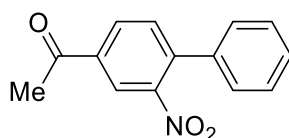
4-Bromo-2-nitrobiphenyl (63)^[163]



Prepared according to general synthesis from 4-bromo-1-iodo-2-nitrobenzene (1.64 g, 5 mmol) and phenylboronic acid (0.67 g, 5.5 mmol). Column chromatography (90:10 hexane: EtOAc) gave the product as a yellow solid (1.11 g, 80% yield). **Figure 42:** ¹H NMR (400 MHz, CDCl₃) δ 8.00 (d, *J* = 2.0 Hz, 1H), 7.75 (dd, *J* = 8.2, 2.0 Hz, 1H), 7.48 - 7.39 (m, 3H), 7.36 - 7.27 ppm (m, 3H). **Figure 43:** ¹³C NMR (101 MHz, CDCl₃) δ 149.57, 136.30, 135.35, 135.24, 133.26, 128.85, 128.61, 127.78, 127.04, 121.34 ppm.

Elemental analysis for C₁₂H₈BrNO₂. Calc.: C 51.83; H 2.90; N 5.04. Found: C 51.70; H 3.02; N 4.92.

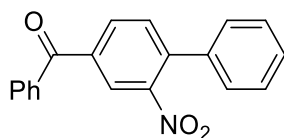
4-Acetyl-2-nitrobiphenyl (64)^[102]



Prepared according to general synthesis from 4-chloro-3-nitroacetophenone (1.0 g, 5 mmol) and phenylboronic acid (0.67 g, 5.5 mmol). Column chromatography (90:10 hexane: EtOAc) gave the product as a pale-yellow solid (1.14 g, 94% yield). **Figure 44:** ¹H NMR (400 MHz, CDCl₃) δ 8.39 (d, *J* = 1.6 Hz, 1H), 8.17 (dd, *J* = 8.0, 1.7 Hz, 1H), 7.57 (d, *J* = 8.2 Hz, 1H), 7.48 - 7.39 (m, 3H), 7.36 - 7.29 (m, 2H), 2.67 ppm (s, 3H). **Figure 45:** ¹³C NMR (101 MHz, CDCl₃) δ 195.50, 149.55, 140.46, 136.87, 136.41, 132.58, 131.50, 129.05, 128.99, 127.83, 124.06, 26.77 ppm.

Elemental analysis for C₁₄H₁₁NO₃. Calc.: C 69.70; H 4.60; N 5.81. Found: C 69.47; H 4.70; N 5.78.

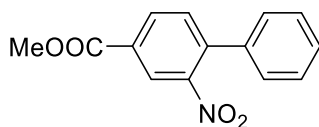
4-Benzoyl-2-nitrobiphenyl (65)^[102]



Prepared according to general synthesis from 4-chloro-3-nitrobenzophenone (1.31 g, 5 mmol) and phenylboronic acid (0.67 g, 5.5 mmol). Column chromatography (90:10 hexane: EtOAc) gave the product as a yellow solid (1.47 g, 97% yield). **Figure 46:** ¹H NMR (400 MHz, CDCl₃) δ 8.26 (d, *J* = 1.6 Hz, 1H), 8.06 (dd, *J* = 7.9, 1.7 Hz, 1H), 7.91 - 7.80 (m, 2H), 7.66 (t, *J* = 7.4 Hz, 1H), 7.63 - 7.51 (m, 3H), 7.51 - 7.42 (m, 3H), 7.42 - 7.33 ppm (m, 2H). **Figure 47:** ¹³C NMR (101 MHz, CDCl₃) δ 194.01, 149.29, 139.88, 137.61, 136.56, 136.51, 133.41, 133.23, 132.31, 130.11, 129.05, 128.87, 127.92, 125.64 ppm.

Elemental analysis for C₁₉H₁₃NO₃. Calc.: C 75.24; H 4.32; N 4.62. Found: C 74.84; H 4.48; N 4.48.

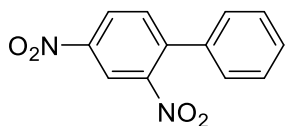
4-Carbomethoxy-2-nitrobiphenyl (66)^[102]



Prepared according to general synthesis from methyl-4-chloro-3-nitrobenzoate (1.08 g, 5 mmol) and phenylboronic acid (0.67 g, 5.5 mmol). Chromatography (1:1 hexane: EtOAc) gave the product as a yellow solid (1.12 g, 87 % yield). **Figure 48:** ¹H NMR (300 MHz, CDCl₃) δ 8.49 (d, *J* = 1.5 Hz, 1H), 8.26 (dd, *J* = 8.0, 1.6 Hz, 1H), 7.55 (d, *J* = 8.0 Hz, 1H), 7.49 - 7.39 (m, 3H), 7.38 - 7.29 (m, 2H), 3.99 ppm (s, 3H). **Figure 49:** ¹³C NMR (75 MHz, CDCl₃) δ 165.04, 149.43, 140.49, 136.54, 132.95, 132.37, 130.52, 129.03, 129.01, 127.90, 125.39, 52.89.

Elemental analysis for C₁₄H₁₁NO₄. Calc.: C 65.37; H 4.31; N 5.45. Found: C 65.19; H 4.38; N 5.48.

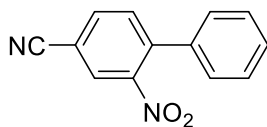
2,4-Dinitrobiphenyl (67)^[164]



Prepared according to general synthesis from 1-chloro-2,4-dinitrobenzene (1.01 g, 5 mmol) and phenylboronic acid (0.67 g, 5.5 mmol). Column chromatography (40:60 hexane: EtOAc) gave the product as a yellow solid (1.06 g, 87% yield). **Figure 50:** ¹H NMR (300 MHz, CDCl₃) δ 8.71 (d, *J* = 2.1 Hz, 1H), 8.47 (dd, *J* = 8.5, 2.2 Hz, 1H), 7.69 (d, *J* = 8.5 Hz, 1H), 7.55 - 7.40 (m, 3H), 7.40 - 7.28 ppm (m, 2H). **Figure 51:** ¹³C NMR (75 MHz, CDCl₃) δ 149.28, 147.05, 142.42, 135.37, 133.36, 129.72, 129.25, 127.83, 126.60, 119.86 ppm.

Elemental analysis for C₁₂H₈N₂O₄. Calc.: C 59.02; H 3.30; N 11.47. Found: C 58.96; H 3.48; N 11.24.

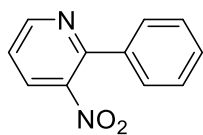
4-Cyano-2-nitrobiphenyl (68)^[102]



Prepared according to general synthesis from 4-chloro-3-nitrobenzonitrile (0.91 g, 5 mmol) and phenylboronic acid (0.67 g, 5.5 mmol). Chromatography (60:40 hexane: EtOAc) gave the product as a yellow solid (1.03 g, 92% yield). **Figure 52:** ¹H NMR (300 MHz, CDCl₃) δ 8.16 (d, *J* = 1.6 Hz, 1H), 7.91 (dd, *J* = 8.0, 1.6 Hz, 1H), 7.63 (d, *J* = 8.0 Hz, 1H), 7.54 - 7.41 (m, 3H), 7.39 - 7.29 (m, 2H). **Figure 53:** ¹³C NMR (75 MHz, CDCl₃) δ 149.41, 140.77, 135.58, 135.29, 133.22, 129.50, 129.16, 127.82, 127.77, 116.62, 112.55 ppm.

Elemental analysis for C₁₃H₈N₂O₂. Calc.: C 69.64; H 3.60; N 12.49. Found: C 69.59; H 3.76; N 12.46.

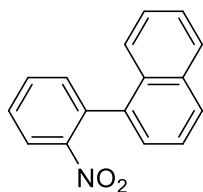
3-Nitro-2-phenylpyridine (69)^[165]



Prepared by modification of the general synthesis. In a 50 mL 2-neck flask, 2-chloro-3-nitropyridine (0.85 g, 5.4 mmol), phenylboronic acid (0.85 g, 7 mmol), K₂CO₃ (1.8 g, 13 mmol), Pd(PPh₃)₄ (118 mg, 0.1 mmol, 2 mol%), were suspended in 1,2-dimethoxyethane (8 mL) and water (3 mL) under a dinitrogen atmosphere. The reaction was heated to 85 °C for 16 h. The reaction was then cooled, CH₂Cl₂ (40 mL) was added and the water phase was separated. The organic phase was dried over Na₂SO₄ and the organic solvent was evaporated under vacuum. Chromatography (70:30 hexane: EtOAc) gave the product as an orange solid (0.99 g, 83% yield). **Figure 54:** ¹H NMR (400 MHz, CDCl₃) δ 8.86 (dd, *J* = 4.7, 1.5 Hz, 1H), 8.14 (dd, *J* = 8.1, 1.5 Hz, 1H), 7.61- 7.53 (m, 2H), 7.52 - 7.40 ppm (m, 4H). **Figure 55:** ¹³C NMR (101 MHz, CDCl₃) δ 153.00, 152.22, 146.40, 136.34, 132.36, 129.96, 128.90, 128.21, 122.53.

Elemental analysis for C₁₁H₈N₂O₂. Calc.: C 66.00; H 4.03; N 13.99. Found: C 66.29; H 3.96; N 14.16.

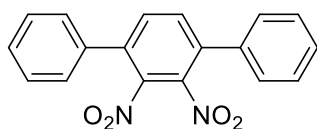
1-(2-Nitrophenyl)naphthalene (70)^[166-167]



Prepared by modification of the general synthesis from 2-bromonitrobenzene (1.01 g, 5 mmol) and 1-naphthaleneboronic acid (0.95 g, 5.5 mmol). DMF was used instead of toluene/water mixture and the reaction was performed at 100 °C for 6 h. After letting the flask cooling to room temperature, the reaction mixture was poured into water (30 mL) and extracted with EtOAc (3 × 30 mL). The combined organic layers were washed with water and brine and dried over Na₂SO₄. Chromatography (90:10 hexane: EtOAc) gave the product as a yellow solid (0.76 g, 61% yield). **Figure 56:** ¹H NMR (400 MHz, CDCl₃) δ 8.08 (dd, *J* = 8.1, 1.2 Hz, 1H), 7.91 (d, *J* = 8.2 Hz, 2H), 7.70 (td, *J* = 7.5, 1.3 Hz, 1H), 7.61 (td, *J* = 7.9, 1.4 Hz, 1H), 7.56 - 7.38 (m, 5H), 7.35 ppm (dd, *J* = 7.0, 1.0 Hz, 1H). **Figure 57:** ¹³C NMR (101 MHz, CDCl₃) δ 149.93, 135.63, 135.40, 133.58, 133.22, 132.68, 131.59, 128.78, 128.70, 128.60, 126.71, 126.19, 125.36, 124.97, 124.37 ppm.

Elemental analysis for C₁₆H₁₁NO₂. Calc.: C 77.10; H 4.45; N 5.62. Found: C 76.79; H 4.61; N 5.58.

2',3'-Dinitro-1,1':4',1''-terphenyl (71)^[168]



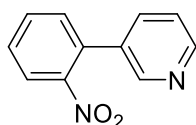
1,4-dibromo-2,3-dinitrobenzene was prepared according to procedure reported above.

Prepared according to general synthesis from 1,4-dibromo-2,3-dinitrobenzene (1.63 g, 5 mmol) and phenylboronic acid (1.83 g, 15 mmol), K_2CO_3 (2.76 g, 20 mmol), $Pd(PPh_3)_4$ (115.6 mg, 0.1 mmol, 2 mol%), toluene (10 mL), water (10 mL). Chromatography (70:30 hexane: EtOAc) gave the product as a yellow solid (1.4 g, 87% yield). **Figure 58:** 1H NMR (400 MHz, $CDCl_3$) δ 7.66 (s, 1H), 7.53 - 7.43 (m, 3H), 7.42 - 7.35 ppm (m, 2H). **Figure 59:** ^{13}C NMR (101 MHz, $CDCl_3$) δ 142.85, 135.65, 134.64, 133.50, 129.60, 129.32, 127.96 ppm.

Elemental analysis for $C_{18}H_{12}N_2O_4$. Calc.: C 67.50; H 3.78; N 8.75. Found: C 67.69; H 4.04; N 8.40.

4.12. Preparation of 2-nitrobiaryls through Ullmann cross-coupling.

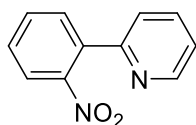
3-(2-Nitrophenyl)pyridine (72)^[137, 169]



3-Iodopyridine (0.47 g, 3.0 mmol), 2-bromonitrobenzene (0.92 g, 4.5 mmol), copper powder (0.76 g, 12 mmol) and $PdCl_2$ (27 mg, 0.15 mmol) were placed 25 mL Schlenk flask and dry DMSO (9 mL) was added under nitrogen. The mixture was heated to 130 °C for 3h while stirring. After letting the flask cooling to room temperature, 10 wt% NH_3 (15 mL) was added and the mixture stirred for one hour. The aqueous phase was then extracted with CH_2Cl_2 (3×25 mL), the combined organic layers dried over Na_2SO_4 , filtered and the solvent was evaporated. Chromatography (gradient elution from 95:5 to 80:20 hexane: EtOAc) gave the product as a dense yellow oil (0.25 g, 42% yield) **Figure 60:** 1H NMR (400 MHz, $CDCl_3$) δ 8.65 (dd, $J = 4.9, 1.5$ Hz, 1H), 8.59 (d, $J = 1.8$ Hz, 1H), 7.99 (dd, $J = 8.1, 1.2$ Hz, 1H), 7.74 - 7.62 (m, 2H), 7.62 - 7.51 (m, 1H), 7.43 (dd, $J = 7.6, 1.4$ Hz, 1H), 7.37 ppm (ddd, $J = 7.9, 4.9, 0.7$ Hz, 1H). **Figure 61:** ^{13}C NMR (101 MHz, $CDCl_3$) δ 148.88, 148.45, 147.66, 136.66, 134.36, 133.16, 132.78, 132.25, 129.57, 124.92, 123.72 ppm.

Elemental analysis for $C_{11}H_8N_2O_2$. Calc.: C 66.00; H 4.03; N 13.99. Found: C 65.67; H 4.37; N 13.60.

2-(2-Nitrophenyl)pyridine (73)^[170-171]

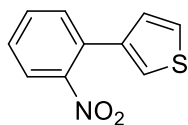


2-Bromonitrobenzene (2.04 g, 10 mmol), copper powder (1.45 g, 23 mmol) and $PdCl_2$ (52 mg, 0.29 mmol) were placed 50 mL Schlenk flask and 2-bromopyridine (0.95 mL, 10 mmol), dry DMSO (10 mL) were added under nitrogen. The mixture was heated to 130 °C for 3h while stirring. After letting the flask cooling to room temperature, 10 wt% NH_3 (100 mL) was added and the mixture stirred for one hour. The reaction was filtered on a Buchner funnel and the solid washed with CH_2Cl_2 . The filtrate was then extracted with CH_2Cl_2 (3×50 mL), the combined organic layers dried over Na_2SO_4 , filtered and the solvent was evaporated. Chromatography (80:20 hexane: EtOAc) gave the product as an orange solid (0.54 g, 27% yield) **Figure 62:** 1H NMR (400 MHz, $CDCl_3$) δ 8.62 (d, $J = 4.3$ Hz, 1H), 7.87 (d, $J = 8.6$ Hz, 1H), 7.77 (td, $J = 7.7, 1.7$ Hz, 1H), 7.70 - 7.56 (m, 2H),

7.56 - 7.40 (m, 2H), 7.35 - 7.20 (m, 1H). **Figure 63:** ^{13}C NMR (101 MHz, CDCl_3) δ 155.50, 149.68, 149.35, 136.96, 135.29, 132.46, 131.29, 129.28, 124.41, 122.97, 122.73 ppm.

Elemental analysis for $\text{C}_{11}\text{H}_8\text{N}_2\text{O}_2$. Calc.: C 66.00; H 4.03; N 13.99. Found: C 65.69; H 4.25; N 13.67.

3-(2-Nitrophenyl)thiophene (74)^[172]



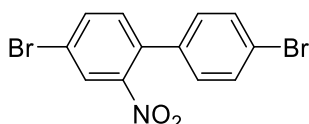
The synthesis was performed following a procedure reported in the literature.^[138]

Copper bronze (2.86 g) was added in portions during 5 min to a mixture of 2-bromonitrobenzene (1.01 g, 5 mmol) and 3-iodothiophene (0.77 mL, 7.5 mmol) at 170-180 °C. The bath temperature was raised and maintained at 200-210 °C for 3 h. On cooling, the products were extracted into hot acetone and the extracts filtered through Celite and evaporated to give a brown residue. Column chromatography (90:10 hexane: EtOAc) gave the product as a yellow oil (0.68 g, 66 % yield). **Figure 64:** ^1H NMR (400 MHz, CDCl_3) δ 7.78 (d, $J = 8.1$ Hz, 1H), 7.60 - 7.52 (m, 1H), 7.51 - 7.40 (m, 2H), 7.39 - 7.35 (m, 1H), 7.34 - 7.29 (m, 1H), 7.09 ppm (dd, $J = 4.9, 1.3$ Hz, 1H). **Figure 65:** ^{13}C NMR (75 MHz, CDCl_3) δ 149.40, 137.12, 132.28, 131.85, 130.94, 128.30, 127.55, 126.36, 124.02, 123.63 ppm.

Elemental analysis for $\text{C}_{10}\text{H}_7\text{NO}_2\text{S}$. Calc.: C 58.52; H 3.44; N 6.82. Found: C 58.65; H 3.61; N 6.61.

4.13. Preparation of 2-nitrobiaryls through simple organic transformations.

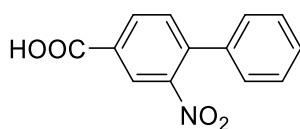
4,4'-Dibromo-2-nitrobiphenyl (75)^[102]



4,4'-Dibromobiphenyl (5 g, 16 mmol) was dissolved in glacial acetic acid (60 mL), and the mixture was stirred and heated to 100 °C. Then, fuming concentrated nitric acid (95%, 20 mL) was added and the resulting mixture was allowed to react for another 6 h. After the reaction solution was cooled to room temperature, the reaction was poured into 1 M NaOH (100 mL) to partially neutralize the acid, resulting in the formation of a yellow precipitate that was extracted with CH_2Cl_2 (2 x 50 mL), washed vigorously with H_2O (2 x 100 mL) and brine, dried over MgSO_4 , and concentrated *in vacuo* to a yellow solid. Recrystallization from ethanol afforded the pure compound (4.74 g, 83% yield). **Figure 66:** ^1H NMR (400 MHz, CDCl_3) δ 8.02 (d, $J = 1.9$ Hz, 1H), 7.75 (dd, $J = 8.2, 2.0$ Hz, 1H), 7.55 (d, $J = 8.5$ Hz, 2H), 7.29 (d, $J = 8.2$ Hz, 1H), 7.15 ppm (d, $J = 8.5$ Hz, 2H). **Figure 67:** ^{13}C NMR (101 MHz, CDCl_3) δ 149.33, 135.69, 135.40, 134.22, 133.14, 132.13, 129.52, 127.43, 123.16, 121.94 ppm.

Elemental analysis for $\text{C}_{12}\text{H}_7\text{Br}_2\text{NO}_2$. Calc.: C 40.37; H 1.98; N 3.92. Found: C 40.59; H 2.24; N 3.69.

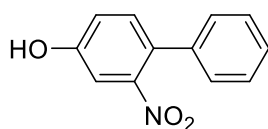
2-Nitrobiphenyl-4-carboxylic acid (76)^[102]



Prepared by hydrolysis of 4-carbomethoxy-2-nitrobiphenyl. To a solution of KOH (0.45 g, 8 mmol, 2 equiv.) in MeOH (10 mL) was added 4-carbomethoxy-2-nitrobiphenyl **66** (1.023 g, 4 mmol). The reaction was stirred for 6 h, during which time a precipitate formed. An additional equivalent of KOH (0.23 g, 4 mmol) and MeOH (5 mL) were added, and the reaction was stirred overnight (20 h). Then the reaction was diluted with H₂O (100 mL) and acidified with concentrated HCl to pH = 2. The mixture was extracted with EtOAc (3 × 100 mL). The combined layers were dried over MgSO₄ and concentrated to dryness, yielding a fluffy pale-yellow solid (0.963 g, 99 % yield). **Figure 68:** ¹H NMR (400 MHz, CDCl₃) δ 11.27 (br s, 1H), 8.58 (d, *J* = 1.4 Hz, 1H), 8.35 (dd, *J* = 8.0, 1.6 Hz, 1H), 7.61 (d, *J* = 8.0 Hz, 1H), 7.53 - 7.41 (m, 3H), 7.40-7.31 (m, 2H). **Figure 69:** ¹³C NMR (101 MHz, CDCl₃) δ 169.68, 149.55, 141.50, 136.35, 133.50, 132.62, 129.44, 129.24, 129.10, 127.89, 126.05 ppm.

Elemental analysis for C₁₃H₉NO₄. Calc.: C 64.20; H 3.73; N 5.76. Found: C 64.39; H 3.95; N 5.49.

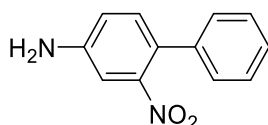
4-Hydroxy-2-nitrobiphenyl (77)^[102]



To an ice-cold solution of 4-methoxy-2-nitrobiphenyl **51** (0.46 g, 2 mmol) in freshly distilled CH₂Cl₂ (5 mL), BBr₃ (0.3 mL, 3 mmol) was added under dinitrogen dropwise via syringe. Upon complete addition, the ice bath was removed, and the reaction continued at room temperature for 5 h. At that time, the reaction mixture was diluted with Et₂O (25 mL), and the resulting solution was carefully treated with 0.5 M HCl (10 mL). The layers were separated, and the aqueous layer extracted with additional Et₂O (2 × 20 mL). The combined organic layers were washed with brine, dried over MgSO₄, and concentrated *in vacuo*. Column chromatography of the residue (05:95, Et₂O:CH₂Cl₂) give the product as a yellow-orange powder (0.32 g, 74% yield). **Figure 70:** ¹H NMR (300 MHz, CDCl₃) δ 7.47 - 7.36 (m, 3H), 7.36 - 7.31 (m, 1H), 7.31 - 7.25 (m, 3H), 7.09 (dd, *J* = 8.4, 2.6 Hz, 1H), 5.20 ppm (s, 1H). **Figure 71:** ¹³C NMR (75 MHz, CDCl₃) δ 155.24, 137.29, 133.25, 129.18, 128.79, 128.16, 128.07, 119.73, 111.27 ppm.

Elemental analysis for C₁₂H₉NO₃. Calc.: C 66.97; H 4.22; N 6.51. Found: C 67.32; H 4.60; N 6.37.

2-Nitro-4-biphenyl amine (78)



The synthesis was performed following a procedure reported in the literature.^[139]

A stirred solution of 2,4-dinitrobiphenyl **67** (2.44 g, 10 mmol) in ethanol (50 mL), and water (13 mL) containing 1-2 drops of concentrated hydrochloric acid (~60 μ L) and iron powder (1.2 g, 20 mmol, 2 equiv.) was refluxed for 3 hours. The red solution was cooled, filtered from iron oxides, then evaporated under reduced pressure to afford a brown residual oil. Column chromatography of the residue (90:10 Hexane: Ethyl acetate) gave the pure product as a bright yellow solid (1.33 g, 62% yield). **Figure 72:** ^1H NMR (400 MHz, CDCl_3) δ 7.44 - 7.31 (m, 3H), 7.31 - 7.23 (m, 2H), 7.20 (d, J = 8.3 Hz, 1H), 7.11 (d, J = 2.4 Hz, 1H), 6.87 (dd, J = 8.3, 2.4 Hz, 1H), 3.98 ppm (br. s, 2H) ppm. **Figure 73:** ^{13}C NMR (101 MHz, CDCl_3) δ 146.65, 137.85, 132.87, 128.68, 128.15, 127.64, 126.18, 118.53, 109.79 ppm. NMR characterization of this compound was not previously reported in the literature.

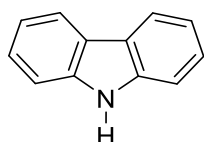
Elemental analysis for $\text{C}_{12}\text{H}_{10}\text{N}_2\text{O}_2$. Calc.: C 67.28; H 4.71; N 13.08. Found: C 67.53; H 4.75; N 13.43.

4.14. General procedure for nitrobiaryls cyclization to carbazoles.

The reaction was performed under dinitrogen atmosphere and the reaction components were assembled at room temperature. To avoid weighing very small amounts of $\text{Na}_2[\text{PdCl}_4]$ and 1,10-phenanthroline, stock solutions of these reagents were prepared by dissolving respectively 32 mg of the former reagent in 20 mL dry DMF (to give 1.6 mg/mL solution) and 98 mg Phen in 20 mL dry DMF (to give 4.9 mg/mL solution).

An ~20 mL pressure tube was placed in a Schlenk tube having a wide mouth and the tube was evacuated and filled with dinitrogen three times. *o*-nitrobiphenyl (107.5 mg, 0.54 mmol) was added first and the tube was evacuated and filled with dinitrogen three times again. Then, in a nitrogen flush, 1 mL of the Phen stock solution was added (corresponding to a ligand amount of 4.9 mg, 0.027 mmol, 5 mol%), followed by 1 mL of the catalyst stock solution (corresponding to a catalyst amount of 1.60 mg, 0.0054 mmol, 1 mol%), and DMF (8.0 mL) and the reaction was stirred for 10 min at rt. Finally, phenyl formate (260 μ L, 2.38 mmol, 4.4 equiv.) and Na_3PO_4 (12 mg, 0.073 mmol, 0.135 equiv.) were added. The pressure tube was closed and transferred to an oil bath preheated at 170 $^\circ\text{C}$. The reaction mixture was heated with continuous stirring for 5 hours. Then the tube was lifted from the oil bath and allowed to cool to room temperature. The reaction was filtered and DMF was evaporated under reduced pressure. Column Chromatography of the residue (Hexane: Ethyl acetate) gave the pure product.

9H-Carbazole (**79**)^[158]

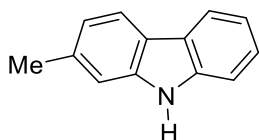


Prepared according to general synthesis from 2-nitrobiphenyl (107.6 mg, 0.54 mmol). Column chromatography of the residue (95:5, hexane: ethyl acetate) gave the pure product as a white lustrous solid (84 mg, 93.0 % yield), R_f = 0.33 (90:10 hexane: ethyl acetate). **Figure 74:** ^1H NMR (400 MHz, $\text{DMSO}-d_6$) δ 11.27 (s, 1H), 8.11 (d, J = 7.8 Hz, 2H), 7.52 (d, J = 8.1 Hz, 2H), 7.40 (t, J = 7.6 Hz, 2H),

7.17 ppm (t, $J = 7.5$ Hz, 2H). **Figure 75:** ^{13}C NMR (101 MHz, $\text{DMSO-}d_6$) δ 139.74, 125.50, 122.42, 120.14, 118.49, 110.93 ppm.

Elemental analysis for $\text{C}_{12}\text{H}_9\text{N}$. Calc.: C 86.20; H 5.43; N 8.38. Found: C 85.94; H 5.63; N 8.33.

2-Methyl-9H-carbazole (80)^[33]



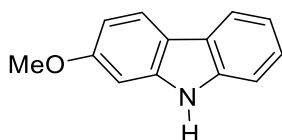
Prepared according to general synthesis from 4-methyl-2-nitrobiphenyl **50** (115.2 mg, 0.54 mmol). Column chromatography afforded the product (96 mg, 98% yield). The same compound was also synthesized from 4'-methyl-2-nitrobiphenyl **54** (115.2 mg, 0.54 mmol). Column chromatography afforded the product (95 mg, 97% yield).

In both cases, column chromatography of the residue (90:10 Hexane: Ethyl acetate) gave the pure product as a lustrous white solid, $R_f = 0.46$ (90:10 Hexane: Ethyl acetate).

Figure 76: ^1H NMR (400 MHz, $\text{DMSO-}d_6$) δ 11.10 (s, 1H), 8.04 (d, $J = 7.8$ Hz, 1H), 7.97 (d, $J = 7.9$ Hz, 1H), 7.44 (d, $J = 8.1$ Hz, 1H), 7.33 (t, $J = 8.2$ Hz, 1H), 7.27 (s, 1H), 7.12 (t, $J = 7.9$ Hz, 1H), 6.98 (dd, $J = 7.9, 0.8$ Hz, 1H), 2.47 ppm (s, 3H). **Figure 77:** ^{13}C NMR (101 MHz, $\text{DMSO-}d_6$) δ 140.25, 139.76, 135.01, 124.97, 122.55, 120.22, 120.07, 119.87, 119.81, 118.39, 110.93, 110.83, 21.73 ppm.

Elemental analysis for $\text{C}_{13}\text{H}_{11}\text{N}$. Calc.: C, 86.15; H, 6.12; N, 7.73 Found: C 86.27; H 6.33; N 7.40.

2-Methoxy-9H-carbazole (82)^[173]



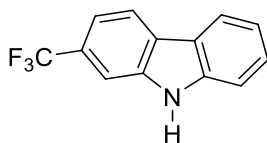
Prepared according to general synthesis from 4-methoxy-2-nitrobiphenyl **51** (123.8 mg, 0.54 mmol). Column Chromatography afforded the product (93.7 mg, 88 % yield). The same compound was also synthesized from 4'-methoxy-2-nitrobiphenyl **55** (123.8 mg, 0.54 mmol). Column Chromatography afforded the product (94.8 mg, 89 % yield)

In both cases, column chromatography of the residue (80:20 Hexane: Ethyl acetate) gave the pure product as a white solid, $R_f = 0.35$ (80:20 Hexane: Ethyl acetate).

Figure 78: ^1H NMR (400 MHz, $\text{DMSO-}d_6$) δ 11.11 (s, 1H), 7.96 (dd, $J = 10.6, 8.2$ Hz, 2H), 7.43 (d, $J = 8.0$ Hz, 1H), 7.29 (t, $J = 7.6$ Hz, 1H), 7.11 (t, $J = 7.4$ Hz, 1H), 6.98 (d, $J = 2.2$ Hz, 1H), 6.77 (dd, $J = 8.5, 2.2$ Hz, 1H), 3.84 ppm (s, 3H). **Figure 79:** ^{13}C NMR (101 MHz, $\text{DMSO-}d_6$) δ 158.56, 141.17, 139.79, 124.17, 122.74, 120.93, 119.28, 118.60, 116.25, 110.66, 107.73, 94.49, 55.25 ppm.

Elemental analysis for $\text{C}_{13}\text{H}_{11}\text{NO}$. Calc.: C, 79.17; H, 5.62; N, 7.10 Found: C 79.02; H 5.65; N 7.07.

2-(Trifluoromethyl)-9H-carbazole (**82**)^[158]



Prepared according to general synthesis from 4-trifluoromethyl-2-nitrobiphenyl **52** (144.3 mg, 0.54 mmol). Column chromatography afforded the product (113 mg, 89% yield), Rf= 0.36 (75:25 Hexane: Ethyl acetate). The same compound was also synthesized from 4'-trifluoromethyl-2-nitrobiphenyl **56** (144.3 mg, 0.54 mmol). Column chromatography afforded the product (102 mg, 80% yield).

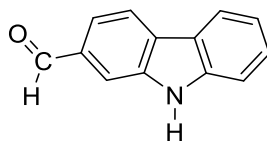
In both cases, column chromatography of the residue (80:20 Hexane: Ethyl acetate) gave the pure product as a lustrous white solid, Rf = 0.36 (75:25 Hexane: Ethyl acetate).

Figure 80: ¹H NMR (400 MHz, DMSO-*d*₆) δ 11.64 (s, 1H), 8.32 (d, *J* = 8.2 Hz, 1H), 8.22 (d, *J* = 7.8 Hz, 1H), 7.83 (s, 1H), 7.60 (d, *J* = 8.2 Hz, 1H), 7.54 - 7.41 (m, 2H), 7.24 ppm (t, *J* = 7.5 Hz, 1H).

Figure 81: ¹³C NMR (101 MHz, DMSO-*d*₆) δ 140.90, 138.85, 127.11, 125.72 (q, *J* = 31.31 Hz), 125.39, 125.37 (q, *J* = 272.70 Hz), 121.50, 121.10, 121.06, 119.39, 114.84 (q, *J* = 4.04 Hz), 111.59, 108.06 (q, *J* = 4.04 Hz) ppm. **Figure 82:** ¹⁹F NMR (376 MHz, DMSO-*d*₆) δ -59.25 (s, 3F) ppm.

Elemental analysis for C₁₃H₈F₃N. Calc.: C, 66.38; H, 3.43; N, 5.96 Found: C 66.06; H 3.65; N 5.81.

2-Formyl-9H-carbazole (**83**)^[102]



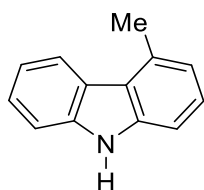
Prepared according to general synthesis from 4-formyl-2-nitrobiphenyl **53** (122.7 mg, 0.54 mmol). Column chromatography afforded the product (96.8 mg, 92 % yield), Rf= 0.34 (80:20 Hexane: Ethyl acetate). The same compound was also synthesized from 4'-formyl-2-nitrobiphenyl **57** (122.7 mg, 0.54 mmol) (96.8 mg, 92 % yield).

In both cases, column chromatography of the residue (80:20 Hexane: Ethyl acetate) gave the pure product as a yellow solid, Rf= 0.34 (80:20 Hexane: Ethyl acetate).

Figure 83: ¹H NMR (400 MHz, CDCl₃) δ 10.14 (s, 1H), 8.40 (br s, 1H), 8.20 (d, *J* = 8.0 Hz, 1H), 8.14 (d, *J* = 7.9 Hz, 1H), 7.99 (s, 1H), 7.77 (dd, *J* = 8.0, 0.8 Hz, 1H), 7.58 - 7.44 (m, 2H), 7.34-7.27 ppm (m, 1H). **Figure 84:** ¹³C NMR (101 MHz, CDCl₃) δ 192.67, 141.39, 139.23, 134.26, 128.79, 127.97, 122.55, 121.73, 121.53, 120.75, 120.40, 112.08, 111.24 ppm.

Elemental analysis for C₁₃H₉NO. Calc.: C, 79.98; H, 4.65; N, 7.17. Found: C, 79.95; H, 4.84; N, 6.97.

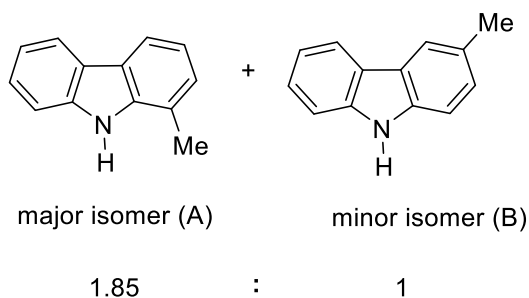
4-Methyl-9H-carbazole (**84**)^[158]



Prepared according to general synthesis from 2'-methyl-2-nitrobiphenyl **59** (115.1 mg, 0.54 mmol). Column chromatography of the residue (95:5, hexane: ethyl acetate) gave the pure product as a white solid (83.2 mg, 85.0 % yield), $R_f = 0.26$ (90:10 hexane: ethyl acetate). **Figure 85:** ^1H NMR (400 MHz, $\text{DMSO-}d_6$) δ 11.30 (s, 1H), 8.12 (d, $J = 7.9$ Hz, 1H), 7.52 (d, $J = 8.1$ Hz, 1H), 7.43 - 7.32 (m, 2H), 7.28 (t, $J = 7.6$ Hz, 1H), 7.18 (t, $J = 7.5$ Hz, 1H), 6.95 (d, $J = 7.1$ Hz, 1H), 2.80 ppm (s, 3H). **Figure 86:** ^{13}C NMR (101 MHz, $\text{DMSO-}d_6$) δ 139.76, 139.71, 132.38, 125.35, 124.91, 122.92, 122.14, 120.89, 119.93, 118.54, 110.73, 108.57, 20.51 ppm.

Elemental analysis for $\text{C}_{13}\text{H}_{11}\text{N}$. Calc.: C 86.15; H 6.12; N 7.73. Found: C 85.31 H 6.28; N 7.60.

1-Methyl-9H-carbazole and 3-methyl-9H-carbazole (**85**)^[173]

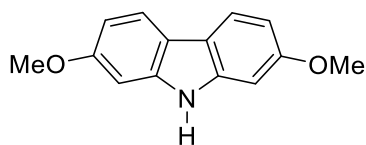


Prepared according to general synthesis from 3'-methyl-2-nitrobiphenyl **59** (115.1 mg, 0.54 mmol). Column chromatography of the residue (95:5 Hexane: Ethyl acetate) afforded two fractions with an overall yield of 99% (96.9 mg), the ratio between the two isomers were recorded from GC chromatogram. First fraction was the pure major isomer (1-methyl-9H-carbazole) obtained as a lustrous white solid, $R_f = 0.22$ (95:5 Hexane: Ethyl acetate). **Figure 87:** ^1H NMR (400 MHz, CDCl_3) δ 8.05 (d, $J = 7.8$ Hz, 1H), 7.92 (br s, 1H), 7.89 (s, 1H), 7.40 (d, $J = 3.6$ Hz, 2H), 7.32 (d, $J = 8.2$ Hz, 1H), 7.28 - 7.16 (m, 2H), 2.54 ppm (s, 3H). **Figure 88:** ^{13}C NMR (101 MHz, CDCl_3) δ 139.95, 137.85, 128.88, 127.31, 125.78, 123.66, 123.36, 120.38, 119.35, 110.69, 110.37, 21.56.

Elemental analysis for the pure isomer $\text{C}_{13}\text{H}_{11}\text{N}$. Calc.: C, 86.15; H, 6.12; N, 7.73 Found: C 85.39; H 6.42; N 7.14.

Second fraction was a mixture of the two isomers, 1-methyl-9H-carbazole **85a** $R_f = 0.22$ (95:5 Hexane: Ethyl acetate) and 3-methyl-9H-carbazole **85b** $R_f = 0.13$ (95:5 Hexane: Ethyl acetate) obtained as a lustrous white solid.

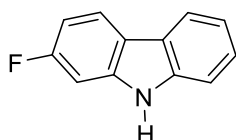
4-Dimethoxy-9H-carbazole (86)^[158]



Prepared according to general synthesis from 4,4'-dimethoxy-2-nitrobiphenyl **60** (140 mg, 0.54 mmol). Column chromatography of the residue (70:30, hexane: ethyl acetate) gave the pure product as a white solid (105.6 mg, 86.0 % yield), $R_f = 0.62$ (60:40 hexane: ethyl acetate). **Figure 89:** ^1H NMR (400 MHz, $\text{DMSO-}d_6$) δ 10.97 (s, 1H), 7.83 (d, $J = 8.5$ Hz, 2H), 6.94 (d, $J = 2.2$ Hz, 2H), 6.73 (dd, $J = 8.5, 2.2$ Hz, 2H), 3.82 ppm (s, 6H). **Figure 90:** ^{13}C NMR (101 MHz, $\text{DMSO-}d_6$) δ 157.55, 141.03, 119.94, 116.46, 107.32, 94.65, 55.22 ppm.

Elemental analysis for $\text{C}_{14}\text{H}_{13}\text{NO}_2$. Calc.: C 73.99; H 5.77; N 6.16. Found: C 74.01 H 5.91; N 5.89.

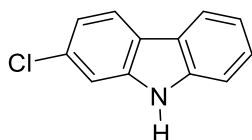
2-Fluoro-9H-carbazole (87)^[158]



Prepared according to general synthesis from 4-fluoro-2-nitrobiphenyl **61** (117.3 mg, 0.54 mmol). Column Chromatography of the residue (90:10 Hexane: Ethyl acetate) gave the pure product as a lustrous white solid (98.9 mg, 99% yield), $R_f = 0.22$ (90:10 Hexane: Ethyl acetate). **Figure 91:** ^1H NMR (400 MHz, $\text{DMSO-}d_6$) δ 11.38 (s, 1H), 8.15 - 8.05 (m, 2H), 7.49 (d, $J = 8.1$ Hz, 1H), 7.37 (t, $J = 7.6$ Hz, 1H), 7.26 (dd, $J = 10.1, 2.3$ Hz, 1H), 7.16 (t, $J = 7.5$ Hz, 1H), 7.04-6.93 ppm (m, 1H). **Figure 92:** ^{13}C NMR (101 MHz, $\text{DMSO-}d_6$) δ 161.18 (d, $J = 283.3$ Hz), 140.40, 140.30, 125.25, 122.07, 121.47 (d, $J = 10.5$ Hz), 119.97, 119.20, 119.00, 111.02, 106.49 (d, $J = 24.4$ Hz), 97.34 (d, $J = 26.2$ Hz) ppm. **Figure 93:** ^{19}F NMR (376 MHz, $\text{DMSO-}d_6$) δ -115.97 (d, $J = 3.4$ Hz, 1F) ppm.

Elemental analysis for $\text{C}_{12}\text{H}_8\text{FN}$. Calc.: C 77.82; H 4.35; N 7.56 Found: C 77.45; H 4.65; N 7.85.

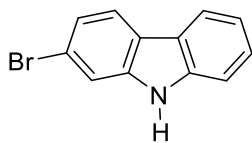
2-Chloro-9H-carbazole (88)^[158]



Prepared according to general synthesis from 4-chloro-2-nitrobiphenyl **62** (126.2 mg, 0.54 mmol). Column chromatography of the residue (90:10 Hexane: Ethyl acetate) gave the pure product as a white solid (107.5 mg, 99 % yield), $R_f = 0.34$ (90:10 Hexane: Ethyl acetate). **Figure 94:** ^1H NMR (400 MHz, $\text{DMSO-}d_6$) δ 11.40 (s, 1H), 8.11 (d, $J = 8.3$ Hz, 2H), 7.59-7.45 (m, 2H), 7.46 - 7.35 (m, 1H), 7.25 - 7.10 ppm (m, 2H). **Figure 95:** ^{13}C NMR (101 MHz, $\text{DMSO-}d_6$) δ 140.29, 140.07, 129.87, 125.94, 121.80, 121.52, 121.31, 120.30, 119.06, 118.65, 111.20, 110.59 ppm.

Elemental analysis for $\text{C}_{12}\text{H}_8\text{ClN}$. Calc.: C 71.48; H 4.00; N, 6.95 Found: C 71.51; H 4.26; N 6.56.

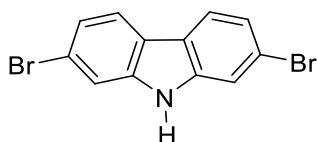
2-Bromo-9H-carbazole (89)^[163]



Prepared according to general synthesis from 4-bromo-2-nitrobiphenyl **63** (150.18 mg, 0.54 mmol). Column chromatography of the residue (90:10 Hexane: Ethyl acetate) gave the pure product as a white solid (105 mg, 79 % yield), Rf= 0.6 (80:20 Hexane: Ethyl acetate). **Figure 96:** ¹H NMR (400 MHz, DMSO-*d*₆) δ 11.40 (s, 1H), 8.11 (d, *J* = 7.8 Hz, 1H), 8.06 (d, *J* = 8.3 Hz, 1H), 7.68 (d, *J* = 1.3 Hz, 1H), 7.52 (d, *J* = 8.1 Hz, 1H), 7.42 (t, *J* = 8.2 Hz, 1H), 7.29 (dd, *J* = 8.3, 1.6 Hz, 1H), 7.18 ppm (t, *J* = 8.0 Hz, 1H). **Figure 97:** ¹³C NMR (101 MHz, DMSO-*d*₆) δ 140.64, 139.91, 126.09, 121.89, 121.81, 121.59, 121.30, 120.35, 119.09, 118.14, 113.52, 111.23 ppm.

Elemental analysis for C₁₂H₈BrN. Calc.: C 58.56; H 3.28; N 5.69 Found: C 58.92; H 3.32; N 5.52.

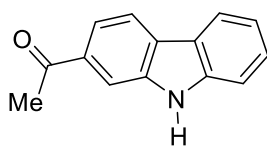
2,7-Dibromo-9H-carbazole (90)^[142]



Prepared according to general synthesis from 4,4'-bromo-2-nitrobiphenyl **75** (192.8 mg, 0.54 mmol). Column chromatography of the residue (80:20 Hexane: Ethyl acetate) gave the pure product as a yellow solid (110.6 mg, 63 % yield), Rf= 0.46 (90:10 Hexane: Ethyl acetate). **Figure 98:** ¹H NMR (400 MHz, DMSO-*d*₆) δ 11.52 (s, 1H), 8.08 (d, *J* = 8.3 Hz, 2H), 7.71 (d, *J* = 1.5 Hz, 2H), 7.32 ppm (dd, *J* = 8.3, 1.8 Hz, 2H). **Figure 99:** ¹³C NMR (101 MHz, DMSO-*d*₆) δ 140.85, 122.18, 122.01, 121.06, 118.78, 113.92 ppm.

Elemental analysis for C₁₂H₇Br₂N. Calc.: C 44.35; H 2.17; N 4.31 Found: C 44.54; H 2.41; N 4.11.

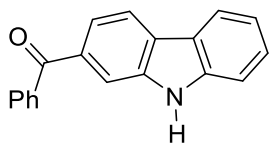
2-Acetyl-9H-carbazole (91)^[174]



Prepared according to general synthesis from 4-acetyl-2-nitrobiphenyl **64** (130.3 mg, 0.54 mmol). Column chromatography of the residue (80:20 Hexane: Ethyl acetate) gave the pure product as a yellow solid (81.5 mg, 72 % yield), Rf= 0.36 (80:20 Hexane: Ethyl acetate). **Figure 100:** ¹H NMR (400 MHz, DMSO-*d*₆) δ 11.53 (s, 1H), 8.21 (dd, *J* = 10.8, 8.1 Hz, 2H), 8.09 (dd, *J* = 1.4, 0.6 Hz, 1H), 7.79 (dd, *J* = 8.2, 1.5 Hz, 1H), 7.56 (d, *J* = 8.2 Hz, 1H), 7.47 (t, *J* = 8.2 Hz, 1H), 7.21 (t, *J* = 7.9 Hz, 1H), 2.68 ppm (s, 3H). **Figure 101:** ¹³C NMR (101 MHz, DMSO-*d*₆) δ 197.80, 141.28, 139.14, 134.09, 126.99, 126.11, 121.58, 121.12, 120.02, 119.09, 118.63, 111.37, 111.32, 26.94 ppm.

Elemental analysis for C₁₄H₁₁NO. Calc.: C 80.36; H 5.30; N 6.69 Found: C 80.03; H 5.44; N 6.74.

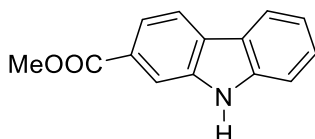
2-Benzoyl-9H-carbazole (92)^[175]



Prepared according to general synthesis from 4-benzoyl-2-nitrobiphenyl **65** (163.8 mg, 0.54 mmol). Column chromatography of the residue (90:10 Hexane: Ethyl acetate) gave the pure product as a yellow solid (127.5 mg, 87 % yield), $R_f = 0.34$ (90:10 Hexane: Ethyl acetate). **Figure 102:** ^1H NMR (400 MHz, $\text{DMSO-}d_6$) δ 11.53 (s, 1H), 8.28 (d, $J = 8.1$ Hz, 1H), 8.22 (d, $J = 7.7$ Hz, 1H), 7.89 (s, 1H), 7.84 -7.74 (m, 2H), 7.69 (t, $J = 7.4$ Hz, 1H), 7.64 -7.53 (m, 4H), 7.48 (t, $J = 8.1$ Hz, 1H), 7.23 ppm (t, $J = 7.4$ Hz, 1H). **Figure 103:** ^{13}C NMR (101 MHz, $\text{DMSO-}d_6$) ^{13}C NMR (101 MHz, D_2O) δ 196.20, 141.25, 138.92, 138.15, 133.87, 132.24, 129.59, 128.51, 127.18, 126.00, 121.66, 121.21, 120.24, 120.13, 119.29, 113.36, 111.47 ppm.

Elemental analysis for $\text{C}_{19}\text{H}_{13}\text{NO}$. Calc.: C 84.11; H 4.83; N 5.16 Found: C 83.87; H 4.94; N 5.37.

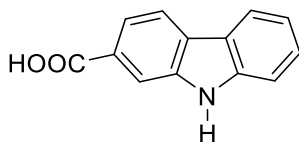
Methyl 9H-carbazole-2-carboxylate (93)^[158]



Prepared according to general synthesis from 4-carbomethoxy-2-nitrobiphenyl **66** (138.9 mg, 0.54 mmol). Column chromatography of the residue (80:20 Hexane: Ethyl acetate) gave the pure product as a white solid (113.2 mg, 93 % yield), $R_f = 0.43$ (70:30 Hexane: Ethyl acetate). **Figure 104:** ^1H NMR (400 MHz, $\text{DMSO-}d_6$) δ 11.55 (s, 1H), 8.20 (dd, $J = 12.2, 8.0$ Hz, 2H), 8.13 (d, $J = 0.9$ Hz, 1H), 7.79 (dd, $J = 8.2, 1.5$ Hz, 1H), 7.57 (d, $J = 8.2$ Hz, 1H), 7.46 (t, $J = 8.2$ Hz, 1H), 7.21 (t, $J = 7.9$ Hz, 1H), 3.90 ppm (s, 3H). **Figure 105:** ^{13}C NMR (101 MHz, $\text{DMSO-}d_6$) δ 166.96, 141.10, 139.05, 127.09, 126.31, 126.21, 121.61, 121.13, 120.17, 119.26, 119.18, 112.36, 111.44, 52.08 ppm.

Elemental analysis for $\text{C}_{14}\text{H}_{11}\text{NO}_2$. Calc.: C 74.65; H 4.92; N 6.22. Found: C 74.95; H 5.05; N 6.08.

9H-Carbazole-2-carboxylic acid (94)^[176]



Prepared according to general synthesis from 2-nitrobiphenyl-4-carboxylic acid **76** (131.3 mg, 0.54 mmol). After evaporation of DMF, the residue was dissolved in ethyl acetate, acidified with 1 M aq. HCl, extracted with ethyl acetate (50 ml x 3), dried with anhydrous Na_2SO_4 , filtered and the solvent was evaporated under reduced pressure. Column chromatography of the residue (60:40 Hexane: Ethyl acetate) gave the pure product as a white solid (23 mg, 20 % yield), $R_f = 0.35$ (50:50 Hexane: Ethyl acetate).

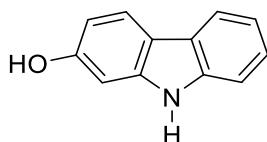
The same compound was also synthesized by hydrolysis of methyl 9*H*-carbazole-2-carboxylate **93**.

93 (225.3 mg, 1 mmole) in ethanol (25 mL) and H₂O (5 mL) was added NaOH (0.6 g, 15 mmole, 15 equiv.), and the reaction mixture was refluxed for 16 h. After cooling to room temperature, ethanol was evaporated, the residue was dissolved in ethyl acetate, acidified with 1 M aq. HCl, extracted with ethyl acetate (50 ml x 3), dried with anhydrous Na₂SO₄, filtered and the solvent was evaporated under reduced pressure to give the desired product **94** (200.7 mg, 95% yield).

Figure 106: ¹H NMR (400 MHz, DMSO-*d*₆) δ 12.86 (br. s, 1H), 11.55 (s, 1H), 8.27 - 8.06 (m, 3H), 7.82 (dd, *J* = 8.2, 1.4 Hz, 1H), 7.57 (d, *J* = 8.2 Hz, 1H), 7.46 (t, *J* = 8.2 Hz, 1H), 7.19 ppm (t, *J* = 7.8 Hz, 1H). **Figure 107:** ¹³C NMR (101 MHz, DMSO-*d*₆) δ 168.18, 141.11, 139.20, 127.64, 126.96, 126.01, 121.77, 121.09, 120.02, 119.65, 119.14, 112.61, 111.45 ppm.

Elemental analysis for C₁₃H₉NO₂. Calc.: C 73.92; H 4.30; N 6.63. Found: C 73.67; H 4.53; N 6.55.

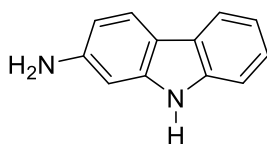
2-Hydroxy-9*H*-carbazole (**95**)^[145]



Prepared according to general synthesis from 4-hydroxy-2-nitrobiphenyl **77** (116.2 mg, 0.54 mmol). After evaporation of DMF, the residue was dissolved in ethyl acetate, acidified with 1N aq. HCl, extracted with ethyl acetate (50 ml x 3), dried with anhydrous Na₂SO₄, filtered and the solvent was evaporated under reduced pressure. Column chromatography of the residue (70:30 Hexane: Ethyl acetate) gave the pure product as a buff solid (76.2 mg, 77.0 % yield), R_f = 0.26 (70:30 Hexane: Ethyl acetate). **Figure 108:** ¹H NMR (400 MHz, DMSO-*d*₆) δ 10.91 (s, 1H), 9.37 (s, 1H), 7.91 (d, *J* = 7.7 Hz, 1H), 7.84 (d, *J* = 8.4 Hz, 1H), 7.36 (d, *J* = 8.0 Hz, 1H), 7.23 (t, *J* = 7.5 Hz, 1H), 7.06 (t, *J* = 7.4 Hz, 1H), 6.81 (s, 1H), 6.63 ppm (dd, *J* = 8.4, 1.7 Hz, 1H). **Figure 109:** ¹³C NMR (101 MHz, DMSO-*d*₆) δ 156.43, 141.41, 139.57, 123.68, 122.98, 120.76, 118.86, 118.31, 115.19, 110.35, 108.31, 96.35 ppm.

Elemental analysis for C₁₂H₉NO. Calc.: C 78.67; H 4.95; N 7.65 Found: C 78.36; H 5.19; N 7.44.

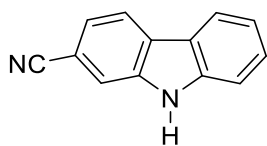
2-Amino-9*H*-carbazole (**96**)^[145]



Prepared according to general synthesis from 4-amino-2-nitrobiphenyl **78** (115.7 mg, 0.54 mmol). Column chromatography of the residue (gradient from 70:30 to 50:50 Hexane: Ethyl acetate) gave the pure product as a light brown solid (81.8 mg, 83.0 % yield), R_f = 0.27 (60:40 Hexane: Ethyl acetate). **Figure 110:** ¹H NMR (400 MHz, DMSO-*d*₆) δ 10.70 (s, 1H), 7.80 (d, *J* = 7.6 Hz, 1H), 7.68 (d, *J* = 8.3 Hz, 1H), 7.28 (d, *J* = 7.9 Hz, 1H), 7.15 (t, *J* = 7.5 Hz, 1H), 7.00 (t, *J* = 7.4 Hz, 1H), 6.58 (s, 1H), 6.45 (dd, *J* = 8.3, 1.7 Hz, 1H), 5.15 ppm (s, 2H). **Figure 111:** ¹³C NMR (101 MHz, DMSO-*d*₆) δ 147.81, 141.90, 139.21, 123.57, 122.80, 120.51, 118.14, 118.03, 113.05, 109.97, 108.09, 94.30 ppm.

Elemental analysis for C₁₂H₉NO. Calc.: C 78.67; H 4.95; N 7.65 Found: C 78.36; H 5.19; N 7.44.

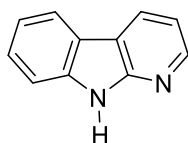
2-Cyano-9H-carbazole (97)^[158]



Prepared according to general synthesis from 4-cyano-2-nitrobiphenyl **68** (121.1 mg, 0.54 mmol). Column chromatography of the residue (gradient elution from 95:5 to 80:20 Hexane: Ethyl acetate) gave the pure product as an off-white solid (68.5 mg, 66.0 % yield), R_f= 0.32 (80:20 Hexane: Ethyl acetate). **Figure 112:** ¹H NMR (400 MHz, DMSO-*d*₆) δ 11.72 (s, 1H), 8.31 (d, *J* = 8.1 Hz, 1H), 8.23 (d, *J* = 7.8 Hz, 1H), 7.98 (s, 1H), 7.59 (d, *J* = 8.2 Hz, 1H), 7.51 (dd, *J* = 13.7, 7.6 Hz, 2H), 7.24 ppm (t, *J* = 7.4 Hz, 1H). **Figure 113:** ¹³C NMR (101 MHz, DMSO-*d*₆) δ 141.00, 138.54, 127.56, 125.95, 121.52, 121.34, 121.28, 120.13, 119.51, 115.21, 111.60, 106.81 ppm.

Elemental analysis for C₁₃H₈N₂. Calc.: C 81.23; H 4.20; N 14.57. Found: C 81.53; H 4.48; N 13.49.

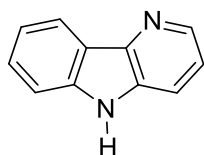
9H-Pyrido[2,3-*b*]indole (98)^[33]



Prepared according to general synthesis from 3-(2-nitrophenyl)pyridine **72** (108.1 mg, 0.54 mmol). Column Chromatography of the residue (70:30 Hexane: Ethyl acetate) gave the pure product as a white solid (67.3 mg, 74.0 % yield), R_f= 0.45 (50:50 Hexane: Ethyl acetate). **Figure 114:** ¹H NMR (400 MHz, DMSO-*d*₆) δ 11.81 (s, 1H), 8.48 (dd, *J* = 7.7, 1.3 Hz, 1H), 8.43 (dd, *J* = 4.8, 1.4 Hz, 1H), 8.15 (d, *J* = 7.8 Hz, 1H), 7.53 (d, *J* = 8.1 Hz, 1H), 7.46 (t, *J* = 7.5 Hz, 1H), 7.28 - 7.10 ppm (m, 2H). **Figure 115:** ¹³C NMR (101 MHz, DMSO-*d*₆) δ 151.95, 146.06, 138.83, 128.33, 126.57, 121.12, 120.40, 119.38, 115.19, 114.93, 111.24 ppm.

Elemental analysis for C₁₁H₈N₂. Calc.: C 78.55; H 4.79; N 16.66 Found: C 77.87; H 4.94; N 16.61.

5H-Pyrido[3,2-*b*]indole (99)^[177]

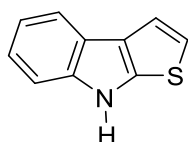


Prepared according to general synthesis from 3-nitro-2-phenylpyridine **69** (108.1 mg, 0.54 mmol). Column chromatography afforded the product (24.6 mg, 27 % yield). The same compound was also synthesized from 2-(2-nitrophenyl)pyridine **73** (108.1 mg, 0.54 mmol). Column chromatography afforded the product (27.3 mg, 30 % yield).

In both cases, column chromatography of the residue (gradient elution from 80:20 to 70:30 Hexane: Ethyl acetate) gave the pure product as a light brown solid, $R_f = 0.18$ (70:30 Hexane: Ethyl acetate). **Figure 116:** ^1H NMR (400 MHz, $\text{DMSO-}d_6$) δ 11.43 (s, 1H), 8.45 (dd, $J = 4.6, 1.3$ Hz, 1H), 8.20 (d, $J = 7.8$ Hz, 1H), 7.88 (dd, $J = 8.2, 1.3$ Hz, 1H), 7.57 (d, $J = 8.2$ Hz, 1H), 7.50 (t, $J = 8.1$ Hz, 1H), 7.38 (dd, $J = 8.2, 4.6$ Hz, 1H), 7.24 ppm (t, $J = 7.8$ Hz, 1H). **Figure 117:** ^{13}C NMR (101 MHz, $\text{DMSO-}d_6$) δ 141.18, 140.51, 132.91, 127.42, 121.56, 120.21, 120.07, 119.36, 117.99, 111.74 ppm.

Elemental analysis for $\text{C}_{11}\text{H}_8\text{N}_2$. Calc.: C 78.55; H 4.79; N 16.66 Found: C 78.42; H 4.91; N 16.47.

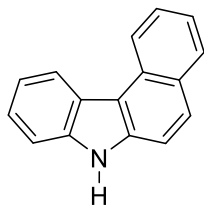
8*H*-Thieno[2,3-*b*]indole (100)^[33]



Prepared by modification of the general synthesis from 3-(2-nitrophenyl)thiophene **74** (110.8 mg, 0.54 mmol) using 2 mol% catalyst and 5 mol% dimethoxyPhen. Column chromatography of the residue (95:05 Hexane: Ethyl acetate) gave the pure product as a light brown solid (32.8 mg, 35 % yield), $R_f = 0.10$ (90:10 Hexane: Ethyl acetate). **Figure 118:** ^1H NMR (400 MHz, $\text{DMSO-}d_6$) δ 11.60 (s, 1H), 7.77 (d, $J = 7.6$ Hz, 1H), 7.43 (dd, $J = 19.8, 6.5$ Hz, 2H), 7.17 (t, $J = 7.4$ Hz, 1H), 7.12 - 6.97 ppm (m, 2H). **Figure 119:** ^{13}C NMR (101 MHz, $\text{DMSO-}d_6$) δ 141.95, 141.33, 123.90, 121.71, 121.39, 118.88, 118.78, 117.72, 117.15, 111.59 ppm.

Elemental analysis for $\text{C}_{10}\text{H}_7\text{NS}$. Calc.: C 69.33; H 4.07; N 8.09 Found: C 69.16; H 4.34; N 7.93.

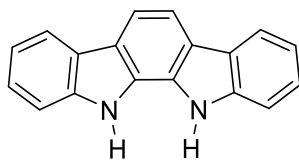
7*H*-Benzo[*c*]carbazole (101)^[33]



Prepared according to general synthesis from 4-(2-nitrobiphenyl) naphthalene **70** (134.6 mg, 0.54 mmol). Column chromatography of the residue (95:05 Hexane: Ethyl acetate) gave the pure product as a lustrous white solid (115 mg, 98 % yield), $R_f = 0.25$ (90:10 Hexane: Ethyl acetate). **Figure 120:** ^1H NMR (400 MHz, $\text{DMSO-}d_6$) δ 11.82 (s, 1H), 8.77 (d, $J = 8.3$ Hz, 1H), 8.58 (d, $J = 8.0$ Hz, 1H), 8.05 (d, $J = 8.0$ Hz, 1H), 7.92 (d, $J = 8.8$ Hz, 1H), 7.78 (d, $J = 8.8$ Hz, 1H), 7.75 - 7.62 (m, 2H), 7.45 (dd, $J = 16.5, 8.3$ Hz, 2H), 7.32 ppm (t, $J = 7.9$ Hz, 1H). **Figure 121:** ^{13}C NMR (101 MHz, $\text{DMSO-}d_6$) δ 138.67, 137.47, 129.41, 129.13, 128.51, 126.92, 126.88, 124.01, 122.95, 122.85, 122.60, 121.58, 119.56, 113.98, 113.48, 111.65 ppm.

Elemental analysis for $\text{C}_{16}\text{H}_{11}\text{N}$. Calc.: C 88.45; H 5.10; N 6.45. Found: C 88.10; H 5.11; N 6.24.

11,12-Dihydroindolo[2,3-a]carbazole (102)^[168]



Prepared according to general synthesis **II** from 2',3'-dinitro-1,1':4',1''-terphenyl **71** (173 mg, 0.54 mmol). Column chromatography of the residue (70:30 Hexane: Ethyl acetate) gave the pure product as a white solid (28 mg, 20 % yield), R_f= 0.35 (70:30 Hexane: Ethyl acetate). **Figure 122:** ¹H NMR (400 MHz, DMSO-*d*₆) δ 11.05 (s, 2H), 8.15 (d, *J* = 7.8 Hz, 2H), 7.91 (s, 2H), 7.68 (d, *J* = 8.1 Hz, 2H), 7.38 (t, *J* = 7.6 Hz, 2H), 7.20 ppm (t, *J* = 7.5 Hz, 2H). **Figure 123:** ¹³C NMR (101 MHz, DMSO-*d*₆) δ 138.97, 125.63, 124.51, 123.76, 120.07, 119.71, 118.91, 111.60 ppm.

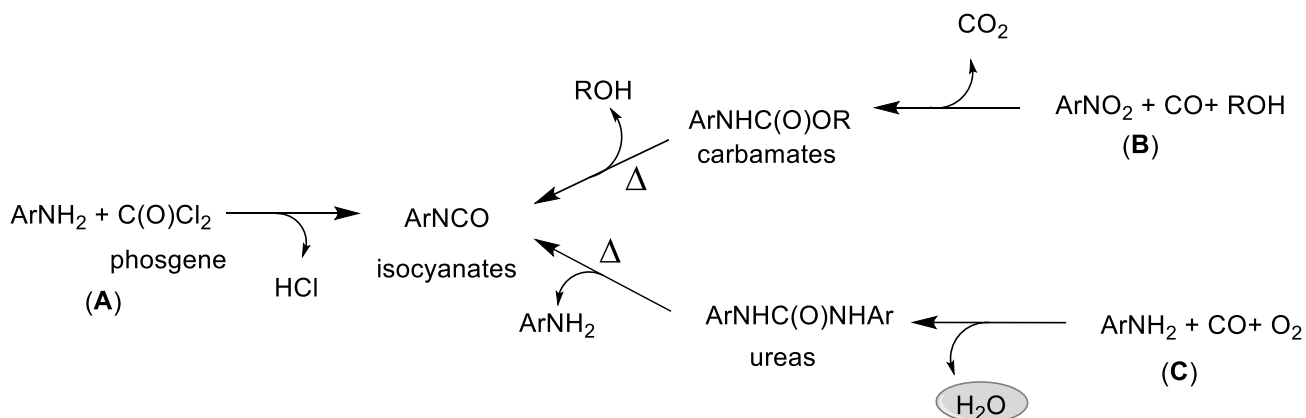
Elemental analysis for C₁₈H₁₂N₂. Calc.: C 84.35; H 4.72; N 10.93. Found: C 84.11; H 4.91; N 10.64.

Chapter II: Oxidative carbonylation of anilines.

1. Introduction.

Isocyanates are important precursors in chemical industry, mostly employed in polyurethane synthesis. Polyurethanes are widely used in almost every part of modern life in the form of plastic foams, coatings, adhesives, sealants, elastomers and binders.^{[178][179]} The annual world production of isocyanates is several millions metric tons and it is steadily increasing. The notable increase of industrial interest for these compounds is evident from the recent investments on new plants by the major producers in both Europe and Asia. The industrial synthesis of isocyanates involves the reaction of an amine with phosgene (**path A in Scheme 35**). From an economical point of view, the phosgene-based route appears to be the most efficient approach and that well-established technology seems to be hard to replace. However, phosgene is a corrosive and very toxic material that is listed as a potential chemical weapon by the Chemical Weapon Convention. In 2006, a large plant producing toluene diisocyanate (TDI) was shut in Italy mainly due to the pressure from the local population and authorities against the use of phosgene close to a densely populated area. Therefore, it is not surprising that a tremendous effort has been made to develop a phosgene-free routes to isocyanates.

The two main alternatives that have been mostly investigated both at an industrial and academic level are the reductive carbonylation of nitroarenes (**path B in Scheme 35**)^[110, 112, 180-181] and the oxidative carbonylation of amines (**path C in Scheme 35**).^[110, 182-184] The former can produce isocyanates in one step, but the direct synthesis of these products requires forcing conditions and the formed isocyanates tend to oligomerize under these conditions. Thus, research in the last few decades have mostly been focused on reactions performed in the presence of an excess of an alcohol or amine. Under these conditions, the obtained products are carbamates and ureas respectively. Both of them can be thermally cracked in a separate step to give the desired isocyanate and regenerate an equivalent of alcohol or amine (**Scheme 35**).^[185-191] Carbamates and ureas are also the products derived from the oxidative carbonylation of amines.



Scheme 35. Reductive carbonylation of nitroarenes and oxidative carbonylation of amines.

Also, it should be noted that carbamates and urea are important chemicals themselves not only possible intermediates in the synthesis of isocyanates. Carbamates are final products and synthetically valuable intermediates for the pharmaceutical ^[192-193] and agrochemical industries ^[194] while, ureas have a variety of applications ^[195], from traditional ones such as fertilizers ^[196] and pesticides ^[197] to the recently developed ones such as receptors for anion recognition ^[198], biosensors ^[199] and pharmaceutically active agents.^[200-201] Thus, the interest in the synthesis of carbamates and ureas extends far beyond their use as intermediates for isocyanate production. The reductive carbonylation route affords carbamates and ureas in one step, but it can only be applied to nitroarenes, since nitroalkanes are much more difficult to reduce and usually exhibit a completely different reactivity compared to their aromatic counterparts. On the other hand, the oxidative carbonylation approach can be applied to both aliphatic and aromatic amines. In the past years, research in our group has been mostly focused on the reductive carbonylation of nitroarenes.^[202-211]

At first sight, it may appear that this reaction and the oxidative carbonylation of amines are very different, but it has been shown that all the most active catalytic procedures for the former reaction involve reduction of the nitroarene to the corresponding aromatic amine, which is subsequently carbonylated.^[212-218] During the latter stage, the metal is reduced. Therefore, the carbonylation step is the same in both pathways and the main difference between them is that the oxidant in one case is the nitroarene and in the other is a separately added oxidant (mostly dioxygen, possibly in the form of air). We thus decided to study the oxidative carbonylation of amines, to see if we could enhance the current state of the art taking advantage of our previous expertise.

Among the different reported catalytic strategies for this reaction, the one that has been most studied and appears to be promising for potential industrial applications is that based on the use of a palladium catalyst with an iodide salt or iodine as a promoter.^[219-248] Fukuoka was the first to report the promoting effect of iodide/iodine while using a heterogeneous catalyst ^[219-222], but the activity of this system was quite low. Later, the activity of heterogeneous systems has been improved by others ^[223, 226-227, 229, 238, 244, 246] However, the turnover frequencies (TOF) that can be achieved are only one or two orders of magnitude lower than those obtained when employing homogeneous palladium catalysts. Therefore, we decided to focus on the use of homogeneous systems.

The possible products of the reaction are ureas, oxamides (double carbonylation products) or carbamates. The latter are produced when an alcohol is employed as solvent. However, similarly to what occurs during the reductive carbonylation of nitroarenes, at least in the case of aromatic amines carbamates are only formed later in the reaction by alcoholysis of the formed urea. Thus, we decided to avoid the use of alcohols in our first investigation to focus on the carbonylation step. Aniline was utilized as substrate because aromatic isocyanates are the most important. In addition, the oxidative carbonylation of aromatic amines is in general harder than that of the more nucleophilic aliphatic amines and achieving suitable conditions for the carbonylation of the former may lead to a strategy that can be extended to the latter easily. However, we also consider the possible extension of the obtained results to aliphatic amines. Thus, as a starting point we choose a system in the literature that is not only highly active but can also give high selectivity for both aromatic and aliphatic amines.

Moreover, some outstanding results were obtained using non-conventional solvents such as supercritical CO₂ and ionic liquids.^[239, 243, 245] Generally, highly polar solvents such as DMF give

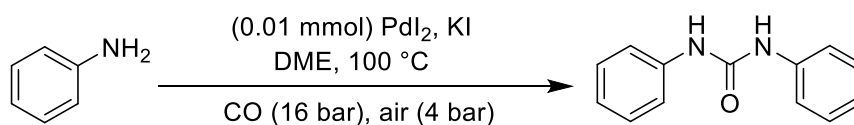
faster reactions, but in case of using aliphatic amines as substrates, significant amounts of oxamide byproducts were formed. Gabriele and coworkers ^[234] were able to obtain the highest selectivity in ureas through the use of dimethoxyethane (DME) as solvent and this was our starting point.

2. Results and discussion.

2.1. Role of iodide.

First, we tried to reproduce some of the best results reported in Gabriele's article.^[234] (Table 16, entries 1 and 2) employing PdI₂ as catalyst and KI as promoter, assembling the reaction in a Teflon-coated autoclave (entry 3). To our surprise, the activity of the catalytic system was much lower than expected.

Table 16. Effect of the autoclave internal coating in the PdI₂ catalyzed oxidative carbonylation of aniline.^(a)



Entry	KI/Pd mol ratio	time (h)	PhNH ₂ conv. (%) ^(b)	urea sel. (%) ^(c)
1 ^d	10	15	89.0	84.3
2 ^d	100	16	96.0	90.6
3 ^e	10	16	33.7	60.6
4 ^f	10	16	100	94.6

(a) Experimental conditions: the reactions were carried out using 10 mmol of aniline at 100 °C under 16 bar of CO and 4 bar of air, in DME (10 mL). PdI₂ = 0.01 mmol. (b) Based on starting aniline and on quantitative GC analysis using benzophenone as an internal standard. (c) Based on reacted aniline and on quantitative HPLC analysis using benzophenone as an internal standard. (d) Data from ref.^[234] (e) Performed in a Teflon-lined stainless steel autoclave. (f) Performed in a stainless-steel autoclave.

Since a stainless-steel autoclave without Teflon coating was used in Gabriele's work, we considered the possibility that iodide ion and the hydriodic acid formed during the reaction could etch the metal from the autoclave walls. For this reason, we performed a reaction in a non-coated stainless-steel autoclave. In this way, the literature results were indeed reproduced (entry 4, Table 16).

The role of iodide has been attributed to various reasons in the previous literature, due to its adsorption onto heterogeneous palladium nanoparticles ^[222-223], to the formation of N-iodoaniline ^[230], to that of carbamoyl iodides (RNHC(O)I) ^[249], to the generation of anionic low valent palladium complexes such as [Pd(CO)₃I]⁻, considered to be the catalytically active species ^[225, 232], and particularly to the ability of iodine, formed by iodide anion by the action of dioxygen, to re-oxidize palladium(0) complexes formed at the end of the catalytic cycle back to palladium(II) ^[233-235, 239, 241, 250]. Direct oxidation of palladium(0) complexes by oxygen is also possible ^[251], but is generally too slow to avoid precipitation of metallic palladium under carbonylation conditions. Indeed, a co-catalyst, that acts as an oxidation catalyst for palladium, is required and the I₂+KI system is able to play this role by oxidizing even

metallic palladium and being quickly re-oxidized by dioxygen.^[250] However, in most of the published oxidative carbonylation works, the reaction was performed in stainless steel autoclaves and only in few cases Hastelloy autoclaves^[223, 226-227, 229] or even less frequently glass reactors^[225, 232, 235] were used and these were not the cases in which the highest activities were observed.

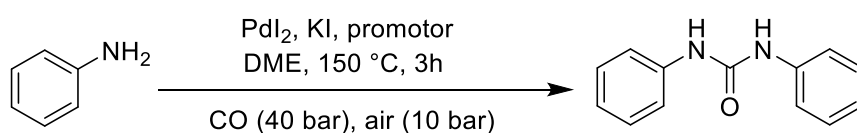
2.2. Effect of iron-containing promoters.

Iron is the most abundant element in stainless steel, so we tested the use of iron salts as promoters for the catalytic reactions.^[252] In the previous literature, some examples have been reported of palladium catalyzed carbonylation reactions of nitroarenes that employ iron as co-catalyst, in which aniline appears to be an intermediate.^[110] Furthermore, recently Krogul and Litwinienko^[242] have investigated the effect of iron on the PdPy₂Cl₂/I₂ catalyzed oxidative carbonylation of amines to carbamates and a considerable effect of iron was recorded mostly on selectivity. However, the effect of iron in the absence of iodine was not studied.

Since the reaction at 100 °C is relatively slow (less than 100 turnovers/hour on average) and aiming for an industrial application, we decided to study the reaction under harsher conditions, 150 °C, 40 bar of carbon monoxide and 10 bar of air. It must be noted that the ratio between the gases is such that the system is outside the CO/O₂ flammability limits.^[253] This has not always been the case for previously reported systems. In general, rising the O₂ relative amount over the lower limit results in faster reactions, but the associated risk would not be acceptable at an industrial level. The catalyst loading was also decreased from 0.1 to 0.02 mol%.

We started by testing different iron promoters, FeCl₃, FeCl₂, FeSO₄·2H₂O, Fe(CO)₅ and Fe(OAc)₂, using PdI₂ as the catalyst. First, as a control experiment, we performed our reactions without the catalyst, both with and without potassium iodide as promoter and we found that no product was formed (entries 1 and 2, Table 17).

Comparing the results of the reactions performed with and without an iron promoter, it can be clearly observed that iron has a positive effect on the catalytic system, both on the conversion and on the selectivity. On the other hand, the effect of iodide is quite ambiguous. Indeed, we confirm that iodide accelerates the reaction when no iron is present (entries 3 and 4, Table 17), but when an iron co-catalyst is present, it inhibits it. Iron acetate and iron sulfate give similar results in the catalytic reactions performed without KI. Addition of the latter has a negative effect mainly on the conversion (entries 8 and 9). This inhibitory effect can be observed also in the reactions carried out with FeCl₃. Comparing the results in entries 15-17, in which the promoter amount is kept the same, the conversion decreases with an increase in the KI amount. Moreover, the negative influence of KI is more evident in the presence of FeCl₂ and FeCl₃ (compare entries 13 with 11 and 17 with 15). The best results were obtained when FeCl₂ and FeCl₃ are used as co-catalysts without potassium iodide, giving a relatively high conversion and selectivity (entries 11 and 15). Further increase of the iron amount over a Fe/Pd = 50 ratio resulted in a decrease in selectivity (compare entries 11 and 12).

Table 17. PdI₂ catalyzed reactions using different iron promoters.^(a)

Entry	KI/Pd mol ratio	promoter	promoter/Pd mol ratio	PhNH ₂ conv. (%) ^(b)	urea sel. (%) ^(c)
1 ^(d)	-	-	-	<1	-
2 ^(d)	100	-	-	<1	-
3	-	-	-	20.3	88.7
4	100	-	-	31.5	51.2
5	100	Fe(CO) ₅	50	40.2	78.1
6	100	Fe(CO) ₅	100	46.8	45.1
7	100	FeSO ₄ ·2H ₂ O	30	19.0	79.0
8	-	FeSO ₄ ·2H ₂ O	50	61.7	80.5
9	100	FeSO ₄ ·2H ₂ O	50	20.0	92.0
10	-	Fe(OAc) ₂	50	64.7	85.8
11	-	FeCl ₂	50	95.8	79.8
12	-	FeCl ₂	100	95.0	70.3
13	100	FeCl ₂	50	38.4	74.0
14	100	FeCl ₂	100	81.6	66.7
15	-	FeCl ₃	50	100	70.4
16	10	FeCl ₃	50	91.8	72.5
17	100	FeCl ₃	50	89.4	68.6
18	100	FeCl ₃	100	95.7	63.6
19	100	FeCl ₃	10	30.4	68.9

(a) Experimental conditions: the reactions were carried out in a Teflon-lined stainless-steel autoclave, using 10 mmol of aniline at 150 °C, for 3 hours, under 40 bar of CO and 10 bar of air, in DME (10 mL). Catalyst amount 2.0×10^{-3} mmol.

(b) Based on starting aniline and measured by GC analysis using benzophenone as an internal standard. (c) Based on converted aniline and measured by HPLC analysis using benzophenone as an internal standard. (d) No palladium was added. The KI/Pd ratio reported is calculated based on a hypothetical 2.0×10^{-3} mmol amount of palladium.

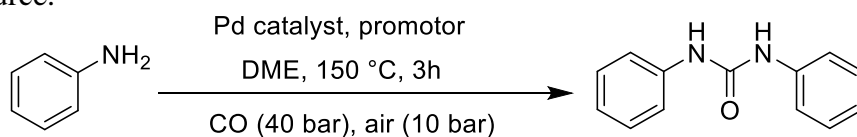
From the data available on the interplay between iron and iodide, it appears that the inhibitory effect of iodide on the iron promoting ability is stronger when the iodide amount is large compared to that of iron and that influence is higher if chloride is also present, despite the effect of chloride is beneficial when no iodide is added.

Taking into account that both iodide and chloride are good ligands for iron(II/III) complexes, the best explanation for the trends observed is that when the total halide concentration highly exceeds that of iron, stable iron complexes (e.g. $[\text{Fe}^{\text{II}}\text{X}_4]^{2-}$ or $[\text{Fe}^{\text{III}}\text{X}_6]^{3-}$) are formed, which are unable to enter the catalytic cycle. In fact, aniline can coordinate both to palladium and iron and the generation of these complexes may influence the outcome of the catalytic reaction. On the other hand, formation of stable halide complexes also decreases the iodide concentration in solution, which in turns can even decrease the promoting effect of iodide. Later, we will discuss this aspect in more depth.

In order to completely avoid the use of iodine which is toxic and difficult to remove from the reaction, we tested both $\text{Pd}(\text{OAc})_2$ and PdCl_2 as catalysts (Table 18).

Use of palladium acetate alone gave a low conversion and a poor selectivity into diphenylurea (entry 1, Table 18). When PdI_2 was used under the same conditions, conversion was comparable, but selectivity was higher (compare entry 1, Table 18, with entry 3 in Table 17). The addition of iron salts not containing halides, such as FeSO_4 and $\text{Fe}(\text{OAc})_2$, had a moderate effect on conversion, which may be positive or even negative depending on the relative amounts, and a positive effect on selectivity (entries 2-4). It can be noted that in the absence of any halide, the addition of $\text{Fe}(\text{CO})_5$ inhibited the reaction (entry 5). This is an important observation because $\text{Fe}(\text{CO})_5$ is a typical contaminant of carbon monoxide, especially when it is stored in steel tanks. We employed aluminum alloy tanks during all of this work, which should minimize the $\text{Fe}(\text{CO})_5$ content in our CO. The tank material was never specified in the previous works, but it is obvious that steel tanks were used at least in the older works, since aluminum alloy tanks have become more commonly used only recently. Therefore, it is clear that iron itself is not a promoter and only when a suitable anion is present it efficiently accelerates the reaction.

Table 18. Pd(OAc)₂ and PdCl₂ catalyzed reactions using different iron promoters and in the absence of any iodide source.^(a)



Entry	catalyst	promoter	promoter/Pd mol ratio	PhNH ₂ conv. (%) ^(b)	urea sel. (%) ^(c)
1	Pd(OAc) ₂	-		22.2	50.0
2	Pd(OAc) ₂	FeSO ₄ ·2H ₂ O	50	30.7	76.7
3	Pd(OAc) ₂	Fe(OAc) ₂	50	19.0	75.3
4	Pd(OAc) ₂	Fe(OAc) ₂	100	8.3	55.4
5	Pd(OAc) ₂	Fe(CO) ₅	50	6.5	55.1
6	Pd(OAc) ₂	FeCl ₂	10	95.0	82.3
7	Pd(OAc) ₂	FeCl ₂	50	97.0	79.4
8	Pd(OAc) ₂	FeCl ₂	100	97.2	74.3
9	Pd(OAc) ₂	FeCl ₃	10	95.3	81.2
10	Pd(OAc) ₂	FeCl ₃	50	99.6	76.9
11	Pd(OAc) ₂	FeCl ₃	100	98.9	72.9
12	PdCl ₂	FeCl ₃	50	99.2	76.6
13	PdCl ₂	FeSO ₄ ·2H ₂ O	50	63.5	70.5
14 ^(d)	Pd(OAc) ₂	FeCl ₂	10	68.0	86.9
15 ^(e)	Pd(OAc) ₂	FeCl ₂	10	41.8	85.0
16		FeCl ₃	50 ^f	3.1	14.3

(a) Experimental conditions: the reactions were carried out in a Teflon-lined stainless-steel autoclave, using 10 mmol of aniline at 150 °C, for 3 hours, under 40 bar of CO and 10 bar of air, in DME (10 mL). Catalyst amount 2.0×10^{-3} mmol. (b) Based on starting aniline and measured by GC analysis using benzophenone as an internal standard. (c) Based on converted aniline and measured by HPLC analysis using benzophenone as an internal standard. (d) Reaction time 1 hour. (e) Reaction time 30 min (see text for a discussion of this reaction). (f) The promoter/Pd ratio is calculated based on the standard 2.0×10^{-3} mmol palladium amount, even if the reaction was run in the absence of any palladium compound.

Much better conversions and selectivity were obtained when palladium acetate was combined with FeCl₂ or FeCl₃ (Table 18, entries 6-11). A graphical representation of the obtained results (**Figure 124**) shows that FeCl₂ and FeCl₃ have very similar effect. Clearly, the initial oxidation state of iron is not

important, both precursors will equilibrate to the same complex under the reaction conditions, and the small observed difference is because of the slightly different chloride content of the catalytic mixture. Notably, only 10 equivalents of iron with respect to palladium (0.2 mol% with respect to aniline) is enough to boost the activity almost to its highest level. A small positive effect on conversion was observed with further increase of the iron amount but the selectivity decreased.

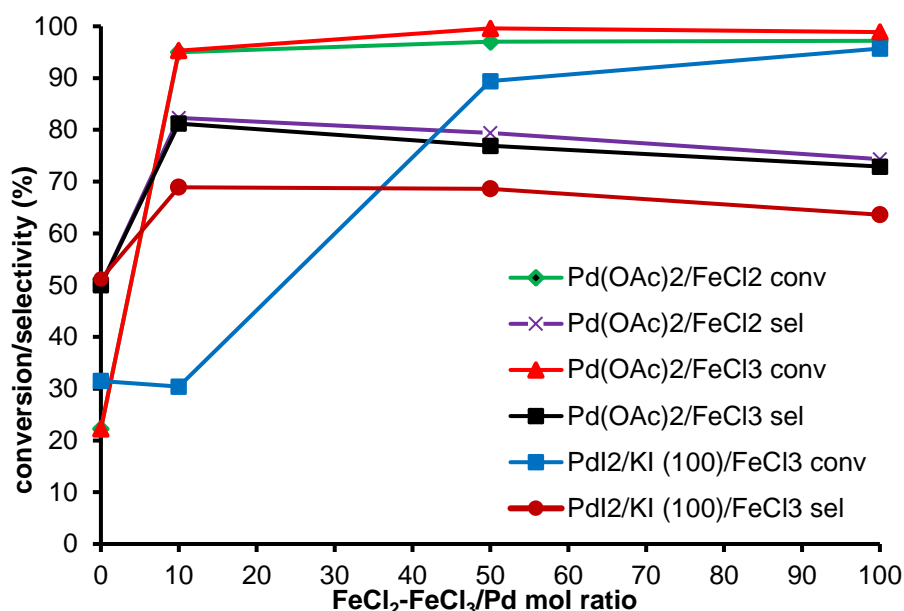


Figure 124. Effect of FeCl₂ and FeCl₃ as co-catalysts in the oxidative carbonylation reactions of aniline catalyzed by Pd(OAc)₂ and PdI₂+KI (mol ratio KI/Pd=100). Data from Tables 17 and 18.

Also, palladium chloride was tested as catalyst in the presence of either FeCl₃ or FeSO₄·2H₂O as promoters. The results were comparable to those obtained using palladium iodide as catalyst under the same conditions (compare entry 12 in Table 18, with 15 in Table 17 and entry 13 in Table 18 with entry 8 in Table 17). On the other hand, it is worth noting that worse results were obtained with the use of Fe(CO)₅, FeSO₄·2 H₂O, and Fe(OAc)₂ as promoters and palladium acetate as catalyst compared to the use of the same promoters with palladium iodide.

As a final experiment, a reaction was carried out in the presence of FeCl₃ and in the absence of any palladium compound (entry 16). A very low conversion and trace amounts of diphenylurea were observed, proving that iron itself has a negligible catalytic activity in this reaction and also that no or insignificant palladium contamination of the Teflon coating of the autoclave occurred.

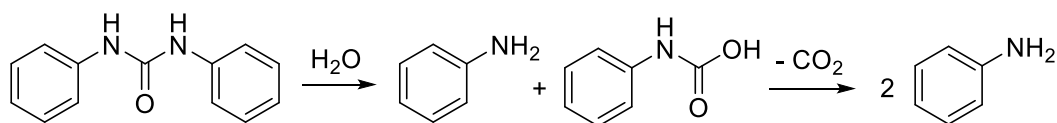
Overall, the trends discussed above show that the best results are achieved when palladium and iron are employed together and in the presence of a halide. Iodide is no better than chloride and it does not seem to be relevant whether the halide is initially bound to either palladium or iron or both.

The results obtained when Fe(CO)₅ is employed as promoter must be taken into consideration. This compound enhance the reaction when PdI₂ is used as catalyst, but inhibits it when Pd(OAc)₂ is employed. This confirm that the presence of a halide is necessary for iron to act as a promoter and a very small amount of it may already have a considerable influence, even if a larger amount is more

effective (see later). This result is important in understanding the data reported in the previous literature. As mentioned before, some $\text{Fe}(\text{CO})_5$ was definitely present in the CO gas employed in most earlier reports and this has likely resulted in the generation of some iron salts even when Hastelloy or glass reactors were used. Therefore, the role of iodide may have been at least in part linked to its interaction with iron even in those cases in which it did not actively provide the required iron by etching the autoclave walls.

The negative effect of an excess of halide has been explained above. The positive effect of a small amounts of halide may be attributed to the formation of bimetallic Pd-Fe complexes with a halogen bridge since halides are much better bridging ligands than all other anions we tested, but a simpler effect of halides on the redox potentials of the palladium and iron species involved must also be considered.

Finally, it should be considered that at 150 °C, in 3 hours, diphenylurea can be hydrolyzed by the water formed during the reaction (**Scheme 36**). The so formed aniline may be carbonylated again but may also give byproducts. Thus, prolonging the reaction time once the reaction is almost complete can only have negative effects. To test this possibility, we repeated the reaction corresponding to entry 6 in Table 18 but stopping it after one hour or after just 30 min. The results (entry 14 and 15 in Table 18) demonstrate that a higher selectivity is obtained in a shorter reaction time.



Scheme 36. Hydrolysis of diphenylurea.

The hydrolysis of diphenylurea was independently tested under the reaction conditions in Table 18, starting from the urea and water concentrations that may be present at the end of the reaction if a complete conversion of aniline into diphenylurea and water took place, without any side reaction. In the absence of any other compound and in the Teflon-lined autoclave, the hydrolysis was negligible, but the presence of a FeCl_3 amount equal to that used in run 12 in Table 18 resulted in the hydrolysis of 16% of the urea. Palladium salts can also catalyze this hydrolysis, but we could not test them because they may have also caused the back carbonylation of some of the formed aniline.

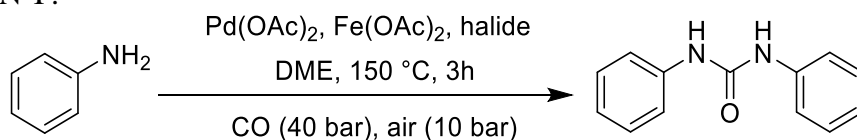
Notably, already a 41.8 % conversion was observed after 30 min, corresponding to a TOF of 4190/h (or 1780/h with respect to the formed urea). However, it must be considered that the TOF values measured at a short reaction time are strongly underestimated in our case. In fact, we placed our autoclaves in a preheated oil bath and counted the time of the reaction from that moment. However, the insertion of the autoclave into the bath caused the oil temperature to drop, which took 15 min to reach again the set temperature. Surely, the content of the autoclave took even longer time to equilibrate due to the insulating power of the Teflon coating (2 mm thickness). Thus, the reaction was stopped very close to the moment in which the reaction solution reached the set temperature or even earlier than it did. ^[254]

2.3. The effect of different I/Fe and Cl/Fe ratios

Comparing the reactions performed in the Teflon lined stainless-steel autoclave using Pd(OAc)₂ in absence of KI with those made using PdI₂ in the presence of KI, with FeCl₃ as co-catalyst (**Figure 124**), it is clear that better results are obtained when iodide is absent. Moreover, there is a strong negative effect on conversion when a low amount of FeCl₃ is used, which further confirms the hypothesis made earlier that iodide coordinates to iron. Indeed, the worse result is obtained when a low amount of FeCl₃ (Fe/Pd = 10) is added to a solution containing a much larger amount of iodide (I/Pd=100). Under these conditions, iron is probably completely deactivated, and its role is to only withdraw iodide from the solution, so that a mutual deactivation occurs.

To better study the effect of the amount of chloride and iodide independently from the amount of iron, we decided to test the effect of different amounts of either tetrabutylammonium chloride or iodide on the activity of a catalytic system, Pd(OAc)₂ + Fe(OAc)₂ (mol ratio Fe/Pd = 50), that does not initially contain any halide. Results are reported in Table 19 and **Figure 125**.

Table 19. Pd(OAc)₂ catalyzed reactions using Fe(OAc)₂ as promoter in the presence of either Bu₄N⁺Cl⁻ or Bu₄N⁺I⁻.^(a)



Entry	halide	halide/Pd mol ratio	PhNH ₂ conv. (%) ^(b)	urea sel. (%) ^(c)
1	-	-	19.0	75.3
2	Cl ⁻	50	54.3	81.2
3	Cl ⁻	100	79.9	79.0
4	Cl ⁻	150	85.2	83.9
5	Cl ⁻	200	93.5	89.0
6	Cl ⁻	250	94.7	89.7
7	I ⁻	50	73.8	85.6
8	I ⁻	100	60.9	82.0
9	I ⁻	150	36.7	85.5
10	I ⁻	200	40.0	83.3
11	I ⁻	250	27.4	74.5

(a) Experimental conditions: the reactions were carried out in a Teflon-lined stainless-steel autoclave, using 10 mmol of aniline at 150 °C, for 3 hours, under 40 bar of CO and 10 bar of air, in DME (10 mL). Catalyst amount 2.0×10^{-3} mmol, mol ratio Fe(OAc)₂/Pd = 50. (b) Based on starting aniline and measured by GC analysis using benzophenone as an internal standard. (c) Based on converted aniline and measured by HPLC analysis using benzophenone as an internal standard.

Tetrabutylammonium was selected as a counter cation to ensure complete solubility of the salt under the reaction conditions and minimize electrostatic interactions between the cation and the halide, which may affect the reactivity of the latter.

Figure 125 demonstrates a clear trend with respect to chloride amount for the catalytic reactions: both conversion and selectivity increase with increasing tetrabutylammonium chloride content. The effect is more noticeable on the conversion but tends to flatten at the highest ratios. The effect on selectivity is more limited, but still significant. The ideal amount of $\text{Bu}_4\text{N}^+\text{Cl}^-$ is 250 to 1 with respect to the catalyst (at a Fe/Pd ratio of 50), that is a 5:1 ratio compared to iron (or about 5:1 with respect to the sum Fe+Pd).

The effect of iodide is quite different, though not unexpected, given the previous results. An amount of iodide equimolar to that of iron promotes the reaction even more efficiently than the same amount of chloride, but a further increase leads to an inhibition of the reaction. At a 5:1 I/Fe mol ratio the results both in term of conversion and selectivity are close to those obtained in the absence of iodide, which are in turn close, at least for the conversion, to those obtained with $\text{Pd}(\text{OAc})_2$ in the absence of both iron and iodide (Table 18, entry 1).

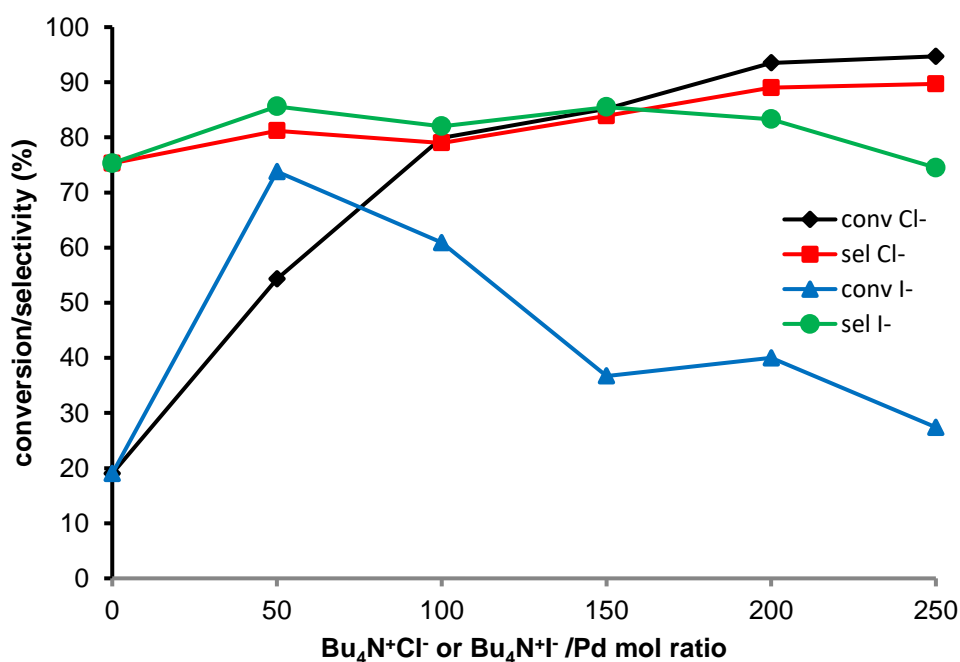


Figure 125. The effect of $\text{Bu}_4\text{N}^+\text{Cl}^-$ and $\text{Bu}_4\text{N}^+\text{I}^-$ on the oxidative carbonylation of aniline catalyzed by $\text{Pd}(\text{OAc})_2 + \text{Fe}(\text{OAc})_2$ (mol ratio Fe/Pd = 50). Data from Table 19.

It may seem surprising that increasing the amount of chloride increases the conversion whereas that of iodide has an inhibiting effect. However, it should be recalled that the reaction produces water and the latter gives strong hydrogen bonds to chloride, markedly decreasing its nucleophilicity and tendency to coordinate to metals^[255-256]. The same occurs with iodide to a much lower extent. Indeed, it is well known that the order of nucleophilicity is $\text{F} > \text{Cl} > \text{Br} > \text{I}$ in non-protic solvents, but exactly the reverse in water and alcohols^[255-256]. Thus, the amount of halide necessary to give the same number of coordinated halide anions is larger for chloride than for iodide. If we naively suppose that the

coordinating ability of iodide is not affected at all by water, then we reach the conclusion that the ideal “coordinated halide”/(Fe+Pd) mol ratio is close to one. This is clearly simplified, but the actual number should be very close. As discussed before, we concluded that the inhibiting effect of halides can be explained by the possible formation of stable iron complexes of the kind $[\text{Fe}^{\text{II}}\text{X}_4]^{2-}$ or $[\text{Fe}^{\text{III}}\text{X}_6]^{3-}$, thus coordination of aniline would be inhibited. However, the results now obtained show that the amount of iodide sufficient to inhibit the reaction is much lower than that required to generate such complexes. An ideal 1:1 “coordinated halide”/(Fe+Pd) ratio is only consistent with the formation of halogen-bridged Pd-X-Fe or Fe-X-Fe species as catalytically active species.^{[257][258-260]} Higher halide concentrations would be sufficient to break such complexes even if considerably lower than those required to completely saturate the coordination sphere of the isolated palladium and iron ions.

As previously mentioned, iron compounds have been utilized in several cases as promoters for palladium-catalyzed reductive carbonylation reactions of nitroarenes. By analyzing the available information, mostly contained in the patent literature, it was noted more than twenty years ago that all active systems also contained chlorides^[180]. Since much evidence also suggested that amines were intermediates in the process, it was proposed for the first time that the role of palladium might be that of carbonylating the amine and that of iron to reduce the nitroarene and re-oxidize palladium. However, it was also considered that a bimetallic Pd-Fe complex with bridging chlorides might be the real catalytic species^[180, 214]. At the time, the comparison between the reductive carbonylation of nitroarenes and the oxidative carbonylation of amines was not stressed for the palladium catalysts because it seemed that the oxidative carbonylation reaction did not need a second metal. However, the results just discussed strengthen the similarity between the two reactions and led support to the hypothesis that bimetallic species may be involved in both cases.

2.4. Reactions under milder conditions

The results discussed above prove that a high conversion can be reached in a short time at 150 °C, but the selectivity of the reaction reaches a maximum around 90%, that would not be enough for an industrial application. To increase the selectivity over this limit, we decided to investigate lower reactions temperatures, even if this means to slow down the reaction. Thus, we lowered the temperature to 100 °C and the pressure to a total of 20 bar and increased the reaction time to 15 h (Table 20).

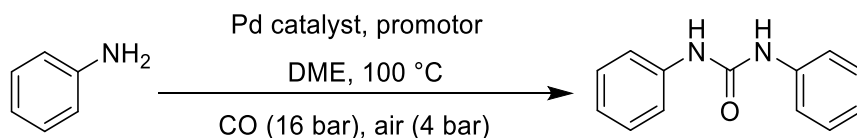
First, we investigated the effect of small amounts of iron promoter (Table 20, entries 1-5). The ideal Fe/Pd ratio is confirmed to be around 10 even under these milder conditions, but it is noteworthy that just a 1:1 ratio Fe/Pd is sufficient to double the conversion with respect to the palladium-only system. This ratio corresponds to just two μmol of iron!

It was also shown that 15 h are not required to reach complete conversion and 6 h are enough (entry 6). However, a shorter time, 3 h, is not enough at this temperature, even when the pressure is increased back to the previously employed values (Entry 7).

Unfortunately, no benefit was observed on selectivity by lowering the reaction temperature. The effect of the catalyst amount was thus investigated by increasing it fivefold at a constant aniline concentration. Both PdI_2 (entries 8-13) and $\text{Pd}(\text{OAc})_2$ (entries 14 and 15) were tested at this catalytic

ratio, in the presence of either KI or FeCl₃ as promoters. The results obtained confirm the generality of the observation made under more forcing conditions: KI is a less effective promoter than FeCl₃ for PdI₂ and the catalytic system lacking any iodide is better than those containing it. However, again better selectivity was not achieved by lowering the catalytic ratio. On the other hand, a direct comparison between entries 6 and 15 confirms that better selectivity is obtained with less catalyst, in agreement with the previously reached conclusion that a higher absolute amount of FeCl₃ causes a decrease in selectivity.

Table 20. Synthesis of diphenylurea under milder conditions.^(a)



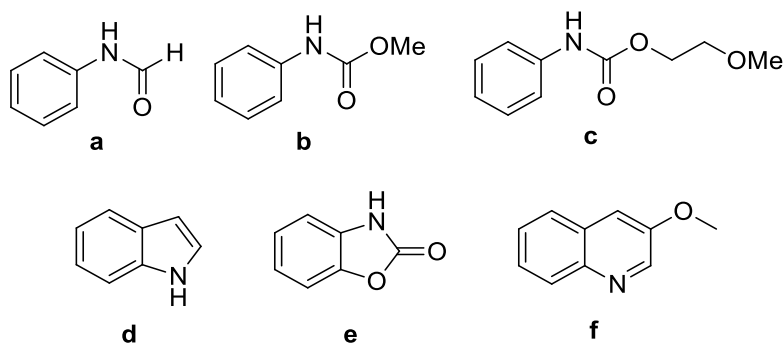
Entry	catalyst	promoter	PhNH ₂ /Pd mol ratio	promoter/Pd mol ratio	t (h)	PhNH ₂ conv. (%) ^b	urea sel. (%) ^c
1	Pd(OAc) ₂	-	5000	-	15	37.2	86.8
2	Pd(OAc) ₂	FeCl ₃	5000	1	15	71.9	83.2
3	Pd(OAc) ₂	FeCl ₃	5000	3	15	90.5	85.5
4	Pd(OAc) ₂	FeCl ₃	5000	10	15	100	83.4
5	Pd(OAc) ₂	FeCl ₃	5000	50	15	100	82.1
6	Pd(OAc) ₂	FeCl ₃	5000	50	6	100	80.8
7 ^d	Pd(OAc) ₂	FeCl ₂	5000	10	3	75.5	87.9
8	PdI ₂	KI	1000	10	3	9.0	28.7
9	PdI ₂	KI	1000	10	6	19.4	26.2
10	PdI ₂	KI	1000	10	16	33.7	60.6
11	PdI ₂	FeCl ₃	1000	10	6	91.5	80.4
12	PdI ₂	FeCl ₃	1000	10	15	96.0	67.7
13	PdI ₂	FeCl ₃	1000	50	15	89.9	66.7
14	Pd(OAc) ₂	FeCl ₃	1000	50	15	100	81.9
15	Pd(OAc) ₂	FeCl ₃	1000	50	6	100	74.6

(a) Experimental conditions: the reactions were carried out in a Teflon lined stainless-steel autoclave, using 10 mmol of aniline at 100 °C under 16 bar of CO and 4 bar of air, in DME (10 mL). (b) Based on starting aniline and measured by GC analysis using benzophenone as an internal standard. (c) Based on converted aniline and measured by HPLC analysis using benzophenone as an internal standard. (d) Under 40 bar of CO and 10 bars of air.

2.5. Reaction byproducts.

Although many studies have been devoted to the oxidative carbonylation of amines with different catalysts, we are not aware of any paper in which the identity of the byproducts (except for oxalamides) were investigated in detail. The observation of formanilide, derived from the reductive elimination from a PhNHC(O)-Pd-H complex, has occasionally been mentioned. ^[261] In order to shed light on the lack of full selectivity for the oxidative carbonylation reaction we subjected the reaction mixture of several of the catalytic reactions showing high conversion, but poor selectivity to GC-MS and HPLC-MS analyses.

From the GC-MS analyses (**Figure 126, 127 and 128**), it immediately emerges that apart from the aniline and phenyl isocyanate peaks (which derive from a thermal cracking of the product diphenylurea, also observable as a weak peak, under the injector conditions) and trace amount of formanilide (**a**), some smaller peaks can be observed. These are clearly identified in the NIRST database as methyl phenylcarbamate (**b**), 2-methoxyethyl phenylcarbamate (**c**) and indole (**d**). Some even smaller peaks could be identified as benzoxazolone (**e**) and 3-methoxyquinoline (**f**) (**Scheme 37**).



Scheme 37. Byproducts observed by GC-MS.

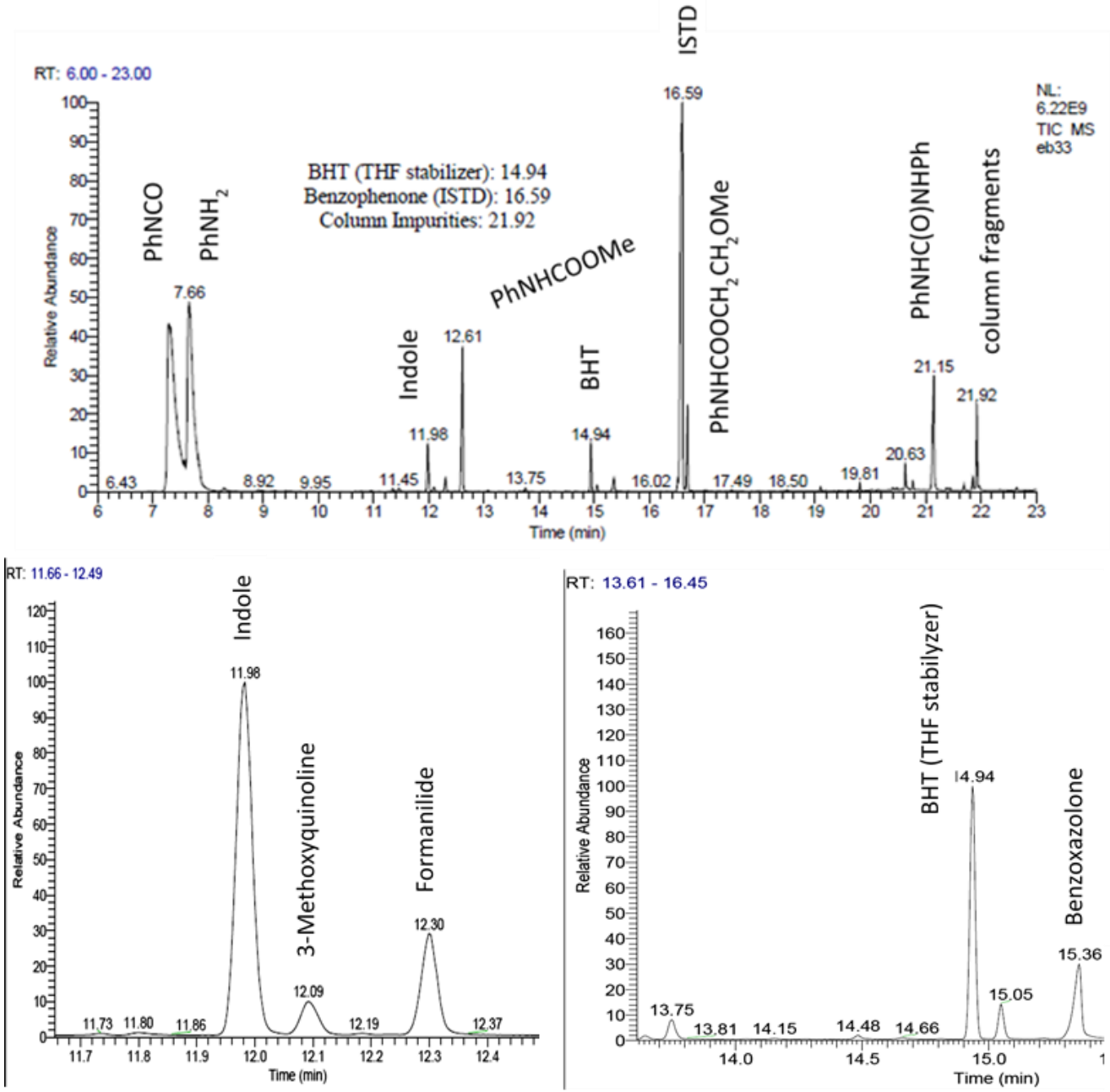


Figure 126. Chromatogram of GC-MS analysis (EI).

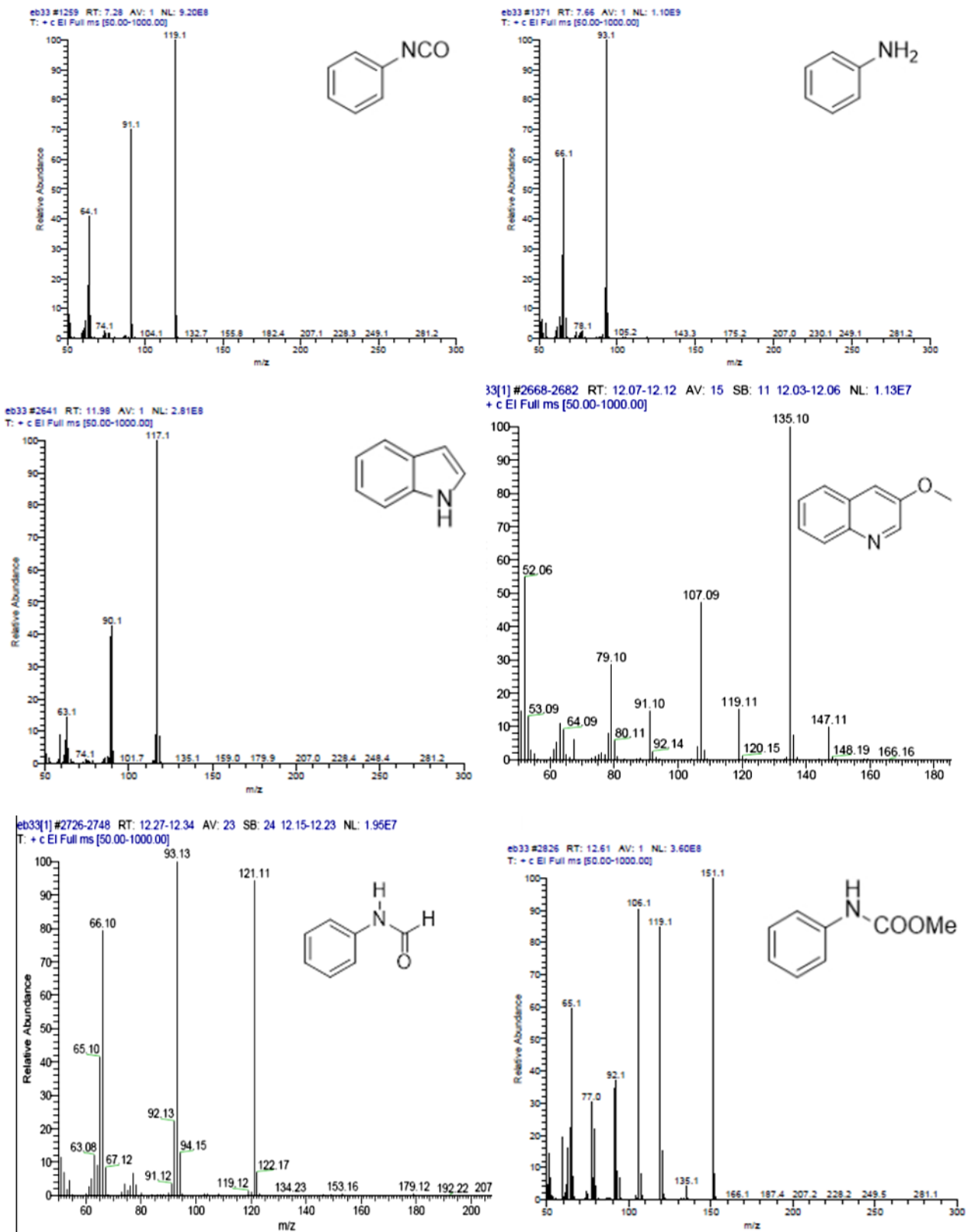


Figure 127. Detailed mass spectrum of each peak in the chromatogram of the GC-MS analysis (EI).

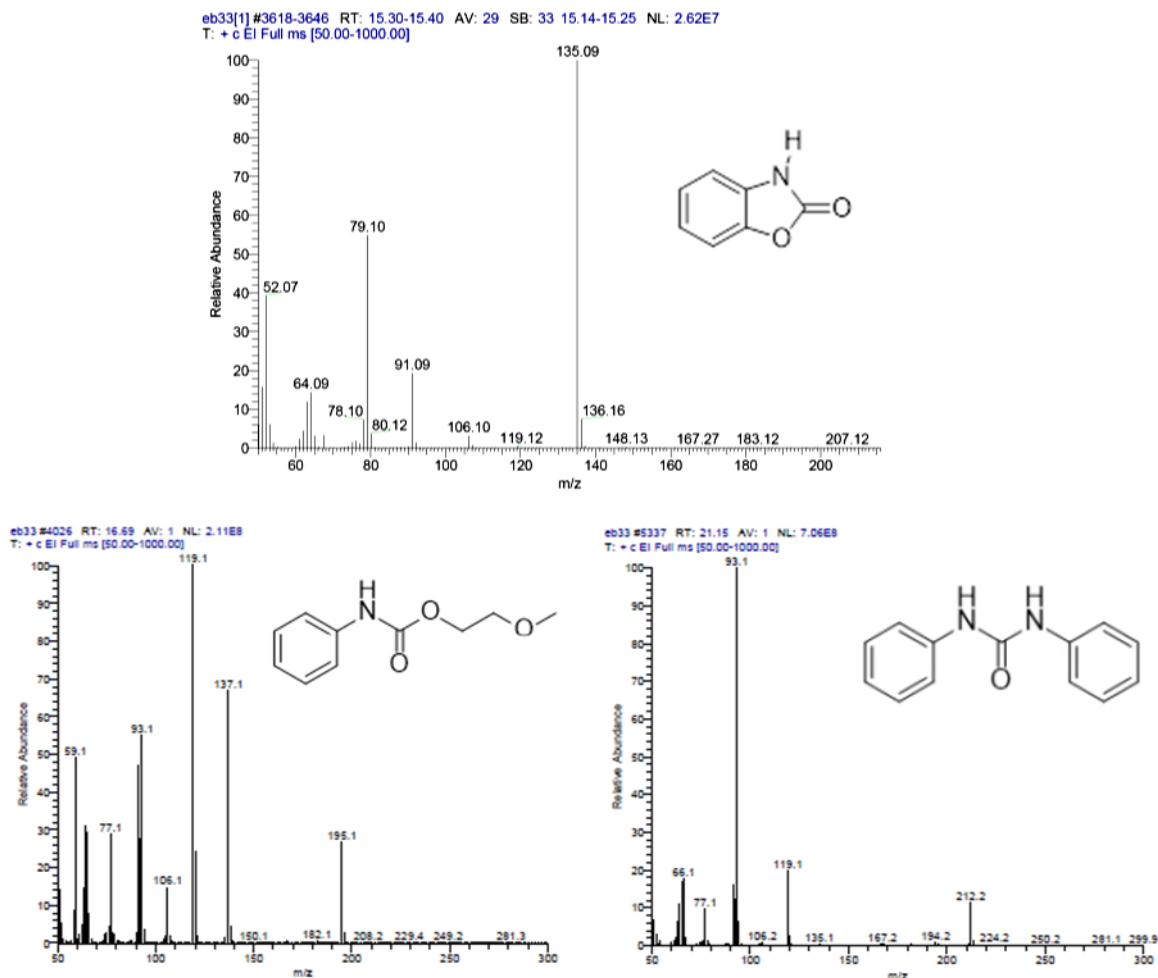


Figure 128. Detailed mass spectrum of each peak in the chromatogram of the GC-MS analysis (EI).

The HPLC chromatogram, on the other hand, was very clean and only the diphenylurea peak could be clearly observed (**Figure 129**). Specifically, no oligomeric polyanilines could be detected by this technique. The latter would result from the direct oxidation of aniline by dioxygen and would easily escape GC analysis.

The observation of phenyl isocyanate by gas-chromatography should not be taken as a proof of its presence in solution without other supporting evidence. Indeed, diphenylurea can extensively thermally crack in the injector of the instrument. For example, no aniline had remained at the end of the reactions investigated by GC-MS in this work and yet the aniline peak is among the most intense in the GC-MS spectrum (**Figure 126**). Gas-chromatographic analysis of aniline and phenyl isocyanate should only be performed by employing a programmed variable temperature injector, so that the temperature can be increased to the final value only after the more volatile (including aniline) compounds of the mixture have left the injector. We routinely used such a procedure in the quantitative analyses of our reaction mixtures and never observed the presence of phenyl isocyanate. Thus, we are confident that the isocyanate observed during the GC-MS analysis is an artefact of the analytical technique.

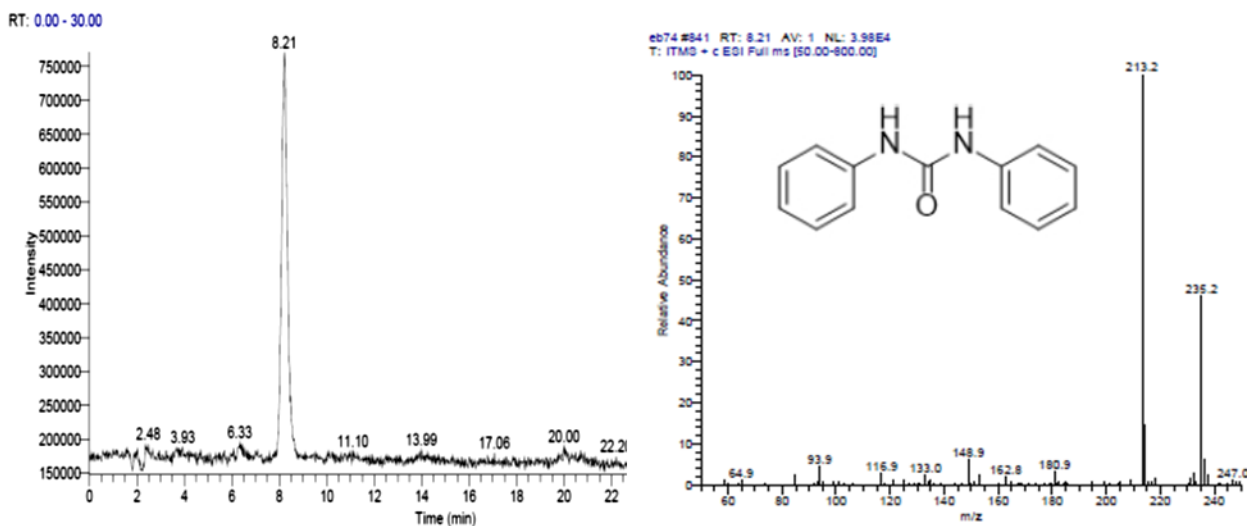
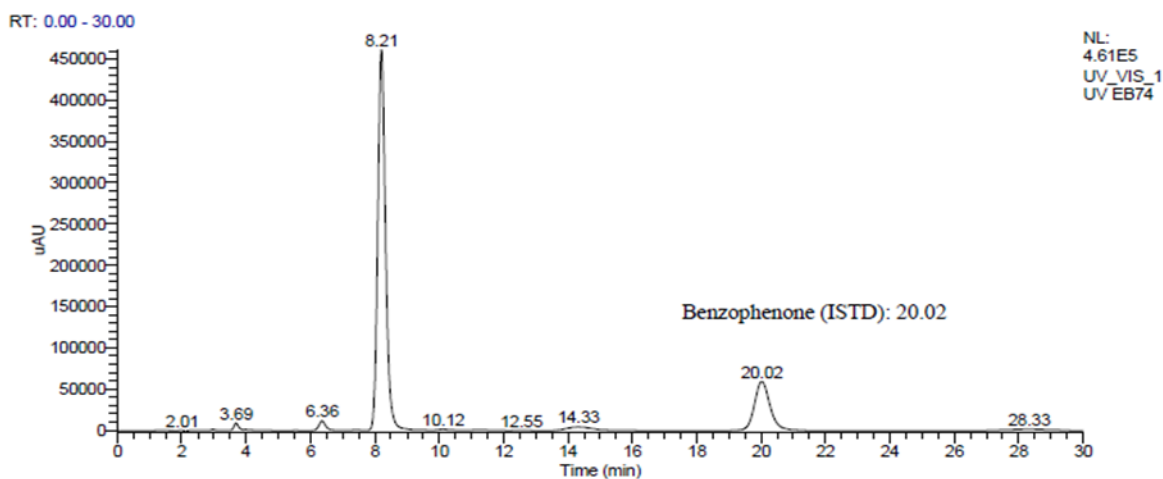


Figure 129. Representative HPLC-MS analysis (ESI+)

Although the formation of the products in **Scheme 37** was unexpected, it is not difficult to trace back their origin. They are all clearly originating from the hydrolysis of the dimethoxyethane used as the solvent by the water formed during the reaction. The two alcohols so formed result in the formation of the two observed carbamates (**b** and **c** in **Scheme 37**). It should be noted that the reaction between diphenylurea and an alcohol to give a carbamate and an aniline equivalent is well known. It typically occurs to a large extent when oxidative carbonylation reactions of amines or the reductive carbonylation of nitroarenes are performed in an alcohol as solvent. However, it is an equilibrium reaction and only becomes significant in the presence of a large excess of alcohol with respect to the free amine.^[212] Thus, the observed carbamates cannot result from the presence of trace amounts of the two alcohols and their formation implies that DME hydrolysis occurs to a significant extent during the reaction.

Indole (**d**), on the other hand, can derive from a reaction of aniline with ethylene glycol, the doubly hydrolyzed DME. Such reaction is known to occur under oxidizing conditions.^[262-263]

Two more byproducts could be identified, which were present in trace amounts. Benzoxazolone (**e**) clearly derives from the oxidation of aniline in the *ortho* position to give *o*-aminophenol. The latter easily gives the cyclic carbamate under the reaction conditions.^[264] The formation of 3-methoxyquinoline (**f**) is less obvious. The presence of the methoxy group anyway suggests that DME is again involved in its formation.

To quantify at least the main byproducts, pure methyl phenylcarbamate, 2-methoxyethyl phenylcarbamate **105**, and indole were used to set a calibration curve at the gas-chromatograph and the reaction was repeated. The selectivities into these three products were respectively 2.4, 1.1 and 1.0%.

The formation of these products raises some concern on the use of DME as the solvent and suggests that one of the reasons for which it seems to be more effective than others may simply be the fact that it acts as internal drying agent, preventing the formed water to hydrolyze the produced urea.

Another solvent that is often employed in oxidative carbonylation reactions is dioxane. Though we did not investigate the use of dioxane in detail, the GC-MS analysis of the solution after a reaction run in this solvent instead of DME evidenced again the formation of carbamates deriving from its hydrolytical ring opening. In this context, it should also be mentioned that the solvent that often gives the best results in most of the cited references, although with low urea/oxalamide selectivity, is dimethylformamide. The declared, and surely at least partly correct, rationale for this is that it has a high dielectric moment, thus stabilizing the likely very polar transition state of the reaction. However, it should not be forgotten that DMF is far from being an inert solvent.^[265] Its hydrolysis reaction has been studied in detail^[266-267] and DMF has even been used as a drying agent.^[268] Clearly, this would not be an acceptable procedure for an industrial production and a different strategy must be pursued to reach complete conversion. This will be the object of future work.

3. Conclusions

In this work we have investigated in more depth the classical Pd/I catalytic system for the oxidative carbonylation reaction of amines to ureas, which has been previously the topic of at least 30 papers. Some surprising results have been found that lead to extensively reconsider what is known of this catalytic system:

- 1) We confirmed that iodide alone promotes the activity of palladium in the oxidative carbonylation reaction of amines, but its promoting ability is much lower than previously estimated.
- 2) Under most of the previously employed experimental conditions, the main role of iodide is to etch the autoclave walls to provide small amounts of iron in solution.

- 3) When iron etching from the autoclave walls cannot occur, small, but sufficient, amounts of iron may still come from the $\text{Fe}(\text{CO})_5$ present as a contaminant of pressurized CO in all those cases in which iron tanks were used to store it.
- 4) The ideal absolute iron amount under the presently employed conditions (930 mg aniline) is just 1.1 mg, but even a tenfold lower amount (around 12 ppm with respect to the whole solution weight) is sufficient to double the activity of the palladium catalyst. It is worth to note that contamination of iron catalysts by noble metals is well known to be responsible for the catalytic activity observed in some cases. However, the present work is a rare, if not unique, case in which the contamination of a palladium catalysts by trace amounts of iron has such a large promoting effect.
- 5) The presence of a halide is anyway required, but chloride can be equally or even more effective than iodide in this respect. The ideal amounts of chloride and iodide differ, likely because chloride coordination to metal ions can be hindered by the formation of strong hydrogen bonds with the water formed during the reaction, whereas iodide is less affected by the presence of water. A molar amount of iodide larger than that of iron causes a deactivation of the system, suggesting that the active catalytic species may be a Pd/Fe dinuclear or higher aggregate held together by bridging halide ligands.
- 6) The reason for the good efficiency of DME as a reaction solvent is at least partly due to its ability to act as a dehydrating agent, but the alcohols formed by its hydrolysis can reenter the reaction and give small amounts of the corresponding carbamates and even some indole. Hydrolysis of the solvent is likely involved even in other cases.
- 7) Though usually not mentioned, iodine is toxic and difficult to remove completely from the reaction products. This is especially a problem if the produced urea is employed as an intermediate in the synthesis of pharmaceuticals. The possibility of substituting it with a very low amount of non-toxic iron chloride should be viewed favorably from an industrial point of view.

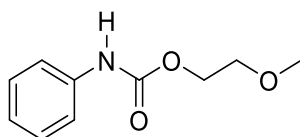
The present work has clarified some previously overlooked aspects of the Pd/I⁻ catalytic system, but at the same time has raised new questions both of industrial and scientific nature: Stainless steel contains other metals apart from iron: do any of them also show any promoting activity? Which is the best way to remove the formed water without resorting to solvent hydrolysis or to the use of any reagent that is stoichiometrically consumed? Which is the exact interplay between palladium, iron and the halide? May a better catalyst can be prepared by knowing this? Work is in progress in our laboratories to answer at least some of them. Our work on the effect of ppm amounts of iron compounds on the classical Pd/I⁻ catalytic system for the oxidative carbonylation reaction of amines to ureas was published in 2019.^[269-270]

4. Experimental work.

4.1. Materials and general procedures.

1,2-Dimethoxyethane used in the catalytic reactions was dried by distillation over Na/benzophenone and stored under a dinitrogen atmosphere. Aniline was distilled over KOH under reduced pressure and stored under dinitrogen. It can be weighed under air without problems but must be stored under an inert atmosphere to avoid oxidation, carbonation, and water uptake. Pd(OAc)₂ [150], and PdI₂ [271] were prepared by literature methods. PdCl₂(CH₃CN)₂ was prepared by refluxing PdCl₂ in acetonitrile until the brown solid had completely dissolved and a yellow solution had formed. The solution was filtered while hot to remove any traces of undissolved material and evaporated to dryness. 2-Methoxyethyl phenylcarbamate was prepared (see below). All the other reagents and solvents were purchased from Sigma-Aldrich or Alfa-Aesar and used without any further purification.

Synthesis and characterization of 2-methoxyethyl phenylcarbamate 105.



1 mL (1.09 g, 9.15 mmol) of phenyl isocyanate was added gradually to an excess of 2-methoxyethanol (4 mL) at RT and the reaction was heated under reflux at 70 °C for 4h. Then the alcohol was removed under reduced pressure and toluene was added to precipitate the urea formed during the reaction because of small water impurities in the solvent or already present in the phenyl isocyanate as a contaminant. The solution was filtered, and toluene was removed from the filtrate under reduced pressure, affording the pure carbamate (1.072 g, 5.49 mmol, 60 % yield).

Figure 130: ¹H NMR (400 MHz, CDCl₃) δ 7.48 (d, *J* = 7.9 Hz, 2H), 7.37 (t, *J* = 7.9 Hz, 2H), 7.14 (t, *J* = 7.9 Hz, 1H), 4.41 (t, *J* = 4 Hz, 2H), 3.72 (t, *J* = 4 Hz, 2H), 3.49 ppm (s, 3H). **Figure 131:** ¹³C NMR (100 MHz, CDCl₃) δ 153.50, 137.94, 128.94, 123.34, 118.69, 70.68, 63.97, 58.79 ppm.

4.2. Catalytic reactions.

All the catalytic reactions were performed in a stainless-steel autoclave lined with Teflon (c.a. 140 mL free volume), or, for the control experiments, directly in a stainless-steel autoclave, both equipped with a stirring bar. Since small amounts of catalyst were used, a stock solution of the catalyst (PdI₂ or PdCl₂, the latter added as PdCl₂(CH₃CN)₂ in aniline) was prepared and stored under dinitrogen atmosphere. The solution already contained the correct Pd/aniline ratio, so that the catalyst was weighed together with aniline. When Pd(OAc)₂ was used as the catalyst it was freshly dissolved in DME and the appropriate amount of the obtained solution was added by volume. In a typical catalytic reaction, the

reagents were transferred to the autoclave always following the same order. First KI, weighted under air, was added. Then the aniline solution, also containing PdI₂ when appropriate, was rapidly weighted under air in a test tube and transferred to the autoclave. To ensure a complete transfer of the reagents to the autoclave, the test tube was washed with the reaction solvent. When Pd(OAc)₂ was used as the catalyst, its solution in DME was added by volume and aniline was weighted in a test tube separately. The remaining amount of solvent was then added by volume, using it to wash the test tube used to weigh aniline. Finally, the iron promoter was added. When the amount of the iron promoter was lower than 10 mg, a freshly prepared solution of it in DME was prepared under dinitrogen atmosphere and then it was added by volume to the reaction mixture.

Reagent amounts or their molar ratios are reported in the tables or in their footnotes. In all cases, the amine concentration was 1 M. The autoclave was then closed, and CO and air were charged in this order at room temperature. The value of pressure after each gas addition was read after complete stabilization of the system (i.e., when it remained constant for at least 5 min). Finally, the autoclave was immersed in an oil bath preheated at the required temperature. This moment was taken as the start of the reaction. At the end of the reaction, the autoclave was quickly cooled in an ice bath and vented. The internal standard, benzophenone, was added to the reaction mixture (1/4 mass ratio with respect to the starting aniline) and 25 mL of THF were also added to completely dissolve both benzophenone and any precipitated diphenylurea. The solution was kept under stirring for half an hour. An aliquot of the obtained solution was then diluted with CH₂Cl₂ to perform the GC and HPLC analyses.

4.3. Quantitative analysis methods for catalytic reactions.

For catalytic reactions, quantitative analyses were performed either on a DANI 86.10 HT gas chromatograph equipped with a SUPELCO Analytical SLBTM-5ms column (Fused Silica Capillary Column 30 m x 0.32 mm x 0.5 μm film thickness), or on a Shimadzu GC-2010 equipped with a Supelco SLBTM-5ms capillary column (GC-FAST technique), or on a HP 1050 series modular HPLC system equipped with a MERCK LiChroCART® 125-4 HPLC-Cartridge Purospher® RP-18e (5μm). HPLC grade solvents - CHROMASOLV® were used for HPLC analyses, which were degassed by sonication in an ultrasonic bath for half an hour before use. Quantitative analyses were carried out using the internal standard method. Benzophenone was used as the internal standard. The wavelength of the UV detector was set at 265 nm because this frequency is close to the maximum absorption of both diphenylurea and benzophenone, thus maximizing the accuracy of the analysis. Unfortunately, aniline absorbs weakly at this wavelength and its analysis is less reliable. This is the reason for which it was routinely quantified by GC.

A standard GC analysis involves the preparation of a sample solution in CH₂Cl₂. An aliquot of the reaction solution, treated as mentioned above, was diluted in CH₂Cl₂ in order to obtain a final standard concentration of 0.05 mg/mL for the analysis made with DANI 86.10 HT and 0.1 mg/mL for the analysis made with Shimadzu GC-2010. Then 1 μL was injected into the GC. This analysis method was used to determine the residual amount of aniline after the catalytic reaction because it showed a higher reproducibility with respect to HPLC analysis. A complete list of the instrumental parameters employed is showed in Table 21 and Table 22.

A standard HPLC analysis involves the preparation of a sample solution in CH₃OH/H₂O 55:45. An aliquot of the previously prepared reaction solution was diluted with CH₃OH/H₂O 55:45 in order to obtain a final standard concentration of 0.01 mg/mL of benzophenone. Then 100 µL of this sample solution were injected into the HPLC (injection loop 20 µL). This analysis method was used to determine the amount of diphenylurea.

Table 21. Instrumental parameters for Gas-chromatographic analyses for **DANI 86.10 HT.**^(a)

COLUMN PROGRAM		
rate (°C/min)	temperature (°C)	time (min)
-	60	6
25	120	-
7	160	-
15	270	20.34

INJECTOR PROGRAM		
rate (°C/min)	temperature(°C)	time (min)
-	50	2
700	120	-
200	275	42

(a) Carrier gas: **He**, carrier gas pressure: **1.2 bar**, air pressure at the detector: **0.7 bar**, hydrogen pressure at the detector: **0.7 bar**, auxiliary gas: **N₂**, auxiliary gas pressure: **1.3 bar**, detector temperature: **300 °C**.

Table 22. Instrumental parameters for Gas-chromatographic analyses for **SHIMADZU GC-2010.**^(a)

COLUMN PROGRAM		
rate (°C/min)	temperature (°C)	time (min)
-	70	-
20	150	2.25
20	200	2.1
100	270	0.5

INJECTOR PROGRAM		
rate (°C/min)	temperature (°C)	time (min)
-	120	-
25	270	3

(a) Carrier gas: **He**, carrier gas pressure: **10 bar**, air flow: **400 mL/min**, hydrogen flow: **40 mL/min**, makeup-gas: **N₂**, makeup flow: **30 mL/min**, detector temperature: **280 °C**.

References

- [1] T. A. Khattab, M. Rehan, *Egypt. J. Chem.* **2018**, *61*, 897-937.
- [2] T. A. Khattab, M. Rehan, *Egypt. J. Chem.* **2018**, *61*, 989-1018.
- [3] P. F. Pagoria, G. S. Lee, A. R. Mitchell, R. D. Schmidt, *Thermochim. Acta* **2002**, *384*, 187-204.
- [4] A. K. Sikder, N. Sikder, *J. Hazard. Mater.* **2004**, *112*, 1-15.
- [5] E. Vitaku, D. T. Smith, J. T. Njardarson, *J. Med. Chem.* **2014**, *57*, 10257-10274.
- [6] G. Brahmachari, in *Green Synthetic Approaches for Biologically Relevant Heterocycles* (Ed.: G. Brahmachari), Elsevier, Boston, **2015**, pp. 1-6.
- [7] N. Kerru, L. Gummidi, S. Maddila, K. K. Gangu, S. B. Jonnalagadda, *Molecules* **2020**, *25*, 1909.
- [8] N. Ono, in *The Nitro Group in Organic Synthesis*, **2001**, pp. 325-363.
- [9] F. Ferretti, D. R. Ramadan, F. Ragaini, *ChemCatChem* **2019**, *11*, 4450-4488.
- [10] F. Ragaini, S. Cenini, D. Brignoli, M. Gasperini, E. Gallo, *J. Org. Chem.* **2003**, *68*, 460-466.
- [11] F. Ragaini, S. Cenini, E. Gallo, A. Caselli, S. Fantauzzi, *Curr. Org. Chem.* **2006**, *10*, 1479-1510.
- [12] F. Ragaini, A. Rapetti, E. Visentin, M. Monzani, A. Caselli, S. Cenini, *J. Org. Chem.* **2006**, *71*, 3748-3753.
- [13] F. Ferretti, M. A. EL-Atawy, S. Muto, M. Hagar, E. Gallo, F. Ragaini, *Eur. J. Org. Chem.* **2015**, *2015*, 5712-5715.
- [14] M. A. El-Atawy, F. Ferretti, F. Ragaini, *Eur. J. Org. Chem.* **2017**, *2017*, 1902-1910.
- [15] F. Ferretti, D. Formenti, F. Ragaini, *Rend. Lincei* **2017**, *28*, 97-115.
- [16] M. A. EL-Atawy, F. Ferretti, F. Ragaini, *Eur. J. Org. Chem.* **2018**, *2018*, 4818-4825.
- [17] M. A. EL-Atawy, D. Formenti, F. Ferretti, F. Ragaini, *ChemCatChem* **2018**, *10*, 4707-4717.
- [18] D. Formenti, F. Ferretti, F. Ragaini, *ChemCatChem* **2018**, *10*, 148-152.
- [19] Y.-S. Wang, H.-P. He, Y.-M. Shen, X. Hong, X.-J. Hao, *J. Nat. Prod.* **2003**, *66*, 416-418.
- [20] C. Ito, S. Katsuno, M. Itoigawa, N. Ruangrunsi, T. Mukainaka, M. Okuda, Y. Kitagawa, H. Tokuda, H. Nishino, H. Furukawa, *J. Nat. Prod.* **2000**, *63*, 125-128.
- [21] A. K. Chakravarty, T. Sarkar, K. Masuda, K. Shiojima, *Phytochemistry* **1999**, *50*, 1263-1266.
- [22] T.-S. Wu, S.-C. Huang, P.-L. Wu, *Chem. Pharm. Bull.* **1998**, *46*, 1459-1461.
- [23] C. Ito, S. Katsuno, H. Ohta, M. Omura, I. Kajiura, H. Furukawa, *Chem. Pharm. Bull.* **1997**, *45*, 48-52.
- [24] C. F. R. Ferreira, M.-J. R. P. Queiroz, G. Kirsch, *J. Heterocycl. Chem.* **2001**, *38*, 749-754.
- [25] J.-F. Morin, M. Leclerc, *Macromolecules* **2001**, *34*, 4680-4682.
- [26] J. Bouchard, S. Wakim, M. Leclerc, *J. Org. Chem.* **2004**, *69*, 5705-5711.
- [27] H. Li, Y. Zhang, Y. Hu, D. Ma, L. Wang, Z. Jing, F. Wang, *Macromol. Chem. Phys.* **2004**, *205*, 247-255.
- [28] A. Kimoto, J.-S. Cho, M. Higuchi, K. Yamamoto, *Macromolecules* **2004**, *37*, 5531-5537.
- [29] K. Karon, M. Lapkowski, *J. Solid State Electrochem.* **2015**, *19*, 2601-2610.
- [30] F. A. Neugebauer, H. Fischer, *Chem. Ber.* **1972**, *105*, 2686-2693.
- [31] M. Kuroki, Y. Tsunashima, *J. Heterocycl. Chem.* **1981**, *18*, 709-714.
- [32] J. A. Joule, in *Adv. Heterocycl. Chem.*, Vol. 35 (Ed.: A. R. Katritzky), Academic Press, **1984**, p. 129.
- [33] J. H. Smitrovich, I. W. Davies, *Org. Lett.* **2004**, *6*, 533-535.
- [34] S. N. Georgiades, P. G. Nicolaou, in *Adv. Heterocycl. Chem.*, Vol. 129 (Eds.: E. F. V. Scriven, C. A. Ramsden), Academic Press, **2019**, pp. 1-88.
- [35] S. Kano, E. Sugino, S. Shibuya, S. Hibino, *J. Org. Chem.* **1981**, *46*, 3856-3859.
- [36] S. Hibino, A. Tonari, T. Choshi, E. Sugino, *Heterocycles* **1993**, *35*, 441-444.
- [37] M. Hussain, S.-M. Tengho Toguem, R. Ahmad, Đ. Thanh Tùng, I. Knepper, A. Villinger, P. Langer, *Tetrahedron* **2011**, *67*, 5304-5318.
- [38] Y. Tao, F. Zhang, C.-Y. Tang, X.-Y. Wu, F. Sha, *Asian J. Org. Chem.* **2014**, *3*, 1292-1301.
- [39] E. Fischer, F. Jourdan, *Ber. Dtsch. Chem. Ges.* **1883**, *16*, 2241-2245.
- [40] W. Borsche, *Justus Liebigs Ann. Chem.* **1908**, *359*, 49-80.
- [41] B. Robinson, *Chem. Rev.* **1963**, *63*, 373-401.
- [42] B. Robinson, *Chem. Rev.* **1969**, *69*, 227-250.
- [43] E. Drechsel, *J. Prakt. Chem.* **1888**, *38*, 65-74.
- [44] C. Graebe, F. Ullmann, *Justus Liebigs Ann. Chem.* **1896**, *291*, 16-17.
- [45] F. Ullmann, *Justus Liebigs Ann. Chem.* **1904**, *332*, 38-81.
- [46] R. W. G. Preston, S. H. Tucker, J. M. L. Cameron, *J. Chem. Soc.* **1942**, 500.
- [47] J. J. Li, *Name Reactions in Heterocyclic Chemistry*, Wiley, Hoboken, NJ, **2005**.
- [48] B. Akermark, L. Ebersson, E. Jonsson, E. Pettersson, *J. Org. Chem.* **1975**, *40*, 1365-1367.
- [49] H.-J. Knölker, *Top. Curr. Chem.* **2005**, *244*, 115.
- [50] H.-J. Knölker, *Modern Alkaloids*, Wiley-VCH, Weinheim, Germany, **2008**.
- [51] H.-J. Knölker, N. O'Sullivan, *Tetrahedron* **1994**, *50*, 10893-10908.

- [52] H.-J. Knölker, W. Fröhner, *J. Chem. Soc., Perkin Trans. 1* **1998**, 173-176.
- [53] H.-J. Knölker, K. R. Reddy, A. Wagner, *Tetrahedron Lett.* **1998**, 39, 8267-8270.
- [54] H.-J. Knölker, W. Fröhner, K. R. Reddy, *Synthesis* **2002**, 557.
- [55] M. P. Krahl, A. Jäger, T. Krause, H.-J. Knölker, *Org. Biomol. Chem.* **2006**, 4, 3215-3219.
- [56] R. Forke, M. P. Krahl, T. Krause, G. Schlechtingen, H.-J. Knölker, *Synlett* **2007**, 2007, 0268-0272.
- [57] R. Forke, A. Jäger, H.-J. Knölker, *Org. Biomol. Chem.* **2008**, 6, 2481-2483.
- [58] R. Forke, M. P. Krahl, F. Däbritz, A. Jäger, H.-J. Knölker, *Synlett* **2008**, 2008, 1870-1876.
- [59] D. E. Ames, A. Opalko, *Tetrahedron* **1984**, 40, 1919-1925.
- [60] S. Bittner, P. Krief, T. Massil, *Synthesis* **1991**, 1991, 215-216.
- [61] B. Åkermark, J. D. Oslob, U. Heuschert, *Tetrahedron Lett.* **1995**, 36, 1325-1326.
- [62] H. Hagelin, J. D. Oslob, B. Åkermark, *Chem. Eur. J.* **1999**, 5, 2413-2416.
- [63] J. Wang, M. Rosingana, D. J. Watson, E. D. Dowdy, R. P. Discordia, N. Soundarajan, W.-S. Li, *Tetrahedron Lett.* **2001**, 42, 8935-8937.
- [64] T. Watanabe, S. Ueda, S. Inuki, S. Oishi, N. Fujii, H. Ohno, *Chem. Commun.* **2007**, 4516-4518.
- [65] B. Liégault, D. Lee, M. P. Huestis, D. R. Stuart, K. Fagnou, *J. Org. Chem.* **2008**, 73, 5022-5028.
- [66] R. B. Bedford, M. Betham, J. P. H. Charmant, A. L. Weeks, *Tetrahedron* **2008**, 64, 6038-6050.
- [67] T. Watanabe, S. Oishi, N. Fujii, H. Ohno, *J. Org. Chem.* **2009**, 74, 4720-4726.
- [68] J. J. Song, J. T. Reeves, D. R. Fandrick, Z. Tan, N. K. Yee, C. H. Senanayake, *ARKIVOC* **2010**, (i), 390.
- [69] B. Weng, R. Liu, J.-H. Li, *Synthesis* **2010**, 2010, 2926-2930.
- [70] T. Gensch, M. Rönnefahrt, R. Czerwonka, A. Jäger, O. Kataeva, I. Bauer, H.-J. Knölker, *Chem. Eur. J.* **2012**, 18, 770-776.
- [71] F. Ullmann, *Ber. Dtsch. Chem. Ges.* **1903**, 36, 2382-2384.
- [72] F. Ullmann, *Ber. Dtsch. Chem. Ges.* **1904**, 37, 853-854.
- [73] I. Goldberg, *Ber. Dtsch. Chem. Ges.* **1906**, 39, 1691-1692.
- [74] S. V. Ley, A. W. Thomas, *Angew. Chem. Int. Ed.* **2003**, 42, 5400-5449.
- [75] J. F. Hartwig, *Angew. Chem. Int. Ed.* **1998**, 37, 2046-2067.
- [76] A. R. Muci, S. L. Buchwald, *Top. Curr. Chem.* **2002**, 219, 131.
- [77] S. L. Buchwald, C. Mauger, G. Mignani, U. Scholz, *Adv. Synth. Catal.* **2006**, 348, 23-39.
- [78] D. S. Surry, S. L. Buchwald, *Angew. Chem. Int. Ed.* **2008**, 47, 6338-6361.
- [79] J. E. R. Sadig, M. C. Willis, *Synthesis* **2011**, 2011, 1-22.
- [80] B. Schlummer, U. Scholz, *Adv. Synth. Catal.* **2004**, 346, 1599-1626.
- [81] Z. Liu, R. C. Larock, *Org. Lett.* **2004**, 6, 3739-3741.
- [82] Z. Liu, R. C. Larock, *Tetrahedron* **2007**, 63, 347-355.
- [83] L. Ackermann, A. Althammer, *Angew. Chem. Int. Ed.* **2007**, 46, 1627-1629.
- [84] L. Ackermann, A. Althammer, P. Mayer, *Synthesis* **2009**, 2009, 3493-3503.
- [85] K. Nozaki, K. Takahashi, K. Nakano, T. Hiyama, H.-Z. Tang, M. Fujiki, S. Yamaguchi, K. Tamao, *Angew. Chem. Int. Ed.* **2003**, 42, 2051-2053.
- [86] A. Kuwahara, K. Nakano, K. Nozaki, *J. Org. Chem.* **2005**, 70, 413-419.
- [87] K. T. H. Y, C. N., *Heterocycles* **2005**, 65, 1561-1567.
- [88] T. Kitawaki, Y. Hayashi, A. Ueno, N. Chida, *Tetrahedron* **2006**, 62, 6792-6801.
- [89] B. J. Stokes, B. Jovanović, H. Dong, K. J. Richert, R. D. Riell, T. G. Driver, *J. Org. Chem.* **2009**, 74, 3225-3228.
- [90] B. J. Stokes, K. J. Richert, T. G. Driver, *J. Org. Chem.* **2009**, 74, 6442-6451.
- [91] H.-J. Knölker, *Chem. Soc. Rev.* **1999**, 28, 151-157.
- [92] H.-J. Knölker, W. Fröhner, *Tetrahedron Lett.* **1997**, 38, 4051-4054.
- [93] H.-J. Knölker, G. Schlechtingen, *J. Chem. Soc., Perkin Trans. 1* **1997**, 349-350.
- [94] H.-J. Knölker, H. Goesmann, C. Hofmann, *Synlett* **1996**, 737.
- [95] T. Chatterjee, G.-b. Roh, M. A. Shoaib, C.-H. Suhl, J. S. Kim, C.-G. Cho, E. J. Cho, *Org. Lett.* **2017**, 19, 1906-1909.
- [96] J. I. G. Cadogan, *Q. Rev. Chem. Soc.* **1962**, 16, 208-239.
- [97] J. I. G. Cadogan, M. Cameron-Wood, *Proc. Chem. Soc.* **1962**, 361.
- [98] J. I. G. Cadogan, M. Cameron-Wood, R. K. Mackie, R. J. G. Searle, *J. Chem. Soc.* **1965**, 4831-4837.
- [99] J. I. G. Cadogan, *Synthesis* **1969**, 1969, 11-17.
- [100] I. Puskas, E. K. Fields, *J. Org. Chem.* **1968**, 33, 4237-4242.
- [101] Y. Tsunashima, M. Kuroki, *J. Heterocycl. Chem.* **1981**, 18, 315-318.
- [102] A. W. Freeman, M. Urvoy, M. E. Criswell, *J. Org. Chem.* **2005**, 70, 5014-5019.
- [103] M. Akazome, T. Kondo, Y. Watanabe, *J. Org. Chem.* **1994**, 59, 3375-3380.
- [104] F. Ragaini, P. Sportiello, S. Cenini, *J. Organomet. Chem.* **1999**, 577, 283-291.
- [105] S. Tollari, S. Cenini, C. Crotti, E. Gianella, *J. Mol. Catal.* **1994**, 87, 203-214.
- [106] T. L. Scott, B. C. G. Söderberg, *Tetrahedron Lett.* **2002**, 43, 1621-1624.

- [107] B. C. Söderberg, S. R. Rector, S. N. O'Neil, *Tetrahedron Lett.* **1999**, *40*, 3657-3660.
- [108] B. C. Söderberg, J. A. Shriver, *J. Org. Chem.* **1997**, *62*, 5838-5845.
- [109] F. Ragaini, in *Reference Module in Chemistry, Molecular Sciences and Chemical Engineering*, Elsevier, **2016**.
- [110] F. Ragaini, *Dalton Trans.* **2009**, 6251-6266.
- [111] F. Paul, *Coord. Chem. Rev.* **2000**, *203*, 269-323.
- [112] A. M. Tafesh, J. Weiguny, *Chem. Rev.* **1996**, *96*, 2035-2052.
- [113] B. C. G. Soderberg, *Curr. Org. Chem.* **2000**, *4*, 727-764.
- [114] S. Cenini, F. Ragaini, *Catalytic Reductive Carbonylation of Organic Nitro Compounds*, Kluwer Academic Publishers, Dordrecht, The Netherlands, **1996**.
- [115] A. Penoni, K. M. Nicholas, *Chem. Commun.* **2002**, 484-485.
- [116] S. Cenini, F. Ragaini, S. Tollari, D. Paone, *J. Am. Chem. Soc.* **1996**, *118*, 11964-11965.
- [117] T. H. H. Hsieh, V. M. Dong, *Tetrahedron* **2009**, *65*, 3062-3068.
- [118] F. Ragaini, S. Cenini, S. Tollari, G. Tummolillo, R. Beltrami, *Organometallics.* **1999**, *18*, 928-942.
- [119] F. Ragaini, S. Cenini, F. Turra, A. Caselli, *Tetrahedron* **2004**, *60*, 4989-4994.
- [120] C.-H. Liu, C.-H. Cheng, *J. Organomet. Chem.* **1991**, *420*, 119-123.
- [121] F. Ragaini, S. Cenini, A. Fumagalli, C. Crotti, *J. Organomet. Chem.* **1992**, *428*, 401-408.
- [122] A. Bontempi, E. Alessio, G. Chanos, G. Mestroni, *J. Mol. Catal.* **1987**, *42*, 67-80.
- [123] P. Wehman, V. E. Kaasjager, F. Hartl, P. C. J. Kamer, P. W. N. M. van Leeuwen, J. Fraanje, K. Goubitz, *Organometallics.* **1995**, *14*, 3751-3761.
- [124] F. Ragaini, C. Cognolato, M. Gasperini, S. Cenini, *Angew. Chem. Int. Ed.* **2003**, *42*, 2886-2889.
- [125] M. Shevlin, X. Guan, T. G. Driver, *ACS Catal.* **2017**, *7*, 5518-5522.
- [126] J. Gui, C.-M. Pan, Y. Jin, T. Qin, J. C. Lo, B. J. Lee, S. H. Spengel, M. E. Mertzman, W. J. Pitts, T. E. La Cruz, M. A. Schmidt, N. Darvatkar, S. R. Natarajan, P. S. Baran, *Science* **2015**, *348*, 886.
- [127] I. W. Davies, J. H. Smitrovich, R. Sidler, C. Qu, V. Gresham, C. Bazaral, *Tetrahedron* **2005**, *61*, 6425-6437.
- [128] P. Wehman, H. M. A. van Donge, A. Hagos, P. C. J. Kamer, P. W. N. M. van Leeuwen, *J. Organomet. Chem.* **1997**, *535*, 183-193.
- [129] M. Pizzotti, S. Cenini, S. Quici, S. Tollari, *J. Chem. Soc., Perkin Trans. 2* **1994**, 913-917.
- [130] C. Crotti, S. Cenini, A. Bassoli, B. Rindone, F. Demartin, *J. Mol. Catal.* **1991**, *70*, 175-187.
- [131] L. Wu, Q. Liu, R. Jackstell, M. Beller, *Angew. Chem. Int. Ed.* **2014**, *53*, 6310-6320.
- [132] H. Konishi, K. Manabe, *Synlett* **2014**, *25*, 1971-1986.
- [133] B. Witulski, C. Alayrac, *Angew. Chem. Int. Ed.* **2002**, *41*, 3281-3284.
- [134] P. G. Sammes, G. Yahioğlu, *Chem. Soc. Rev.* **1994**, *23*, 327-334.
- [135] A. Bencini, V. Lippolis, *Coord. Chem. Rev.* **2010**, *254*, 2096-2180.
- [136] B. V. Popp, J. L. Thorman, S. S. Stahl, *J. Mol. Catal. A: Chem.* **2006**, *251*, 2-7.
- [137] N. Shimizu, T. Kitamura, K. Watanabe, T. Yamaguchi, H. Shigyo, T. Ohta, *Tetrahedron Lett.* **1993**, *34*, 3421-3424.
- [138] J. W. Barton, D. J. Lapham, D. J. Rowe, *J. Chem. Soc., Perkin Trans. 1* **1985**, 131-133.
- [139] J. Forrest, *J. Chem. Soc. (Resumed)* **1960**, 566-573.
- [140] W. Jiang, L. Duan, J. Qiao, G. Dong, D. Zhang, L. Wang, Y. Qiu, *J. Mater. Chem.* **2011**, *21*, 4918-4926.
- [141] T. Tong, C. Tan, T. Keller, B. Li, C. Zheng, U. Scherf, D. Gao, W. Huang, *Macromolecules* **2018**, *51*, 7407-7416.
- [142] T.-C. Lin, W. Chien, S.-W. Dai, H.-W. Lin, Y.-C. Liu, *Dyes Pigm.* **2019**, *168*, 140-150.
- [143] A. W. Schmidt, K. R. Reddy, H.-J. Knölker, *Chem. Rev.* **2012**, *112*, 3193-3328.
- [144] R. Sanz, J. Escribano, M. R. Pedrosa, R. Aguado, F. J. Arnáiz, *Adv. Synth. Catal.* **2007**, *349*, 713-718.
- [145] Y. Ou, N. Jiao, *Chem. Commun.* **2013**, *49*, 3473-3475.
- [146] I. W. Davies, V. A. Guner, K. N. Houk, *Org. Lett.* **2004**, *6*, 743-746.
- [147] Y. Liu, Y. Lu, M. Prashad, O. Repič, T. J. Blacklock, *Adv. Synth. Catal.* **2005**, *347*, 217-219.
- [148] T. Ueda, H. Konishi, K. Manabe, *Org. Lett.* **2012**, *14*, 3100-3103.
- [149] M. Rimoldi, F. Ragaini, E. Gallo, F. Ferretti, P. Macchi, N. Casati, *Dalton Trans.* **2012**, *41*, 3648-3658.
- [150] V. I. Bakmutov, J. F. Berry, F. A. Cotton, S. Ibragimov, C. A. Murillo, *Dalton Trans.* **2005**, 1989-1992.
- [151] A. C. Cope, E. C. Friedrich, *J. Am. Chem. Soc.* **1968**, *90*, 909-913.
- [152] S. Mao, Z. Chen, L. Wang, D. B. Khadka, M. Xin, P. Li, S.-Q. Zhang, *J. Org. Chem.* **2019**, *84*, 463-471.
- [153] R. J. Sundberg, R. W. Heintzelman, *J. Org. Chem.* **1974**, *39*, 2546-2552.
- [154] W. J. Mijs, S. E. Hoekstra, R. M. Ulmann, E. Havinga, *Recl. Trav. Chim. Pays-Bas* **1958**, *77*, 746-752.
- [155] G. S. Hammond, F. J. Modic, R. M. Hedges, *J. Am. Chem. Soc.* **1953**, *75*, 1388-1392.
- [156] C. J. Sunde, G. Johnson, C. F. Kade, *J. Org. Chem.* **1939**, *04*, 548-554.
- [157] J. Tang, A. Biafora, L. J. Goossen, *Angew. Chem. Int. Ed.* **2015**, *54*, 13130-13133.
- [158] H. Gao, Q.-L. Xu, M. Yousufuddin, D. H. Ess, L. Kürti, *Angew. Chem. Int. Ed.* **2014**, *53*, 2701-2705.
- [159] V. Elumalai, A. H. Sandtorv, H.-R. Bjørsvik, *Eur. J. Org. Chem.* **2016**, *2016*, 1344-1354.
- [160] J. Hassan, C. Hathroubi, C. Gozzi, M. Lemaire, *Tetrahedron* **2001**, *57*, 7845-7855.

- [161] M.-Q. Yan, J. Yuan, F. Lan, S.-H. Zeng, M.-Y. Gao, S.-H. Liu, J. Chen, G.-A. Yu, *Org. Biomol. Chem.* **2017**, *15*, 3924-3929.
- [162] M. L. N. Rao, S. Meka, *Tetrahedron Lett.* **2019**, *60*, 150971.
- [163] C.-L. Ho, L.-C. Chi, W.-Y. Hung, W.-J. Chen, Y.-C. Lin, H. Wu, E. Mondal, G.-J. Zhou, K.-T. Wong, W.-Y. Wong, *J. Mater. Chem.* **2012**, *22*, 215-224.
- [164] W. Yang, C. Liu, J. Qiu, *Chem. Commun.* **2010**, *46*, 2659-2661.
- [165] H. Natsugari, *J. Med. Chem.* **1995**, *38*, 3106-3120.
- [166] Y.-H. Zheng, H.-Y. Lu, M. Li, C.-F. Chen, *Eur. J. Org. Chem.* **2013**, *2013*, 3059-3066.
- [167] D. Hackenberger, B. Song, M. F. Grünberg, S. Farsadpour, F. Menges, H. Kelm, C. Groß, T. Wolff, G. Niedner-Schatteburg, W. R. Thiel, L. J. Gooßen, *ChemCatChem.* **2015**, *7*, 3579-3588.
- [168] A. Kistenmacher, K. Müllen, *J. Heterocycl. Chem.* **1992**, *29*, 1237-1239.
- [169] G. Cahiez, A. Moyeux, O. Gager, M. Poizat, *Adv. Synth. Catal.* **2013**, *355*, 790-796.
- [170] E. C. Bigham, M. J. Bishop, D. H. Drewry, D. T. Garrison, S. J. Hodson, F. Navas III, J. D. Speake, *united states*, US6884801 B1 (**2005**), to SmithKline Beecham Corporation (Philadelphia, PA).
- [171] A. d. A. Bartolomeu, R. C. Silva, T. J. Brocksom, T. Noël, K. T. de Oliveira, *J. Org. Chem.* **2019**, *84*, 10459-10471.
- [172] X. Chen, L. Zhou, Y. Li, T. Xie, S. Zhou, *J. Org. Chem.* **2014**, *79*, 230-239.
- [173] K. Takamatsu, K. Hirano, T. Satoh, M. Miura, *Org. Lett.* **2014**, *16*, 2892-2895.
- [174] T. M. Gøgsig, J. Kleimark, S. O. Nilsson Lill, S. Korsager, A. T. Lindhardt, P.-O. Norrby, T. Skrydstrup, *J. Am. Chem. Soc.* **2012**, *134*, 443-452.
- [175] C. Suzuki, K. Hirano, T. Satoh, M. Miura, *Org. Lett.* **2015**, *17*, 1597-1600.
- [176] H.-R. Bjørsvik, V. Elumalai, *Eur. J. Org. Chem.* **2016**, *2016*, 5474-5479.
- [177] W. D. Guerra, R. A. Rossi, A. B. Pierini, S. M. Barolo, *J. Org. Chem.* **2015**, *80*, 928-941.
- [178] H.-W. Engels, H.-G. Pirkl, R. Albers, R. W. Albach, J. Krause, A. Hoffmann, H. Casselmann, J. Dormish, *Angew. Chem., Int. Ed.* **2013**, *52*, 9422-9441.
- [179] See the American Chemistry Council site at <http://polyurethane.americanchemistry.com/> (accessed May 10, 2018)
- [180] S. Cenini, F. Ragaini, *Catalytic Reductive Carbonylation of Organic Nitro Compounds*, Kluwer Academic Publishers, Dordrecht, The Netherlands, **1996**.
- [181] F. Paul, *Coord. Chem. Rev.* **2000**, *203*, 269-323.
- [182] B. Gabriele, G. Salerno, M. Costa, *Top. Organomet. Chem.* **2006**, *18*, 239-272.
- [183] D. J. Diaz, A. K. Darko, L. McElwee-White, *Eur. J. Org. Chem.* **2007**, 4453-4465.
- [184] X.-F. Wu, H. Neumann, M. Beller, *ChemSuschem* **2013**, *6*, 229-241.
- [185] Y. Dai, Y. Wang, J. Yao, Q. Wang, L. Liu, W. Chu, G. Wang, *Catal Lett* **2008**, *123*, 307-316.
- [186] M. Kloetzer, H.-j. Blankertz, G. Georgi, E. Stroefler, V. Krase, G. Schulz, A. Warzecha, *United States US* 8193385 B2 (**2012**), to BASF SE (Ludwigshafen, DE).
- [187] A. Y. Samuilov, F. B. Balabanova, Y. D. Samuilov, A. I. Konovalov, *Russ J Gen Chem* **2012**, *82*, 1110-1114.
- [188] R. Rosenthal, J. G. Zajacek, *United States US* 3936484 (**1976**), to Atlantic Richfield Company (Los Angeles, CA).
- [189] E. T. Shawl, H. S. Kesling, Jr., *US Patent US* 4871871 (**1989**), to (Arco Chemical Technology, Inc., USA).
- [190] E. Stroefler, W. Mackenroth, M. Sohn, C. Knoesche, O. Schweers, *PCT Int. Appl. WO* 2008031755 A1 20080320 (**2008**), to (BASF Aktiengesellschaft, Germany).
- [191] F. L. Serrano Fernandez, B. Almuna Munoz, A. Padilla Polo, A. Orejon Alvarez, C. Claver Cabrero, S. Castillon Miranda, P. Salagre Carnero, A. Aghmiz, *U.S. Pat. Appl. Publ. US* 2007293696 A1 20071220, (**2007**), to (Repsol-Ypf,S.A., Spain).
- [192] S. Ray, D. Chaturvedi, *Drug Future* **2004**, *29*, 343-357.
- [193] S. Ray, S. A. Pathak, D. Chaturvedi, *Drug Future* **2005**, *30*, 161-180.
- [194] R. L. Metcalf, in *Ullmann's Encyclopedia of Industrial Chemistry*, Wiley-VCH Verlag GmbH & Co. KGaA, **2000**.
- [195] N. Volz, J. Clayden, *Angew. Chem., Int. Ed.* **2011**, *50*, 12148-12155.
- [196] T. Li, S. Y. Lv, J. Chen, C. M. Gao, S. F. Zhang, M. Z. Liu, *Acta Polym. Sin.* **2018**, 336-348.
- [197] S. R. Sorensen, G. D. Bending, C. S. Jacobsen, A. Walker, J. Aamand, *FEMS Microbiol. Ecol.* **2003**, *45*, 1-11.
- [198] V. Amendola, L. Fabbrizzi, L. Mosca, *Chem. Soc. Rev.* **2010**, *39*, 3889-3915.
- [199] G. Dhawan, G. Sumana, B. D. Malhotra, *Biochem. Eng. J.* **2009**, *44*, 42-52.
- [200] H. Q. Li, P. C. Lv, T. Yan, H. L. Zhu, *Anti-Cancer Agents Med. Chem.* **2009**, *9*, 471-480.
- [201] J. Dumas, R. A. Smith, T. B. Lowinger, *Curr. Opin. Drug Discov. Dev.* **2004**, *7*, 600-616.
- [202] S. Cenini, M. Pizzotti, C. Crotti, F. Ragaini, F. Porta, *J. Mol. Catal.* **1988**, *49*, 59-69.
- [203] F. Ragaini, S. Cenini, A. Fumagalli, C. Crotti, *J. Organomet. Chem.* **1992**, *428*, 401-408.
- [204] F. Ragaini, E. Gallo, S. Cenini, *J. Organomet. Chem.* **2000**, *594*, 109-118.
- [205] F. Ragaini, C. Cognolato, M. Gasperini, S. Cenini, *Angew. Chem., Int. Ed.* **2003**, *42*, 2886-2889.

- [206] F. Ragaini, M. Gasperini, S. Cenini, *Adv. Synth. Catal.* **2004**, *346*, 63-71.
- [207] M. Gasperini, F. Ragaini, C. Cazzaniga, S. Cenini, *Adv. Synth. Catal.* **2005**, *347*, 105-120.
- [208] M. Gasperini, F. Ragaini, S. Cenini, E. Gallo, *J. Mol. Catal. A: Chem.* **2003**, *204-205*, 107-114.
- [209] F. Ferretti, F. Ragaini, R. Lariccia, E. Gallo, S. Cenini, *Organometallics* **2010**, *29*, 1465-1471.
- [210] F. Ferretti, E. Gallo, F. Ragaini, *J. Organomet. Chem.* **2014**, *771*, 59-67.
- [211] F. Ferretti, E. Gallo, F. Ragaini, *ChemCatChem* **2015**, *7*, 2241-2247.
- [212] J. D. Gargulak, W. L. Gladfelter, *J. Am. Chem. Soc.* **1994**, *116*, 3792-3800.
- [213] F. Ragaini, S. Cenini, F. Demartin, *Organometallics* **1994**, *13*, 1178-1189.
- [214] F. Ragaini, S. Cenini, *J. Mol. Catal. A: Chem.* **1996**, *109*, 1-25.
- [215] F. Ragaini, M. Macchi, S. Cenini, *J. Mol. Catal. A: Chem.* **1997**, *127*, 33-42.
- [216] F. Ragaini, A. Ghitti, S. Cenini, *Organometallics* **1999**, *18*, 4925-4933.
- [217] F. Ragaini, S. Cenini, *J. Mol. Catal. A: Chem.* **2000**, *161*, 31-38.
- [218] F. Ragaini, M. Gasperini, S. Cenini, L. Arnera, A. Caselli, P. Macchi, N. Casati, *Chem. Eur. J.* **2009**, *15*, 8064-8077.
- [219] S. Fukuoka, M. Chono, *Eur. Pat. Appl.*, (**1983**), to Asahi Chemical Industry Co., Ltd., Japan .
- [220] S. Fukuoka, M. Chono, M. Kohno, *CHEMTECH* **1984**, *14*, 670-676.
- [221] S. Fukuoka, M. Chono, M. Kohno, *J. Chem. Soc., Chem. Commun.* **1984**, 399-400.
- [222] S. Fukuoka, M. Chono, M. Kohno, *J. Org. Chem.* **1984**, *49*, 1458-1460.
- [223] S. P. Gupte, R. V. Chaudhari, *J. Catal.* **1988**, *114*, 246-258.
- [224] I. Pri-Bar, H. Alper, *Can. J. Chem.* **1990**, *68*, 1544-1547.
- [225] S. A. R. Mulla, S. P. Gupte, R. V. Chaudhari, *J. Mol. Catal.* **1991**, *67*, L7-L10.
- [226] S. P. Gupte, R. V. Chaudhari, *Ind. Eng. Chem. Res.* **1992**, *31*, 2069-2074.
- [227] A. A. Kelkar, D. S. Kolhe, S. Kanagasabapathy, R. V. Chaudhari, *Ind. Eng. Chem. Res.* **1992**, *31*, 172-176.
- [228] K. L. Loh, P. Shieh, J. L. Chen, T. K. Chuang, *US Pat.*, (**1992**), to Industrial Technology Research Institute, Taiwan .
- [229] S. Kanagasabapathy, S. P. Gupte, R. V. Chaudhari, *Ind. Eng. Chem. Res.* **1994**, *33*, 1-6.
- [230] I. Pri-Bar, J. Schwartz, *J. Org. Chem.* **1995**, *60*, 8124-8125.
- [231] V. L. K. Valli, H. Alper, *Organometallics* **1995**, *14*, 80-82.
- [232] S. A. R. Mulla, C. V. Rode, A. A. Kelkar, S. P. Gupte, *J. Mol. Catal. A: Chem.* **1997**, *122*, 103-109.
- [233] B. Gabriele, R. Mancuso, G. Salerno, M. Costa, *Chem. Commun.* **2003**, 486-487.
- [234] B. Gabriele, G. Salerno, R. Mancuso, M. Costa, *J. Org. Chem.* **2004**, *69*, 4741-4750.
- [235] K. Hiwatari, Y. Kayaki, K. Okita, T. Ukai, I. Shimizu, A. Yamamoto, *Bull. Chem. Soc. Jpn.* **2004**, *77*, 2237-2250.
- [236] S. Zheng, X. Peng, J. Liu, W. Sun, C. Xia, *Helv. Chim. Acta* **2007**, *90*, 1471-1476.
- [237] M. R. Didgikar, S. S. Joshi, S. P. Gupte, M. M. Diwakar, R. M. Deshpande, R. V. Chaudhari, *J. Mol. Catal. A: Chem.* **2010**, *334*, 20-28.
- [238] M. R. Didgikar, D. Roy, S. P. Gupte, S. S. Joshi, R. V. Chaudhari, *Ind. Eng. Chem. Res.* **2010**, *49*, 1027-1032.
- [239] N. Della Ca, P. Bottarelli, A. Dibenedetto, M. Aresta, B. Gabriele, G. Salerno, M. Costa, *J. Catal.* **2011**, *282*, 120-127.
- [240] M. R. Didgikar, S. S. Joshi, S. P. Gupte, M. M. Diwakar, R. M. Deshpande, R. V. Chaudhari, *J. Mol. Catal. A: Chem.* **2011**, *334*, 20-28.
- [241] R. Mancuso, D. S. Raut, N. Della Ca, F. Fini, C. Carfagna, B. Gabriele, *Chemsuschem* **2015**, *8*, 2204-2211.
- [242] A. Krogul, G. Litwinienko, *J. Mol. Catal. A: Chem.* **2015**, *407*, 204-211.
- [243] N. Zahrtmann, C. Claver, C. Godard, A. Riisager, E. J. Garcia-Suarez, *ChemCatChem* **2018**.
- [244] P. Toochinda, S. S. C. Chuang, *Ind. Eng. Chem. Res.* **2004**, *43*, 1192-1199.
- [245] X. Peng, F. Li, X. Hu, C. Xia, C. A. Sandoval, *Chin. J. Catal.* **2008**, *29*, 638-642.
- [246] M. Liang, T. J. Lee, C. C. Huang, K. Y. Lin, *J. Chin. Chem. Soc.* **2007**, *54*, 885-892.
- [247] S. T. Gadge, E. N. Kusumawati, K. Harada, T. Sasaki, D. Nishio-Hamane, B. M. Bhanage, *J. Mol. Catal. A: Chem.* **2015**, *400*, 170-178.
- [248] Z. Shu-Zhan, P. Xin-Gao, L. Jian-Ming, S. Wei, X. Chun-Gu, *Chin. J. Chem.* **2007**, *25*, 1065-1068.
- [249] M. Aresta, P. Giannoccaro, I. Tommasi, A. Dibenedetto, A. M. Manotti Lanfredi, F. Ugozzoli, *Organometallics* **2000**, *19*, 3879-3889.
- [250] B. Gabriele, M. Costa, G. Salerno, G. P. Chiusoli, *J. Chem. Soc., Perkin Trans. 1* **1994**, 83-87.
- [251] S. S. Stahl, *Angew. Chem., Int. Ed.* **2004**, *43*, 3400-3420.
- [252] Reaction 4 in Table 16 was repeated to check the presence of iron in solution and the result was compared with that obtained when a reaction is performed under exactly the same conditions, but with palladium acetate as a catalyst and without any source of iodine. The results showed indeed a higher iron content in the reaction solution after the reaction when iodide was present, but technical problems in completely mineralizing the organic compounds prevented us to get reliable quantitative data by ICP.

- [253] The flammability range of CO in O₂ is 16.7–93.5% at RT. Kirk-Othmer Encyclopedia of Chemical Technology. 3rd ed. Vol 4. pp 774 John Wiley and Sons.
- [254] Higher TOF values have been reported in a few cases among the cited literature. While it is difficult to compare rate values obtained by using different pressure equipment and we claim no record, we want to emphasize that the highest TOF values have been obtained by running reactions for a short time (15-20 min). Moreover, it appears that the reaction time was measured from the onset of the reaction temperature, which may take up to one hour to be reached. Clearly, the reaction start before and the heating time contributes to the proceeding of the reaction is a non-negligible way. On the contrary, we placed our autoclaves in a preheated oil bath and considered that moment as the start of the reaction.
- [255] D. M. Branan, N. W. Hoffman, E. A. McElroy, N. C. Miller, D. L. Ramage, A. F. Schott, S. H. Young, *Inorg. Chem.* **1987**, *26*, 2915-2917.
- [256] D. Forster, *Inorg. Chem.* **1972**, *11*, 1686-1687.
- [257] A few dimeric Pd-Fe complexes with bridging halide ligands are known [258-260]. Countless di- and oligonuclear iron complexes with bridging halides are known. The latter complexes cannot be active catalysts by themselves, but they may be involved at some stage of the reaction, following or preceding a palladium-catalyzed reaction.
- [258] P. Braunstein, E. Colomer, M. Knorr, A. Tiripicchio, M. Tiripicchio Camellini, *J. Chem. Soc., Dalton Trans.* **1992**, 903-909.
- [259] F. Balegroune, P. Braunstein, J. Durand, T. Faure, D. Grandjean, M. Knorr, M. Lanfranchi, C. Massera, X. Morise, A. Tiripicchio, *Monatsh. Chem.* **2001**, *132*, 885-896.
- [260] D. Serra, M. C. Correia, L. McElwee-White, *Organometallics* **2011**, *30*, 5568-5577.
- [261] Alkylated amines and alkylquinolines have been detected as byproducts when the synthesis of carbamates is performed and an alcohol is employed as solvent [242]. However, these byproducts derive from secondary reactions involving the alcohol.
- [262] M. Campanati, S. Franceschini, O. Piccolo, A. Vaccari, *J. Catal.* **2005**, *232*, 1-9.
- [263] T. Nishida, Y. Tokuda, M. Tsuchiya, *J. Chem. Soc., Perkin Trans. 2* **1995**, 823-830.
- [264] B. Gabriele, R. Mancuso, G. Salerno, *Eur. J. Org. Chem.* **2012**, 6825-6839.
- [265] J. Muzart, *Tetrahedron* **2009**, *65*, 8313-8323.
- [266] A. D. Burrows, K. Cassar, R. M. W. Friend, M. F. Mahon, S. P. Rigby, J. E. Warren, *Crystengcomm* **2005**, *7*, 548-550.
- [267] W. C. Cooper, A. Chilukoorie, S. Polam, D. Scott, F. Wiseman, *J. Phys. Org. Chem.* **2017**, *30*.
- [268] P. Supsana, T. Liaskopoulou, P. G. Tsoungas, G. Varvounis, *Synlett* **2007**, 2671-2674.
- [269] F. Ferretti, E. Barraco, C. Gatti, D. R. Ramadan, F. Ragaini, *J. Catal.* **2019**, *369*, 257-266.
- [270] F. Ragaini, F. Ferretti, C. Gatti, D. R. Ramadan, *J. Catal.* **2019**, *380*, 391-395.
- [271] U. Nagel, B. Rieger, A. Bublewitz, *J. Organomet. Chem.* **1989**, *370*, 223-239.

Appendix.

1. NMR spectra

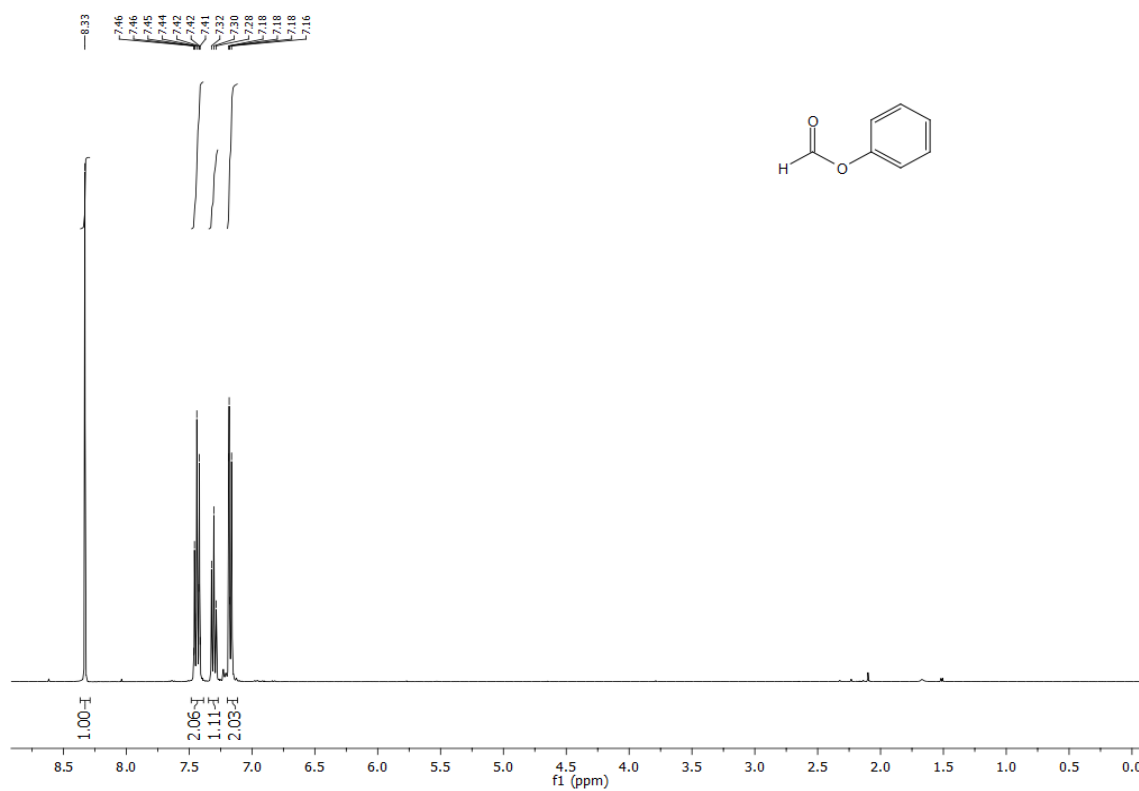


Figure 5: ^1H NMR spectrum of phenyl formate in CDCl_3 .

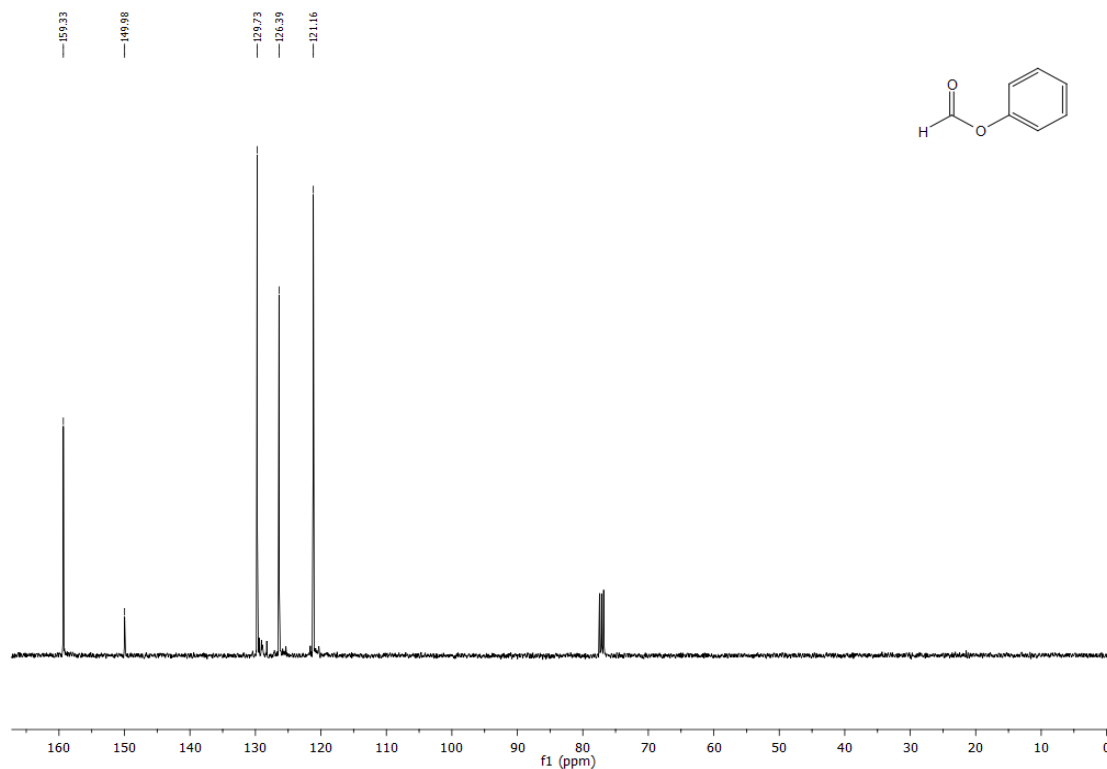


Figure 6: ^{13}C NMR spectrum of phenyl formate in CDCl_3 .

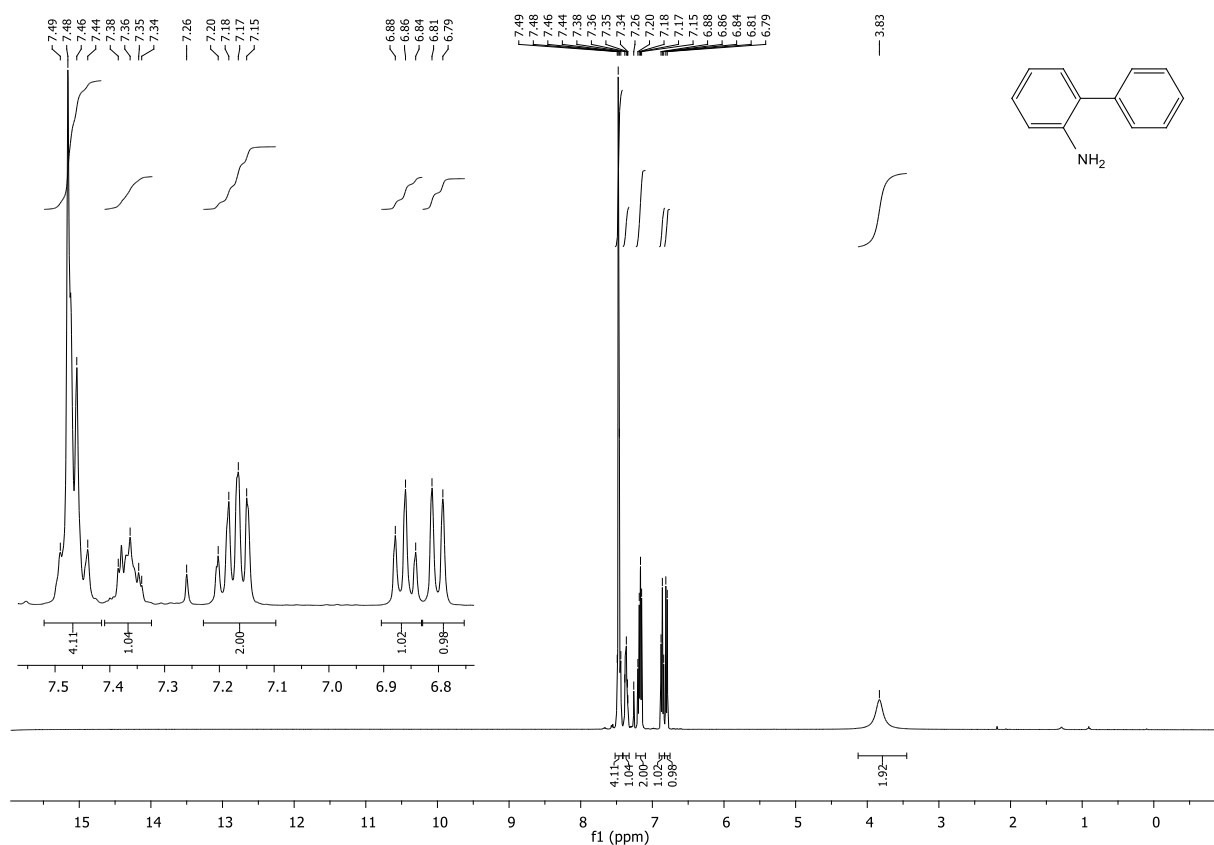


Figure 7: ^1H NMR of *o*-amino-biphenyl **103** spectrum in CDCl_3 .

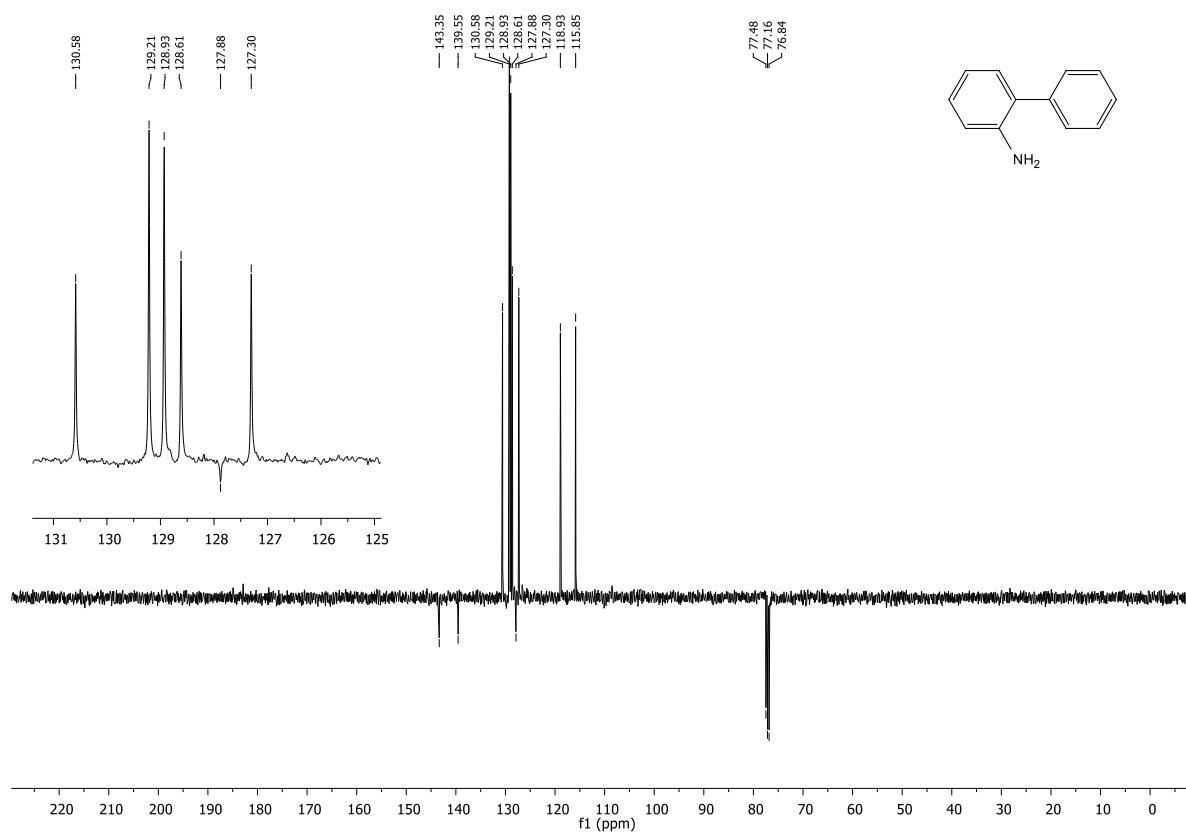


Figure 8: ^{13}C NMR of *o*-amino-biphenyl **103** spectrum in CDCl_3 .

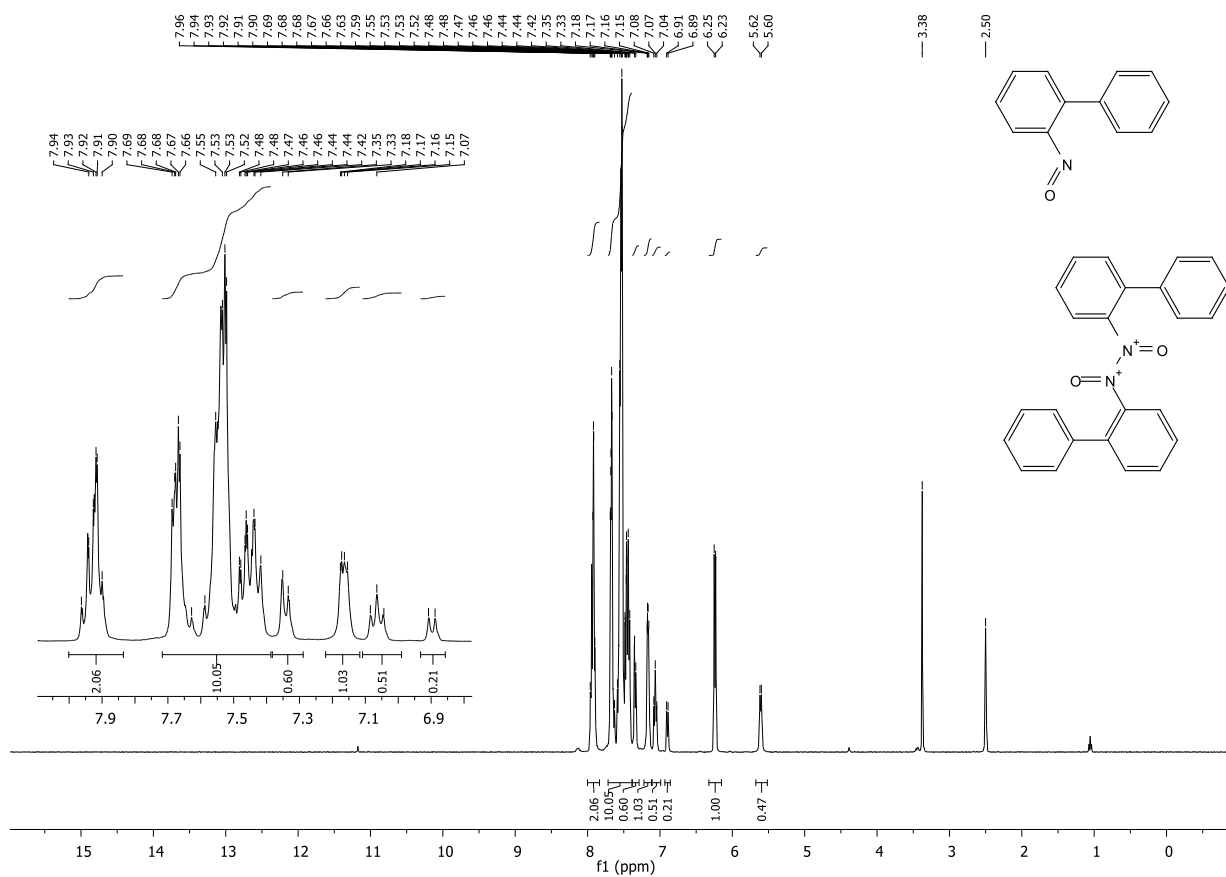


Figure 9: ^1H NMR of *o*-nitroso-biphenyl **104** spectrum in $\text{DMSO-}d_6$.

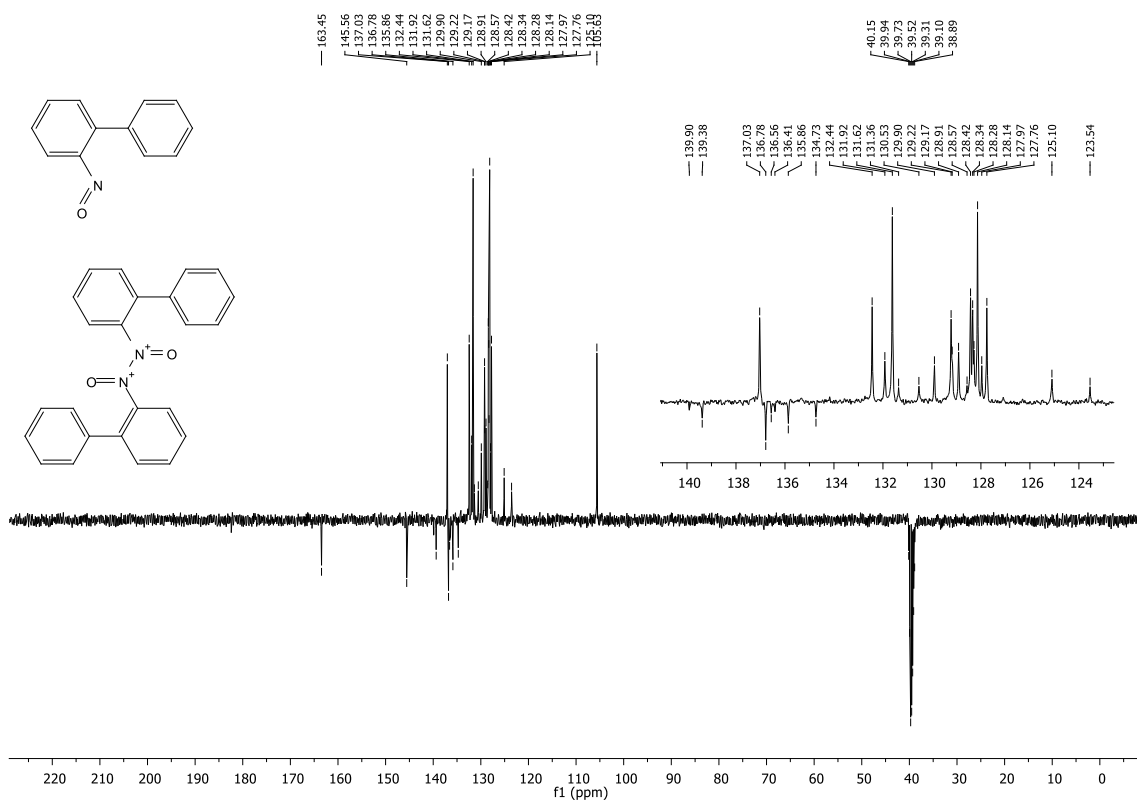


Figure 10: ^{13}C NMR of *o*-nitroso-biphenyl **104** spectrum in $\text{DMSO-}d_6$.

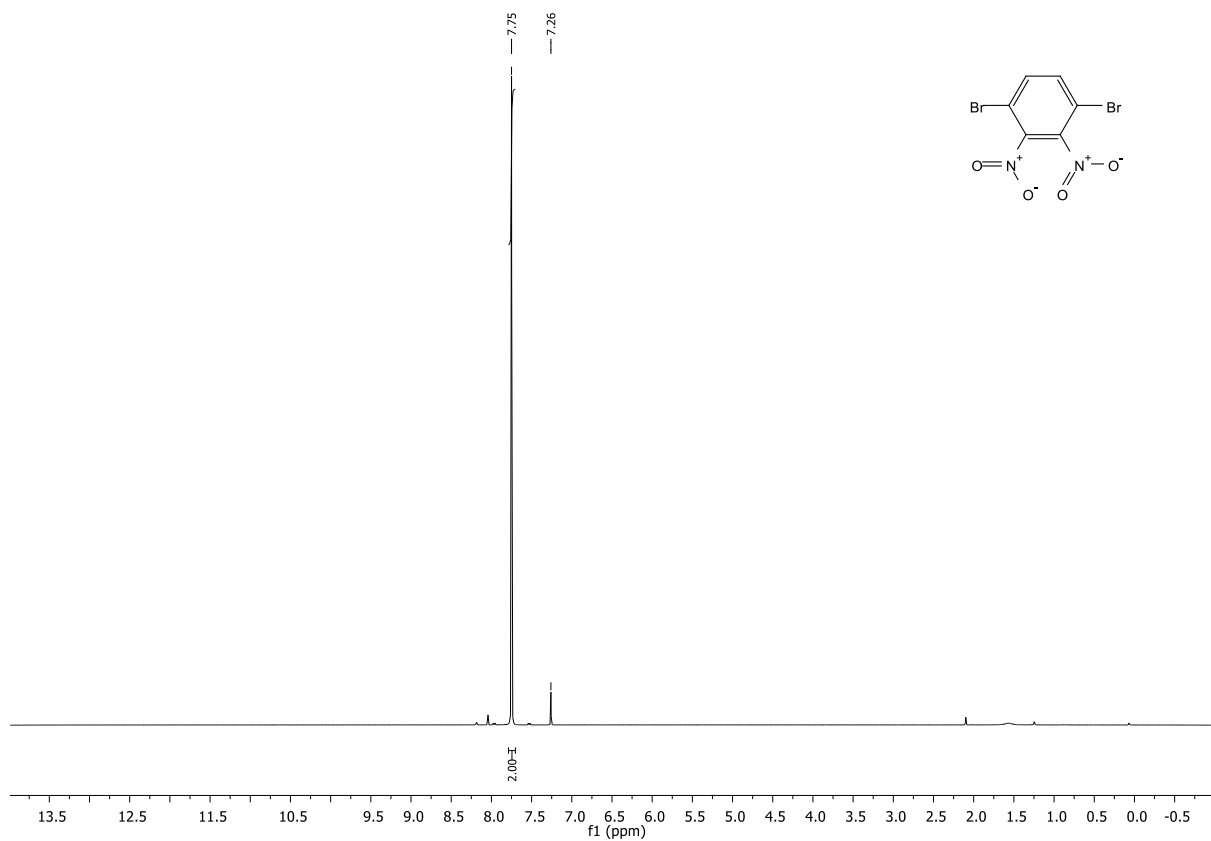


Figure 11: ^1H NMR of 1,4-dibromo-2,3-dinitrobenzene spectrum in CDCl_3 .

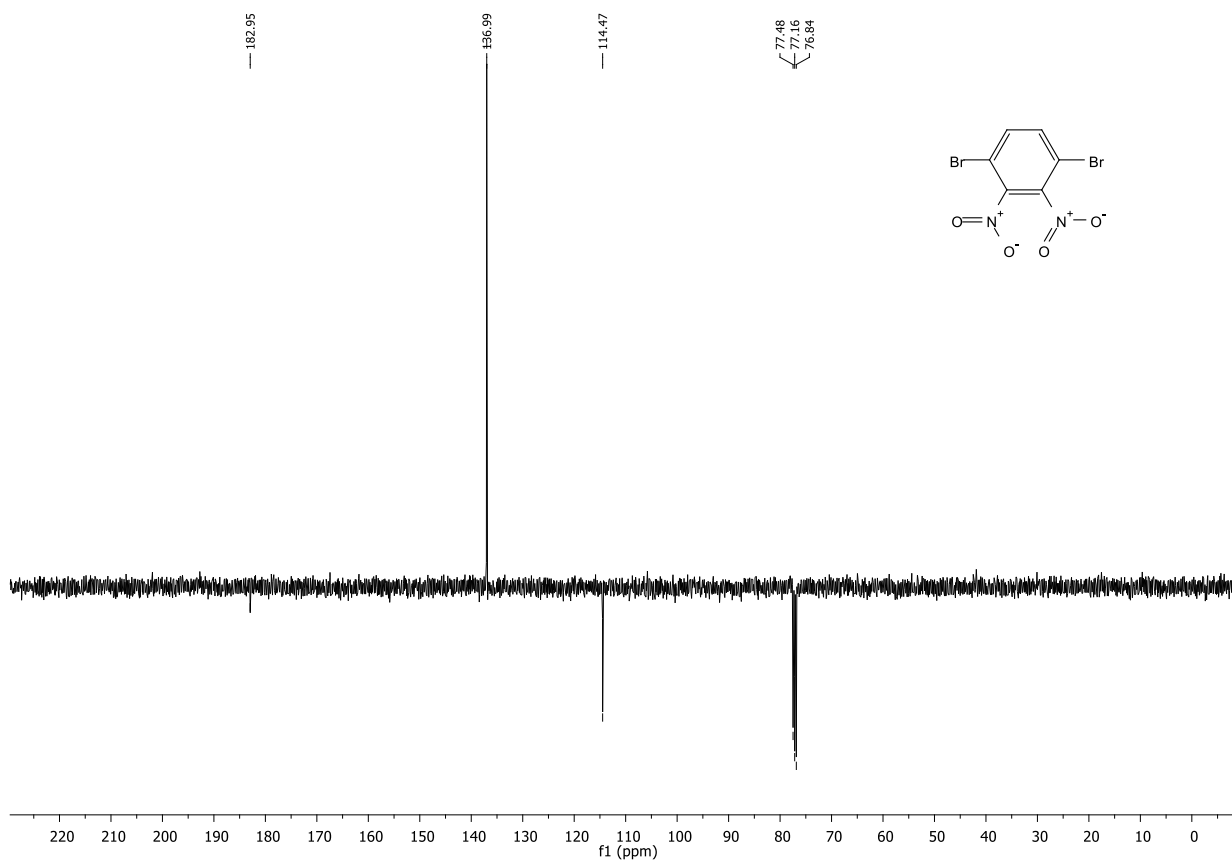
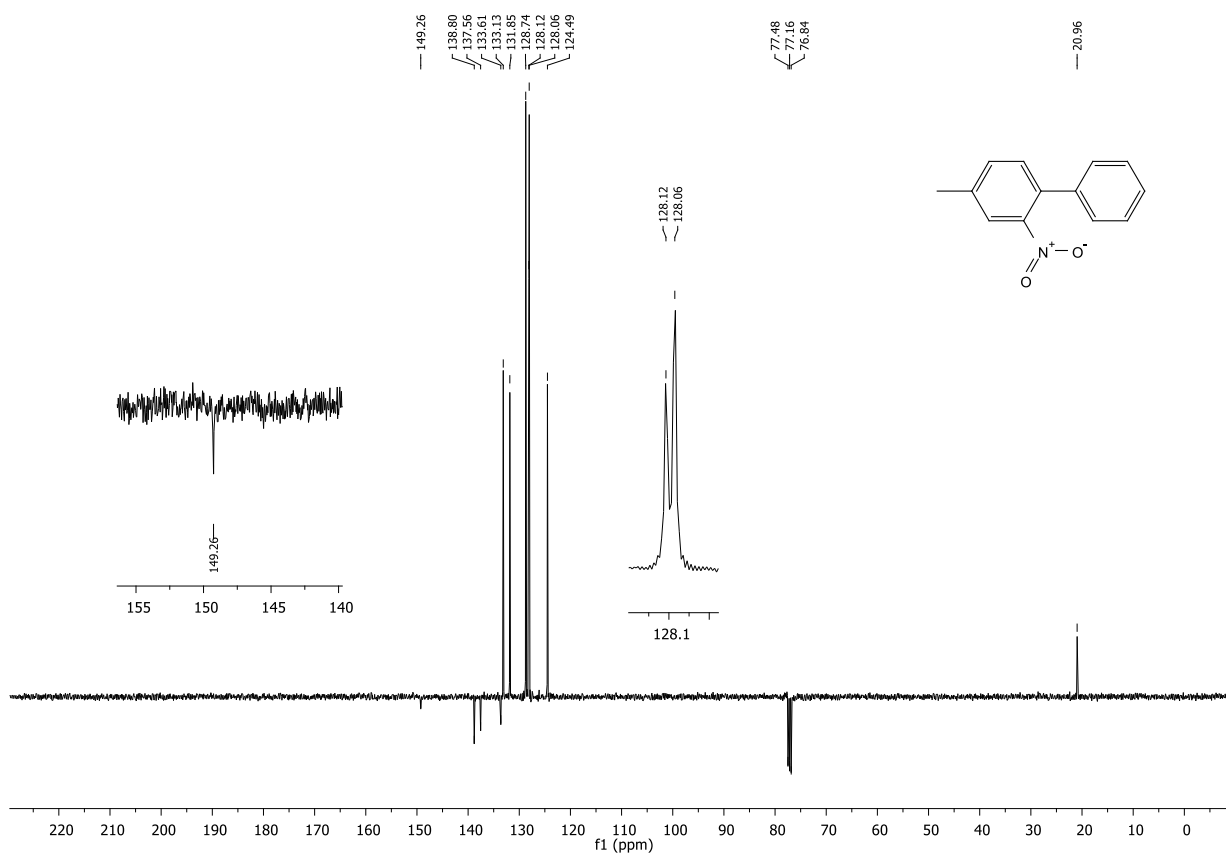
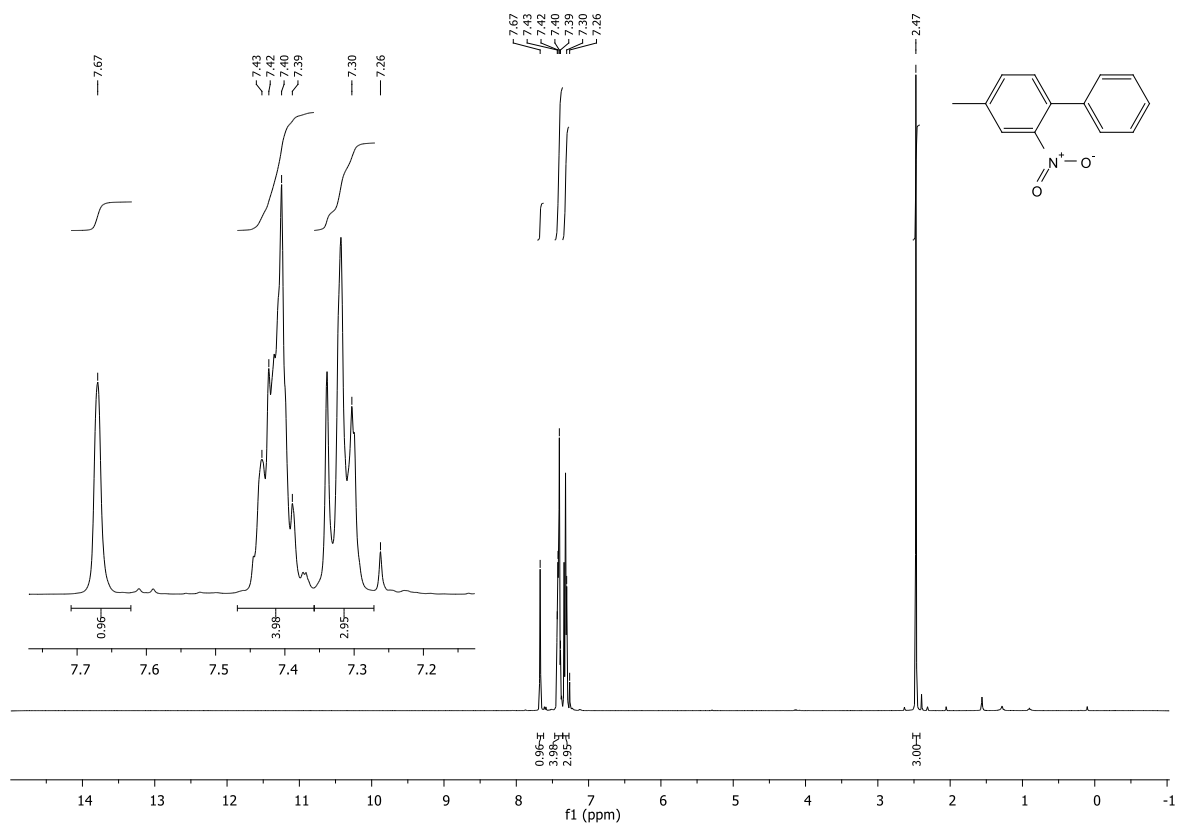


Figure 12: ^{13}C NMR of 1,4-dibromo-2,3-dinitrobenzene spectrum in CDCl_3 .



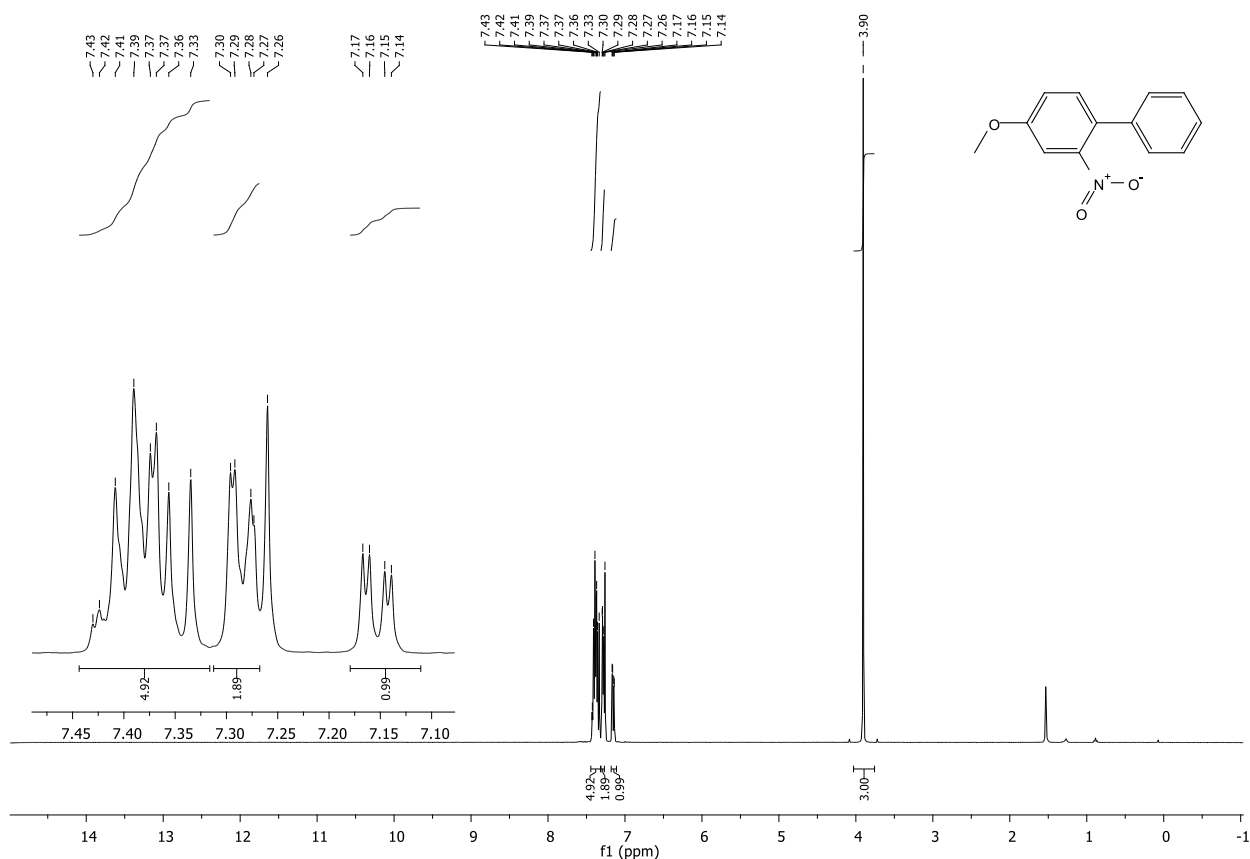


Figure 15: ^1H NMR of 4-methoxy-2-nitrophenyl **51** spectrum in CDCl_3 .

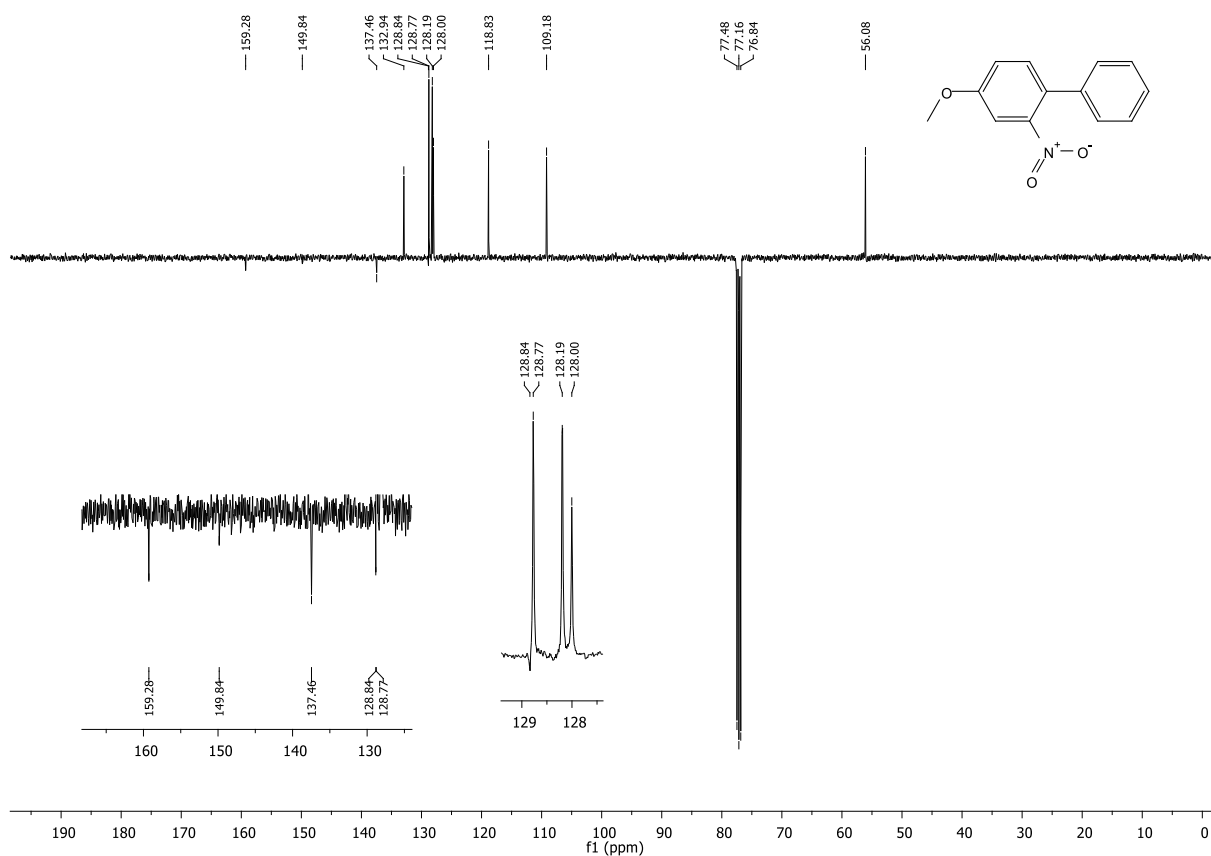


Figure 16: ^{13}C NMR of 4-methoxy-2-nitrophenyl **51** spectrum in CDCl_3 .

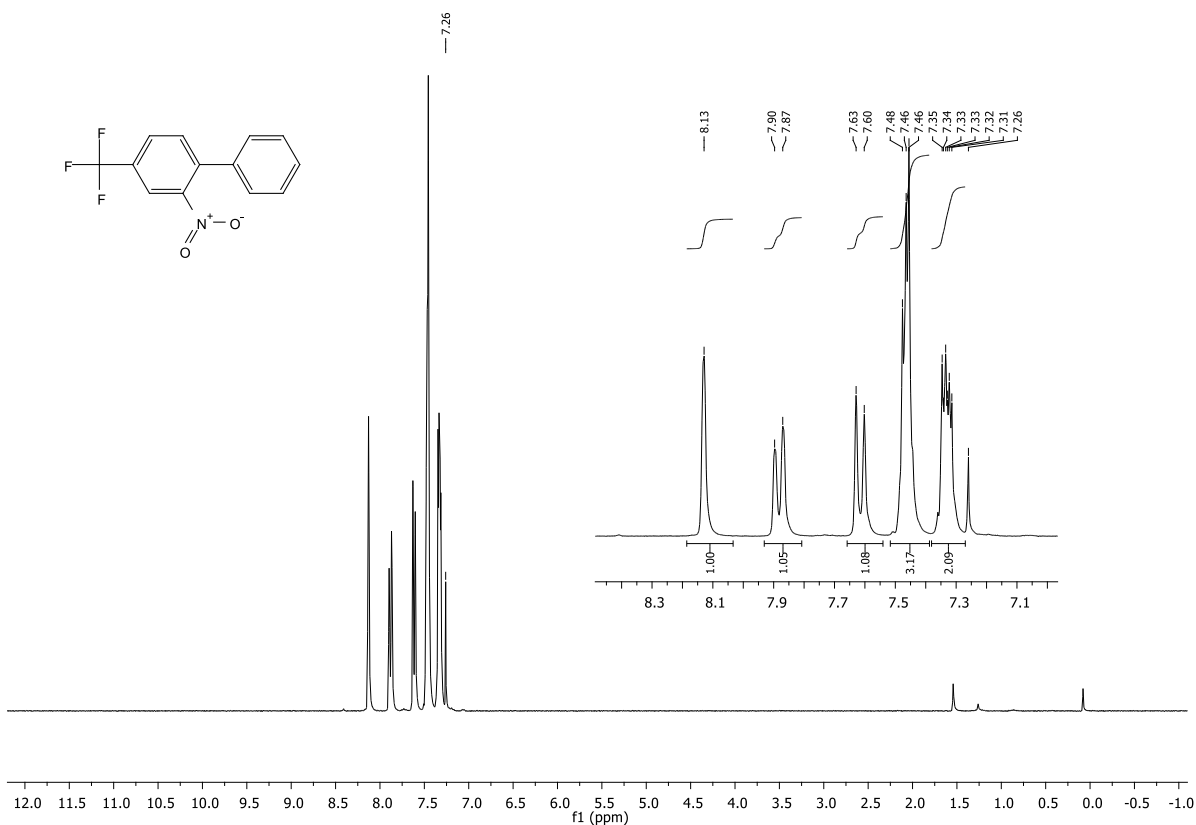


Figure 17: ¹H NMR of 4-trifluoromethyl-2-nitrobiphenyl **52** spectrum in CDCl₃.

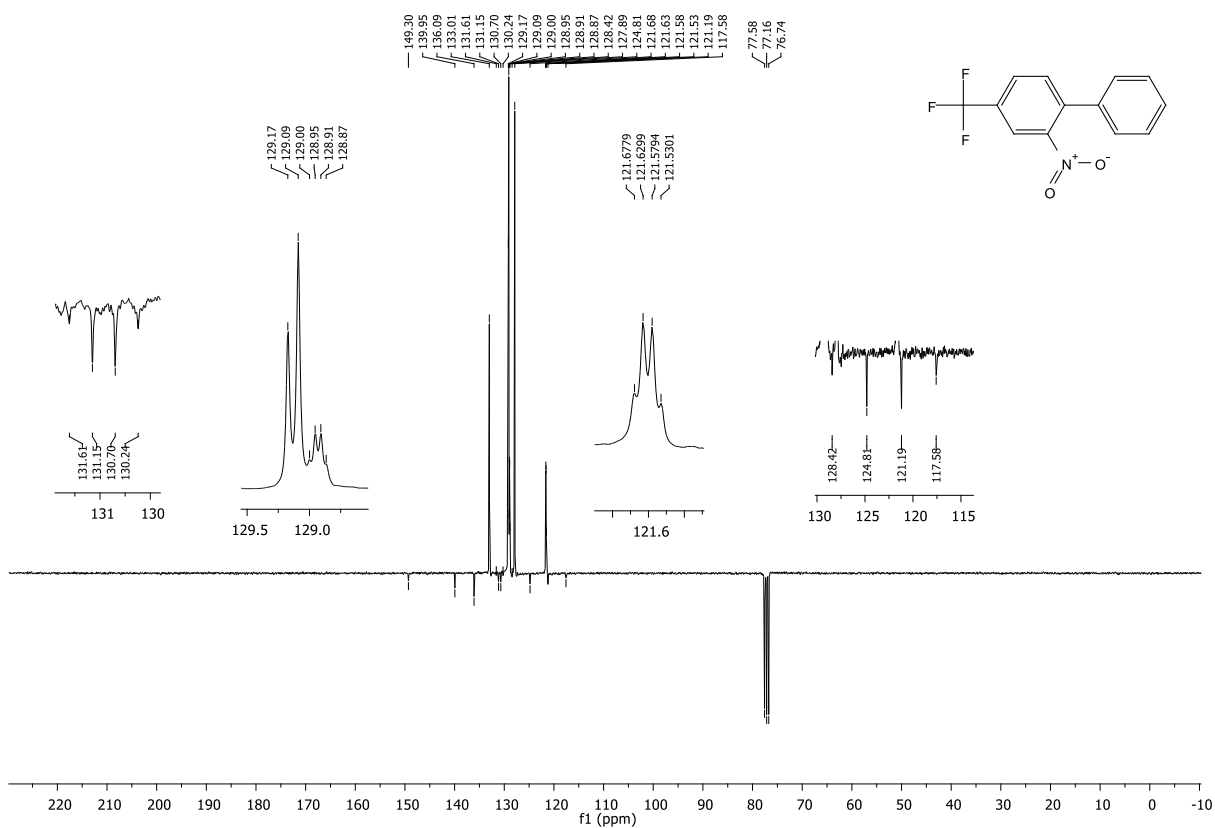


Figure 18: ¹³C NMR of 4-trifluoromethyl-2-nitrobiphenyl **52** spectrum in CDCl₃.

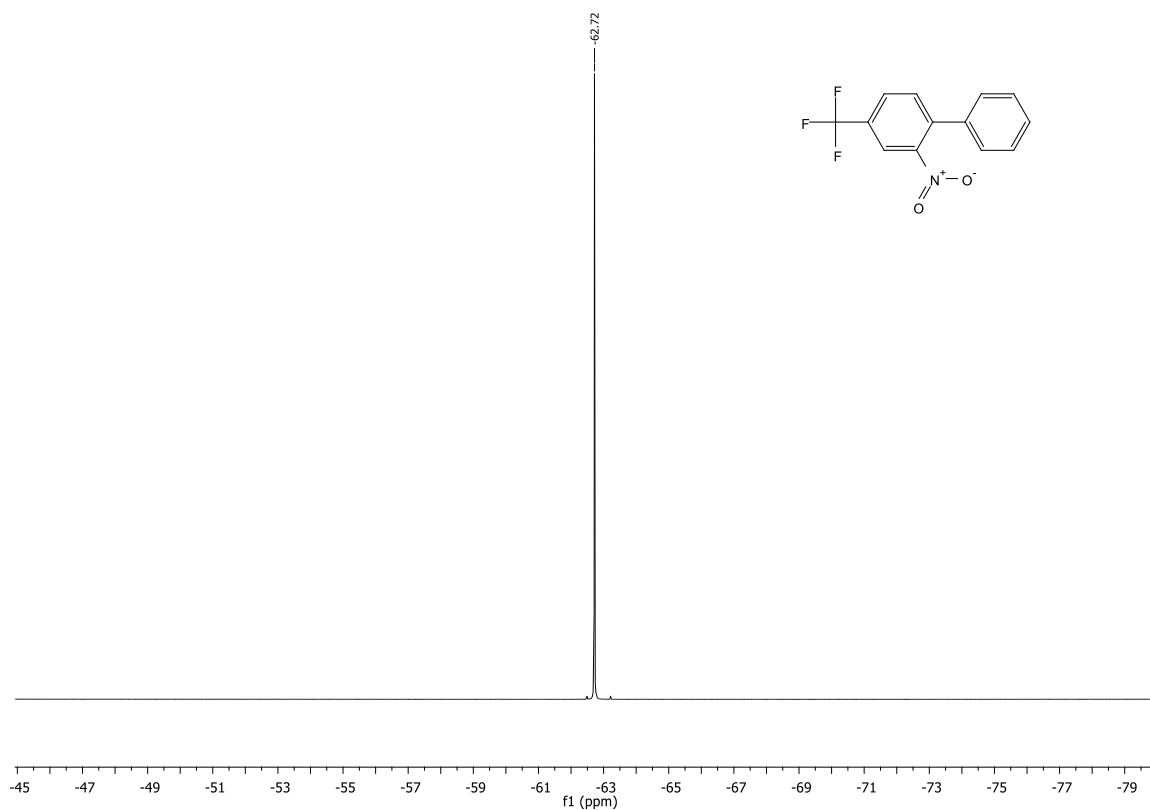


Figure 19: ^{19}F NMR of 4-trifluoromethyl-2-nitrophenyl **52** spectrum in CDCl_3 .

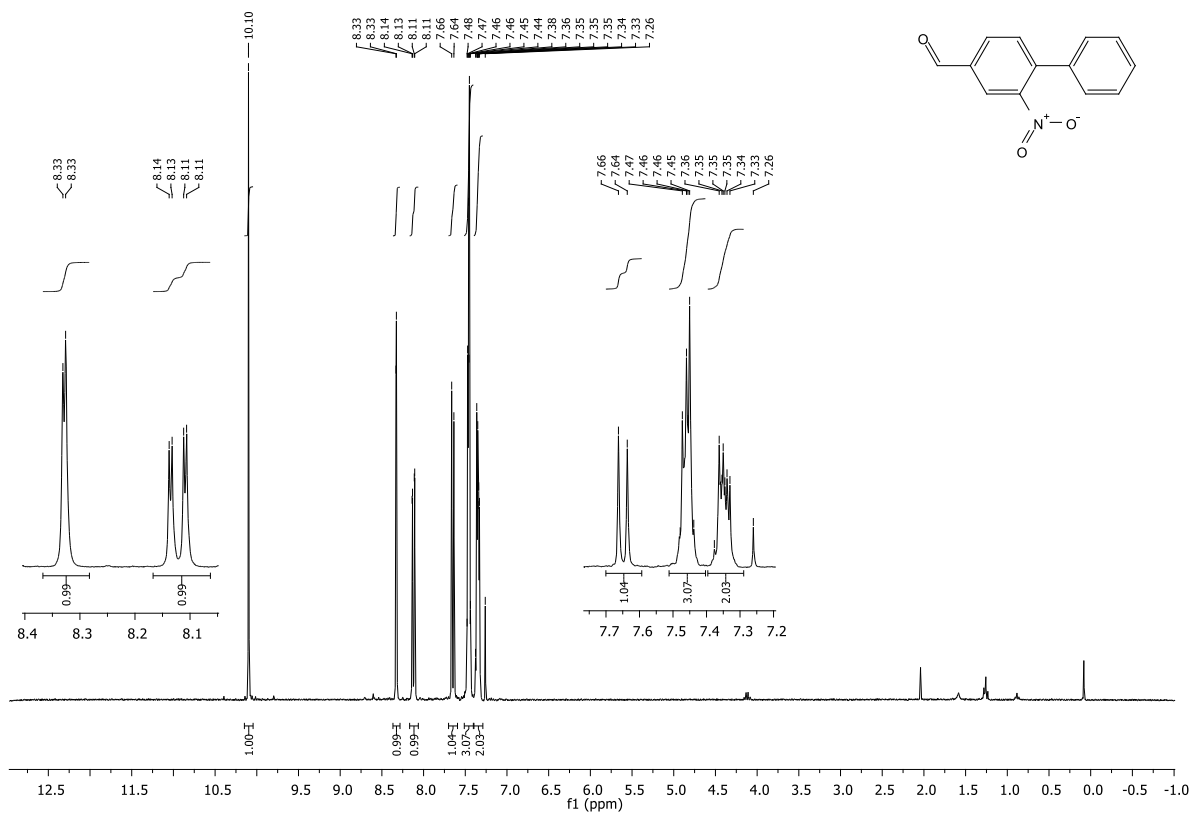


Figure 20: ^1H NMR of 4-formyl-2-nitrophenyl **53** spectrum in CDCl_3 .

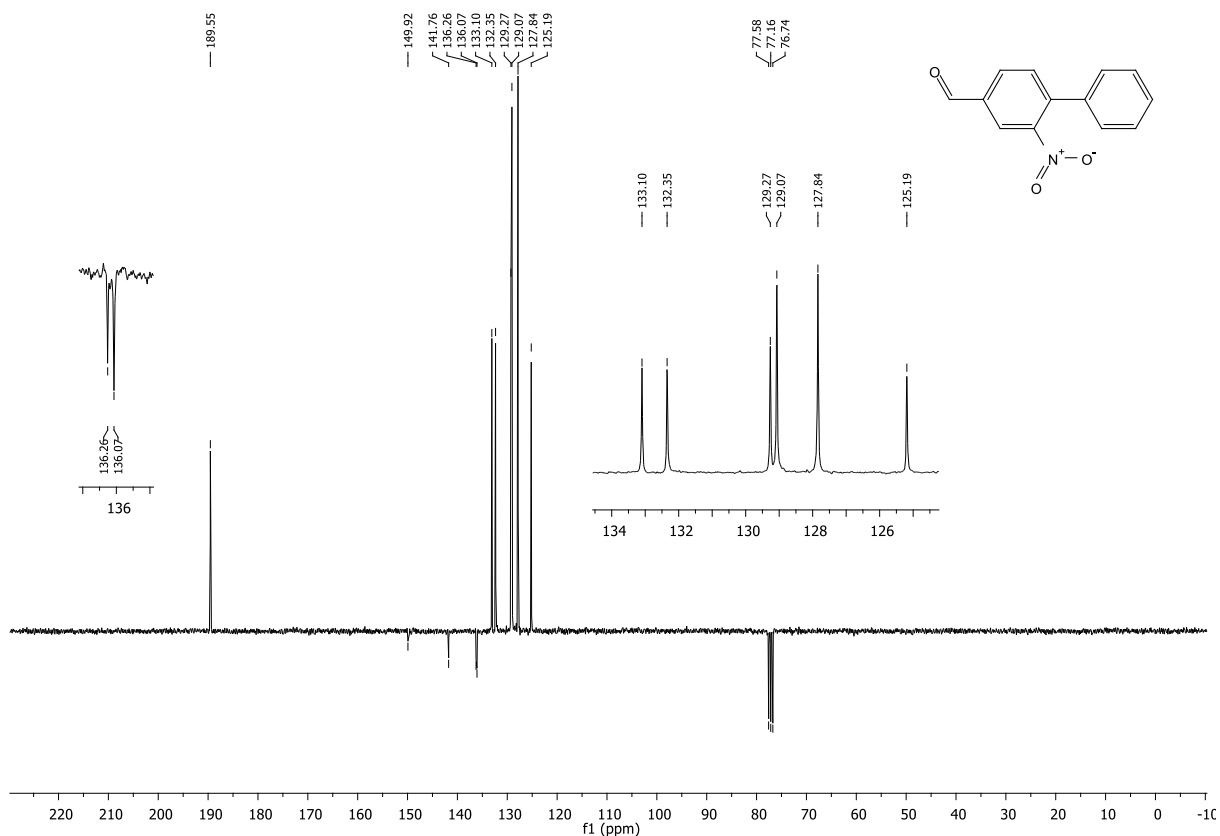


Figure 21: ^{13}C NMR of 4-formyl-2-nitrophenyl **53** spectrum in CDCl_3 .

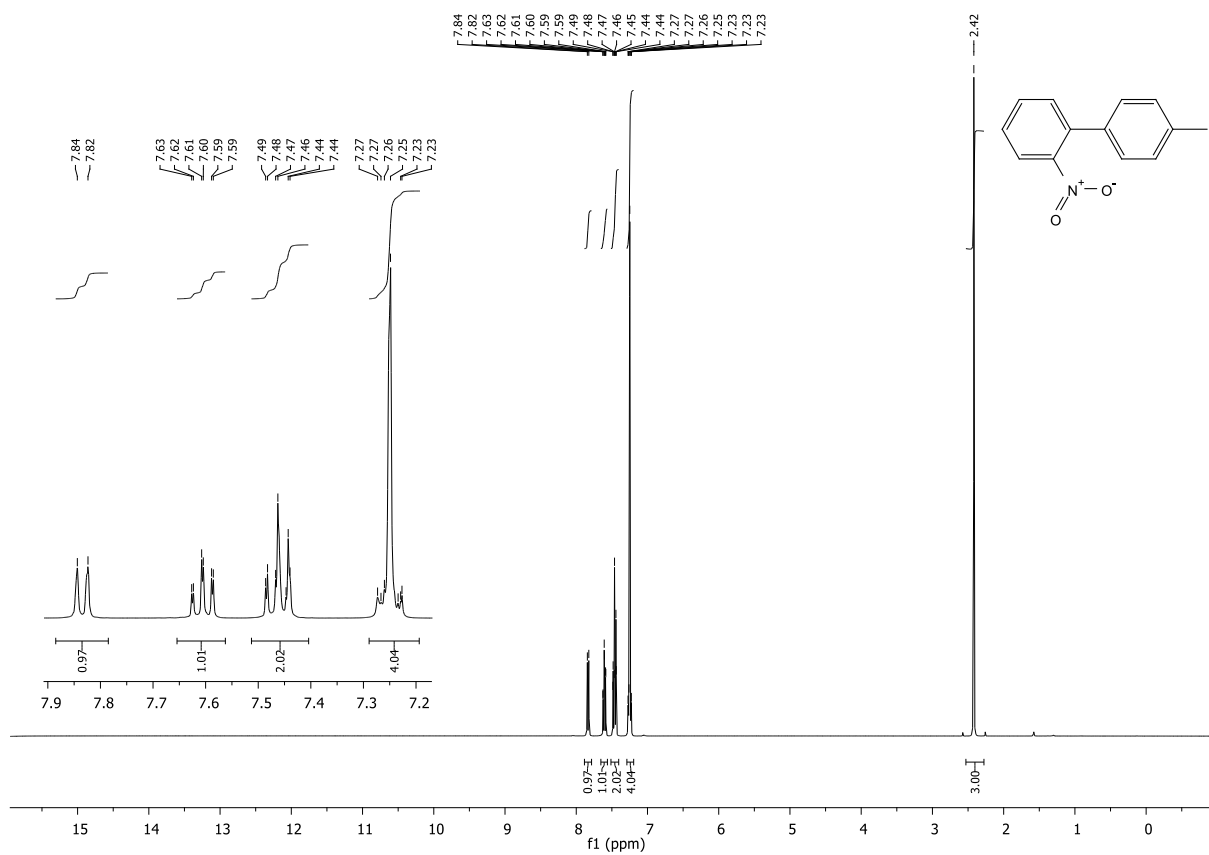


Figure 22: ^1H NMR of 4'-methyl-2-nitrophenyl **54** spectrum in CDCl_3 .

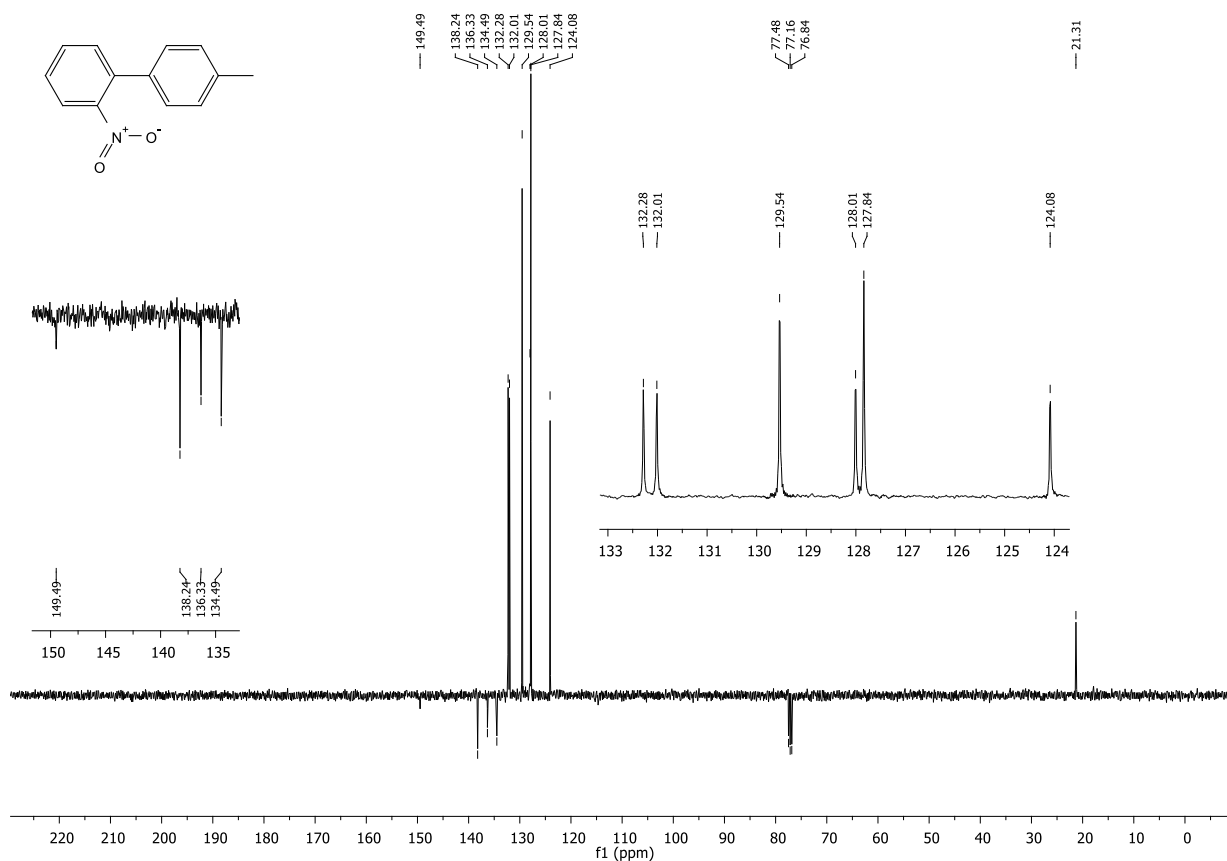


Figure 23: ^{13}C NMR of 4'-methyl-2-nitrophenyl **54** spectrum in CDCl_3 .

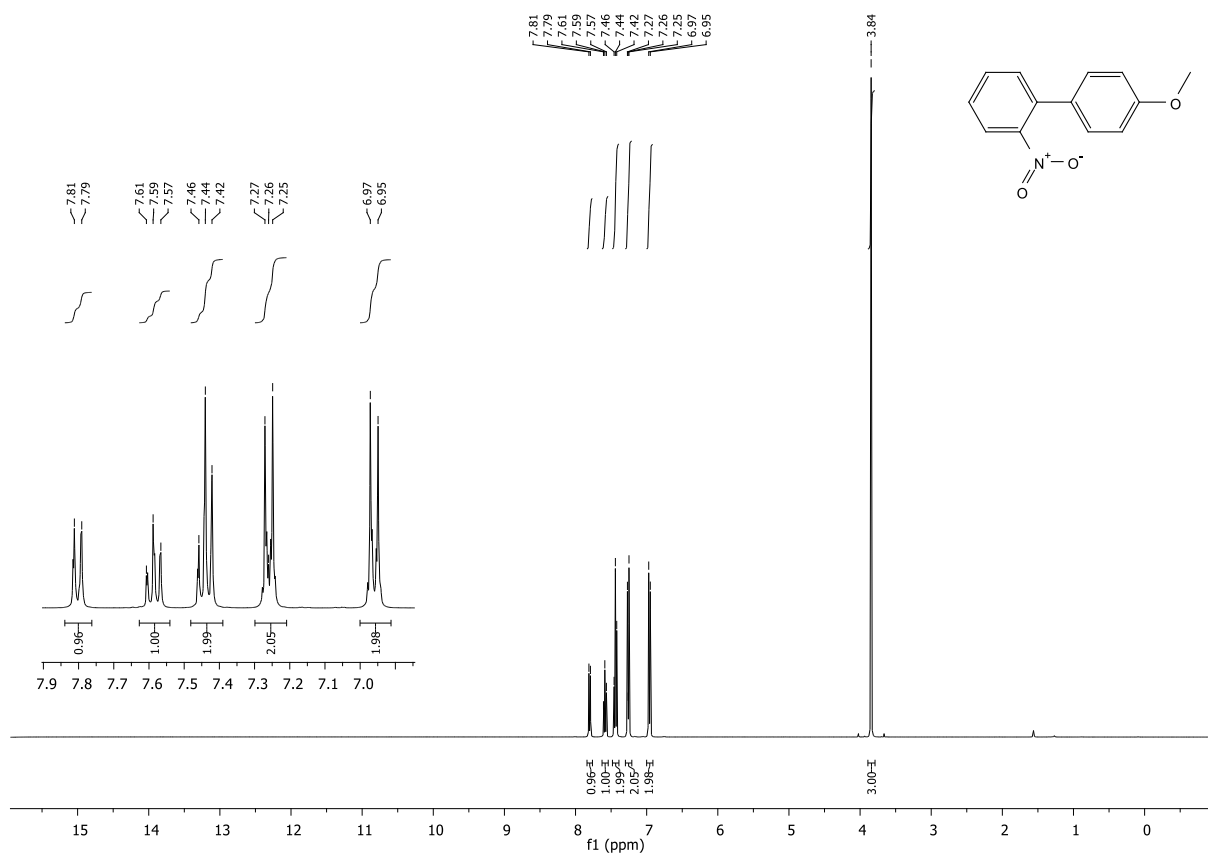
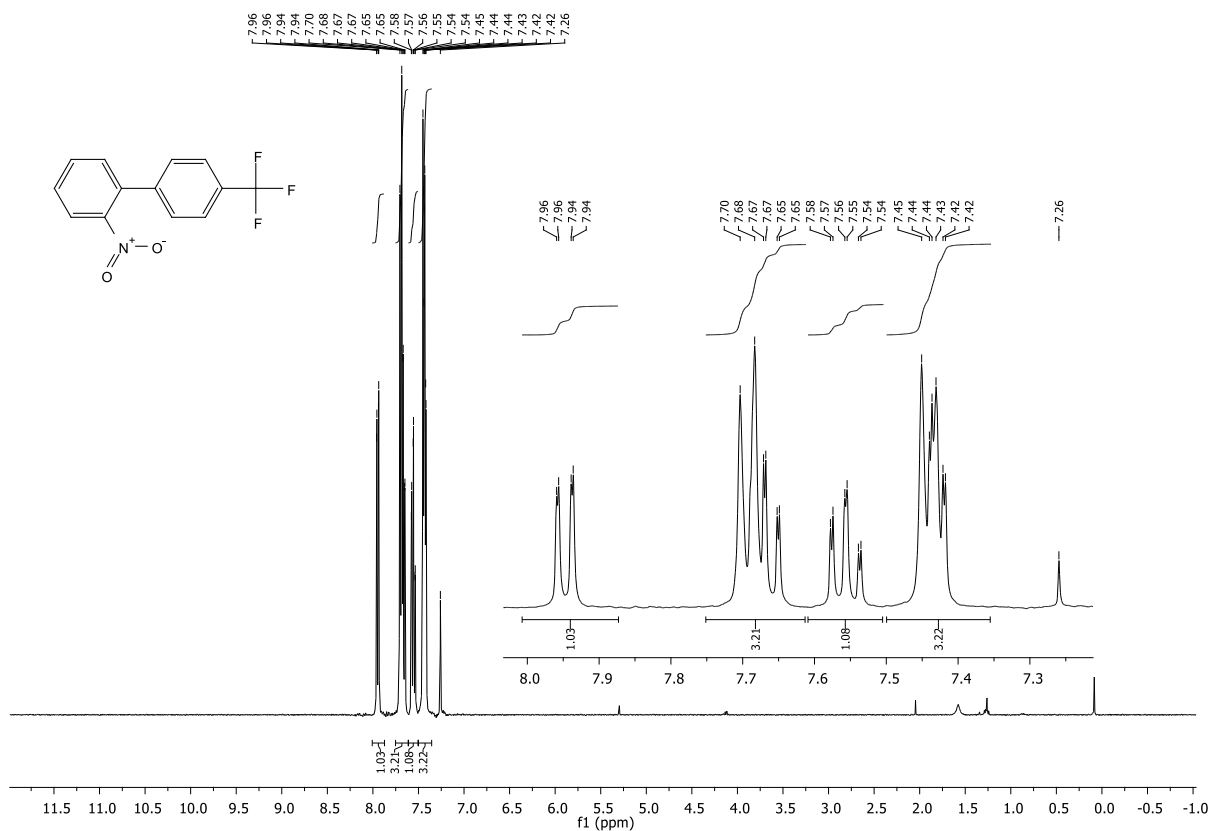
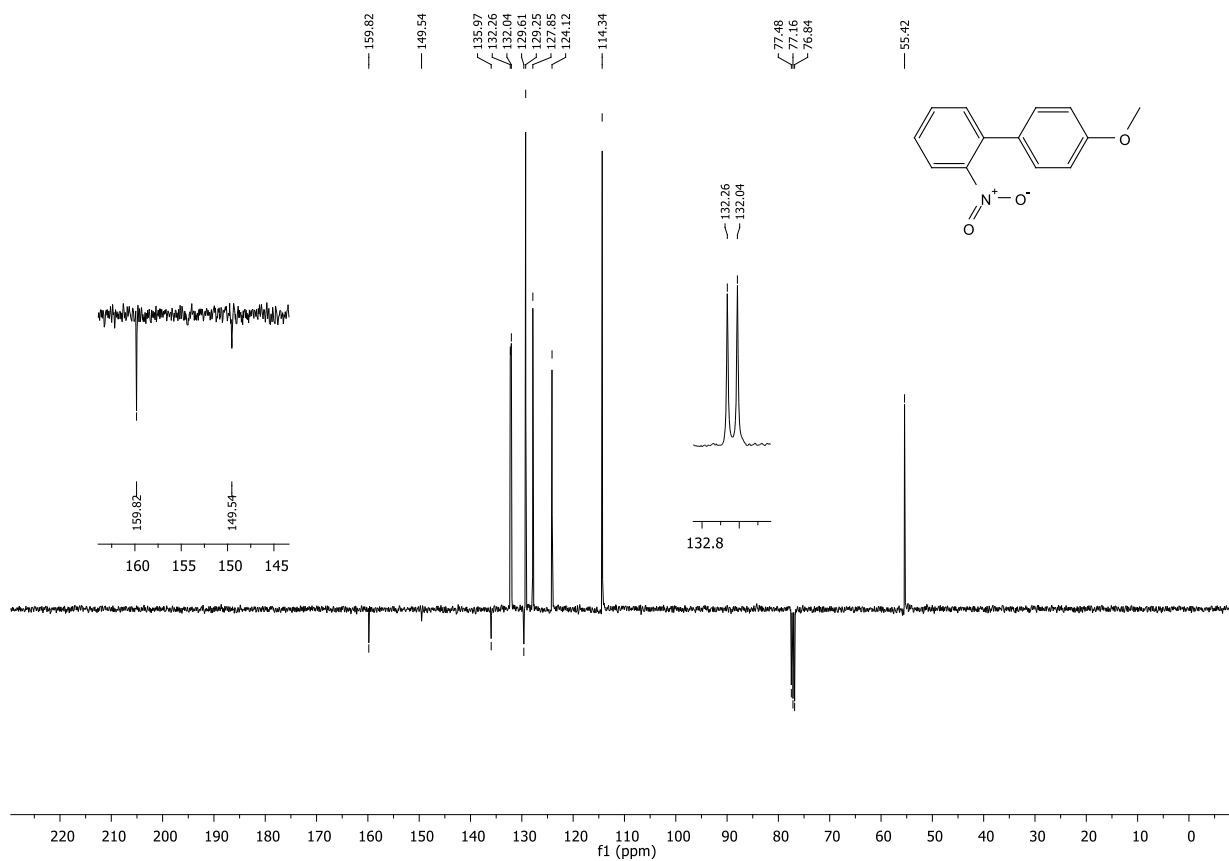


Figure 24: ^1H NMR of 4'-methoxy-2-nitrophenyl **55** spectrum in CDCl_3 .



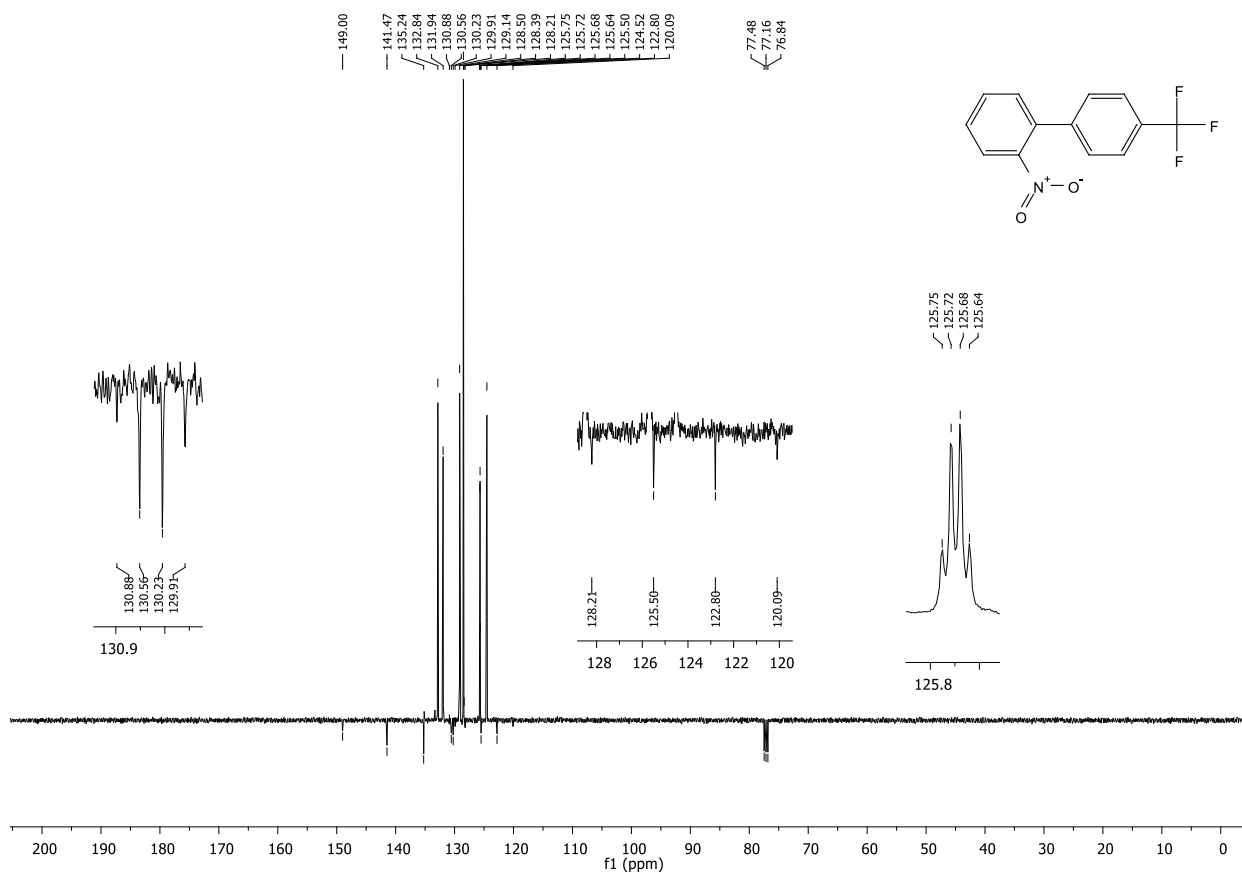


Figure 27: ^{13}C NMR of 4'-trifluoromethyl-2-nitrobiphenyl **56** spectrum in CDCl_3 .

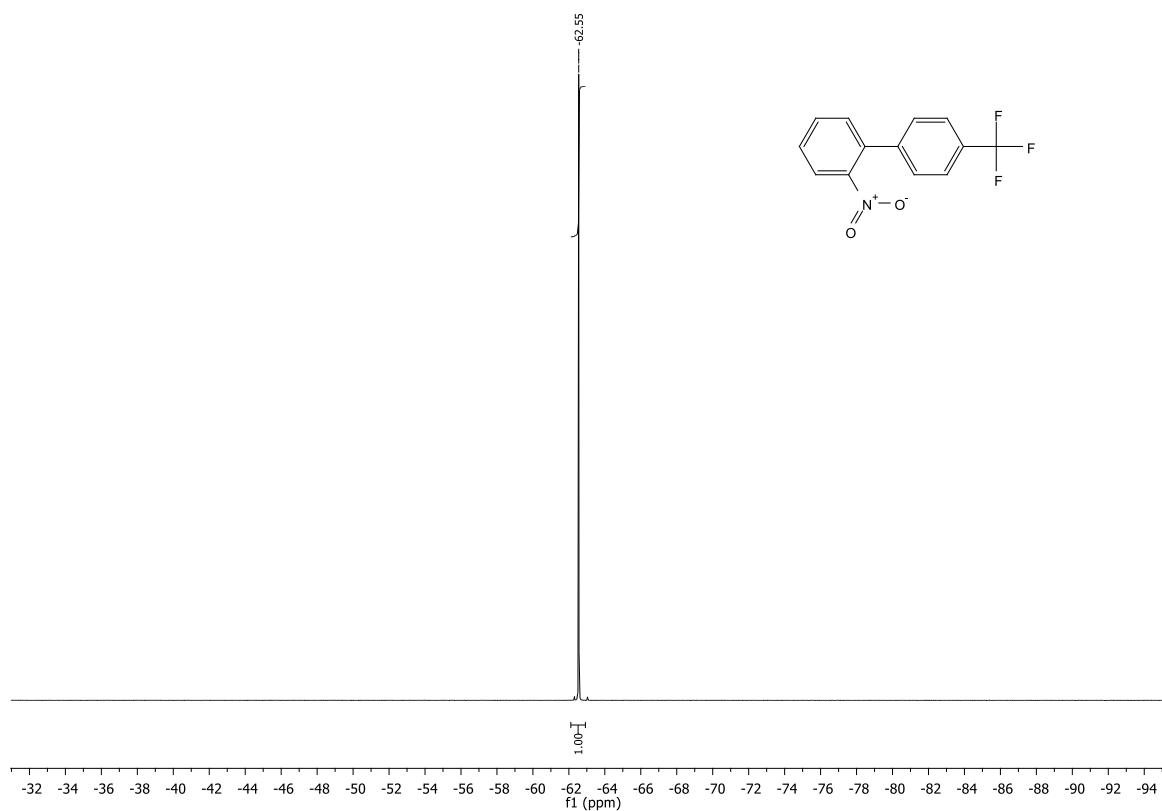


Figure 28: ^{19}F NMR of 4'-trifluoromethyl-2-nitrobiphenyl **56** spectrum in CDCl_3 .

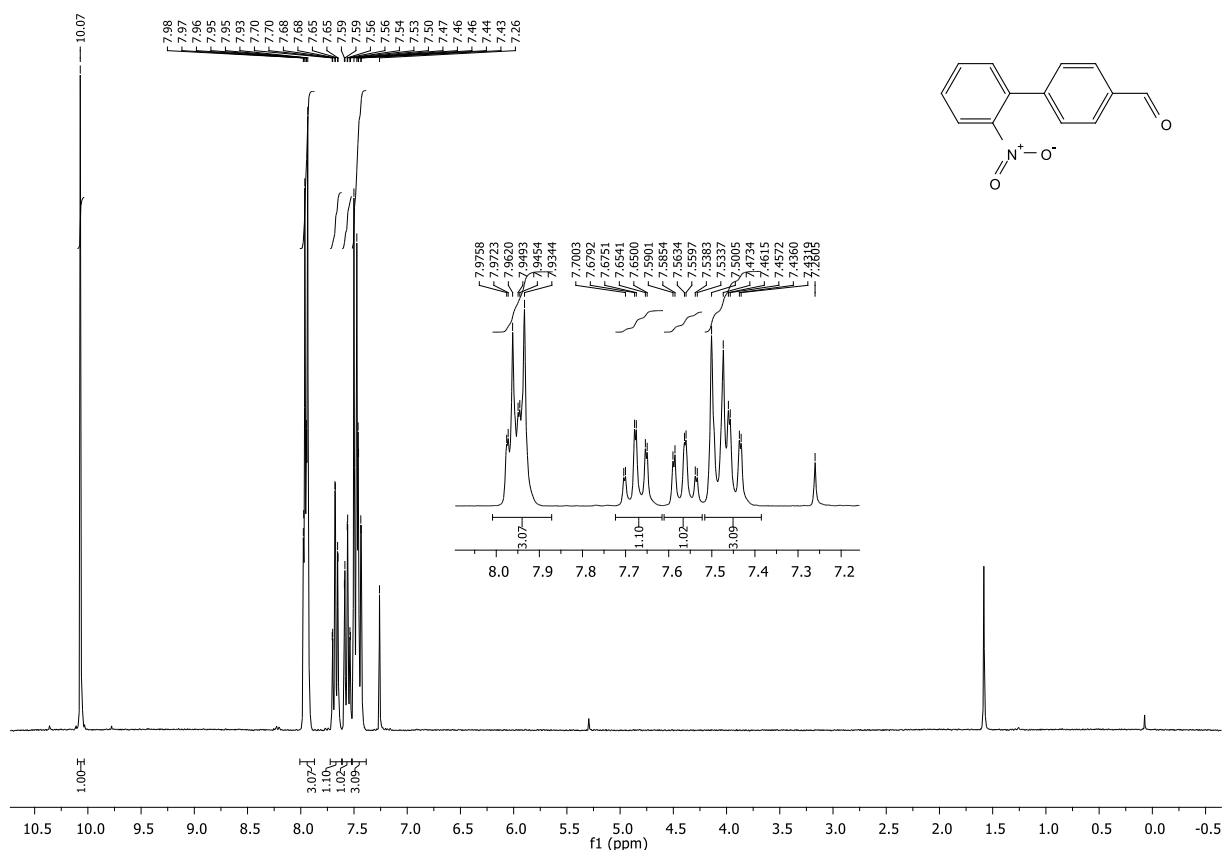


Figure 29: ¹H NMR of 4'-formyl-2-nitrophenyl **57** spectrum in CDCl₃.

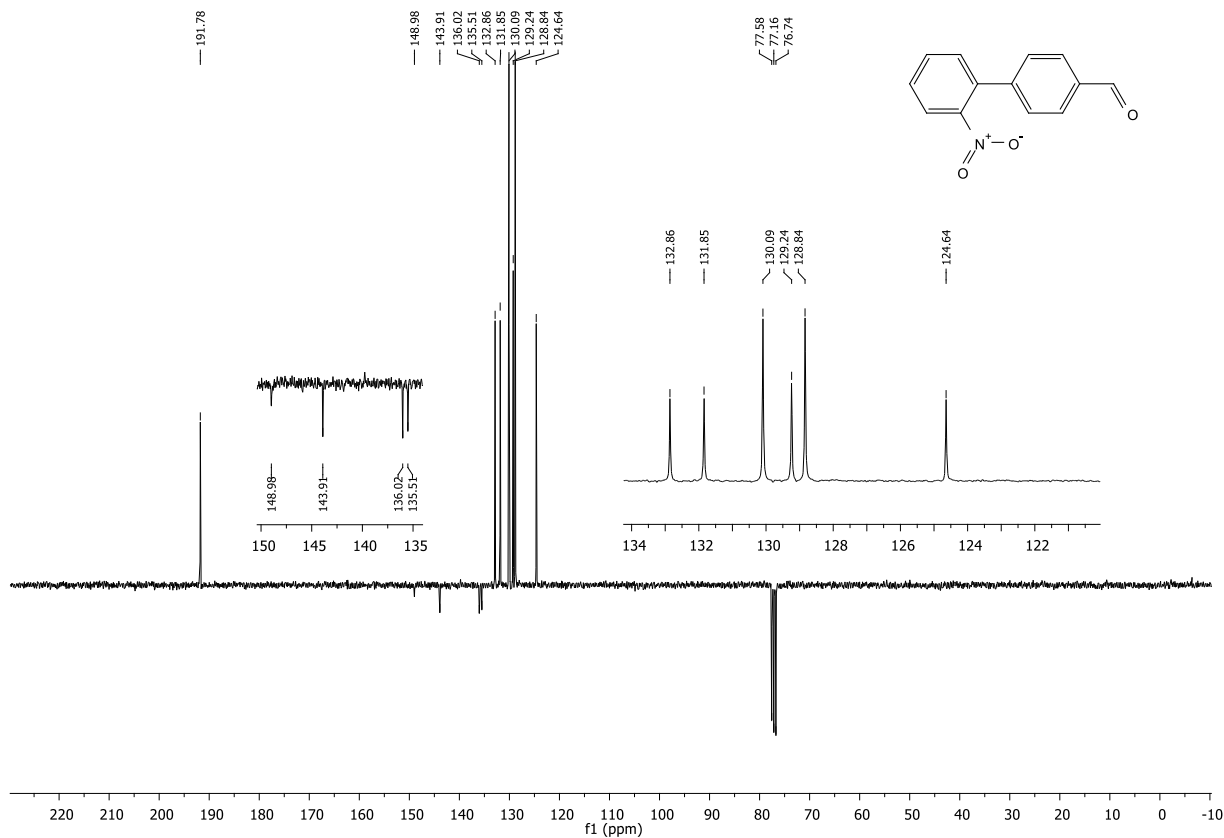
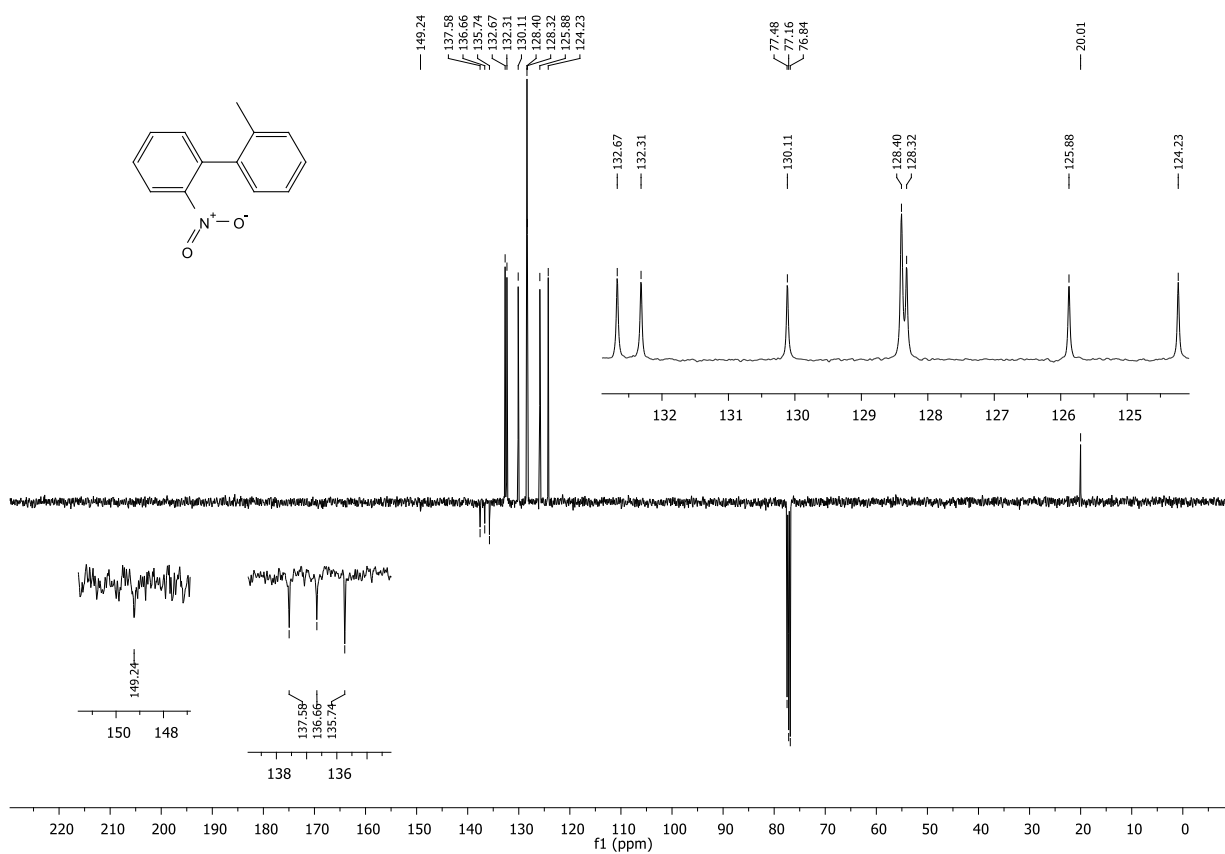
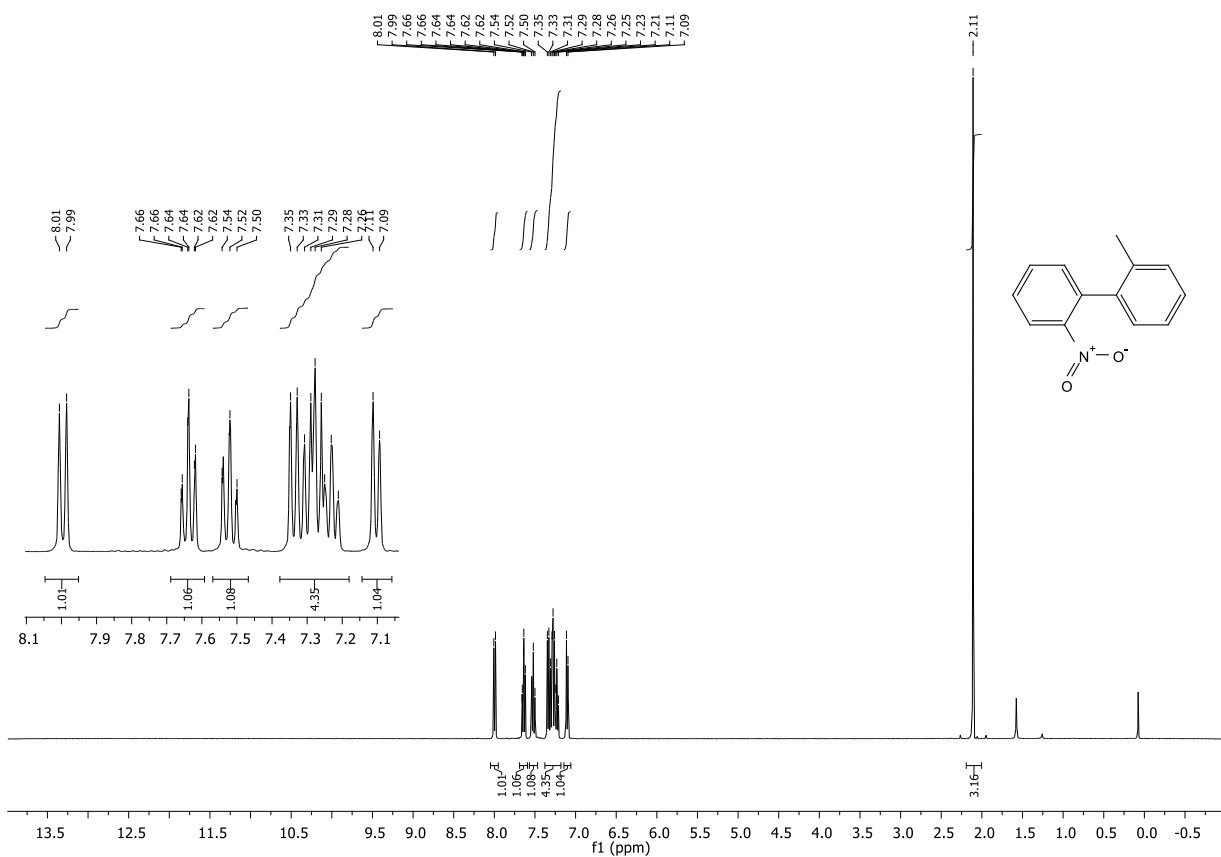
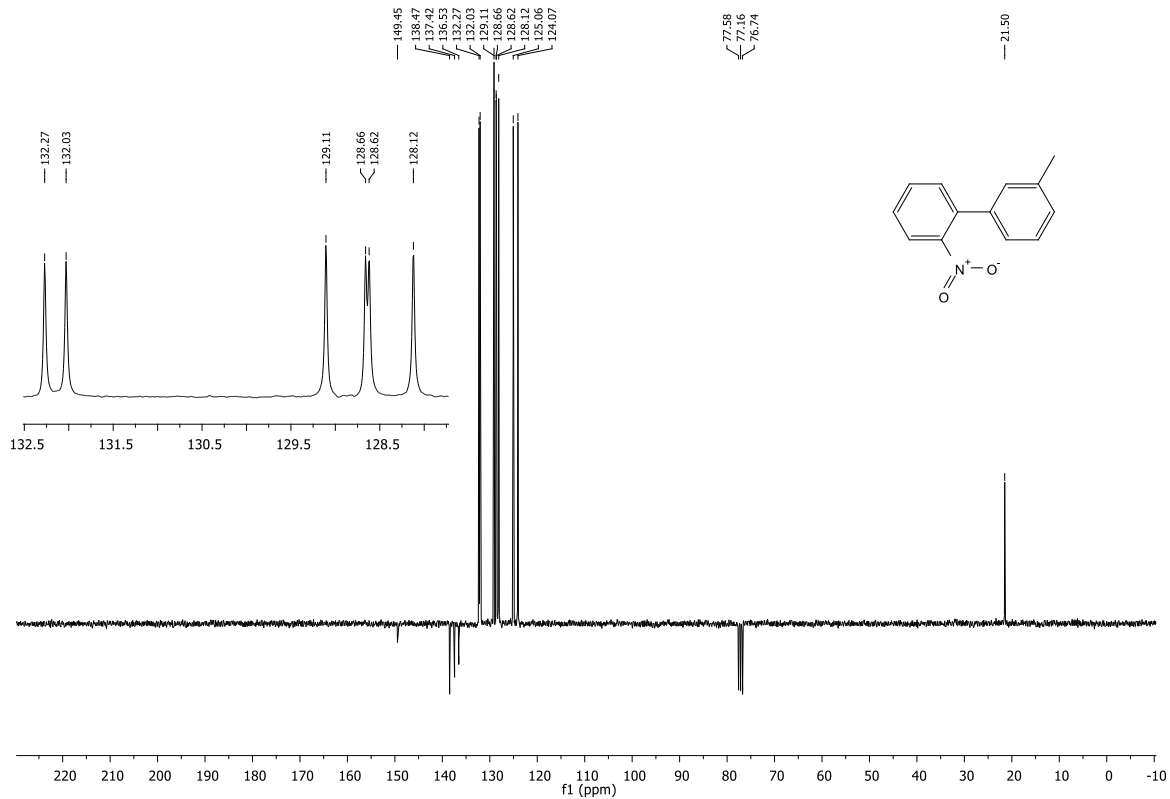
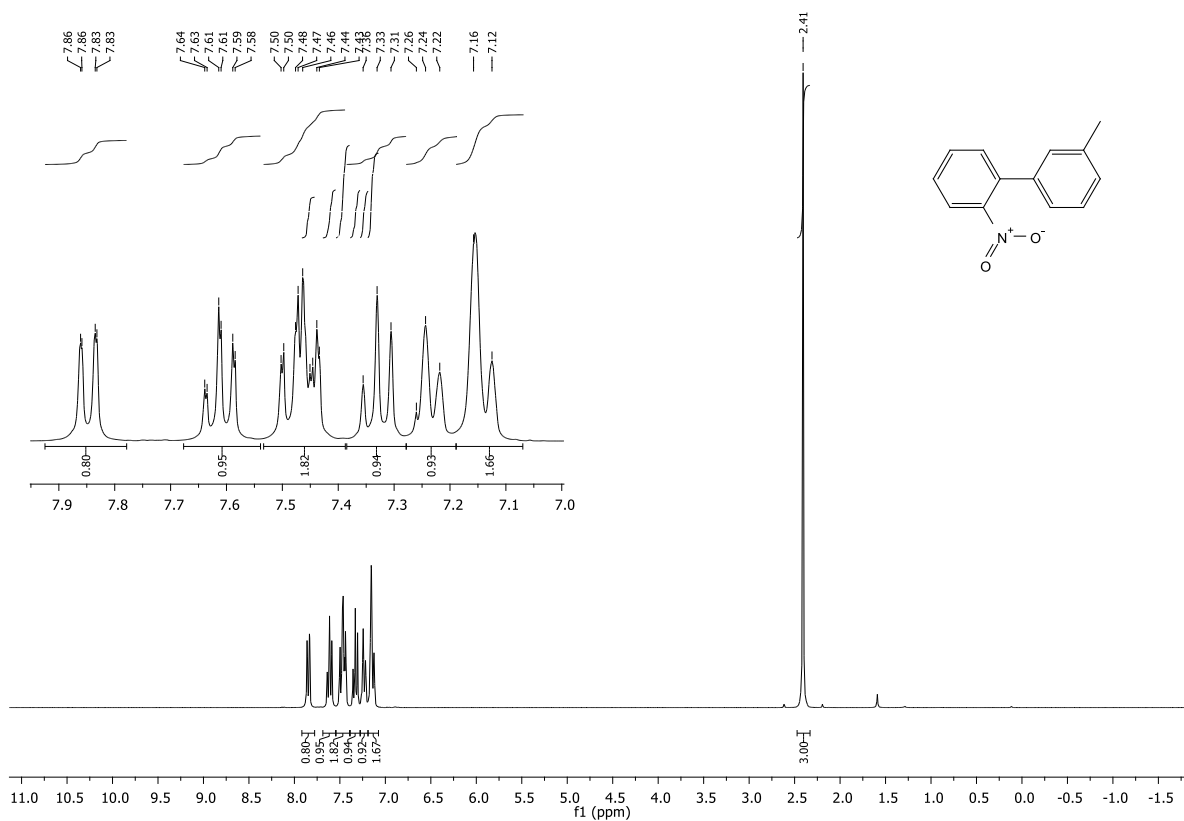
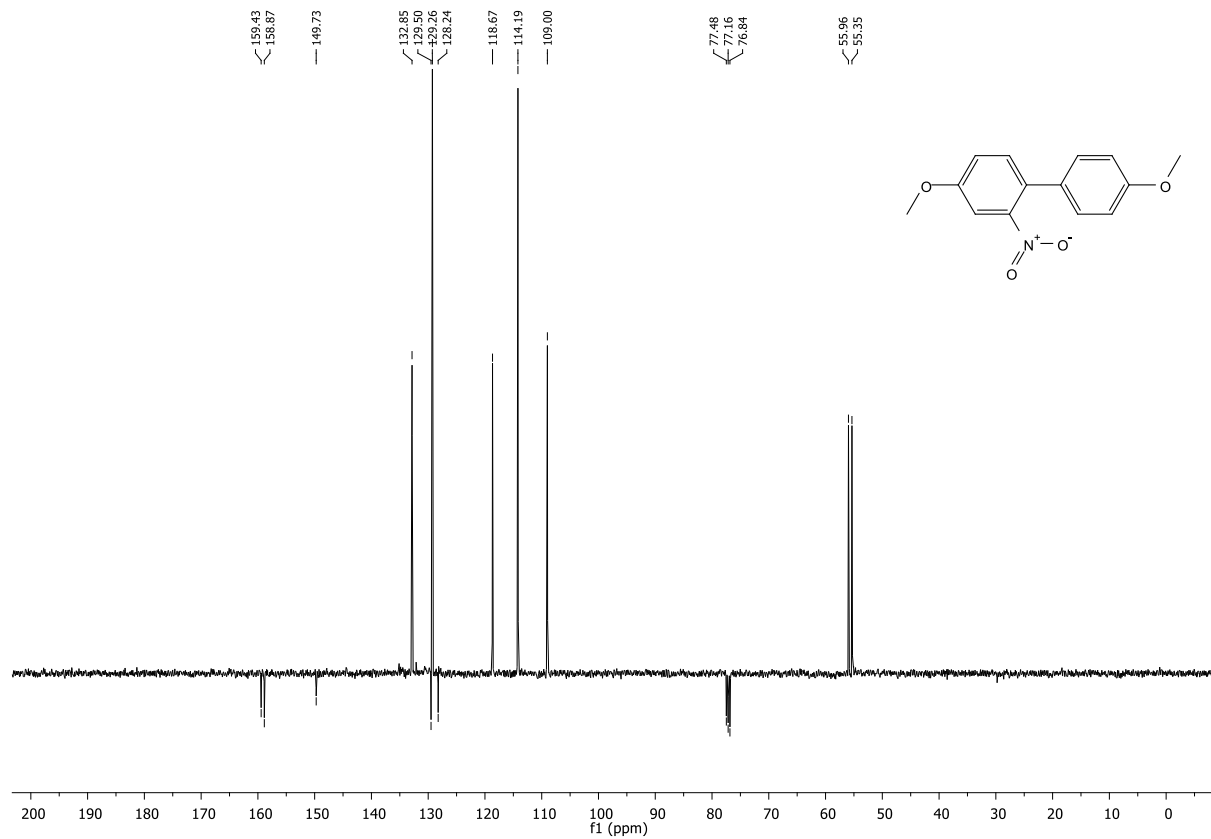
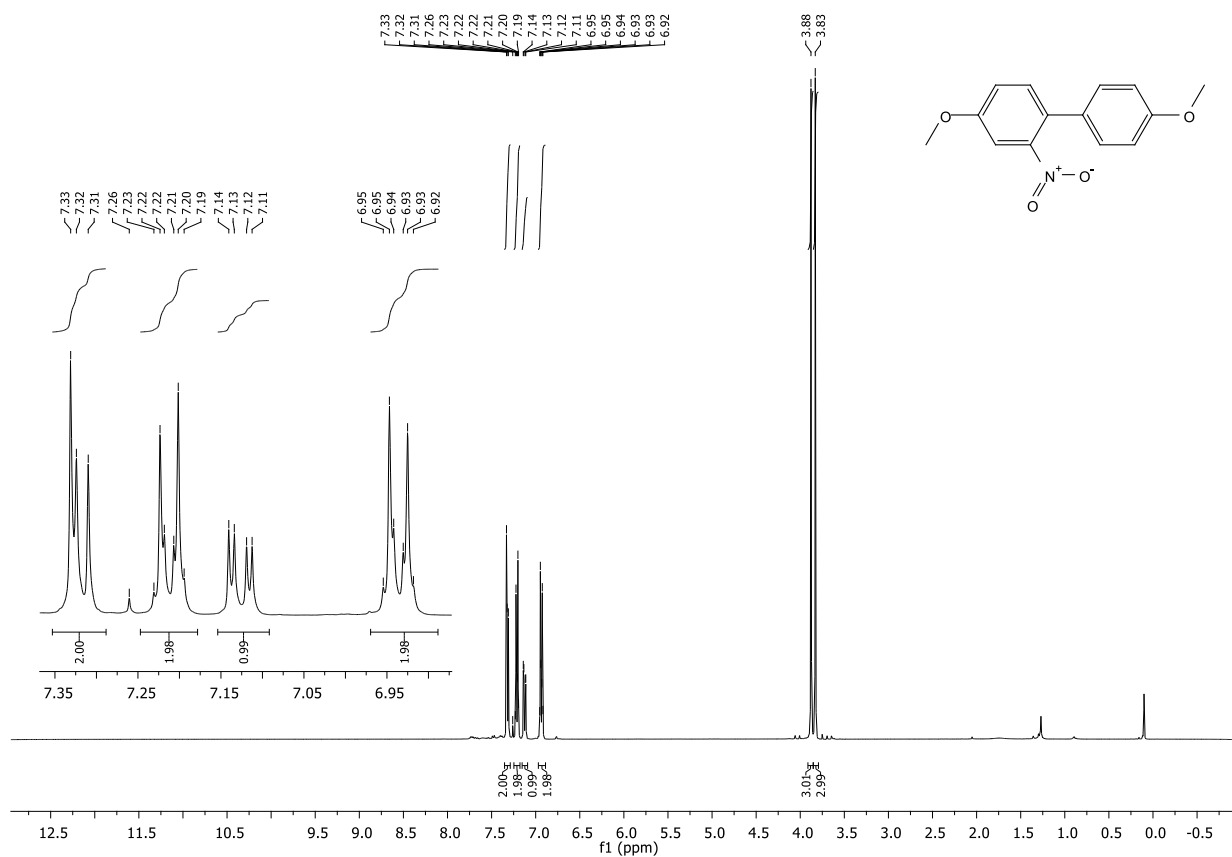


Figure 30: ¹³C NMR of 4'-formyl-2-nitrophenyl **57** spectrum in CDCl₃.







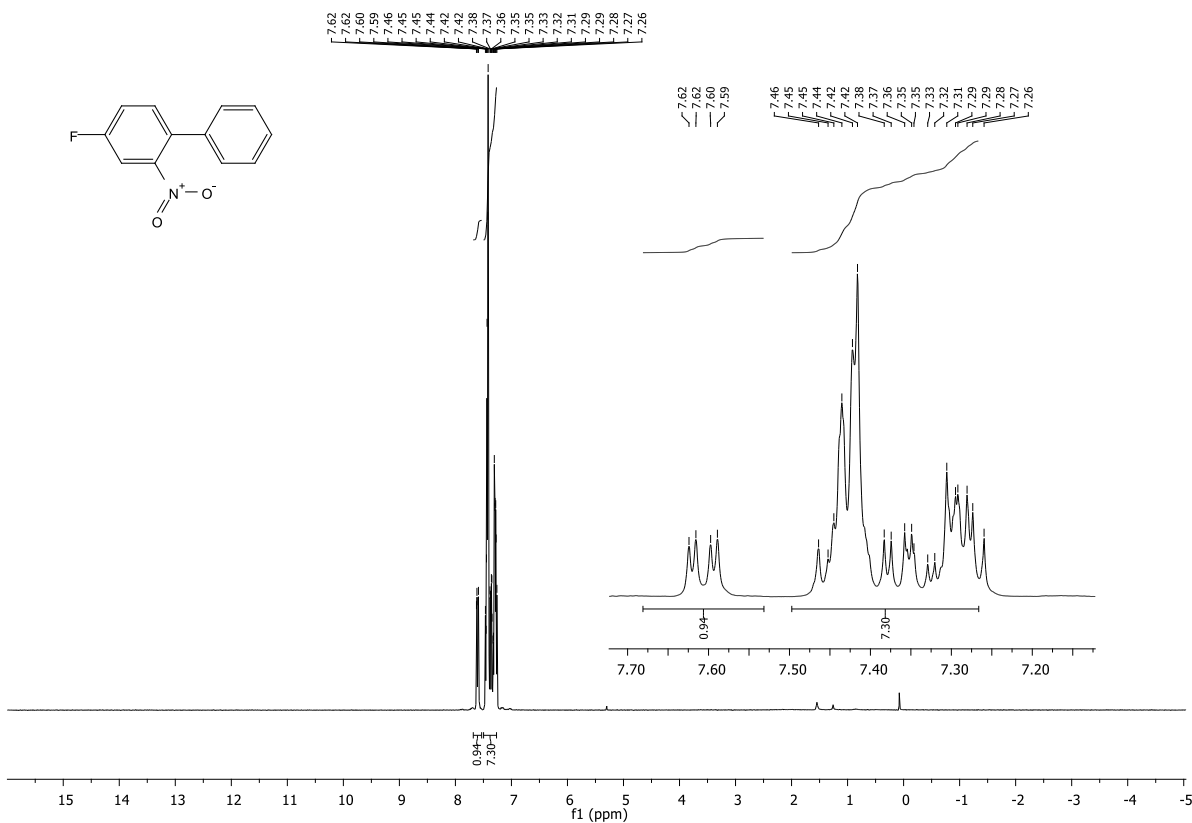


Figure 37: ¹H NMR of 4-fluoro-2-nitrophenyl **61** spectrum in CDCl₃.

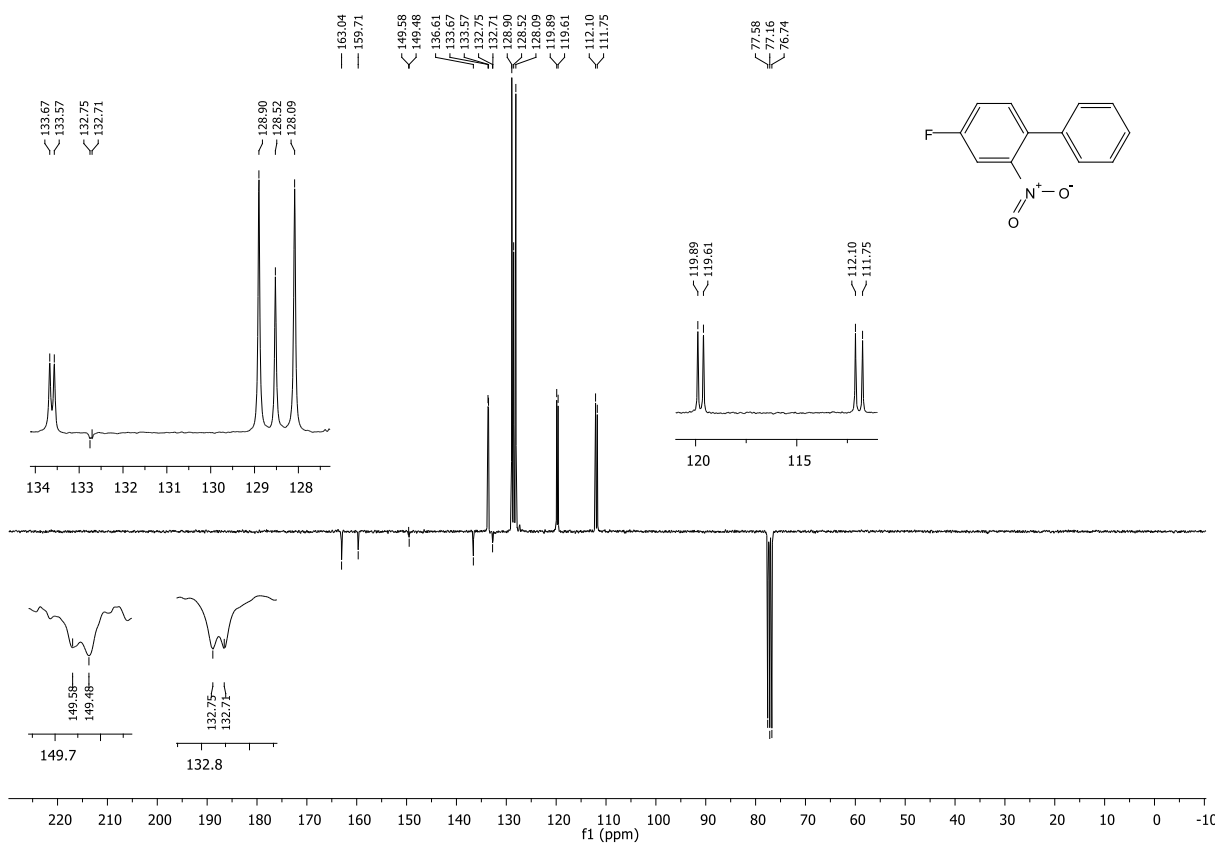


Figure 38: ¹³C NMR of 4-fluoro-2-nitrophenyl **61** spectrum in CDCl₃.

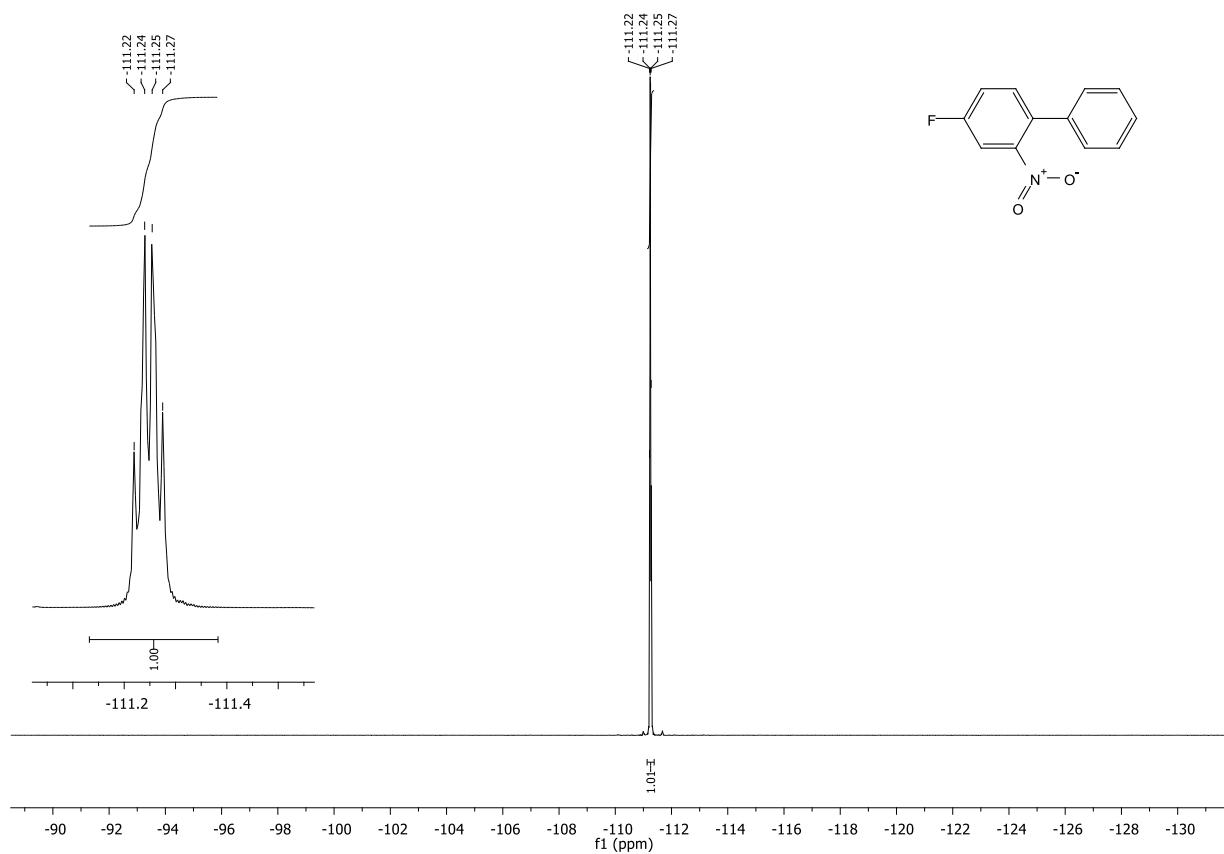


Figure 39: ¹⁹F NMR of 4-chloro-2-nitrophenyl **62** spectrum in CDCl₃.

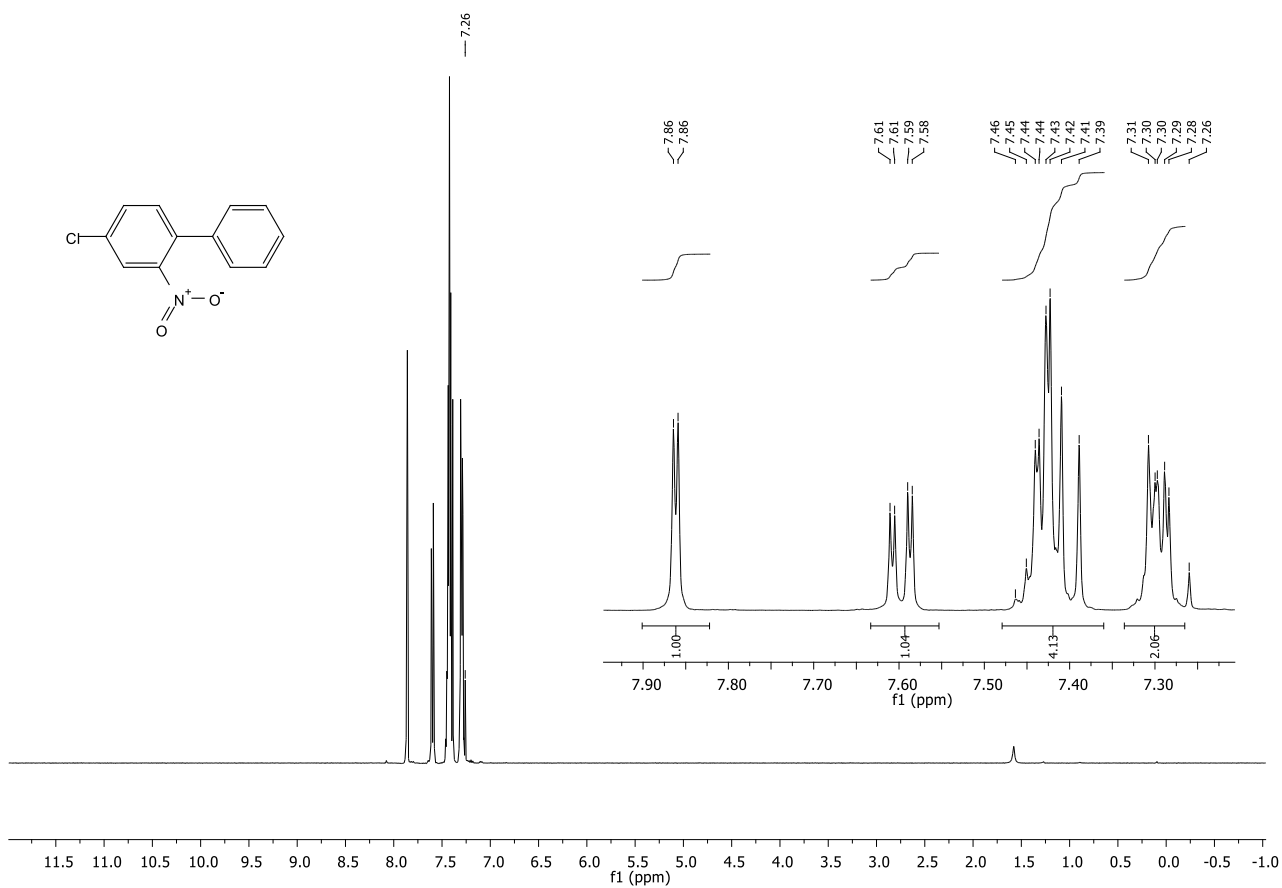


Figure 40: ¹H NMR of 4-chloro-2-nitrophenyl **62** spectrum in CDCl₃.

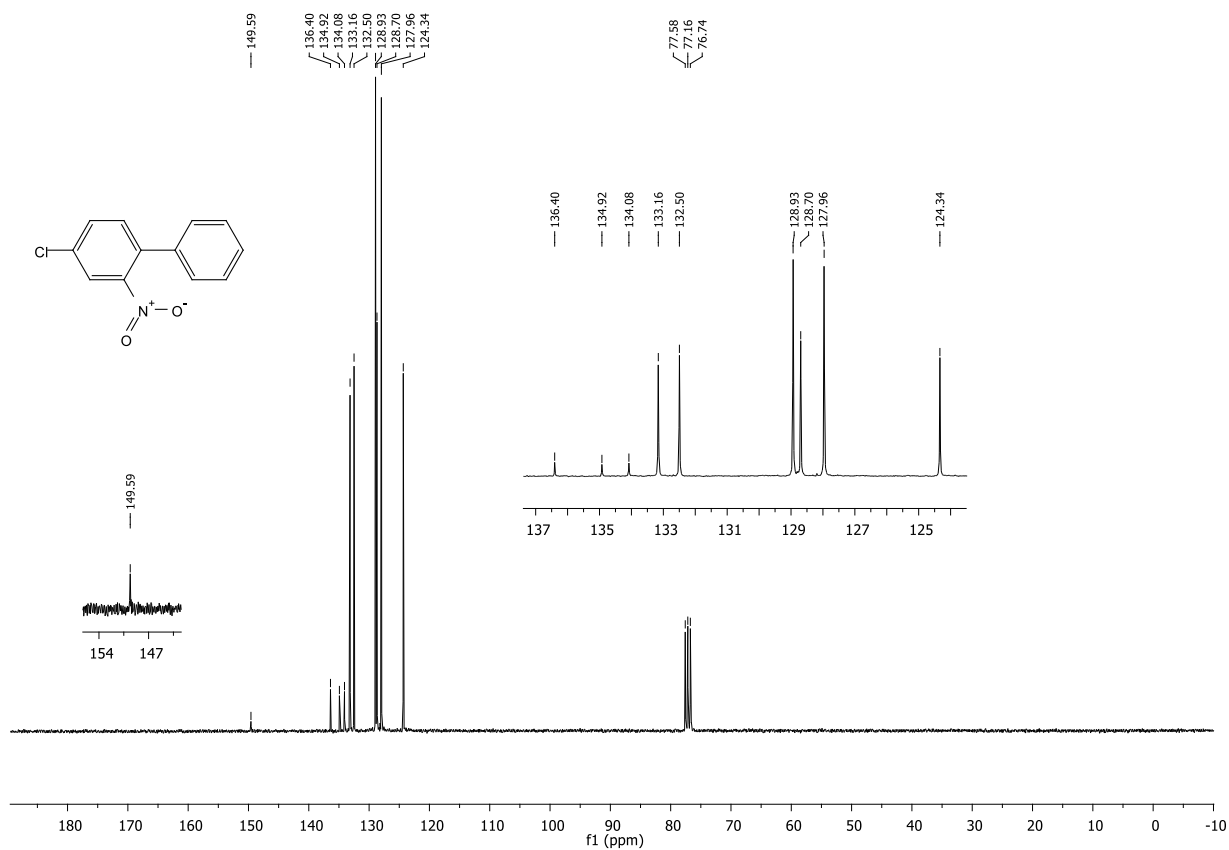


Figure 41: ¹³C NMR of 4-chloro-2-nitrobiphenyl **62** spectrum in CDCl₃.

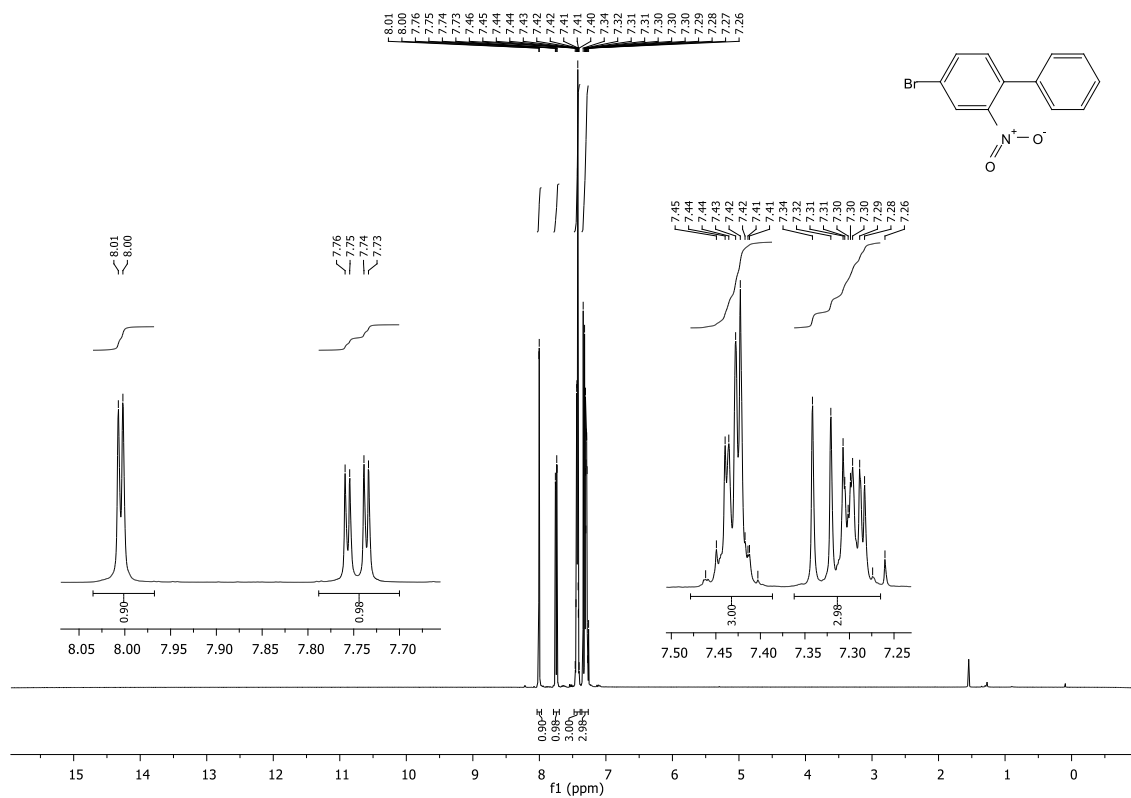


Figure 42: ¹H NMR of 4-bromo-2-nitrobiphenyl **63** spectrum in CDCl₃.

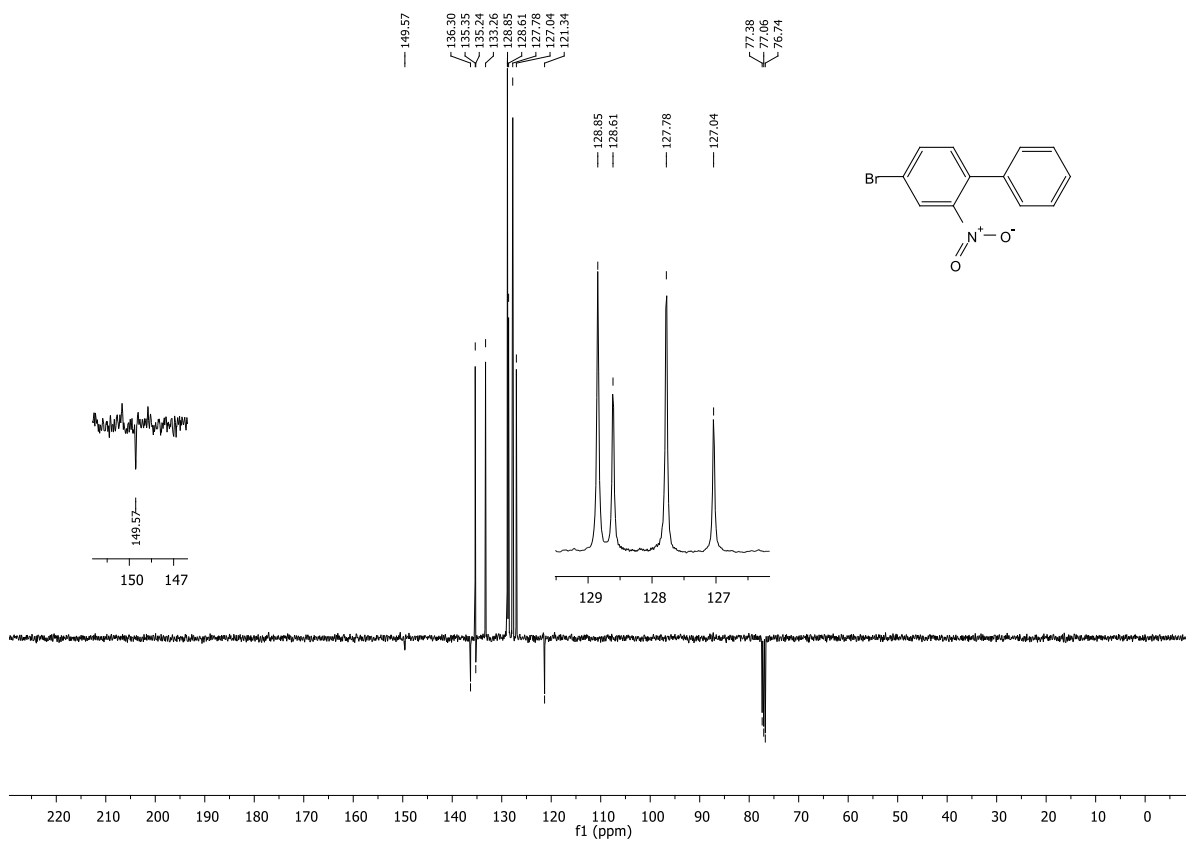


Figure 43: ^{13}C NMR of 4-bromo-2-nitrophenyl **63** spectrum in CDCl_3 .

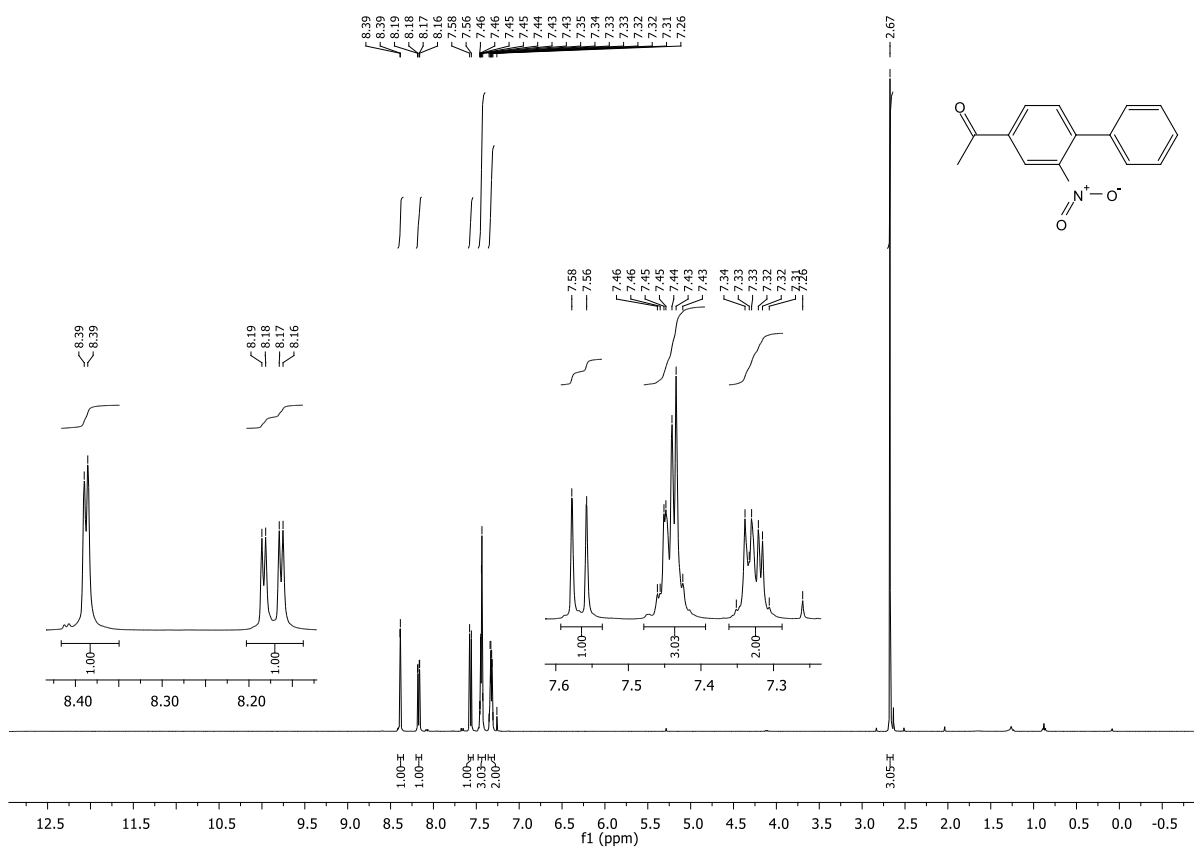


Figure 44: ^1H NMR of 4-acetyl-2-nitrophenyl **64** spectrum in CDCl_3 .

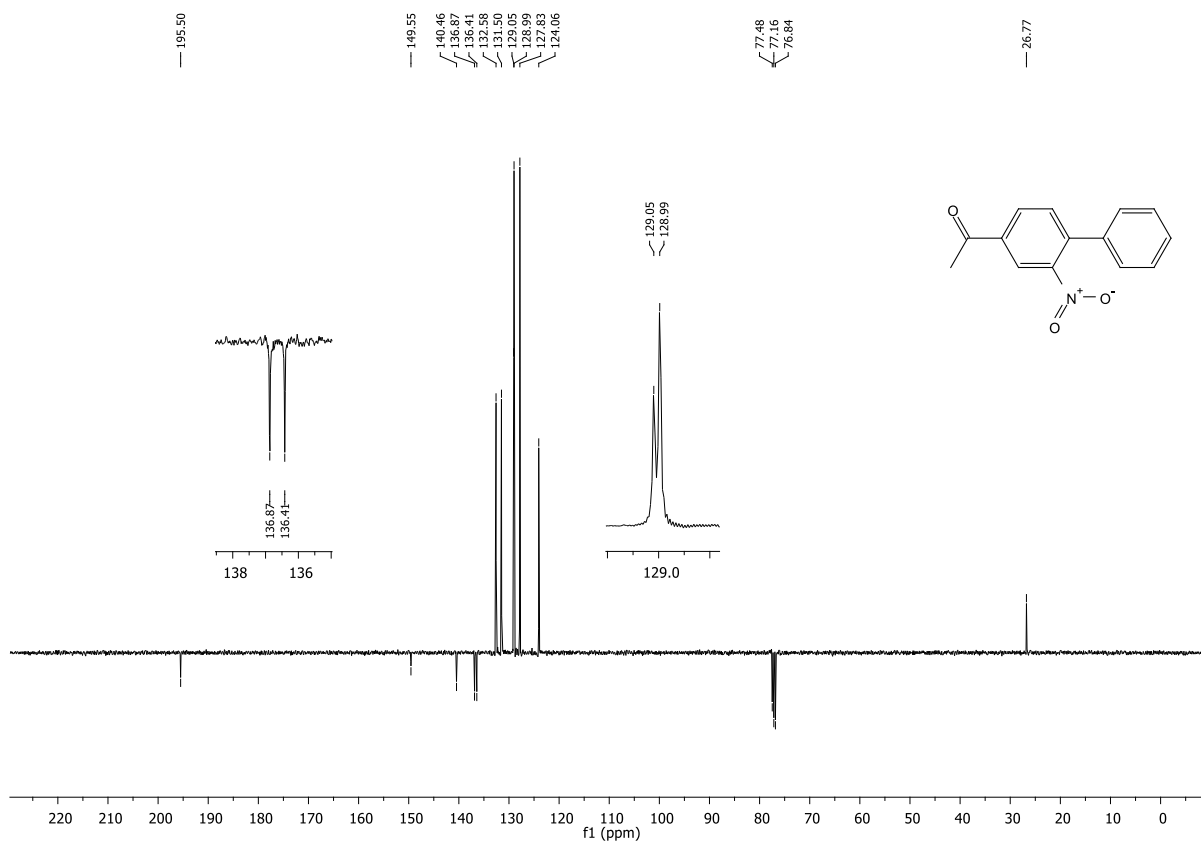


Figure 45: ^{13}C NMR of 4-Acetyl-2-nitrophenyl **64** spectrum in CDCl_3 .

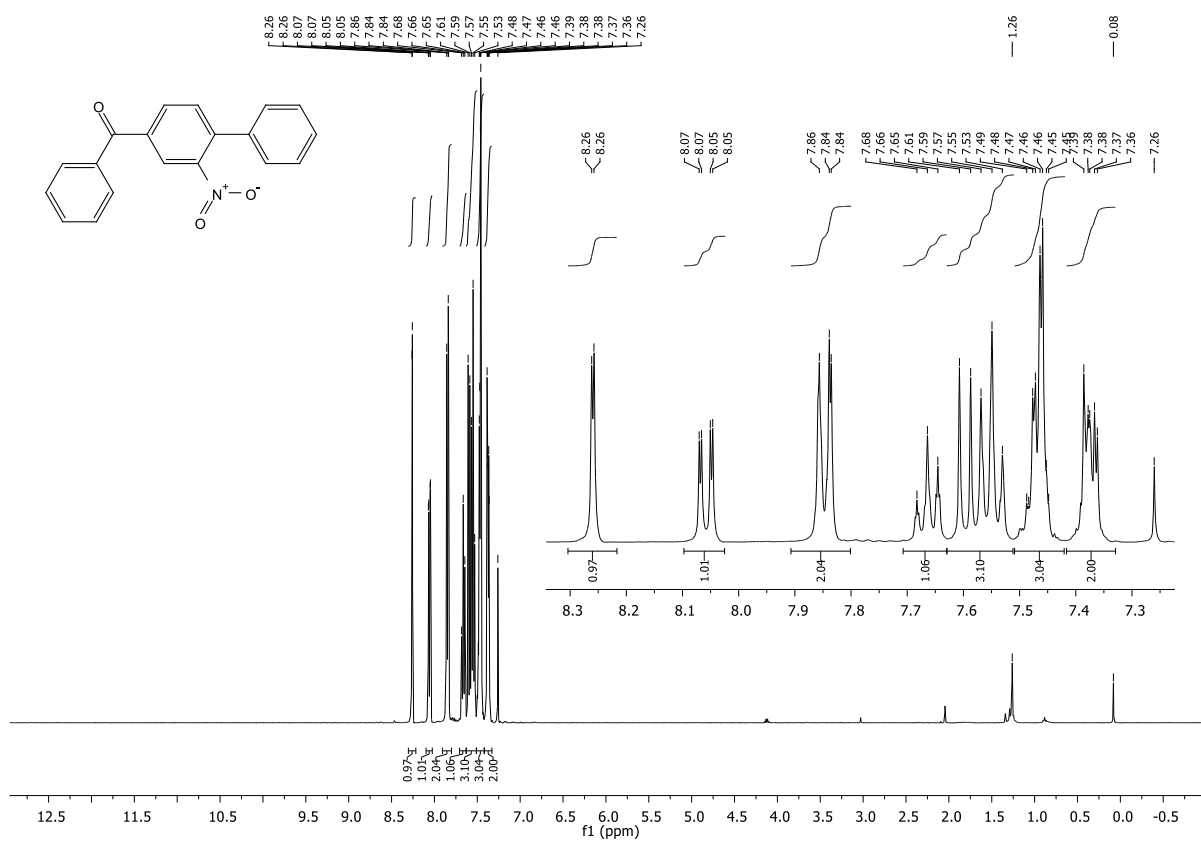


Figure 46: ^1H NMR of 4-benzoyl-2-nitrophenyl **65** spectrum in CDCl_3 .

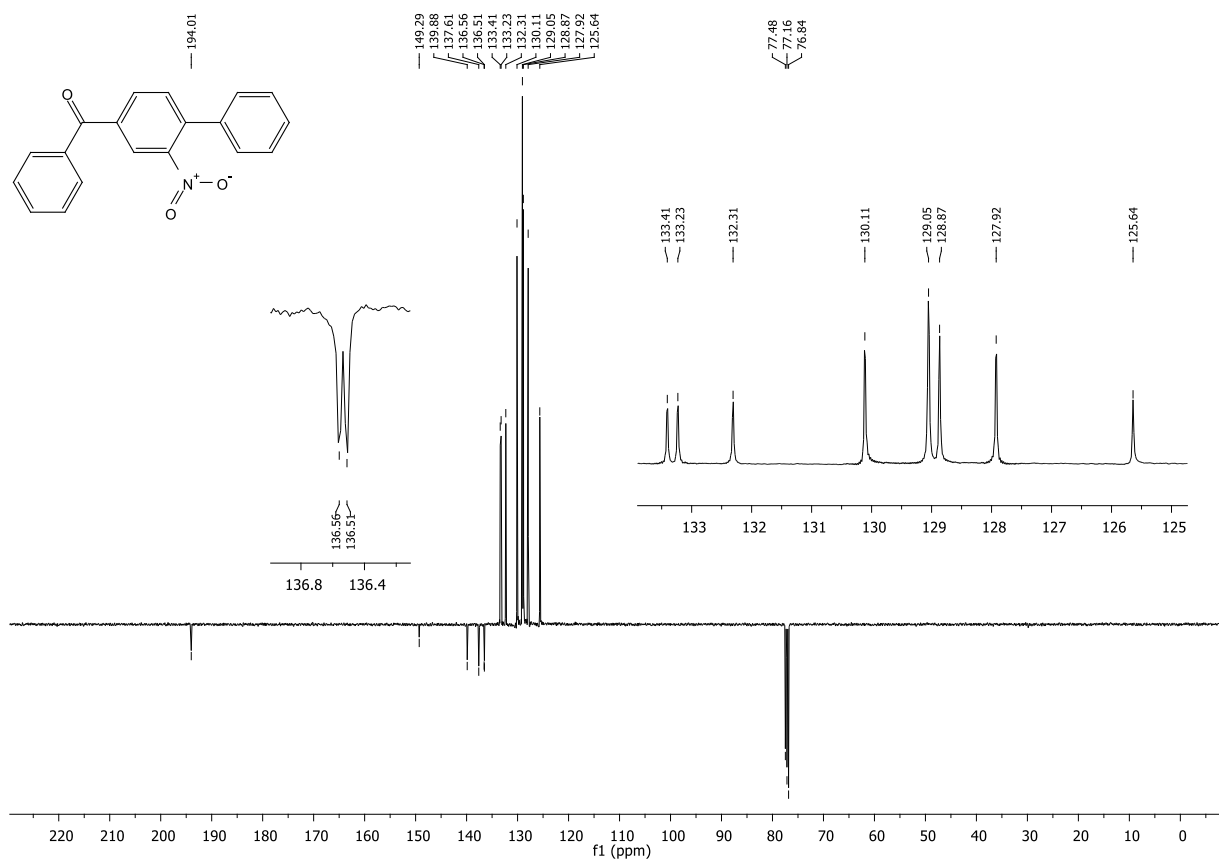


Figure 47: ^{13}C NMR of 4-benzoyl-2-nitrophenyl **65** spectrum in CDCl_3 .

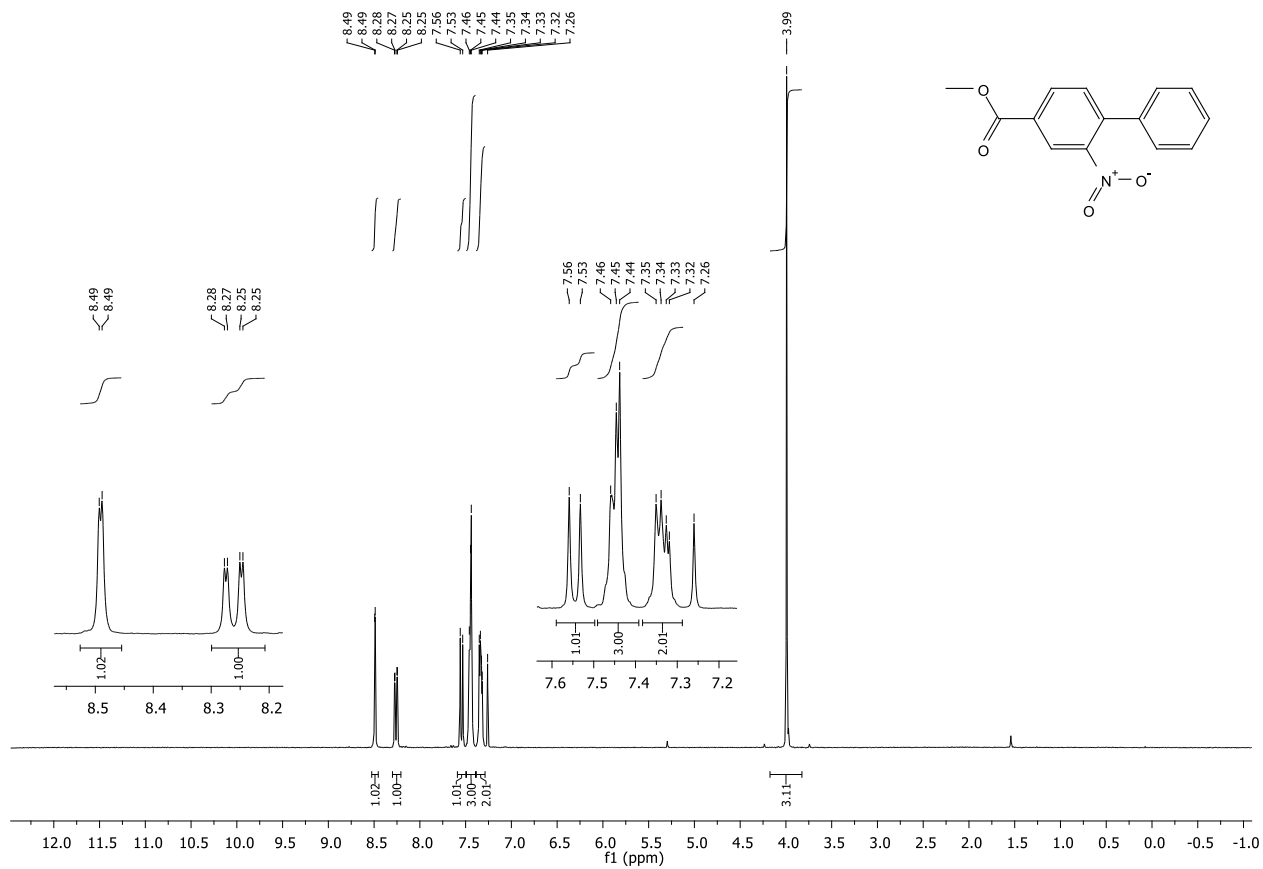


Figure 48: ^1H NMR of 4-carbomethoxy-2-nitrophenyl **66** spectrum in CDCl_3 .

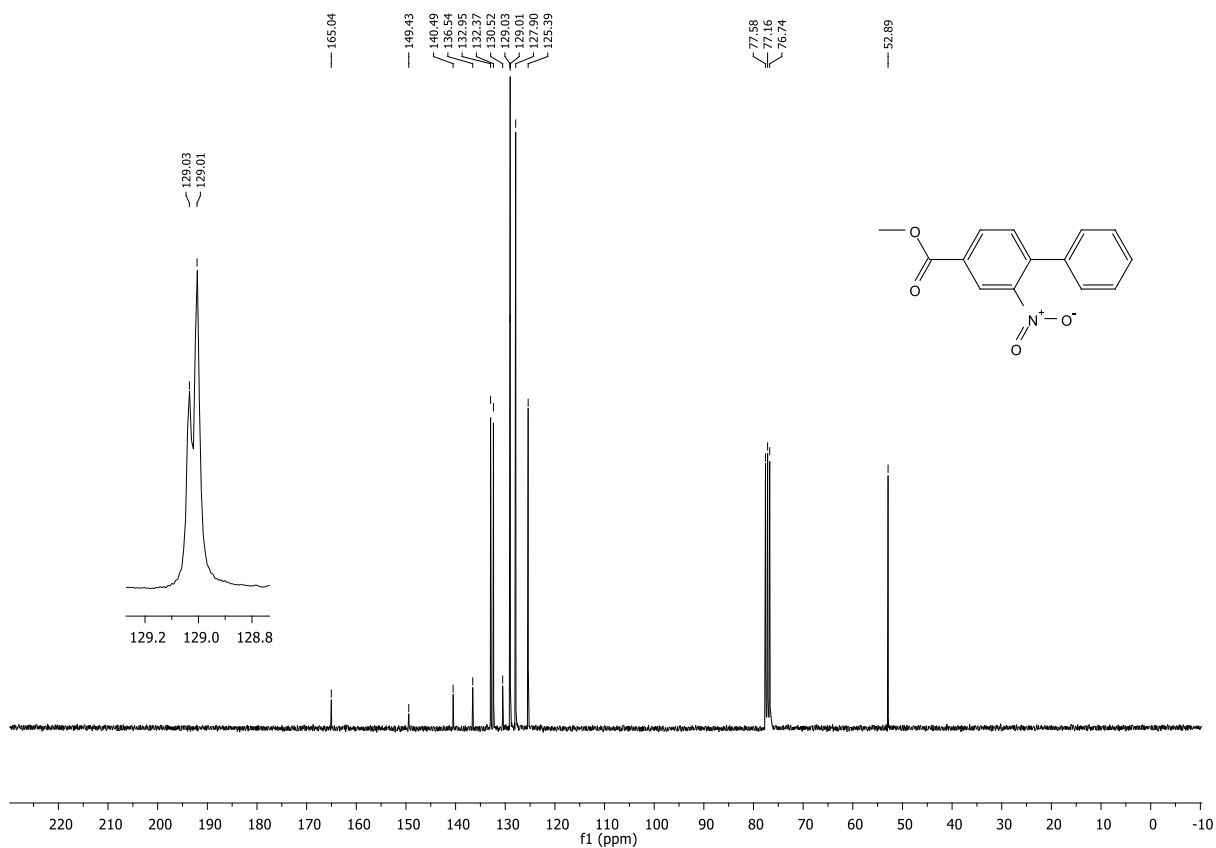


Figure 49: ^{13}C NMR of 4-carbomethoxy-2-nitrophenyl **66** spectrum in CDCl_3 .

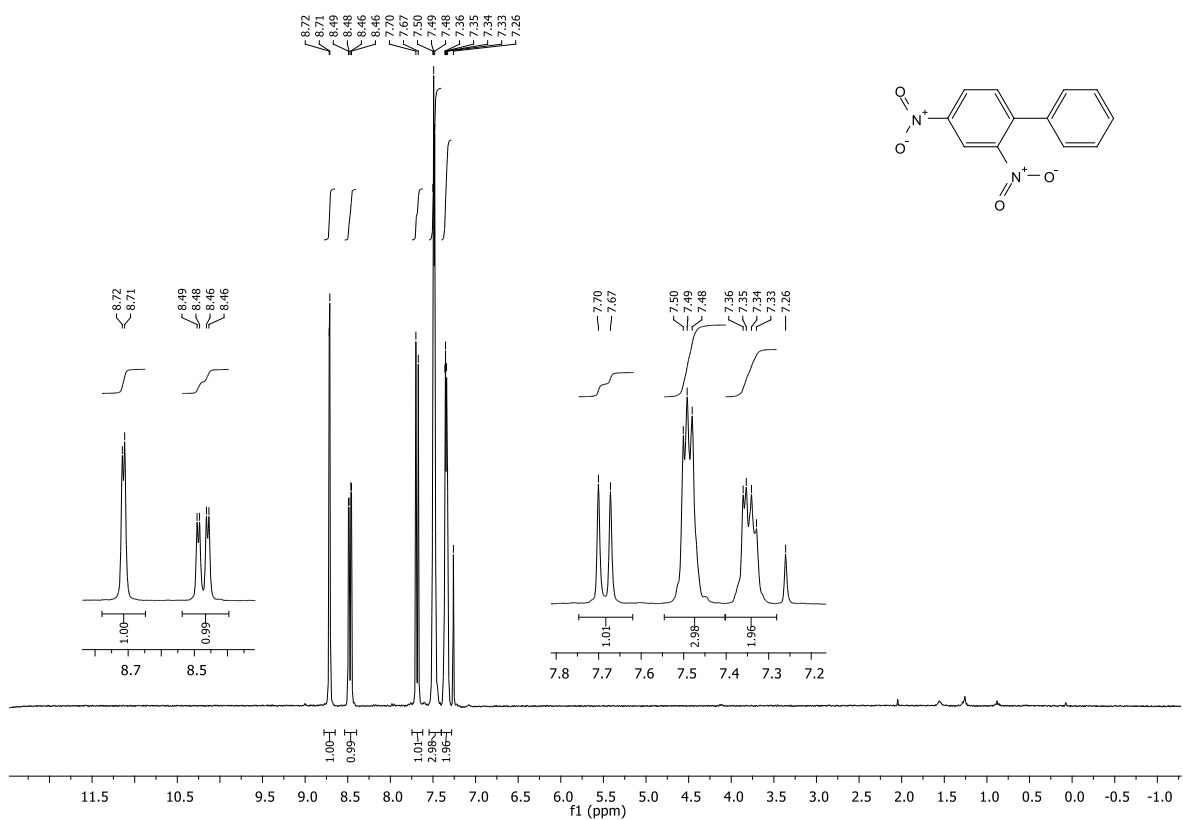


Figure 50: ^1H NMR of 2,4-dinitrophenyl **67** spectrum in CDCl_3 .

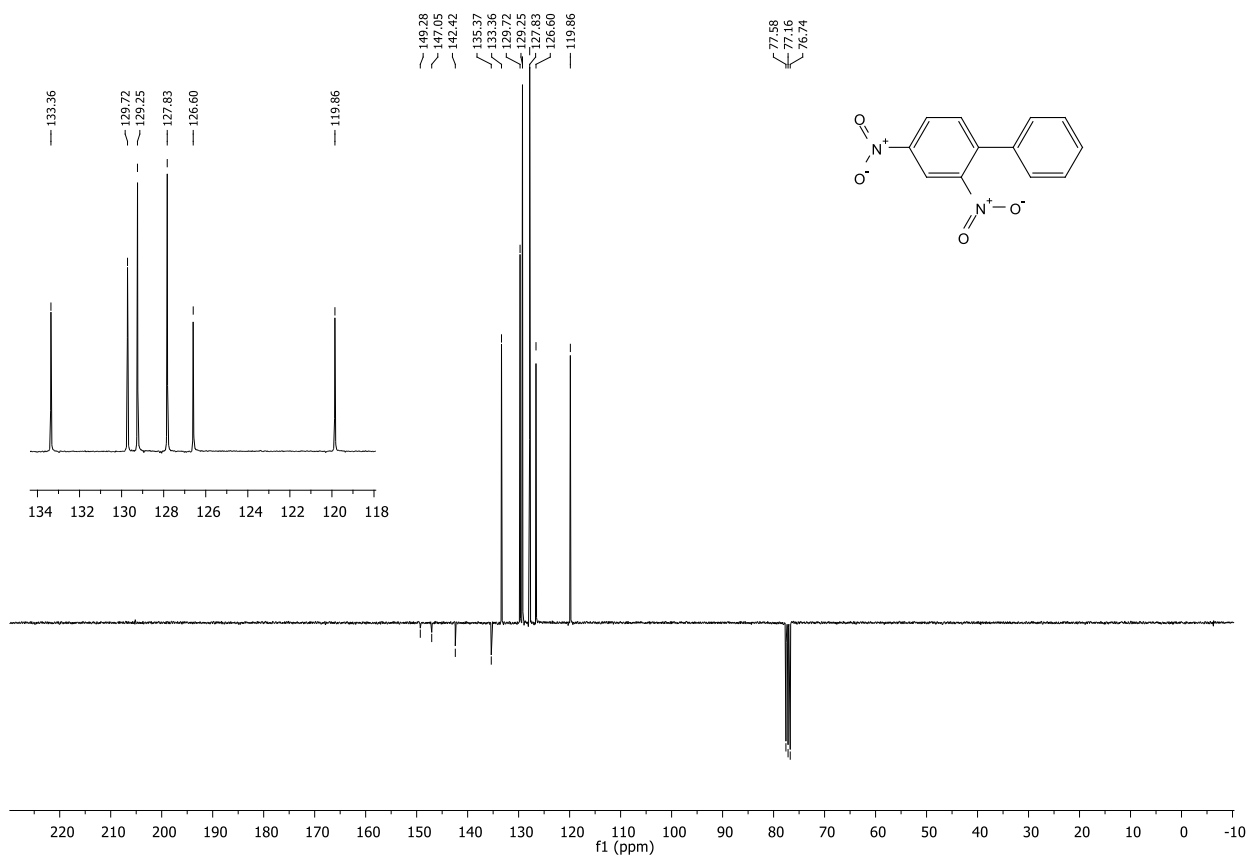


Figure 51: ¹³C NMR of 2,4-dinitrophenyl **67** spectrum in CDCl₃.

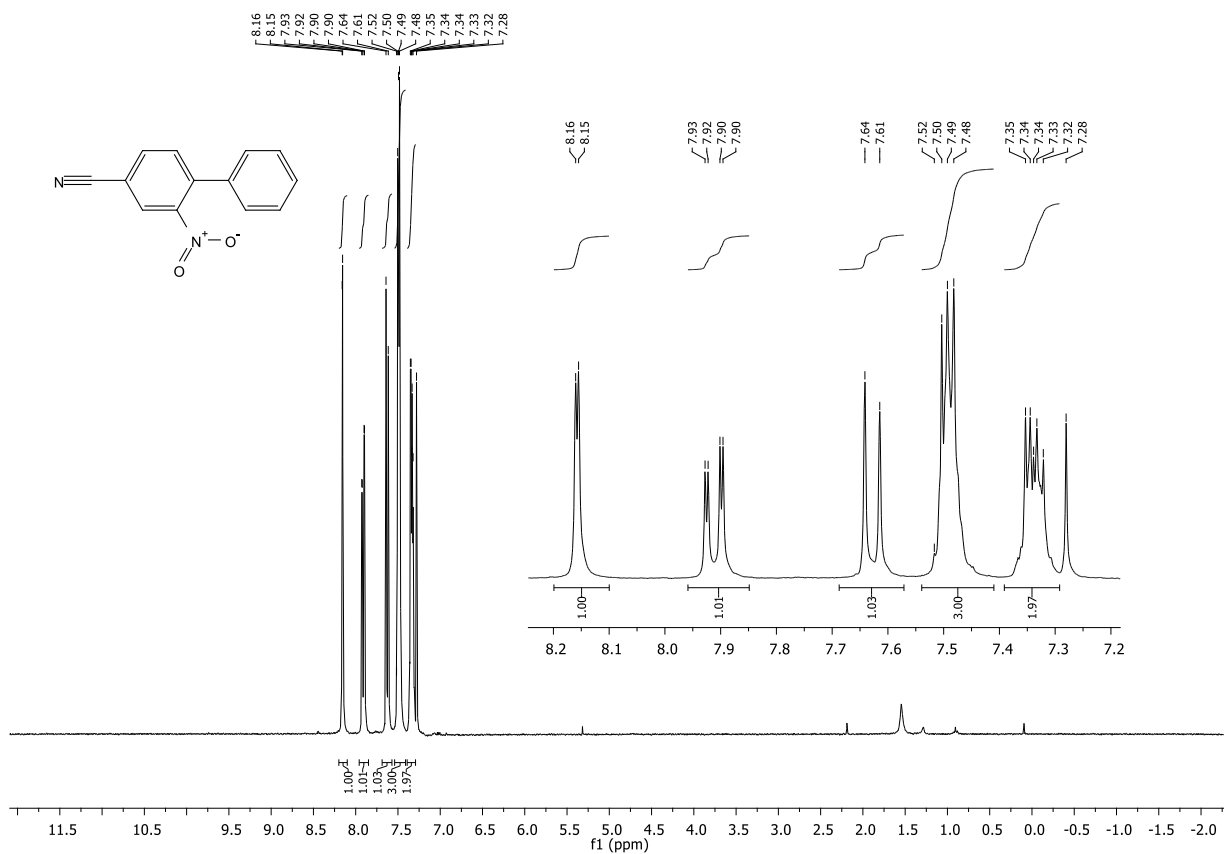


Figure 52: ¹H NMR of 4-cyano-2-nitrophenyl **68** spectrum in CDCl₃.

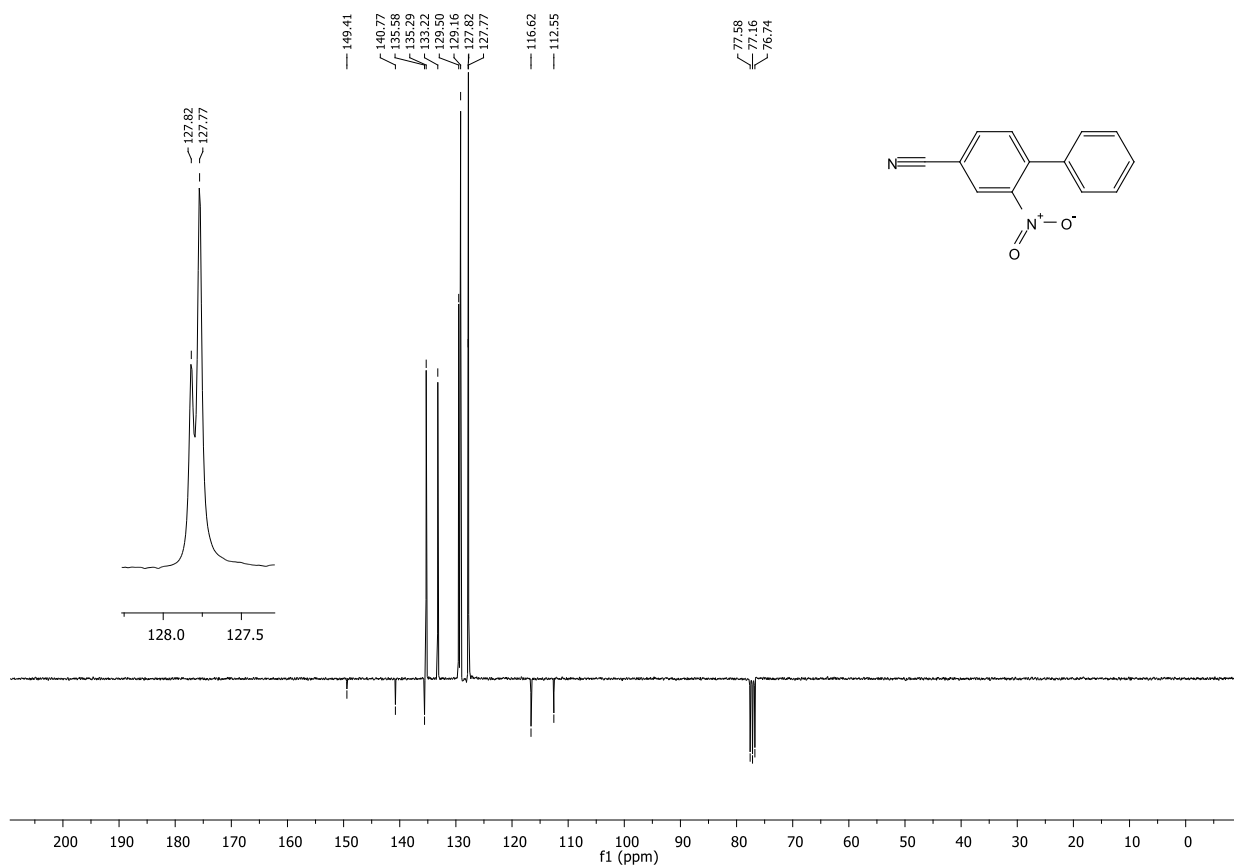


Figure 53: ^{13}C NMR of 4-cyano-2-nitrophenyl **68** spectrum in CDCl_3 .

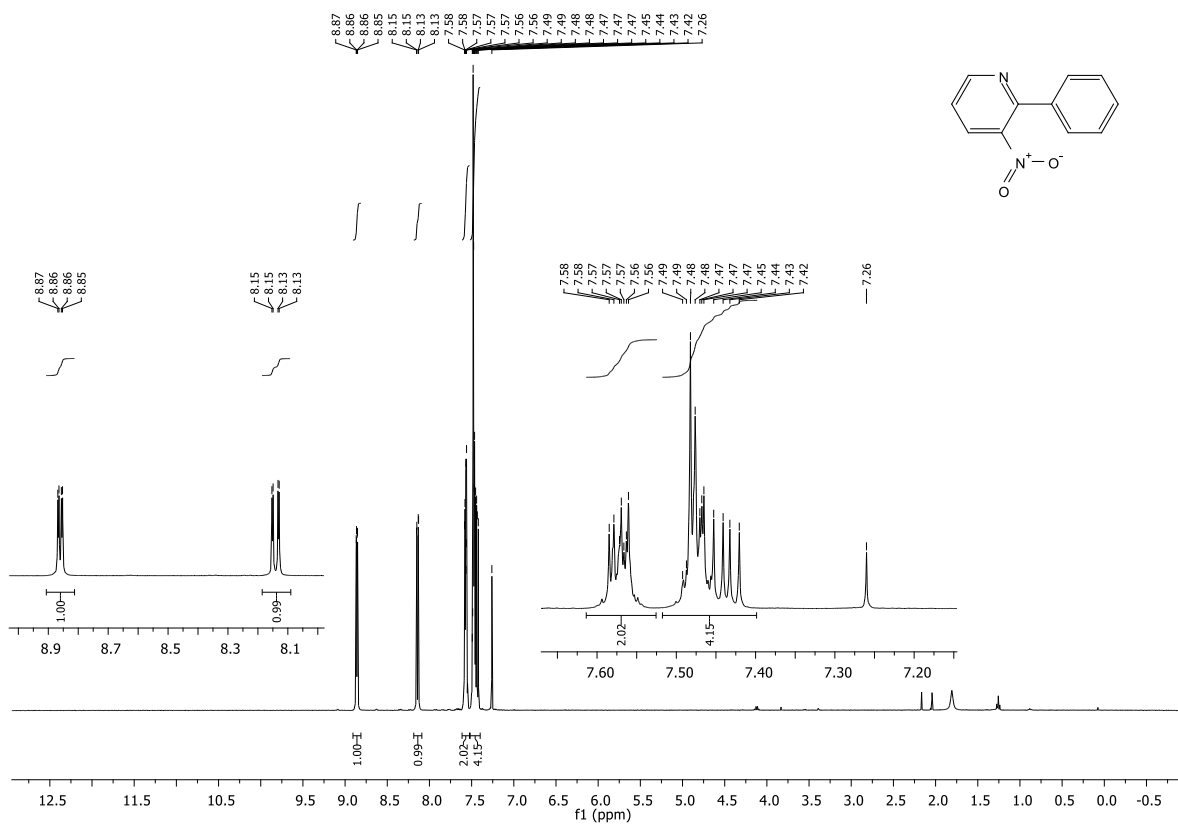


Figure 54: ^1H NMR of 3-nitro-2-phenylpyridine **69** spectrum in CDCl_3 .

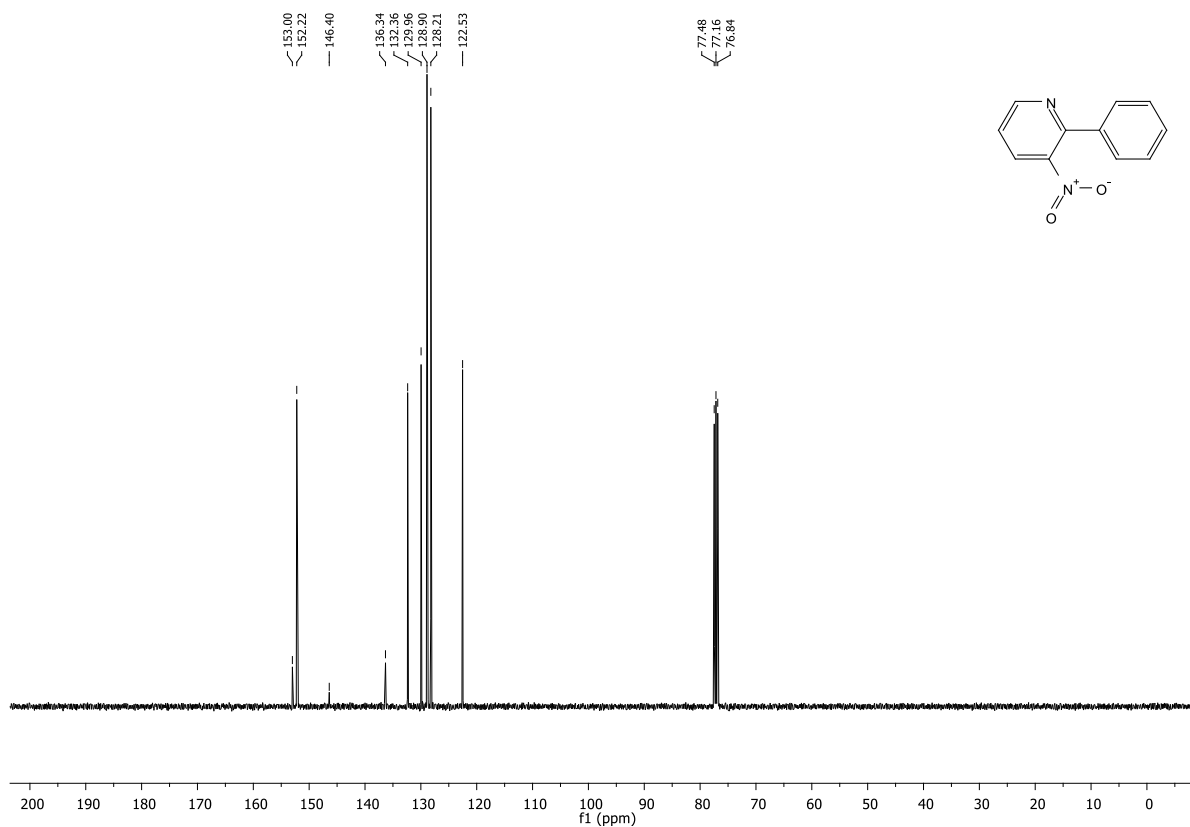


Figure 55: ^{13}C NMR of 3-nitro-2-phenylpyridine **69** spectrum in CDCl_3 .

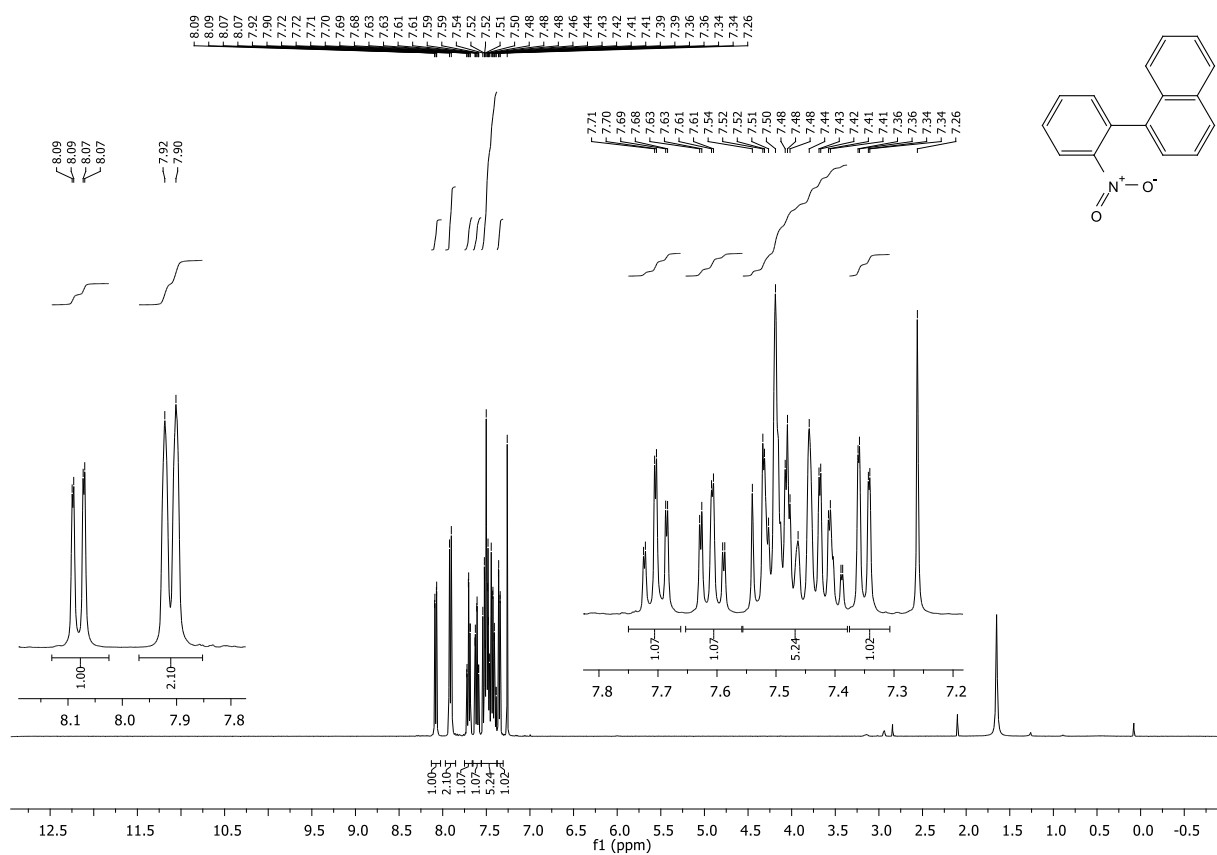


Figure 56: ^1H NMR of 1-(2-nitrophenyl)naphthalene **70** spectrum in CDCl_3 .

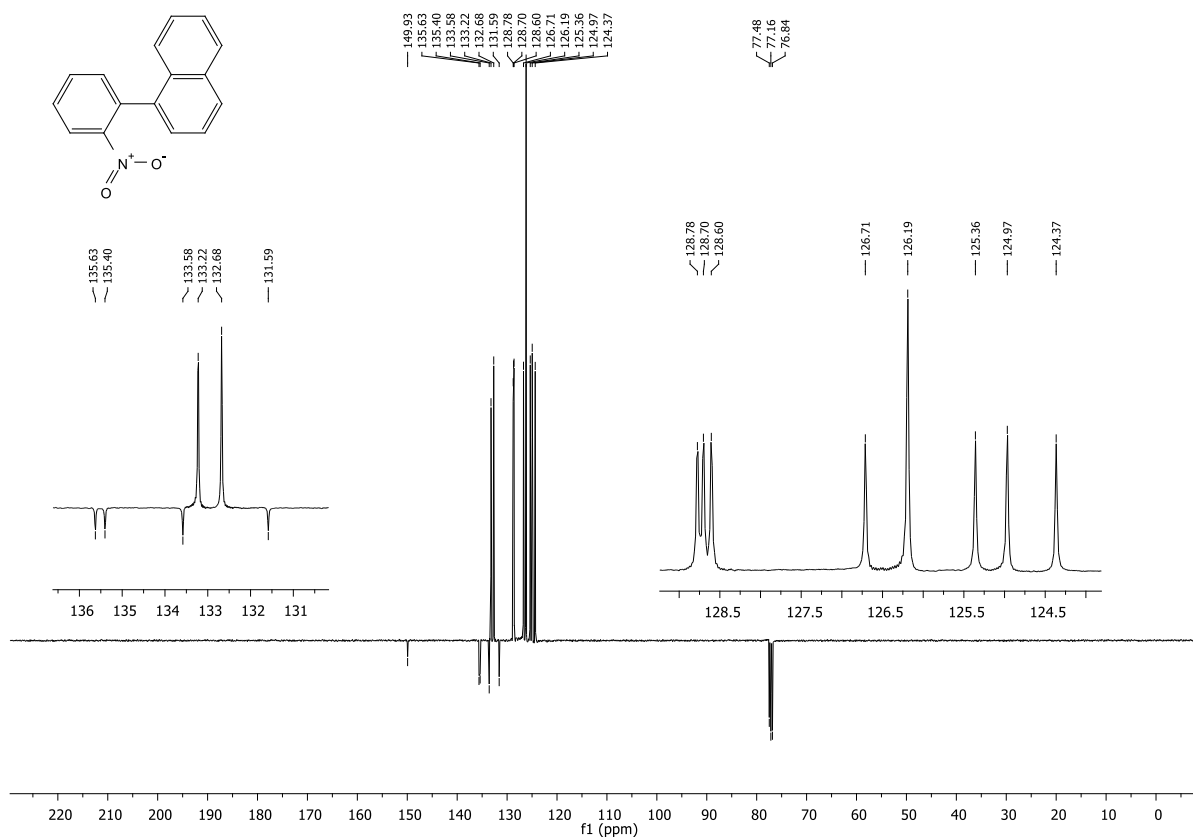


Figure 57: ^{13}C NMR of 1-(2-nitrophenyl)naphthalene **70** spectrum in CDCl_3 .

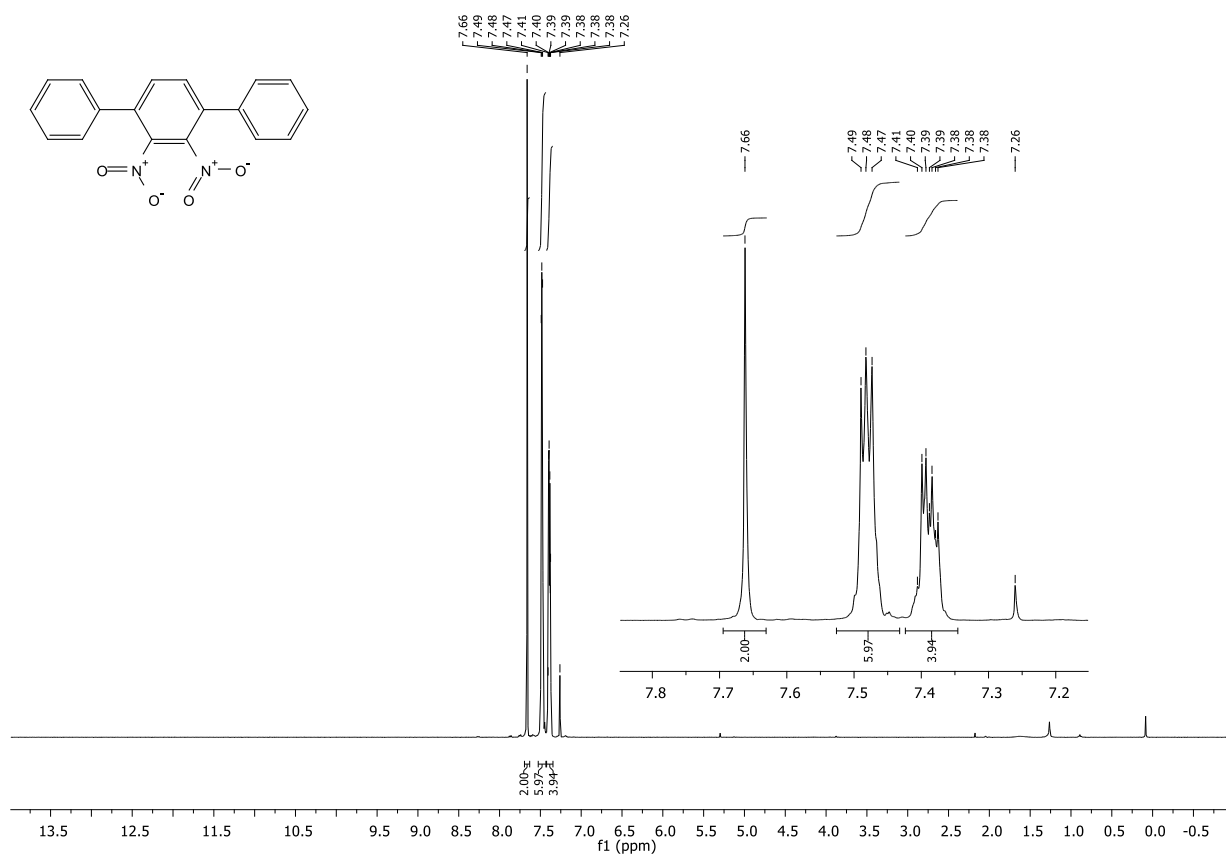


Figure 58: ^1H NMR of 2,3'-dinitro-1,1':4,1''-terphenyl **71** spectrum in CDCl_3 .

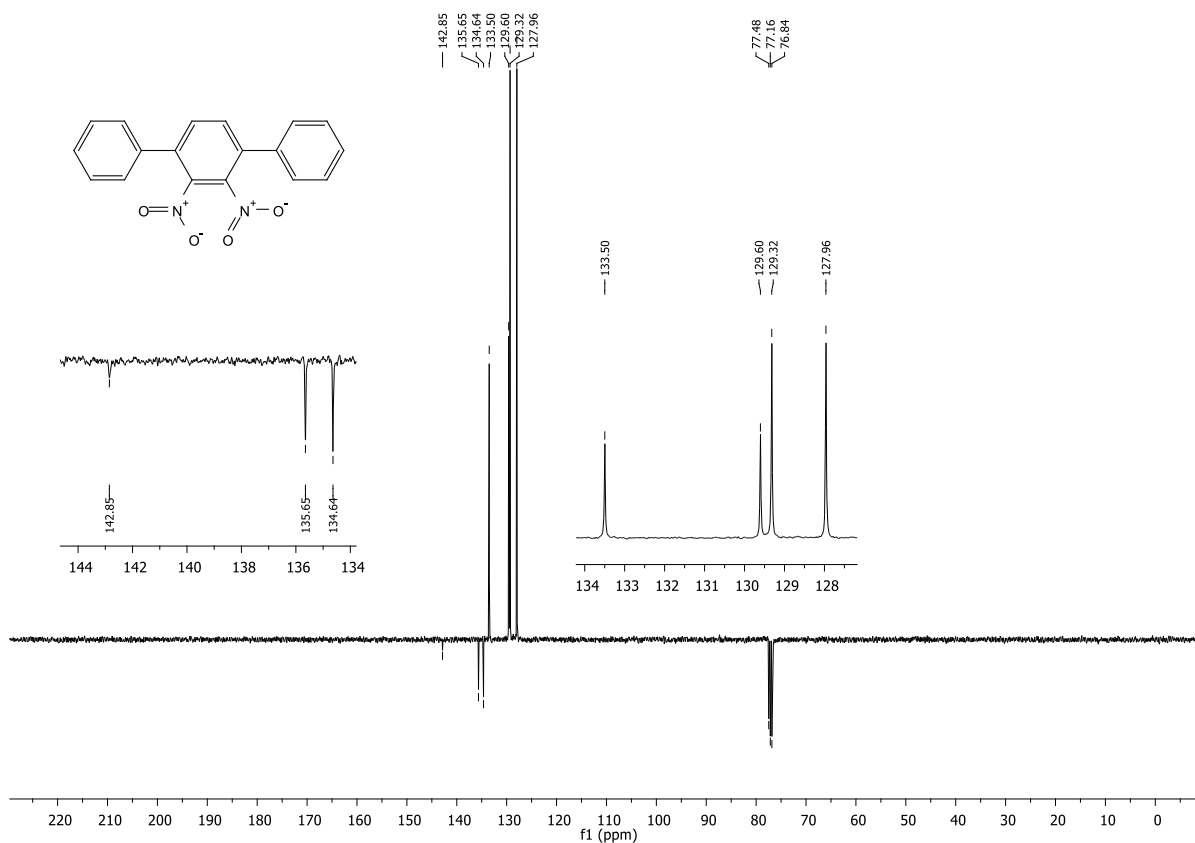


Figure 59: ¹³C NMR of 2',3'-dinitro-1,1':4',1''-terphenyl **71** spectrum in CDCl₃.

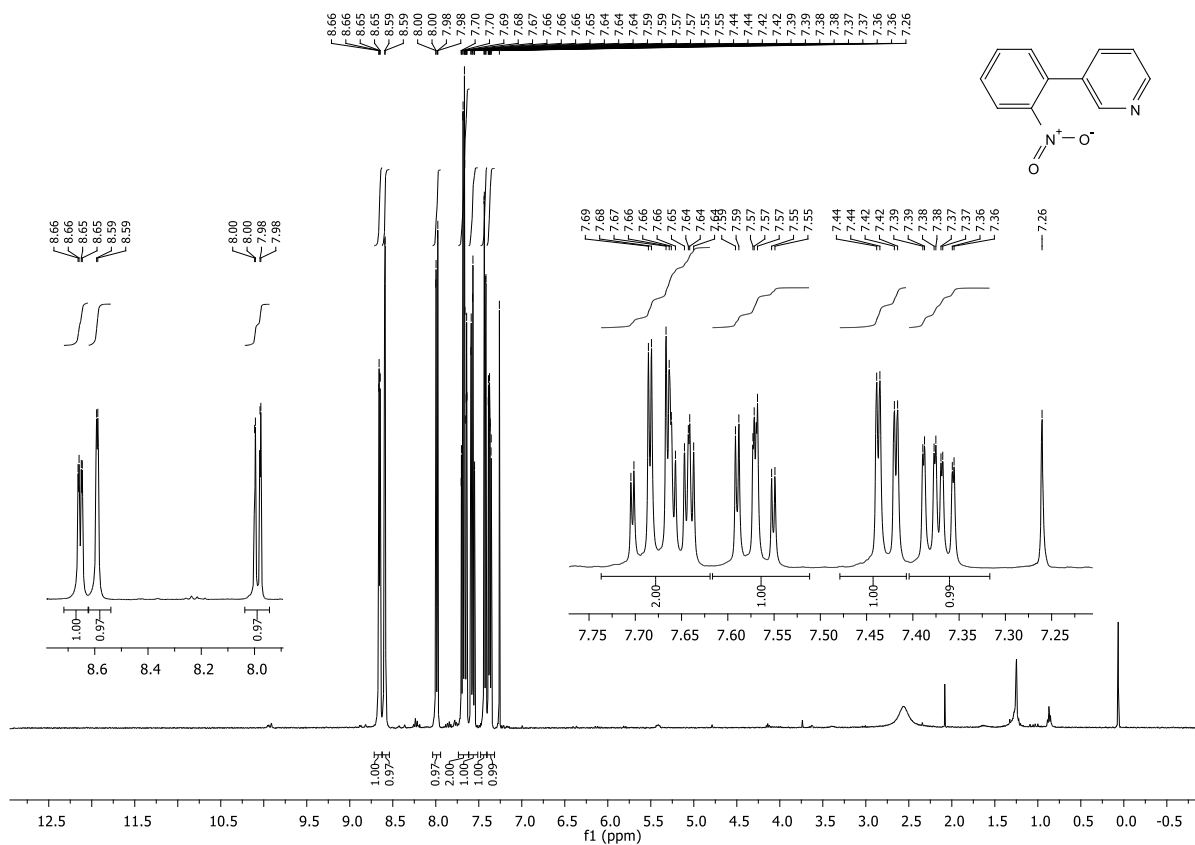


Figure 60: ¹H NMR of 3-(2-nitrophenyl)pyridine **72** spectrum in CDCl₃.

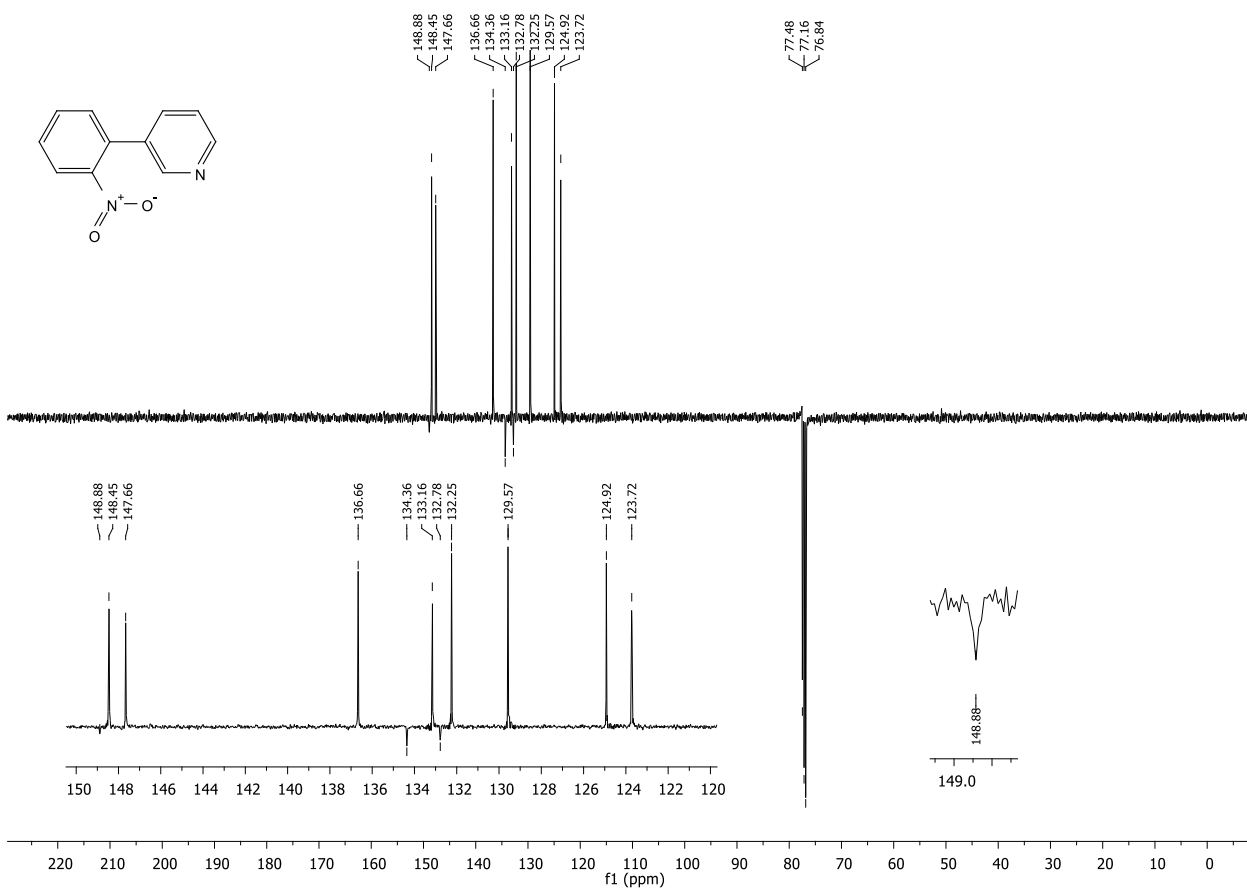


Figure 61: ^{13}C NMR of 3-(2-nitrophenyl)pyridine **72** spectrum in CDCl_3 .

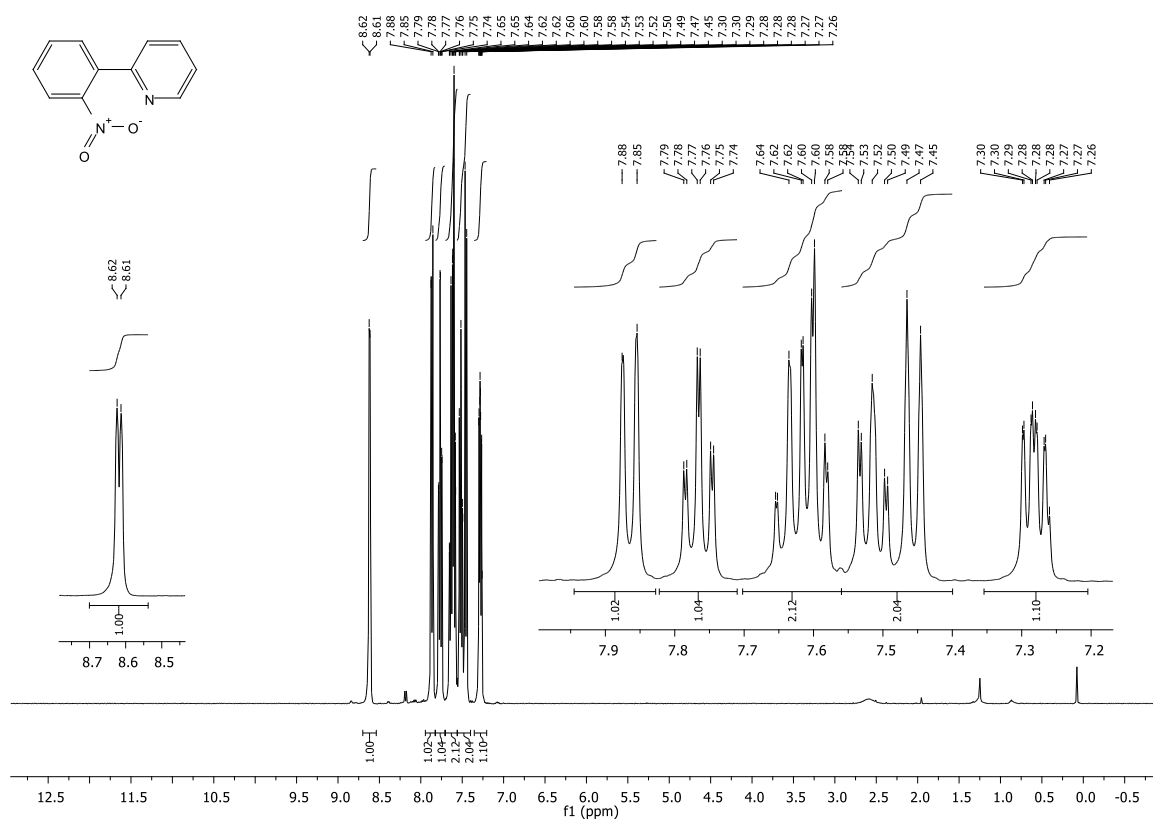


Figure 62: ^1H NMR of 2-(2-nitrophenyl)pyridine **73** spectrum in CDCl_3 .

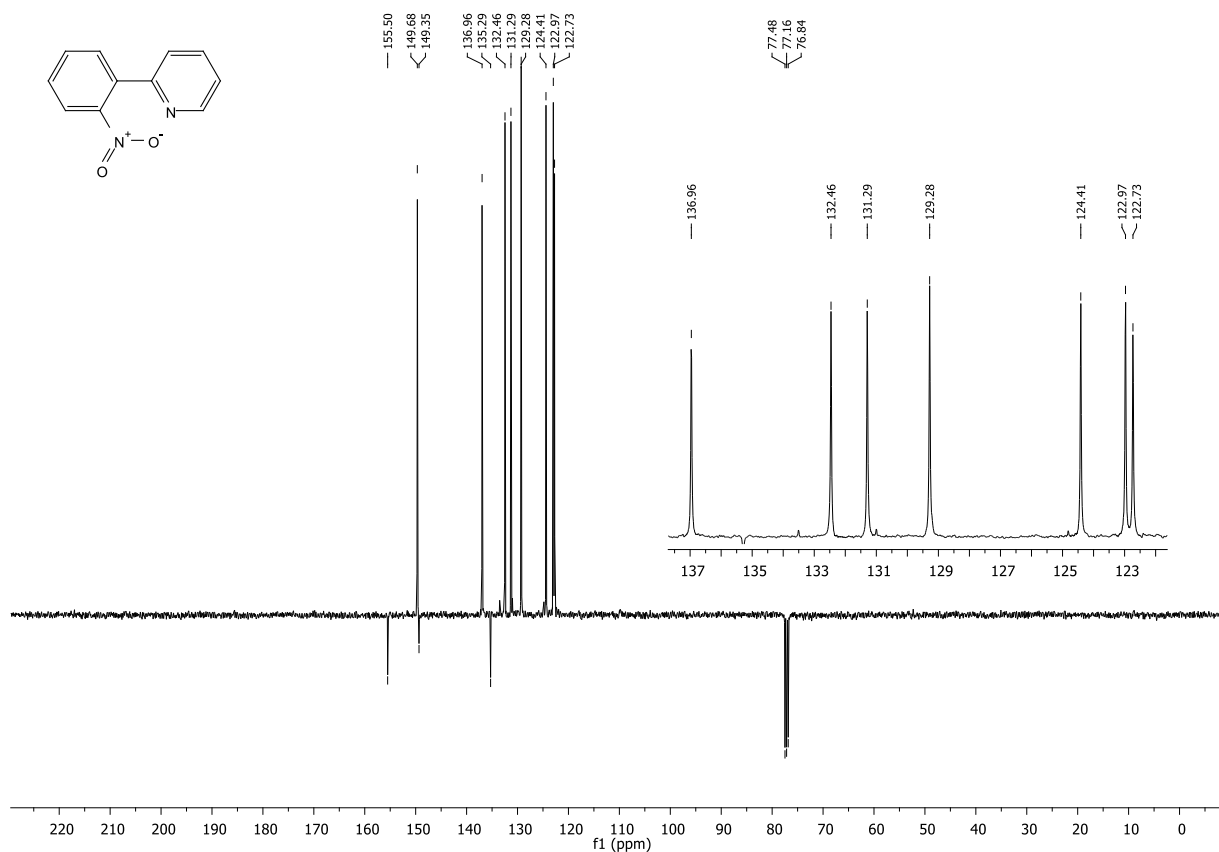


Figure 63: ^{13}C NMR of 2-(2-nitrophenyl)pyridine **73** spectrum in CDCl_3 .

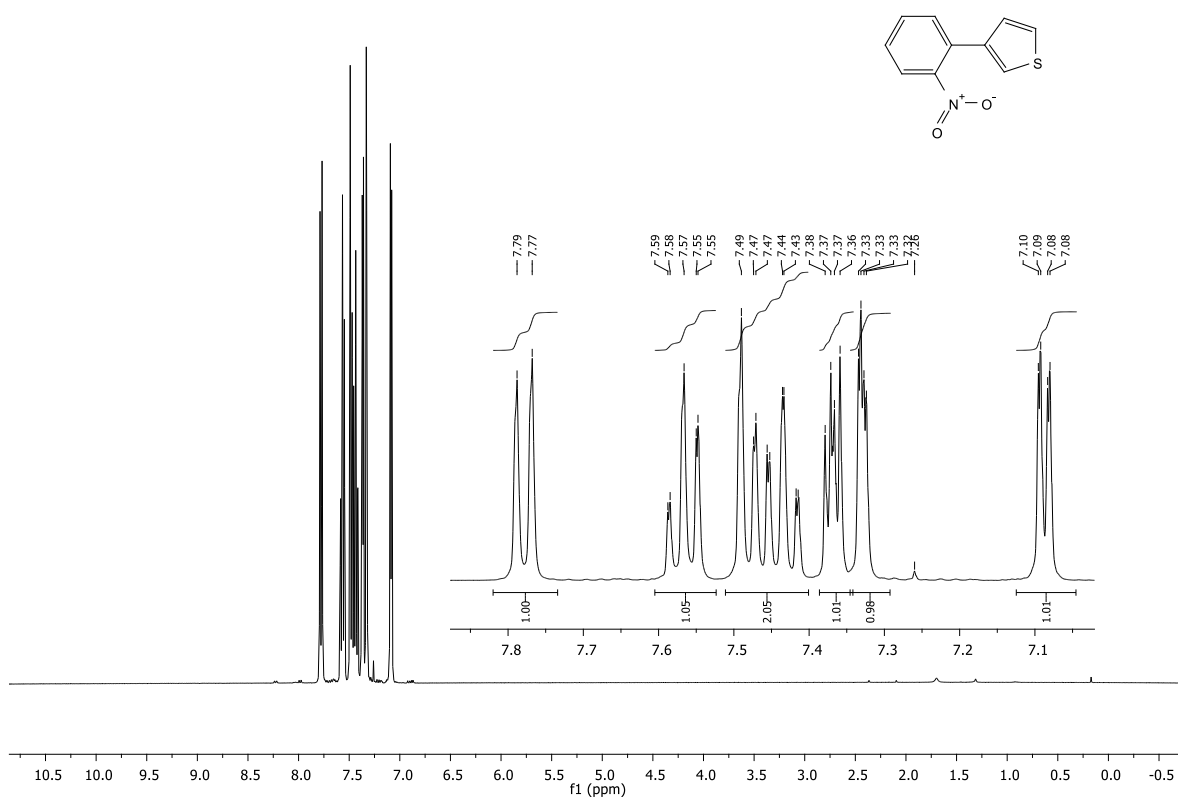


Figure 64: ^1H NMR of 2-(2-nitrophenyl)thiophene **74** spectrum in CDCl_3 .

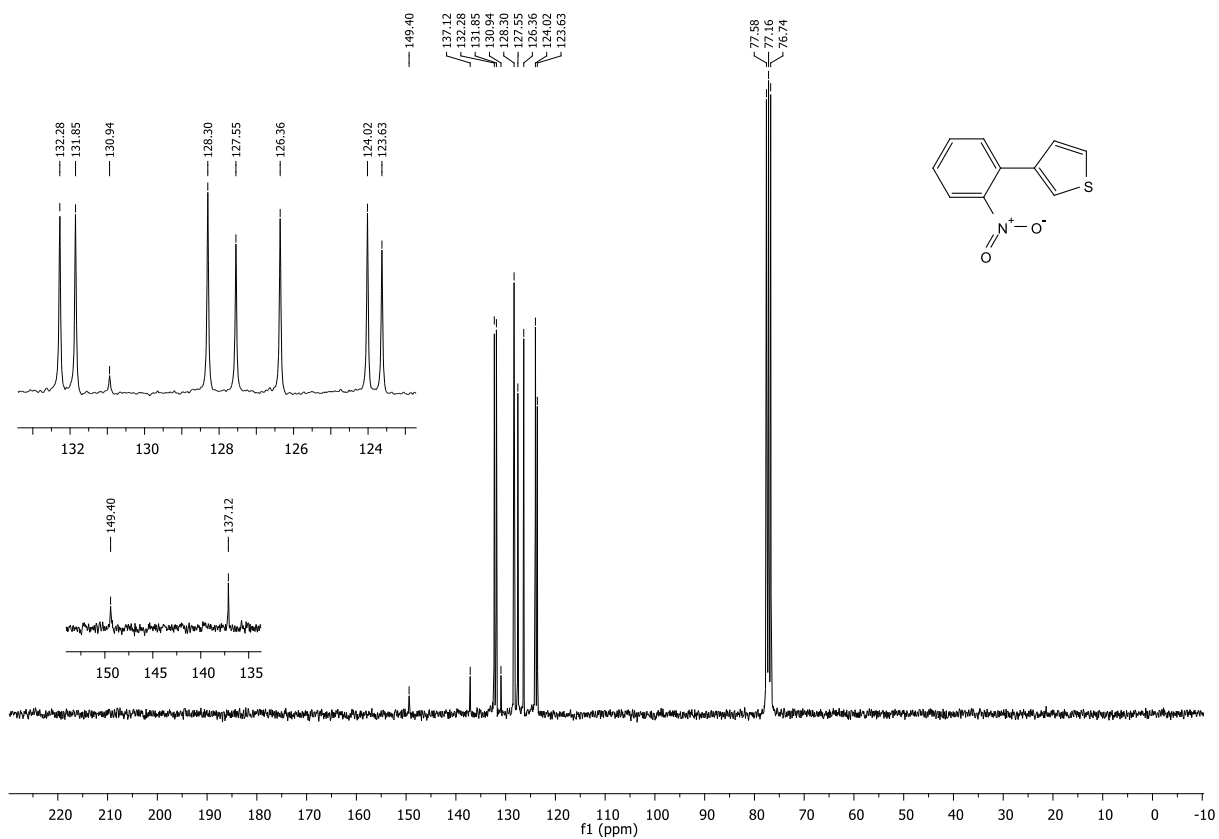


Figure 65: ¹³C NMR of 2-(2-nitrophenyl)thiophene **74** spectrum in CDCl₃.

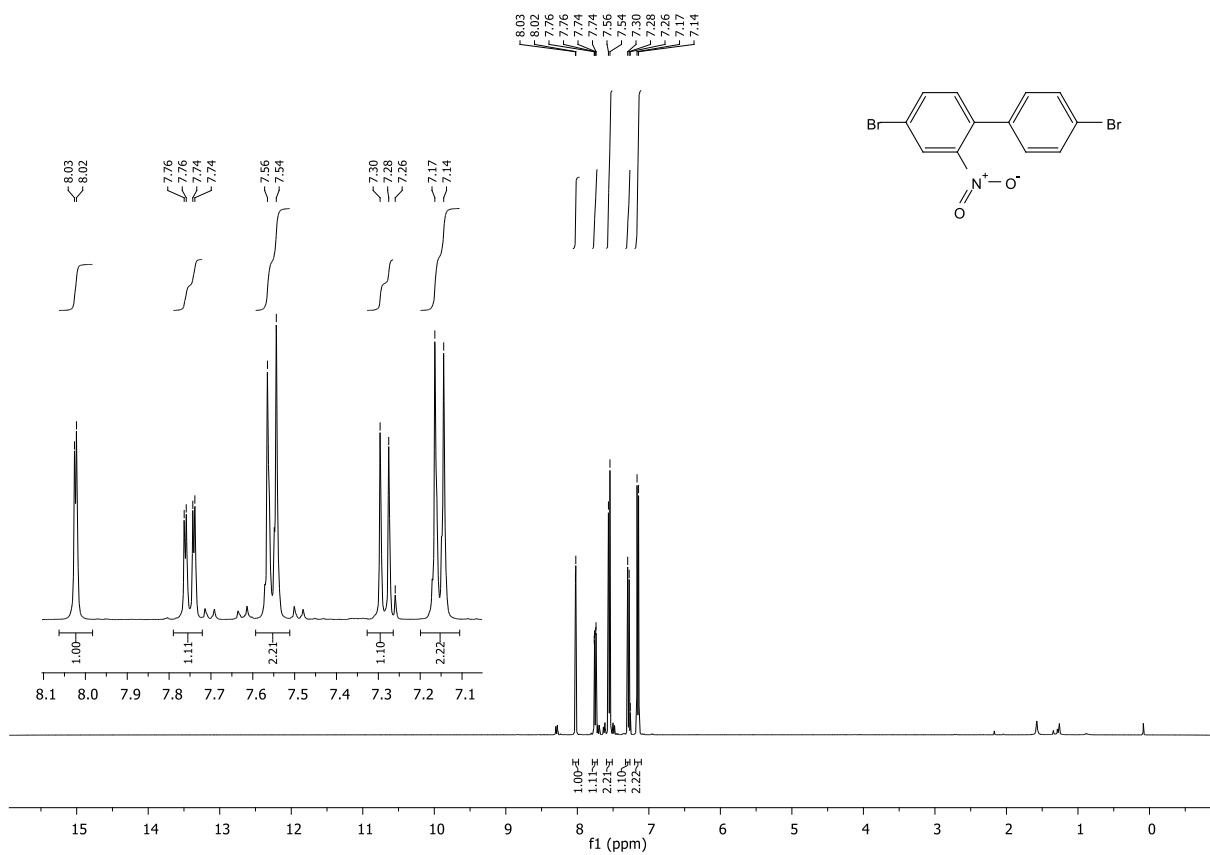


Figure 66: ¹H NMR of 4,4'-dibromo-2-nitrophenyl **75** spectrum in CDCl₃.

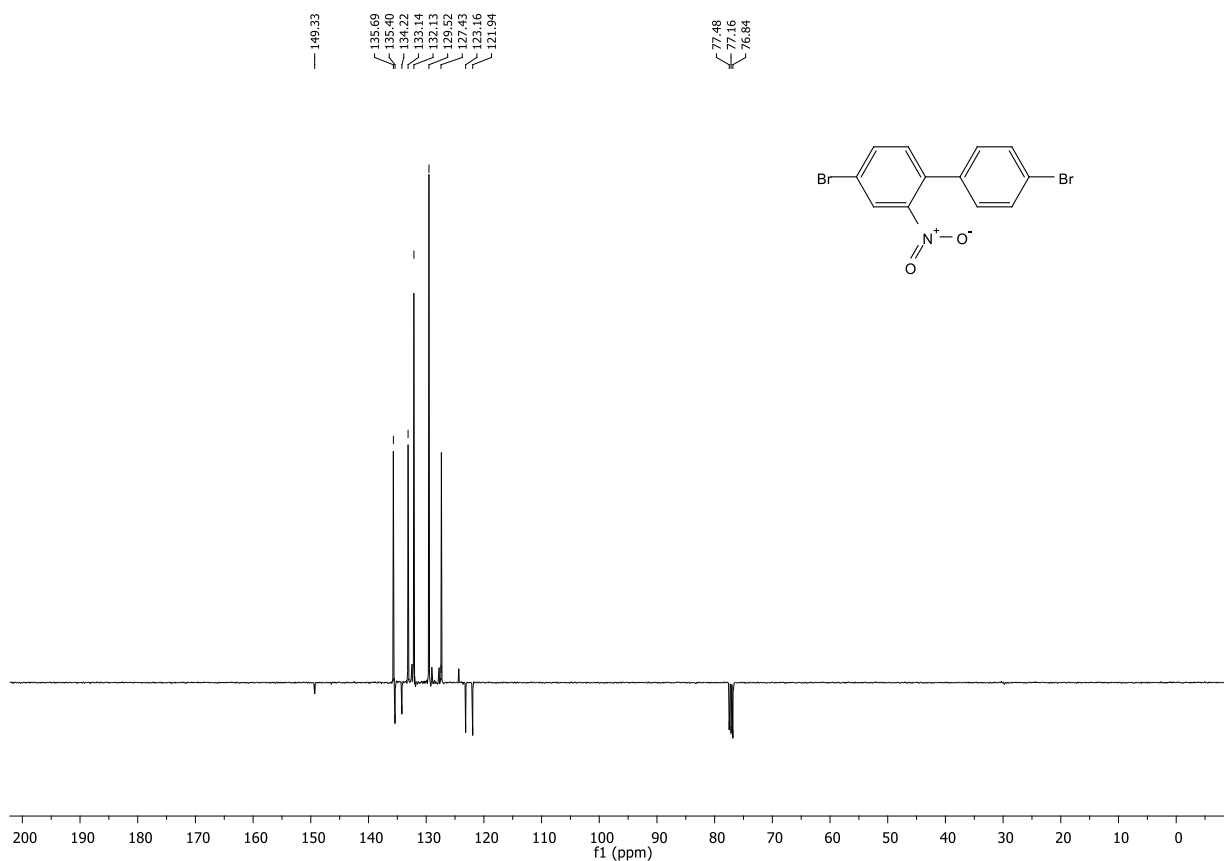


Figure 67: ^{13}C NMR of 4,4'-dibromo-2-nitrophenyl **75** spectrum in CDCl_3 .

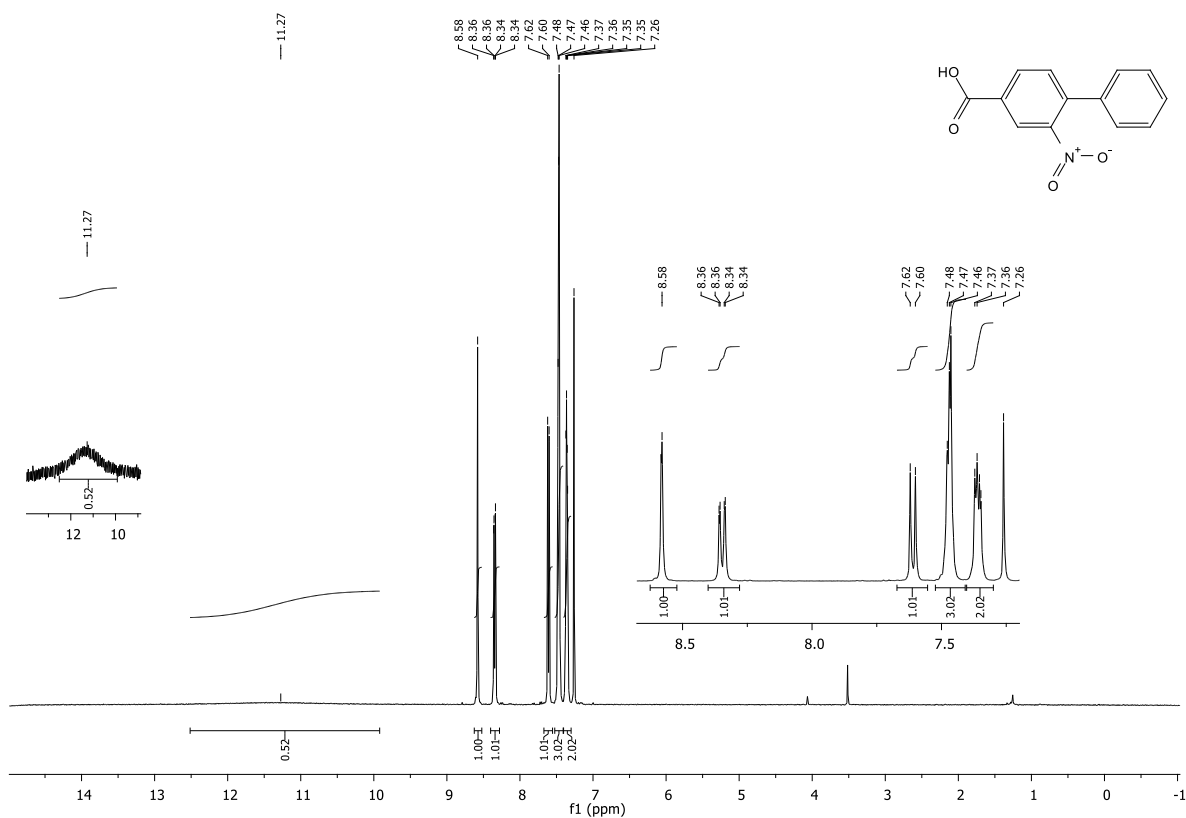
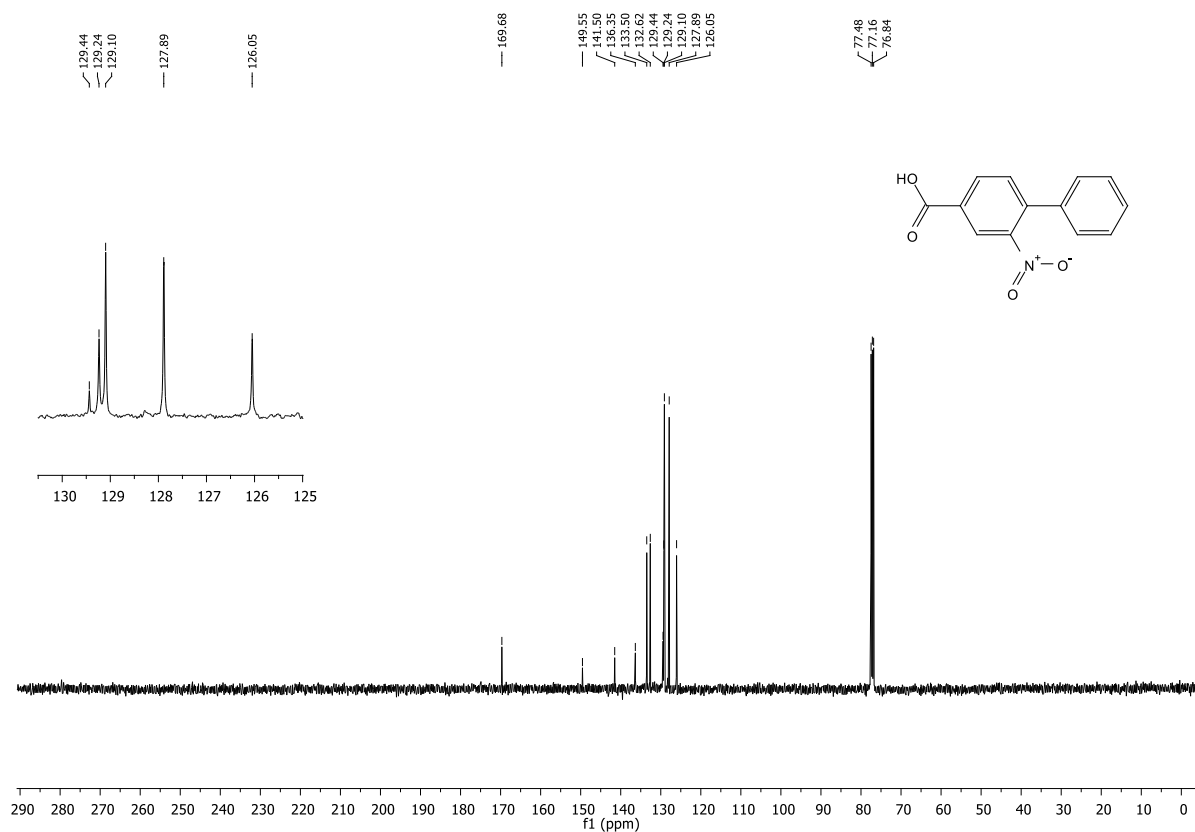


Figure 68: ^1H NMR of 2-nitrophenyl-4-carboxylic acid **76** spectrum in CDCl_3 .



69: ^{13}C NMR of 2-nitrobiphenyl-4-carboxylic acid **76** spectrum in CDCl_3 .

Figure

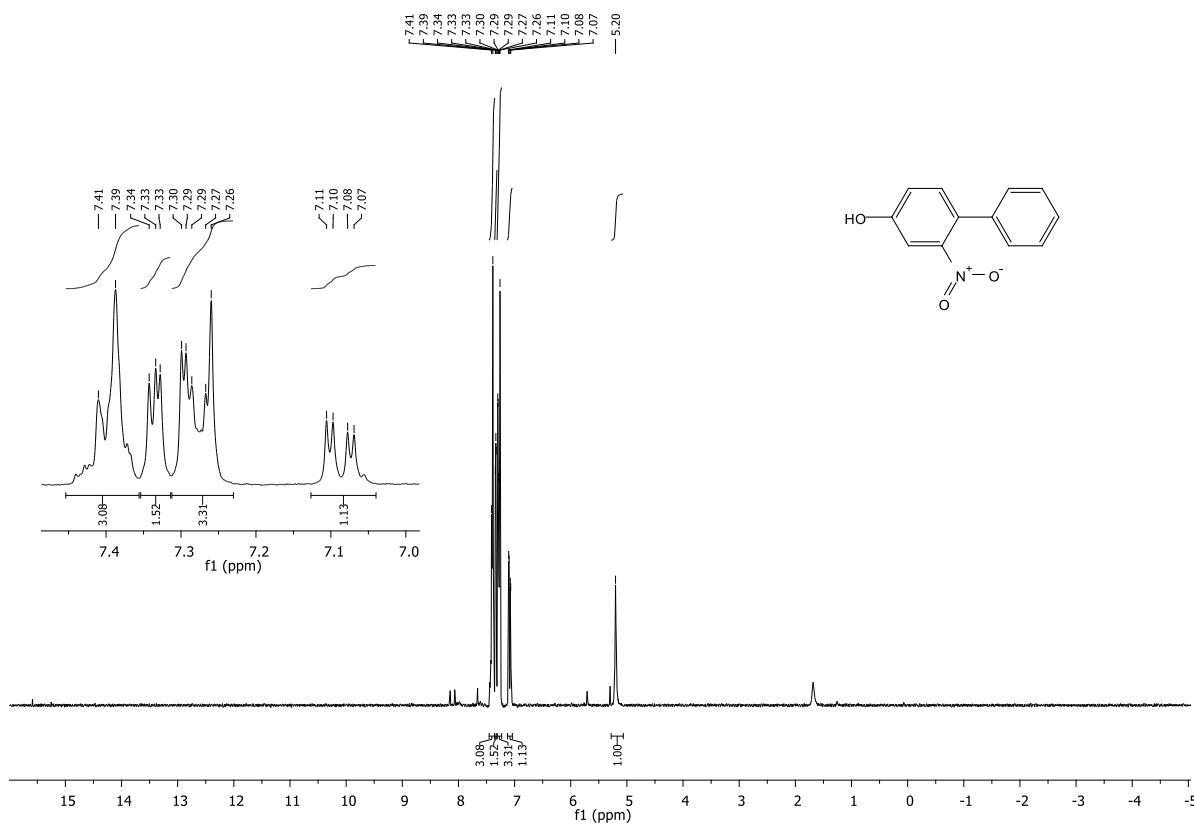
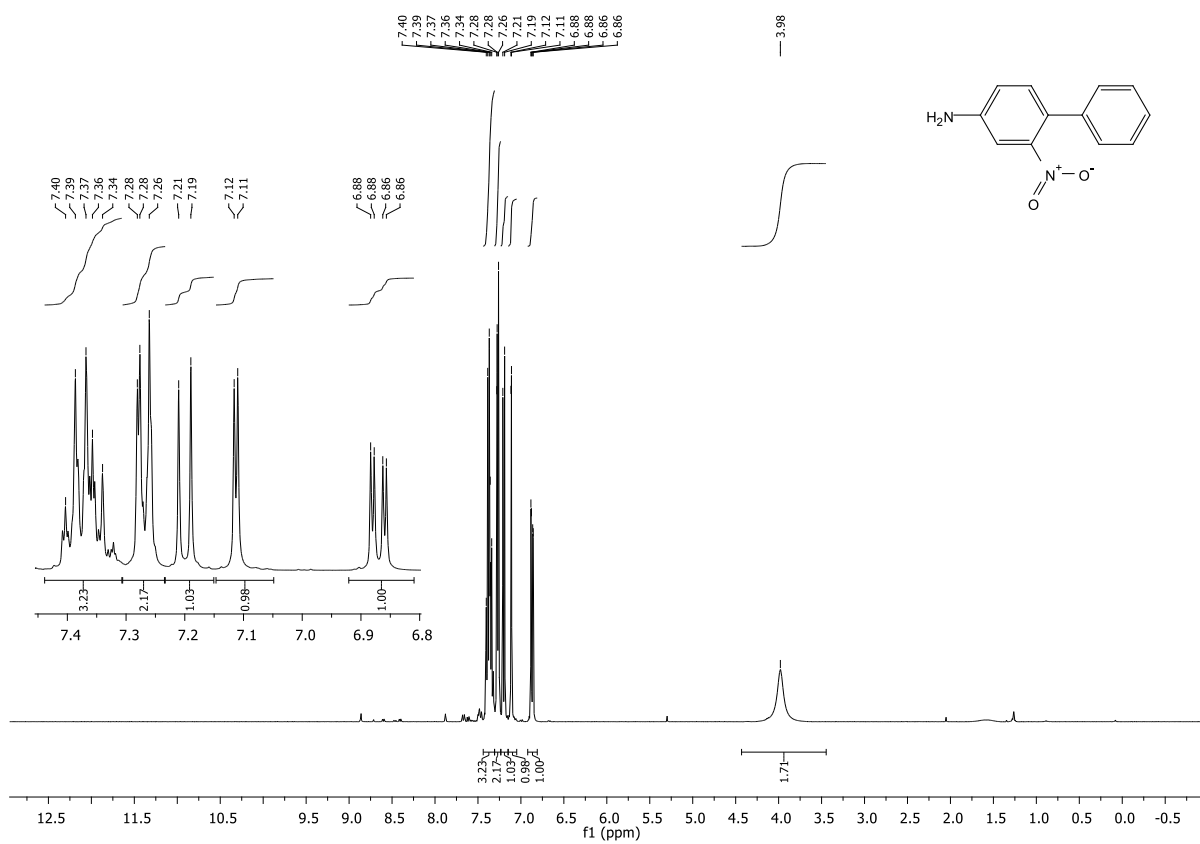
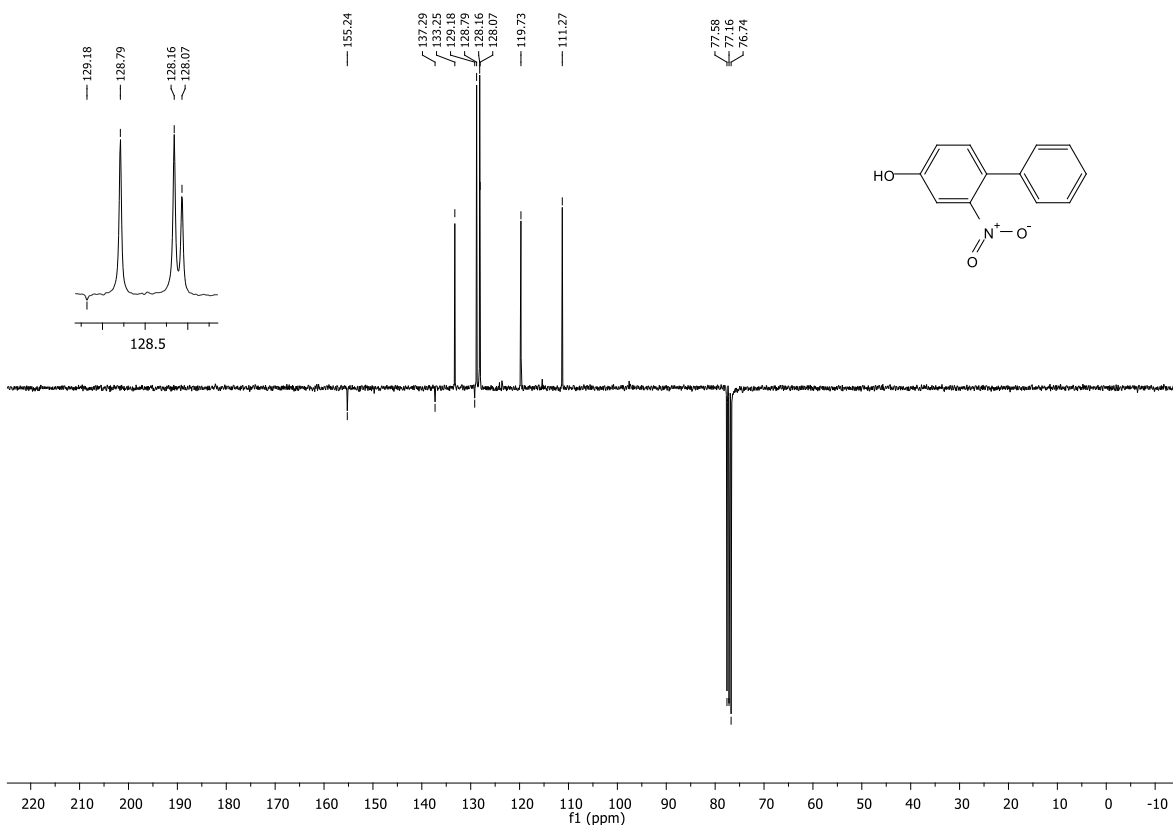


Figure 70: ^1H NMR of 4-hydroxy-2-nitrophenyl **77** spectrum in CDCl_3 .



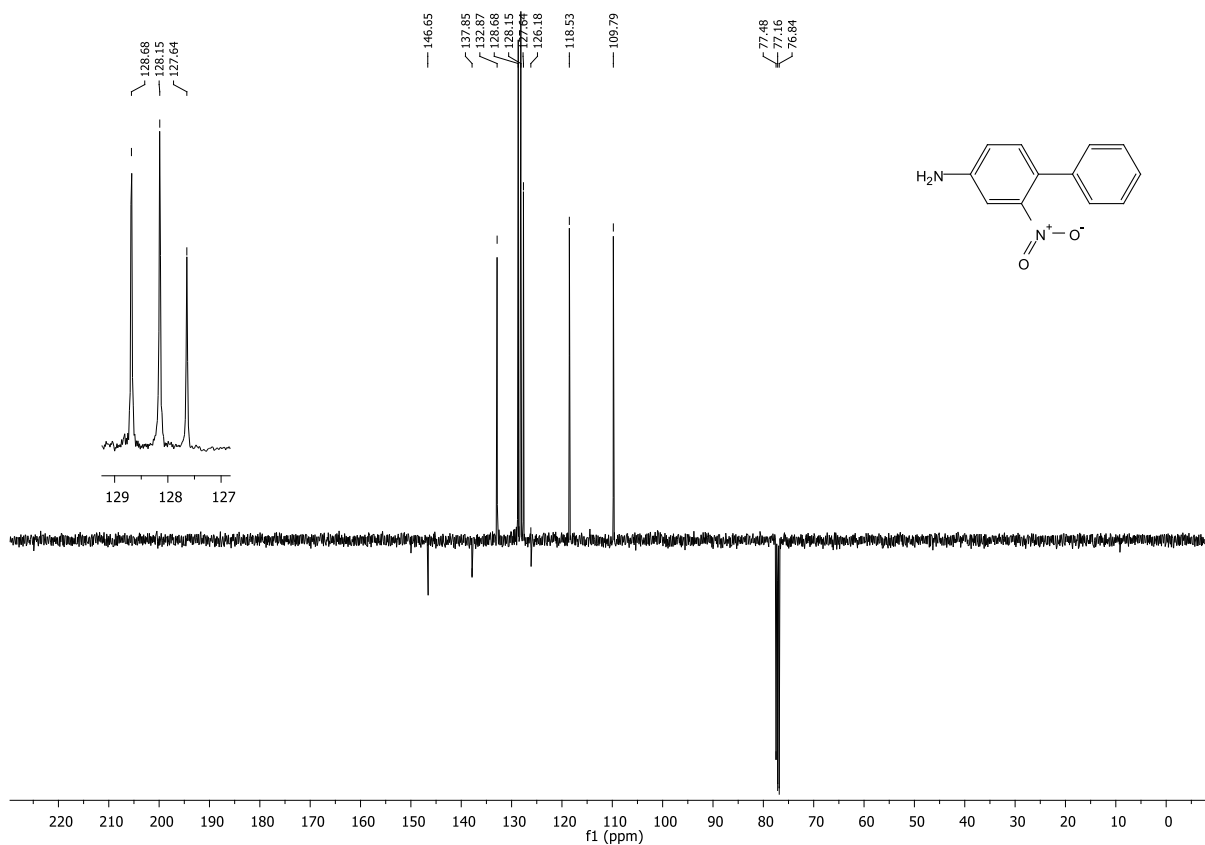


Figure 73: ^{13}C NMR of 2-nitro-4-biphenyl amine **78** spectrum in CDCl_3 .

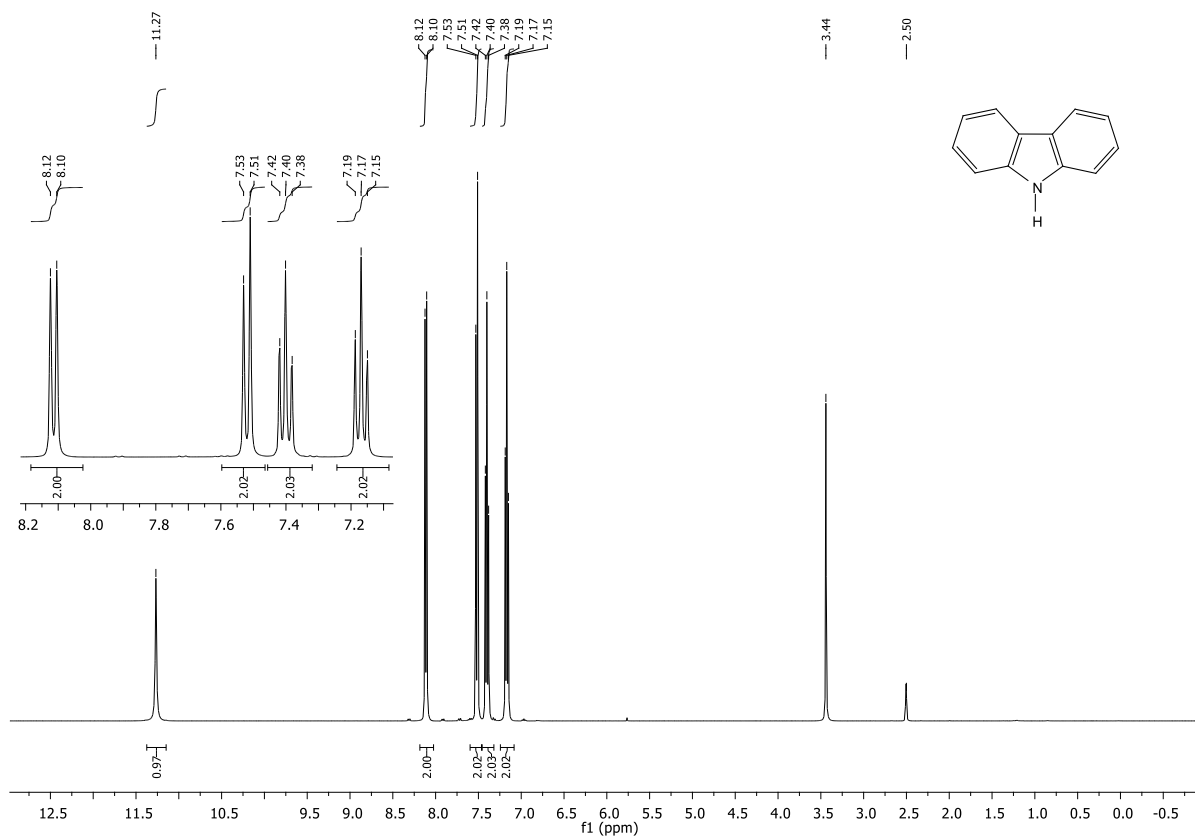


Figure 74: ^1H NMR of 9H-carbazole **79** spectrum in $\text{DMSO}-d_6$.

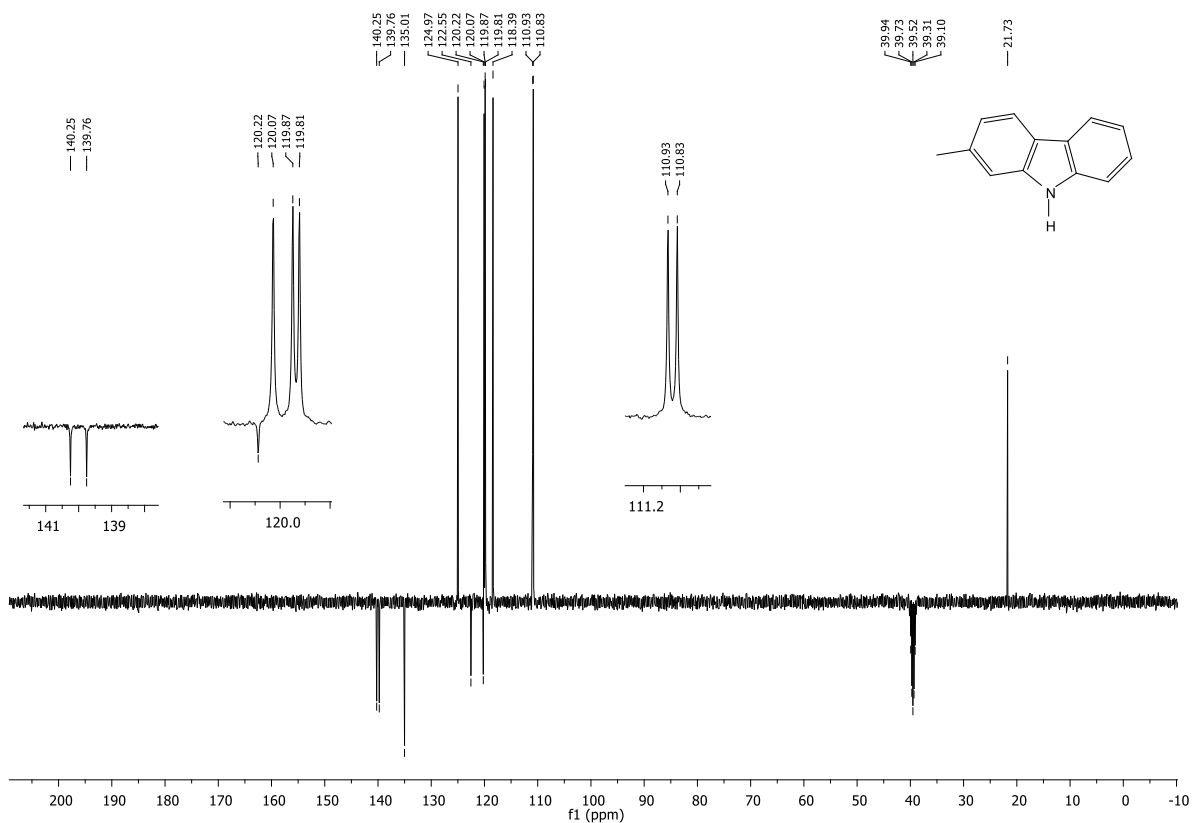


Figure 77: ^{13}C NMR of 2-methyl-9H-carbazole **80** spectrum in $\text{DMSO-}d_6$.

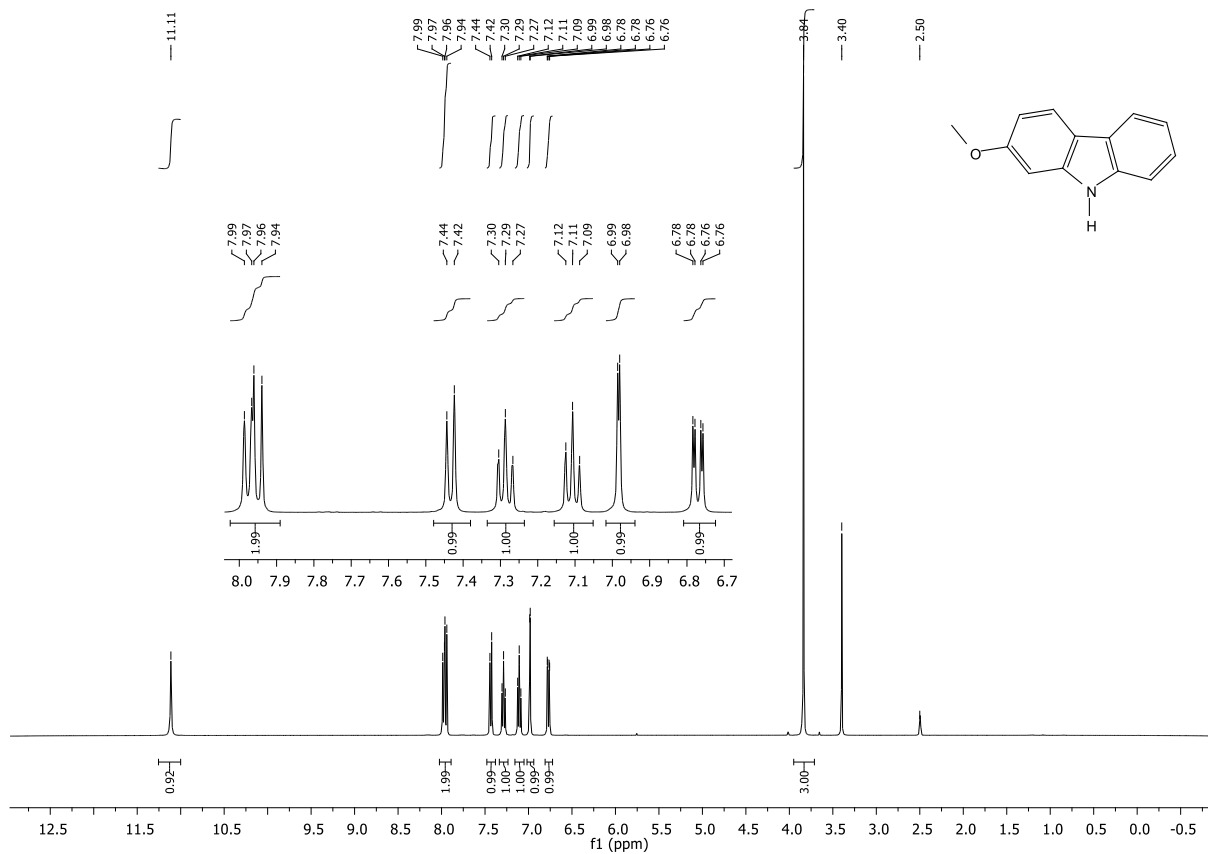


Figure 78: ^1H NMR of 2-methoxy-9H-carbazole **81** spectrum in $\text{DMSO-}d_6$.

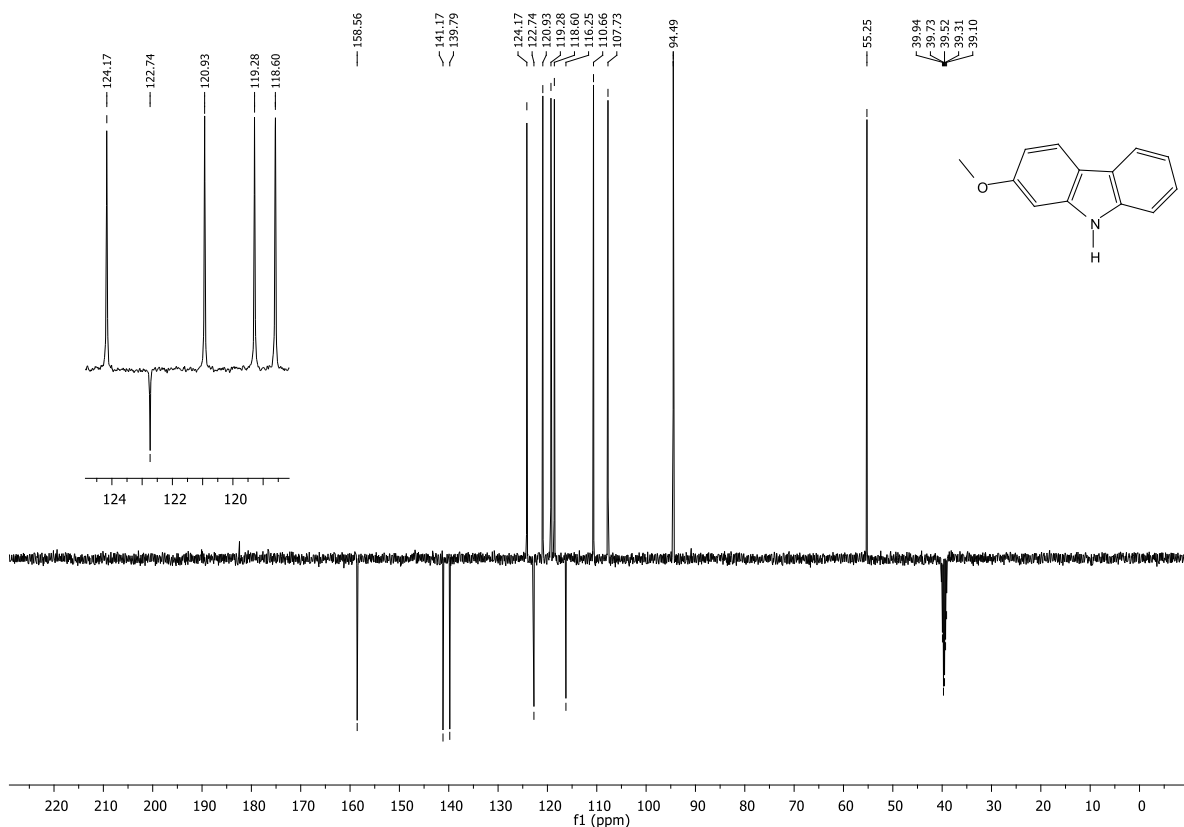


Figure 79: ^{13}C NMR of 2-methoxy-9H-carbazole **81** spectrum in $\text{DMSO-}d_6$.

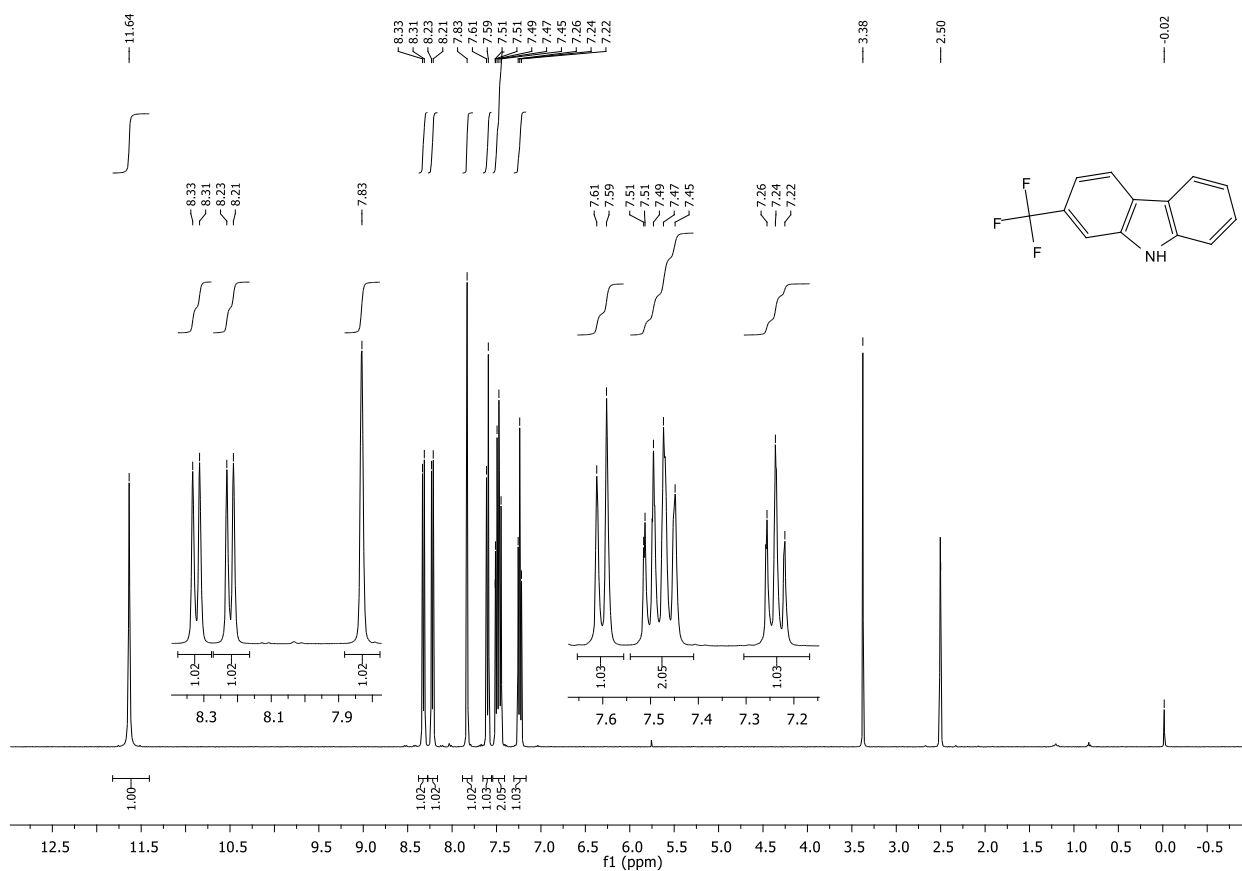


Figure 80: ^1H NMR of 2-(trifluoromethyl)-9H-carbazole **82** spectrum in $\text{DMSO-}d_6$.

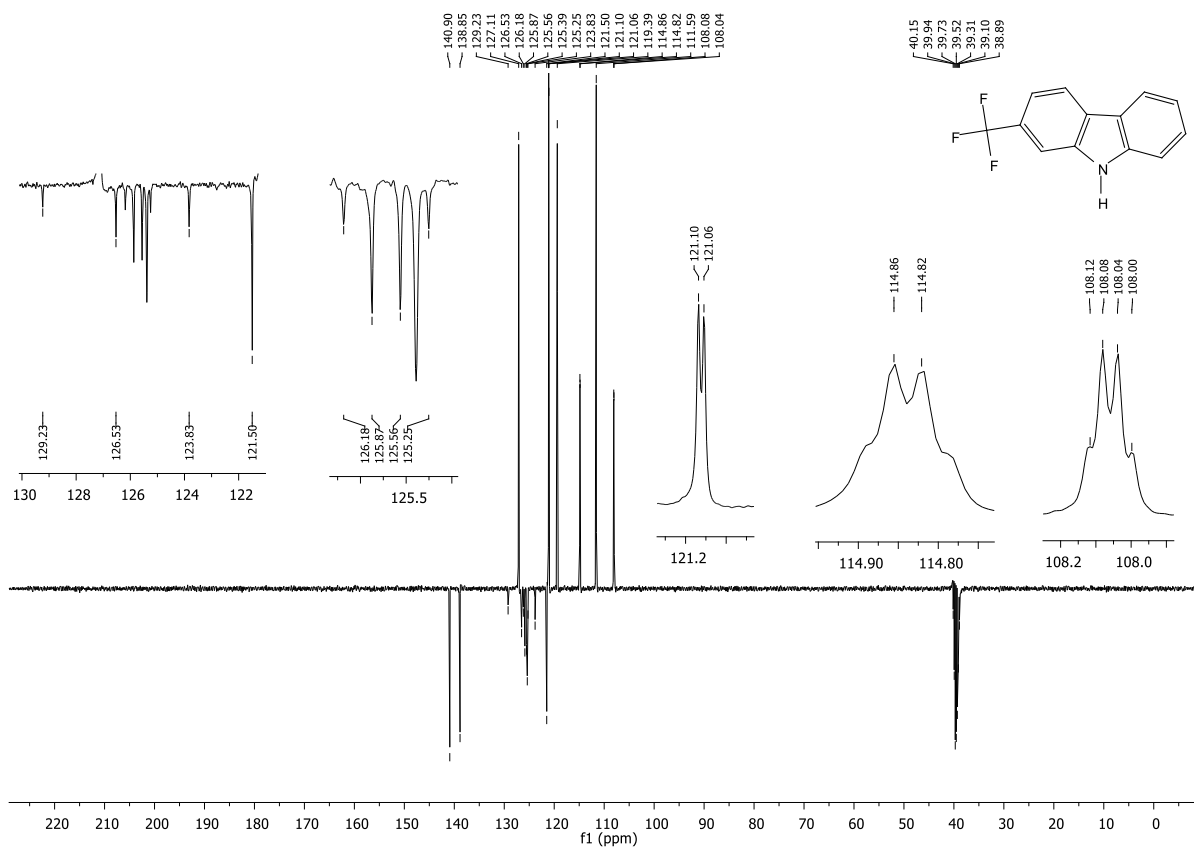


Figure 81: ¹³C NMR of 2-(trifluoromethyl)-9H-carbazole **82** spectrum in DMSO-*d*₆.

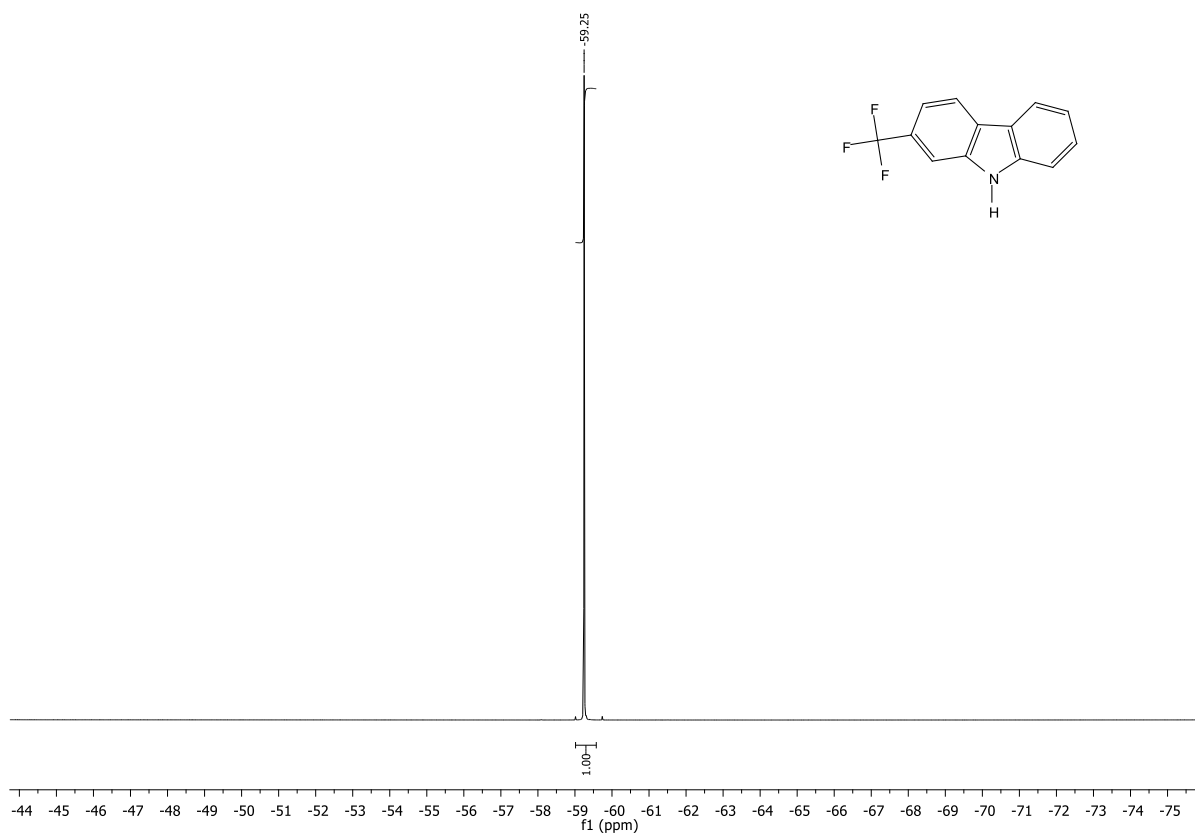
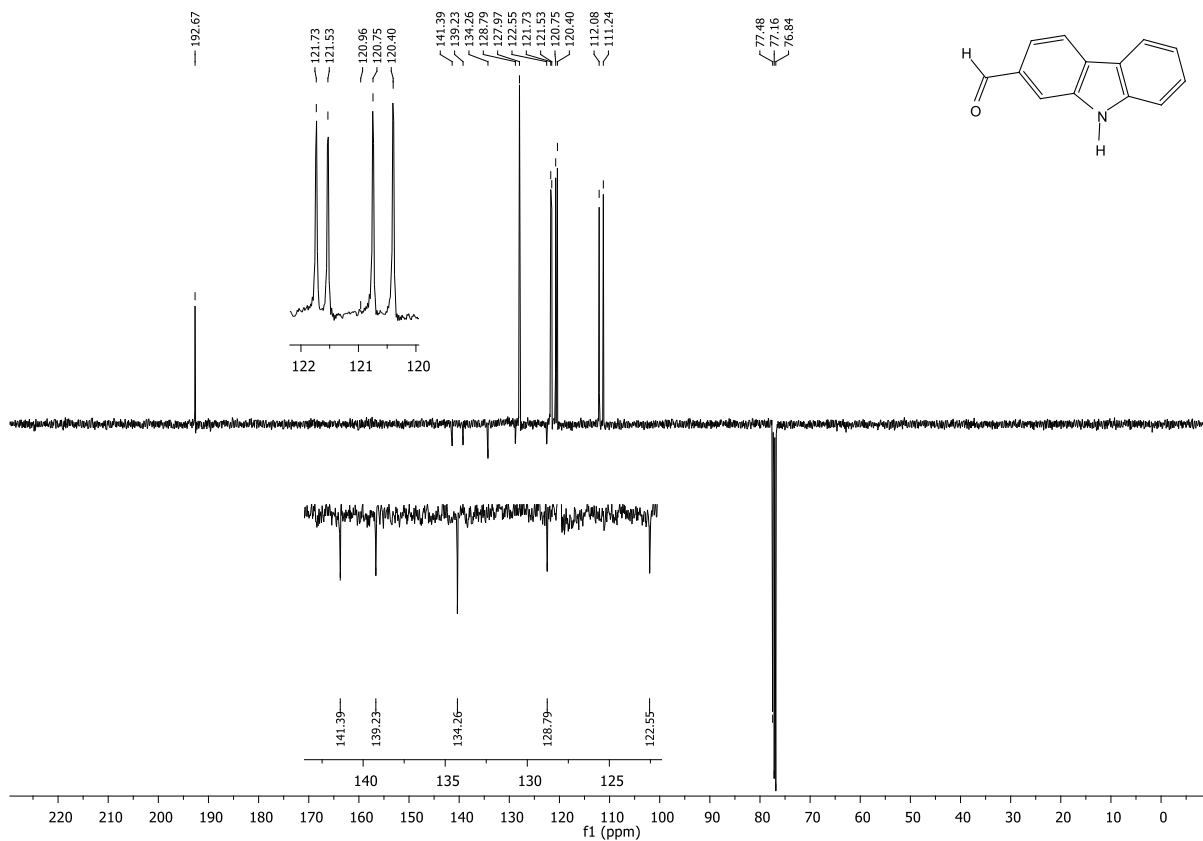
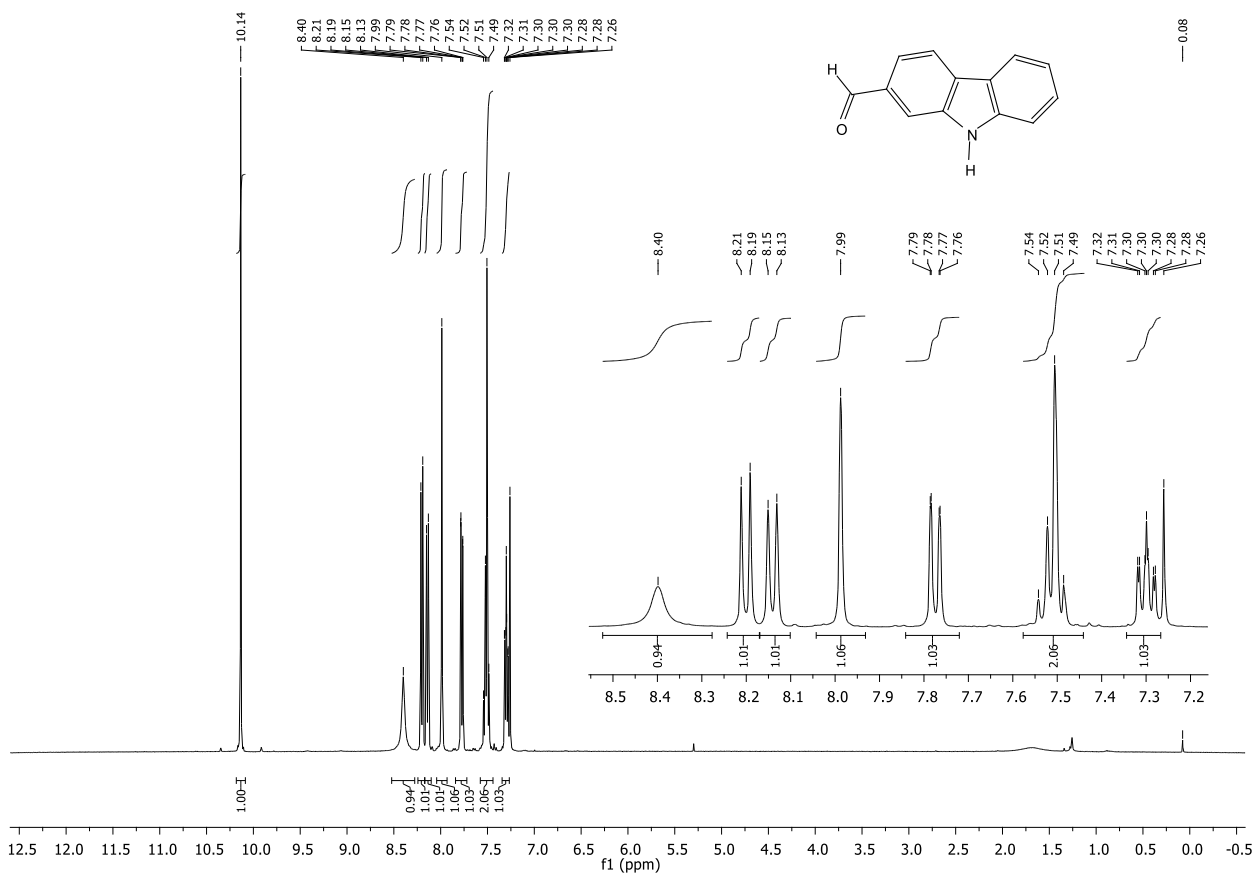
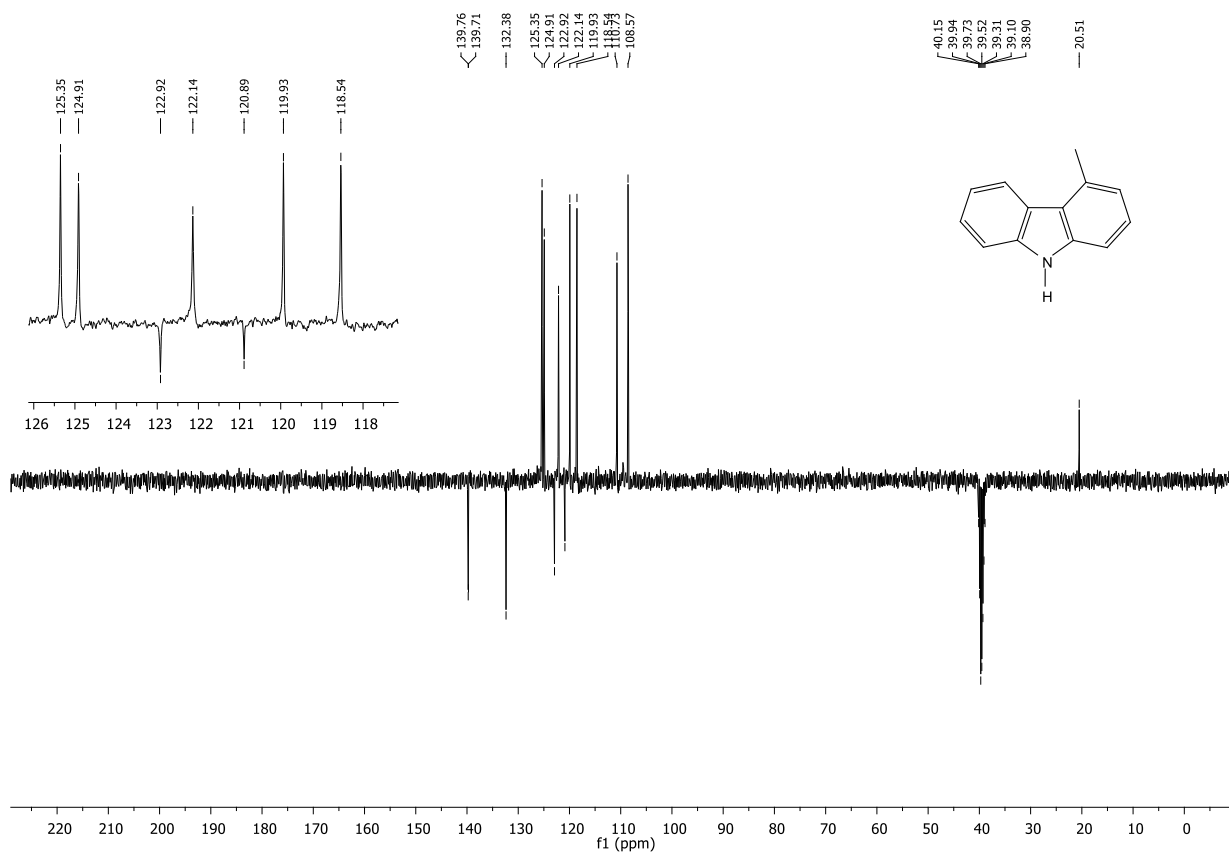
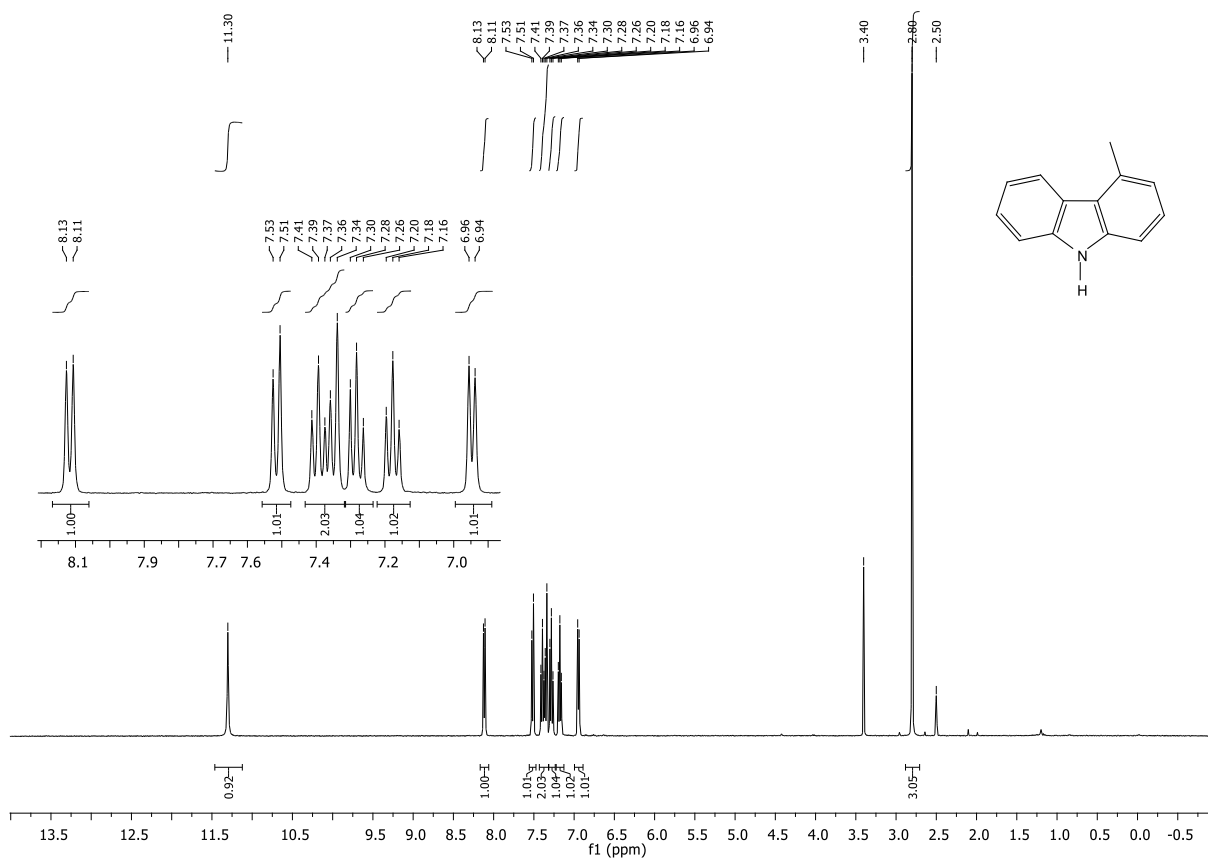
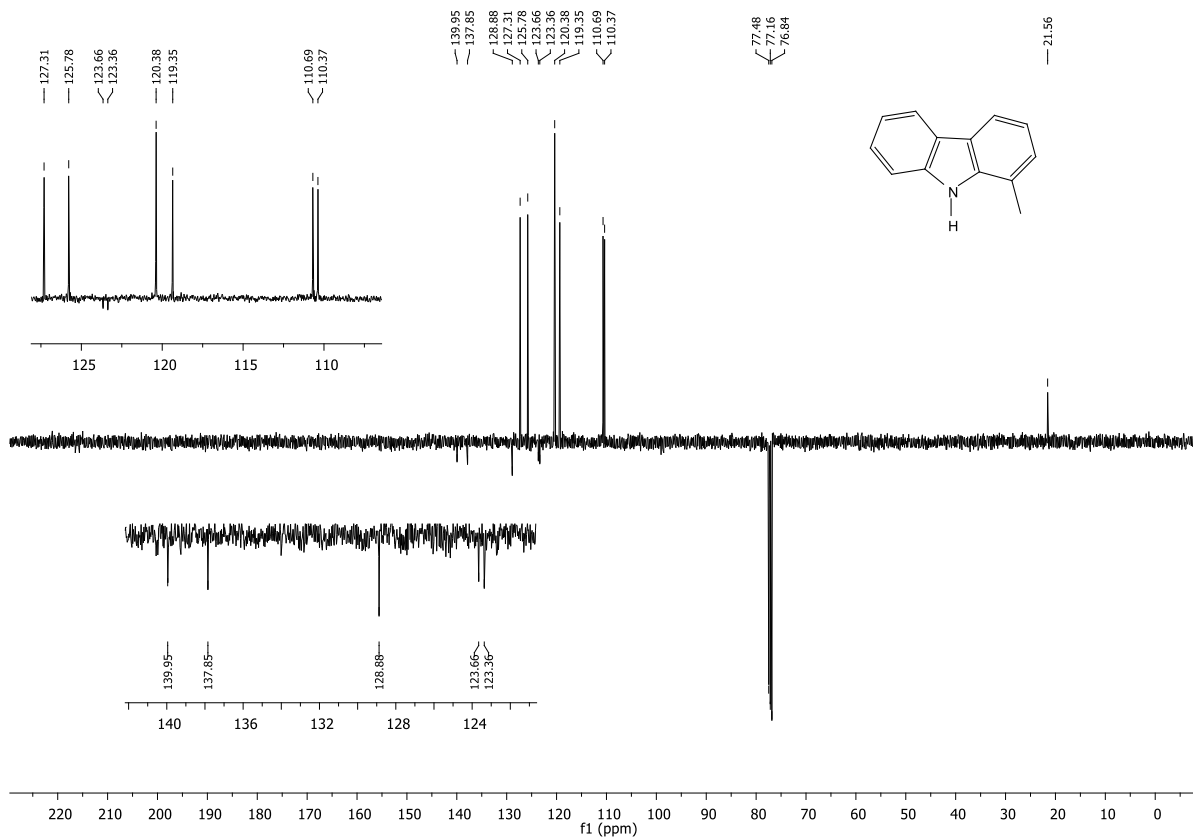
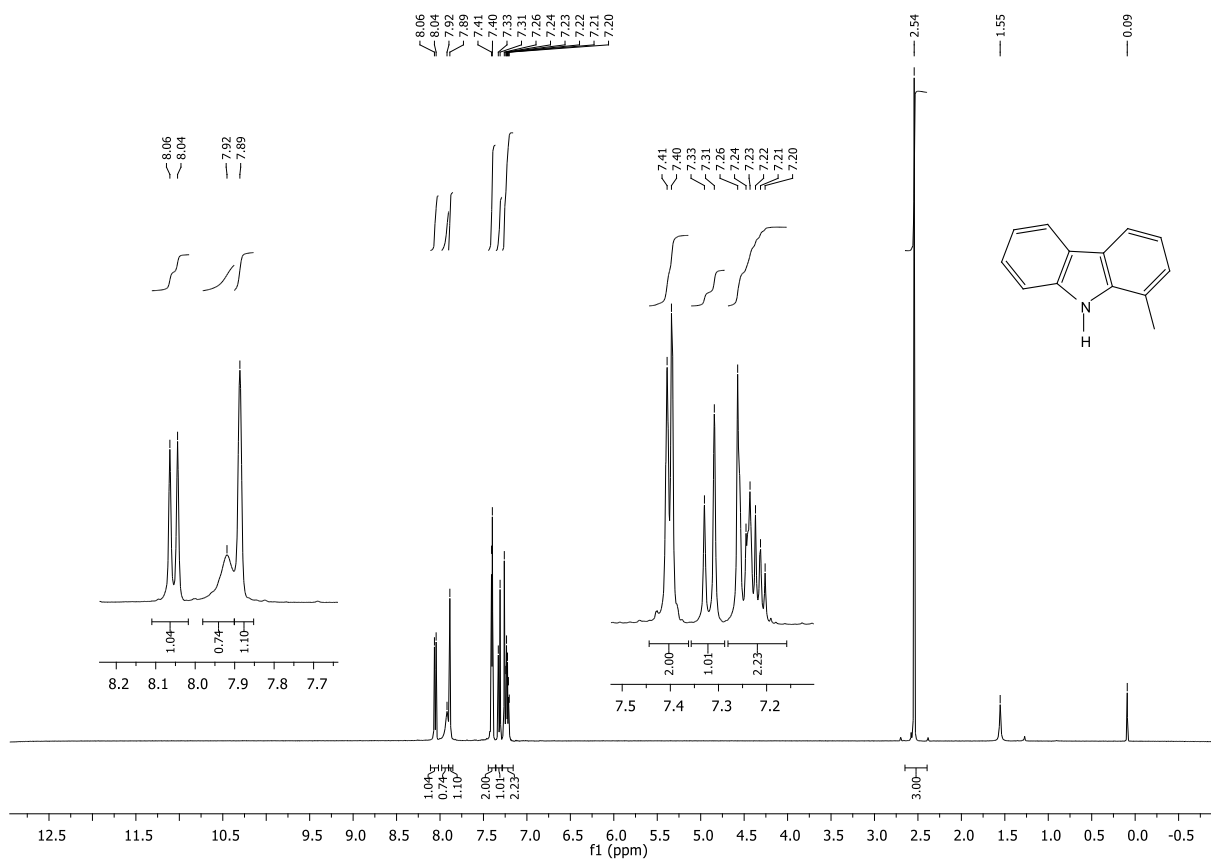


Figure 82: ¹⁹F NMR of 2-(trifluoromethyl)-9H-carbazole **82** spectrum in DMSO-*d*₆.







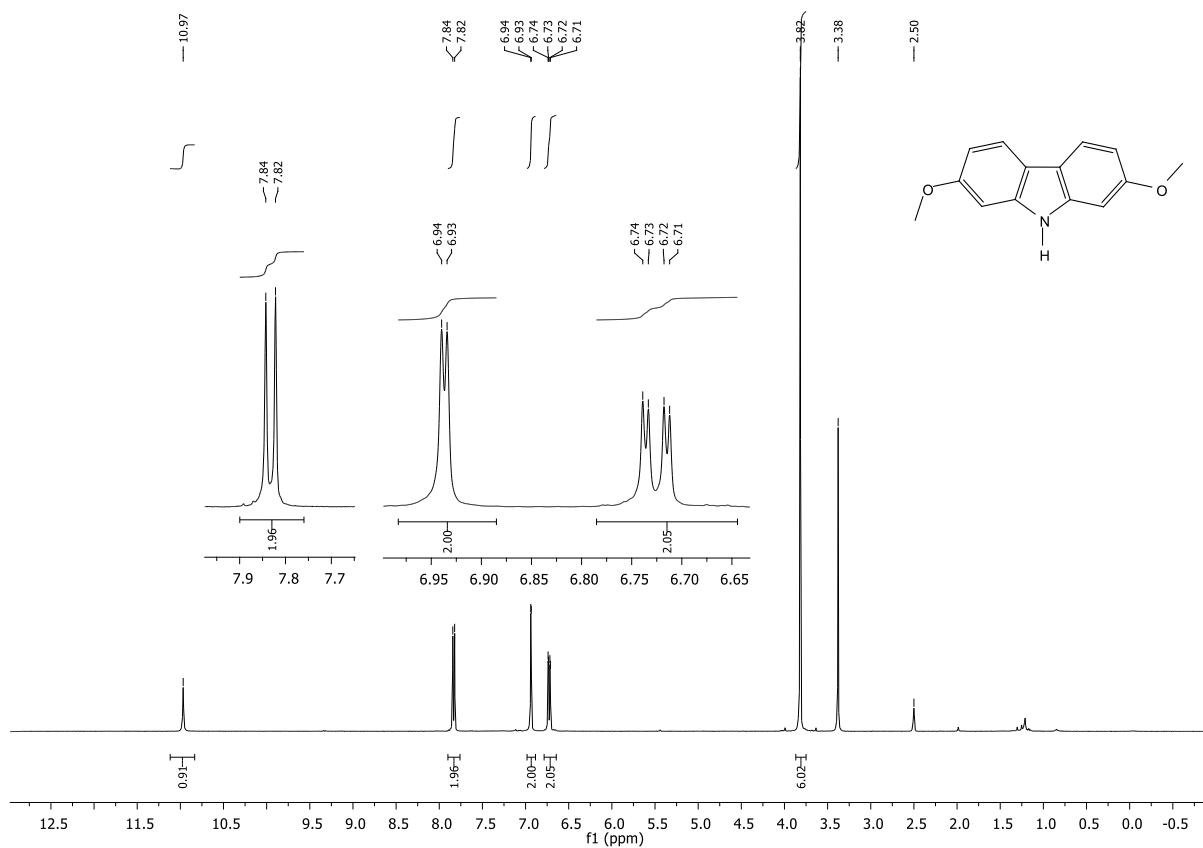


Figure 89: ^1H NMR of 4-dimethoxy-9H-carbazole **86** spectrum in $\text{DMSO-}d_6$.

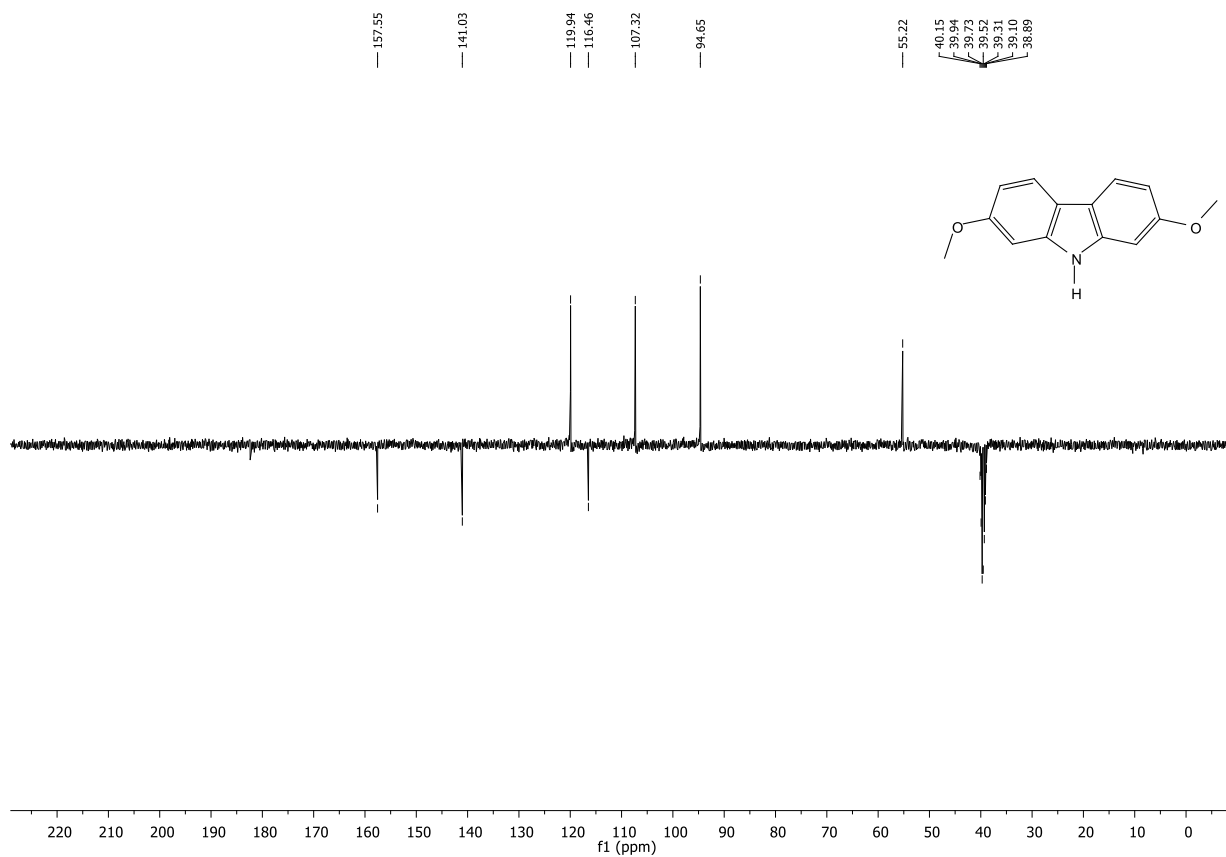


Figure 90: ^{13}C NMR of 4-dimethoxy-9H-carbazole **86** spectrum in $\text{DMSO-}d_6$.

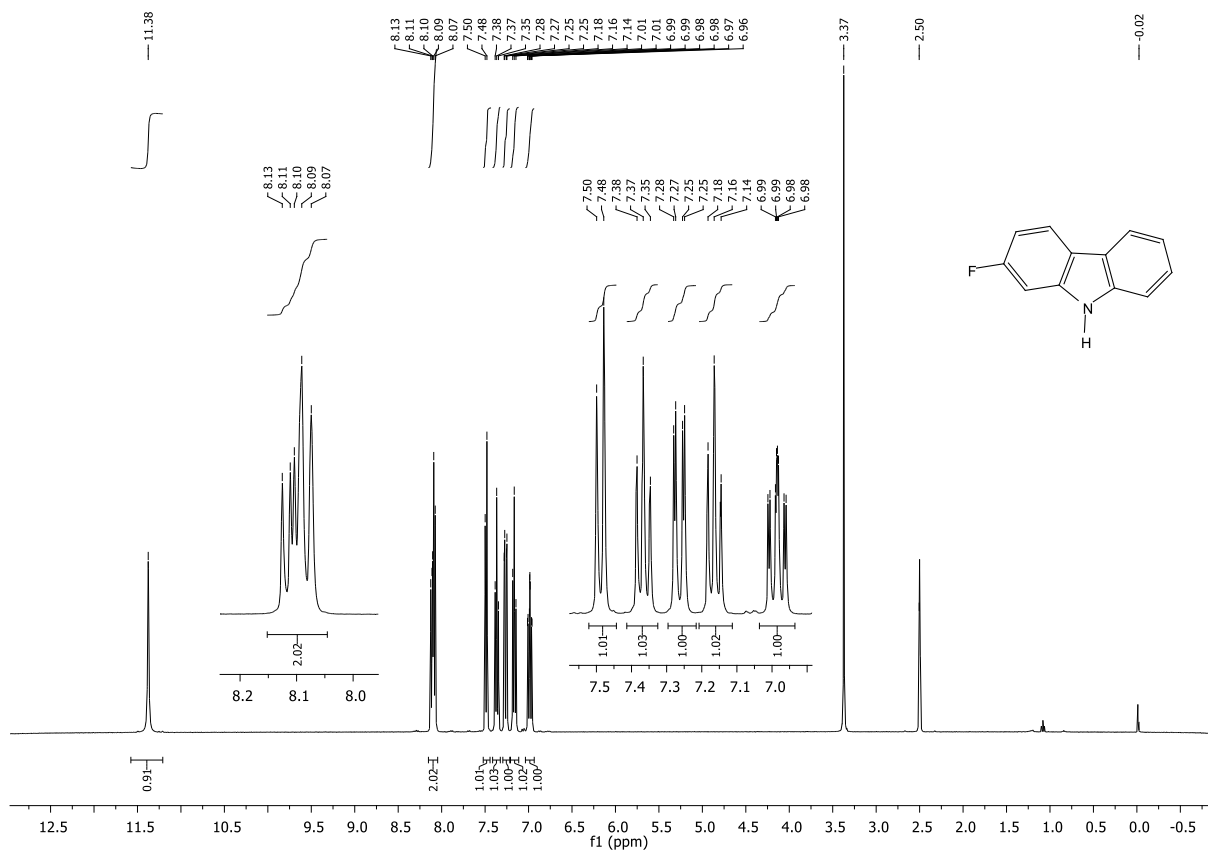


Figure 91: $^1\text{H NMR}$ of 2-fluoro-9H-carbazole **87** spectrum in $\text{DMSO-}d_6$.

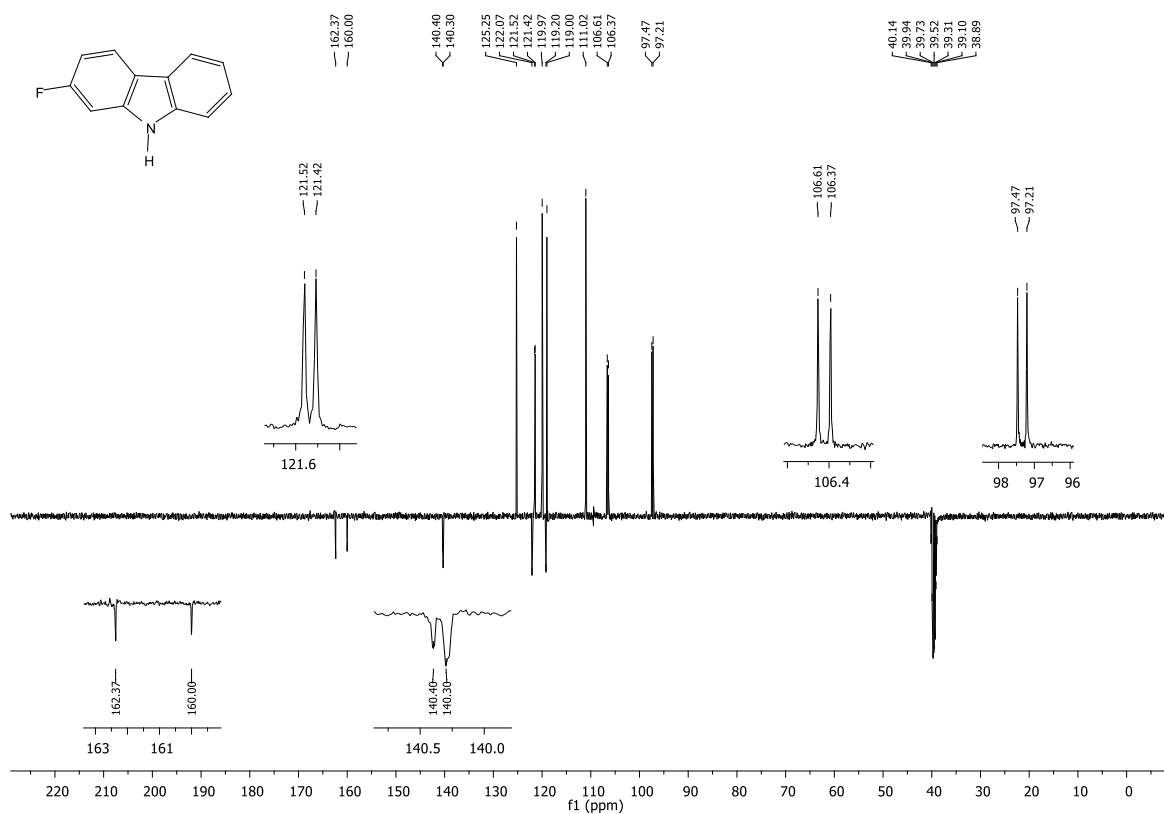


Figure 92: $^{13}\text{C NMR}$ of 2-fluoro-9H-carbazole **87** spectrum in $\text{DMSO-}d_6$.

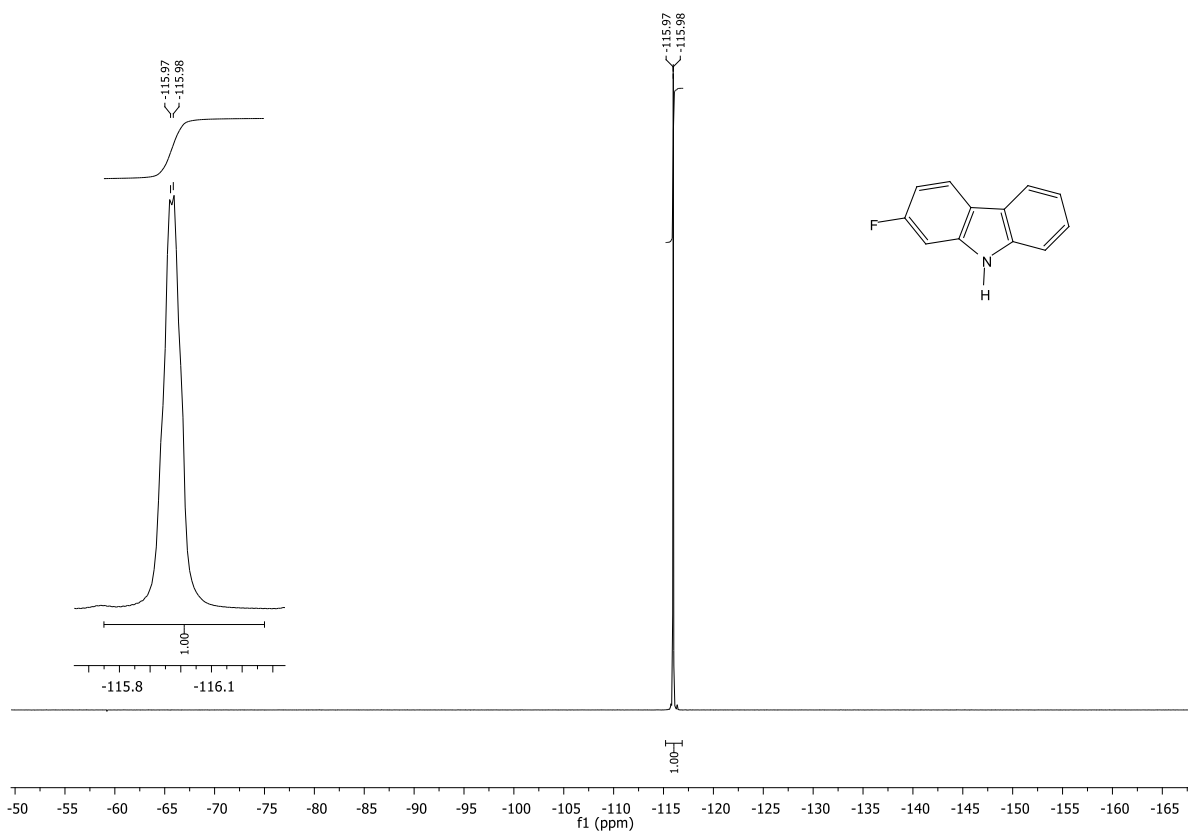


Figure 93: ^{19}F NMR of 2-fluoro-9H-carbazole **87** spectrum in $\text{DMSO-}d_6$.

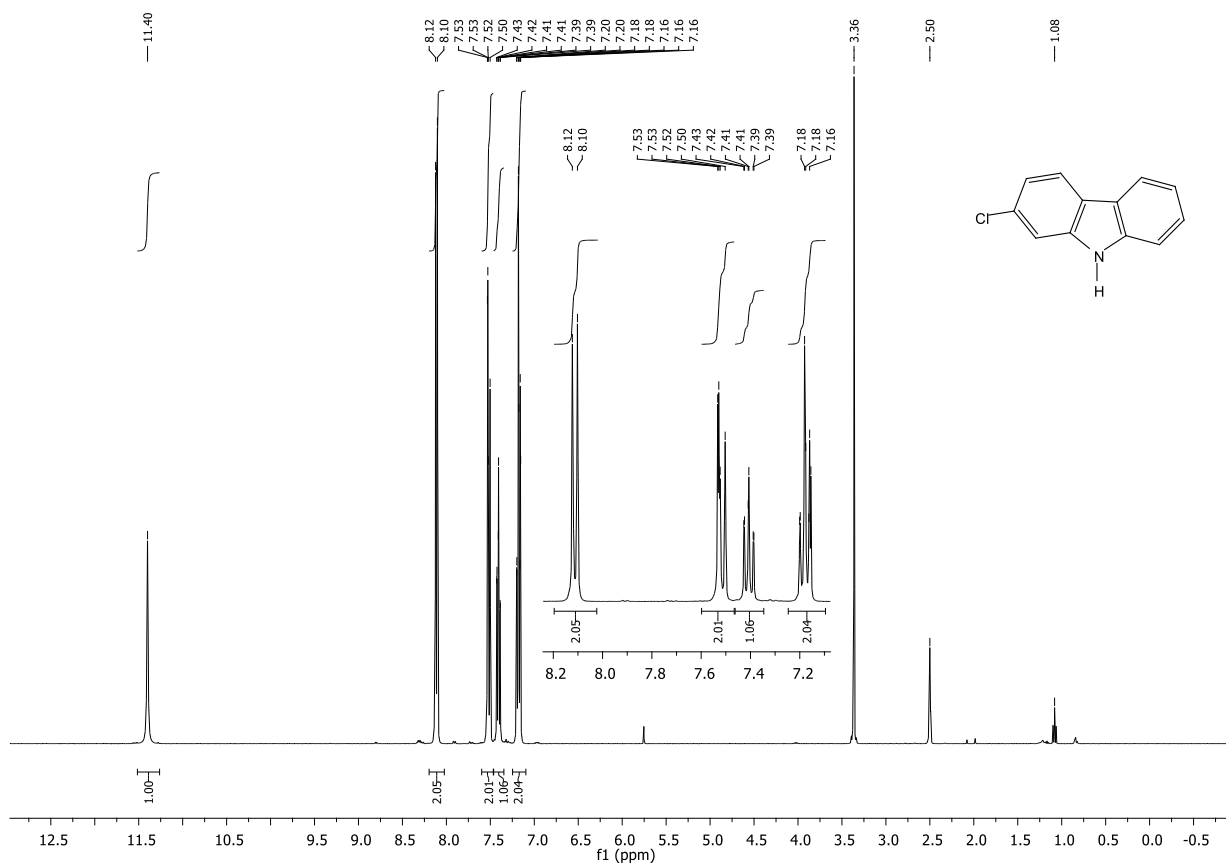


Figure 94: ^1H NMR of 2-chloro-9H-carbazole **88** spectrum in $\text{DMSO-}d_6$.

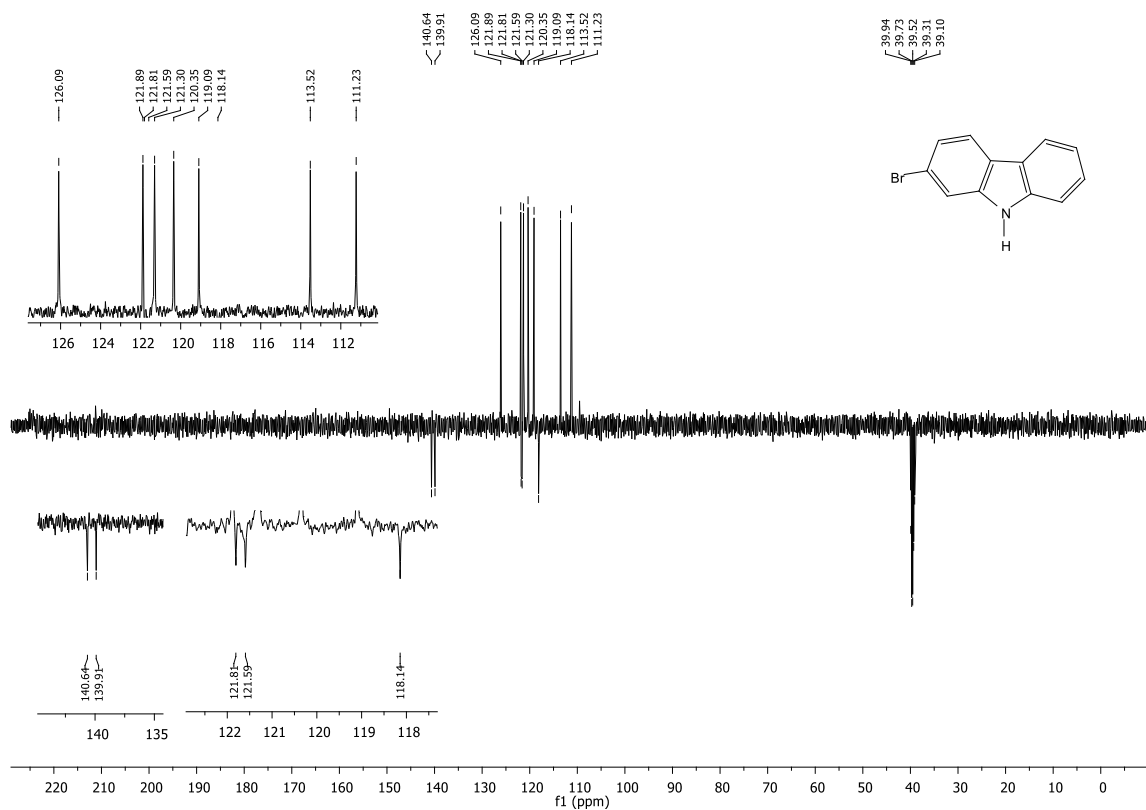


Figure 97: ^{13}C NMR of 2-bromo-9H-carbazole **89** spectrum in $\text{DMSO-}d_6$.

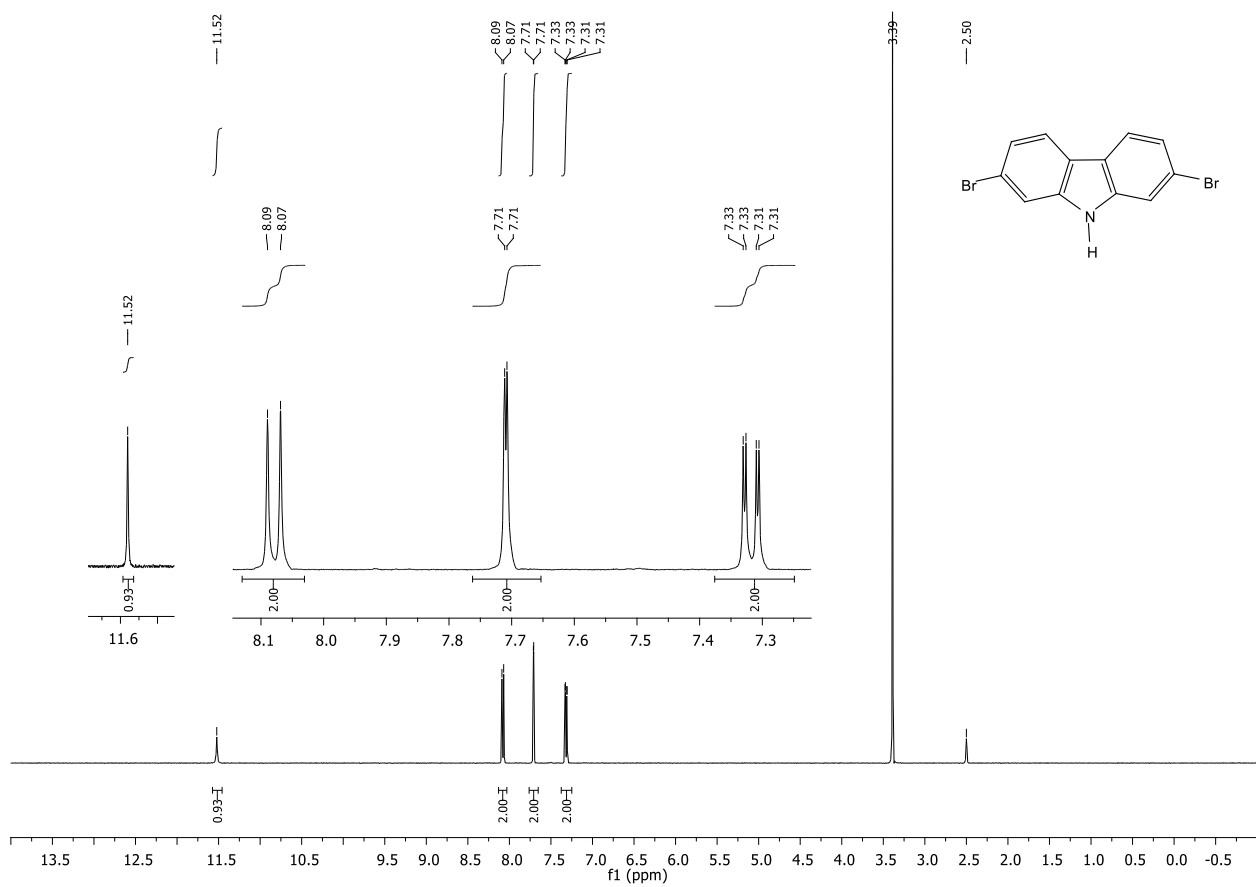


Figure 98: ^1H NMR of 2,7-dibromo-9H-carbazole **90** spectrum in $\text{DMSO-}d_6$.

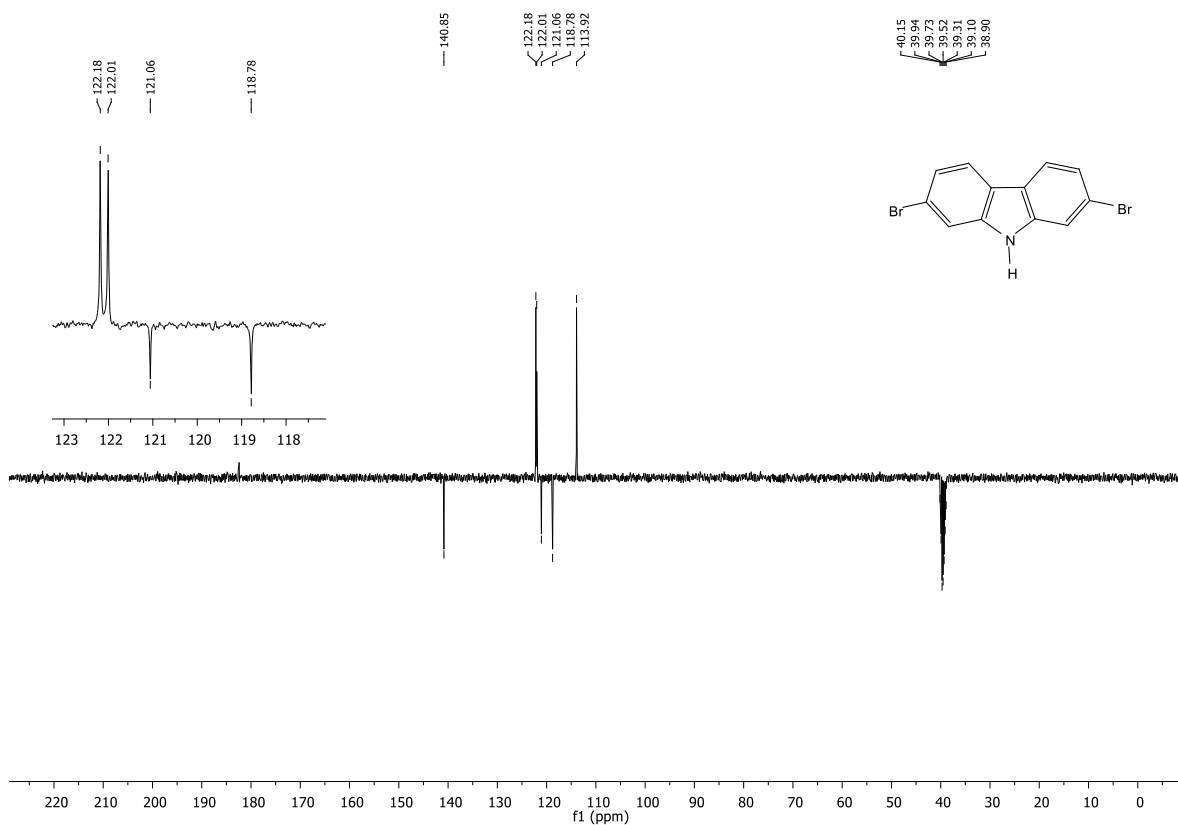


Figure 99: ^{13}C NMR of 2,7-dibromo-9H-carbazole **90** spectrum in $\text{DMSO-}d_6$.

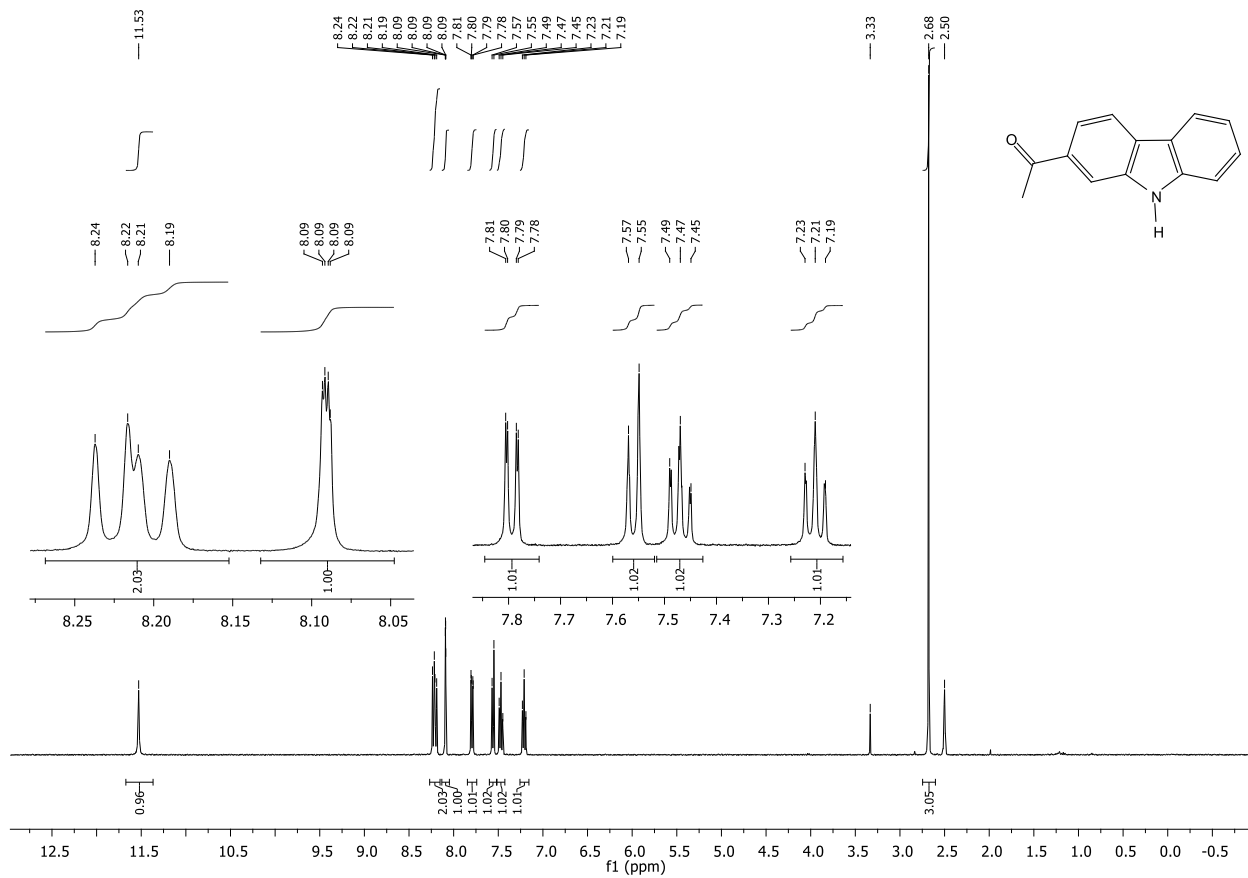


Figure 100: ^1H NMR of 2-acetyl-9H-carbazole **91** spectrum in $\text{DMSO-}d_6$.

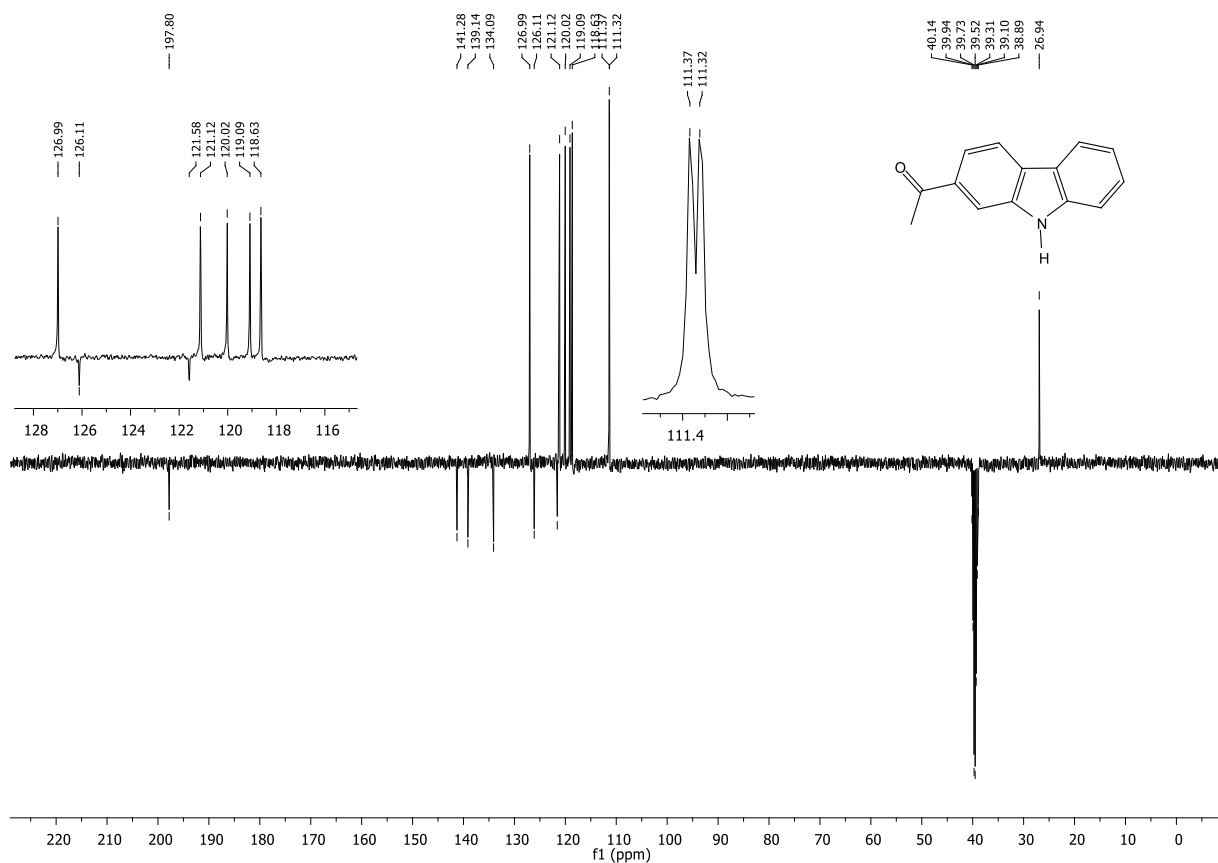


Figure 101: ^{13}C NMR of 2-acetyl-9H-carbazole **91** spectrum in $\text{DMSO-}d_6$.

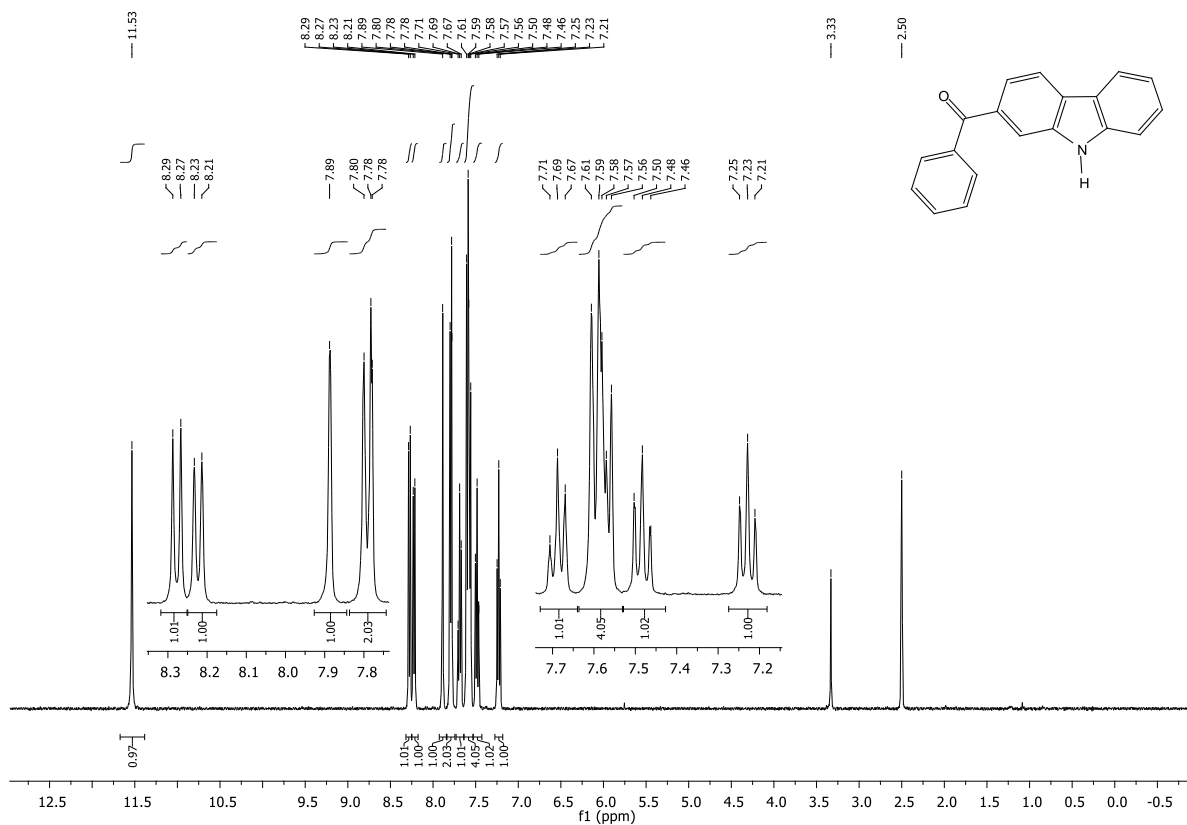


Figure 102: ^1H NMR of 2-benzoyl-9H-carbazole **92** spectrum in $\text{DMSO-}d_6$.

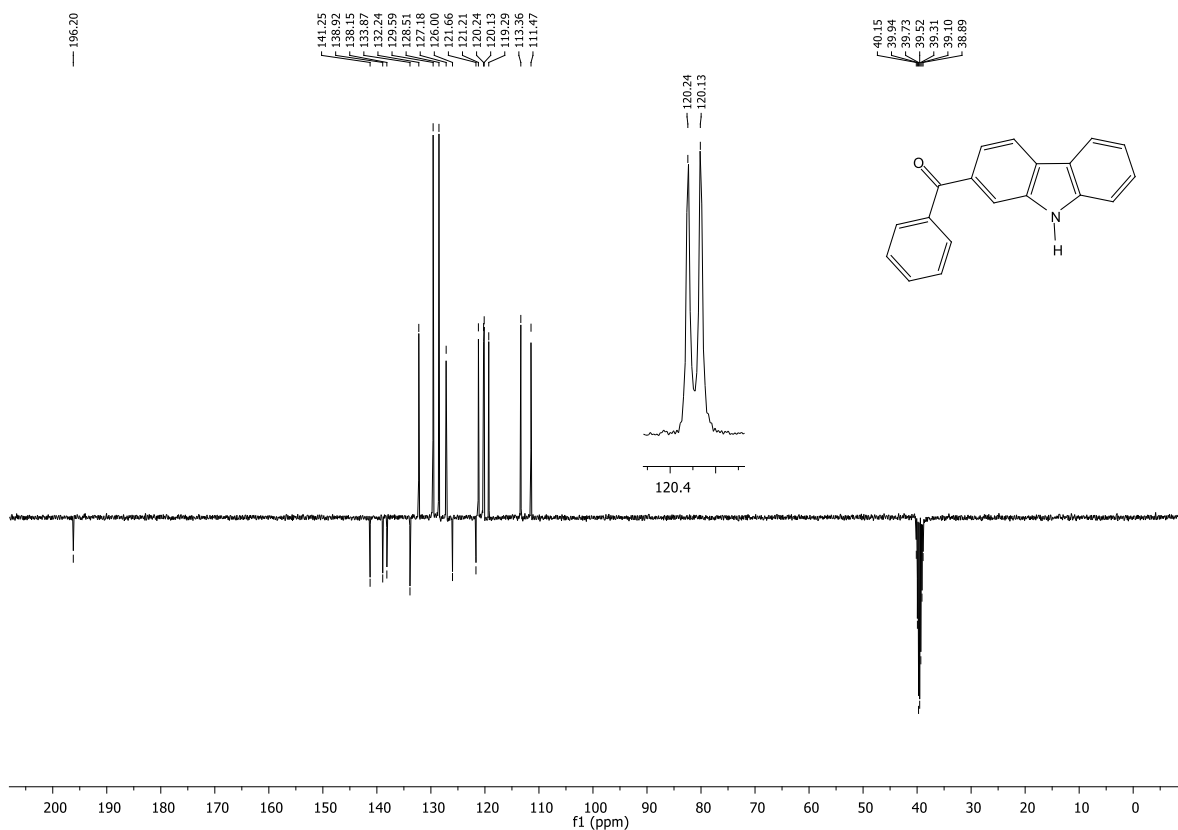


Figure 103: ^{13}C NMR of 2-benzoyl-9H-carbazole **92** spectrum in $\text{DMSO-}d_6$.

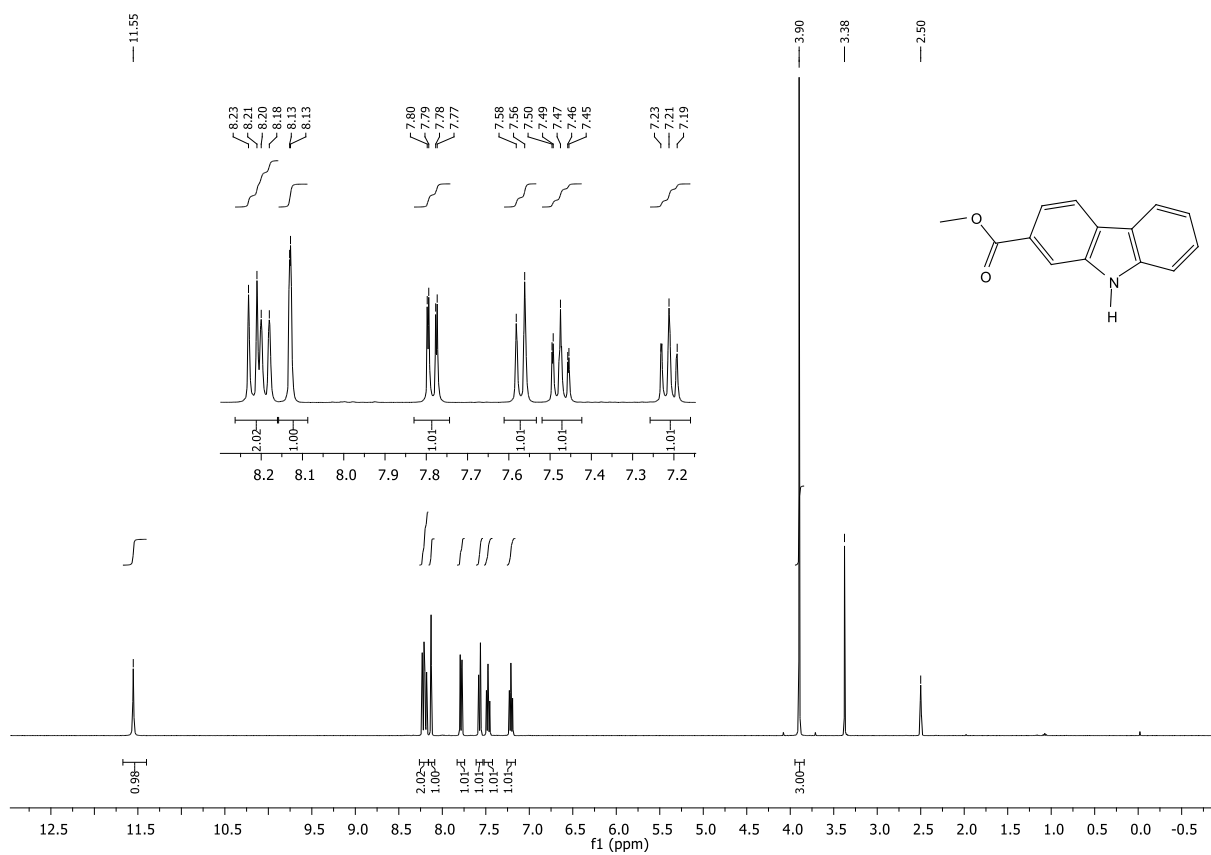


Figure 104: ^1H NMR of methyl 9H-carbazole-2-carboxylate **93** spectrum in $\text{DMSO-}d_6$.

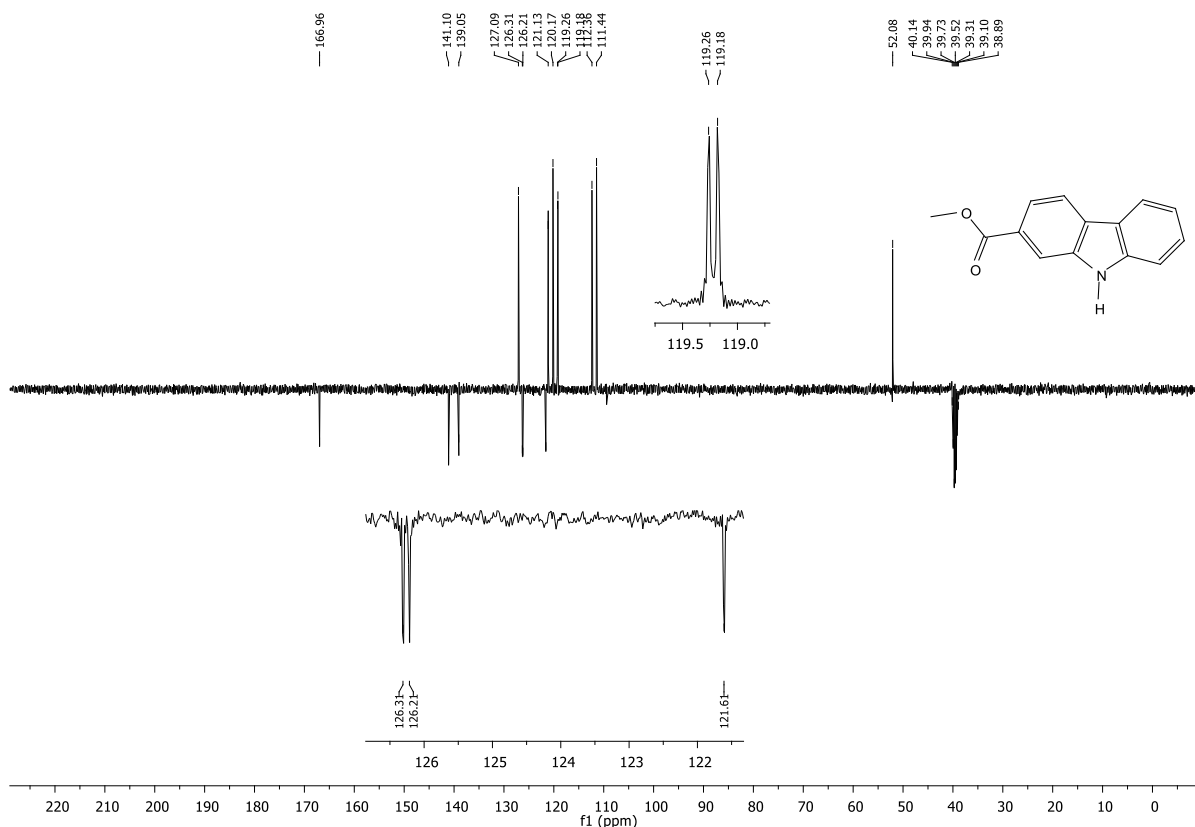


Figure 105: ^{13}C NMR of methyl 9H-carbazole-2-carboxylate **93** spectrum in $\text{DMSO-}d_6$.

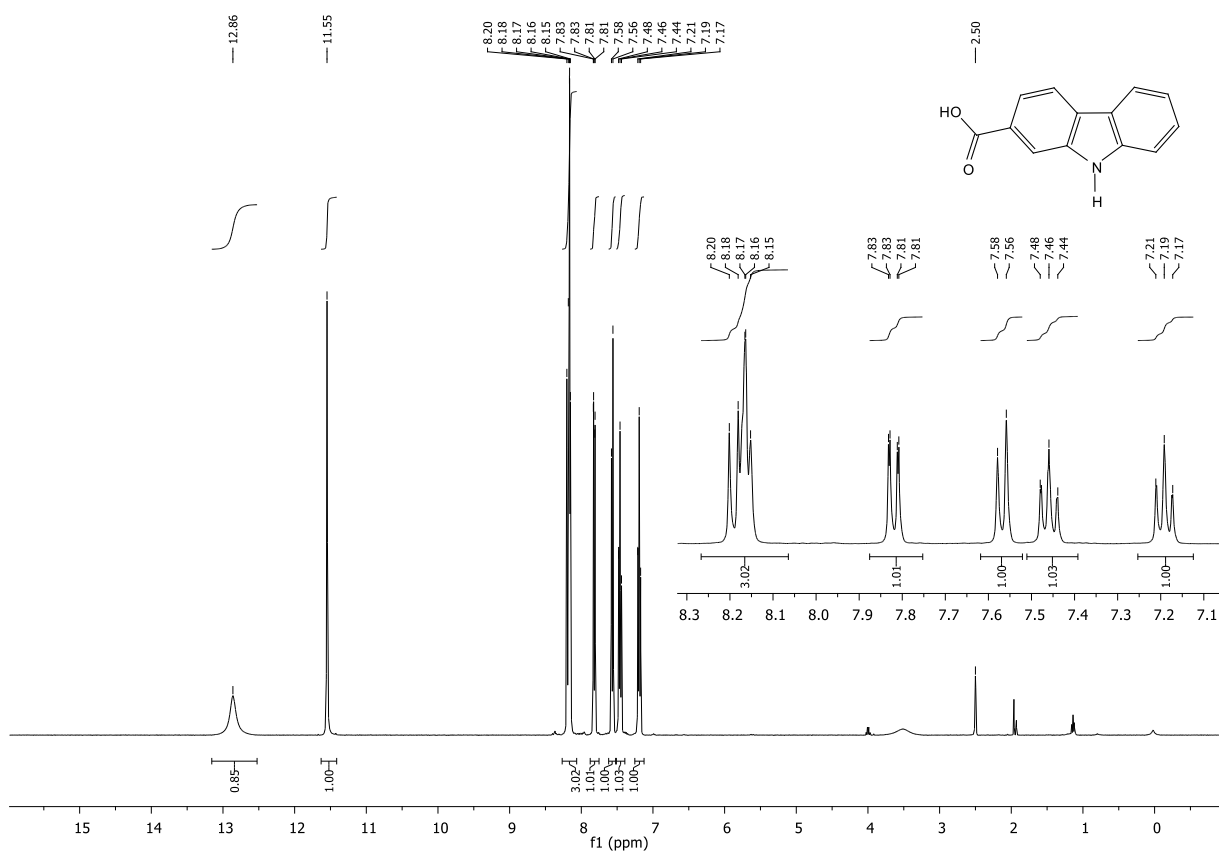


Figure 106: ^1H NMR of 9H-carbazole-2-carboxylic acid **94** spectrum in $\text{DMSO-}d_6$.

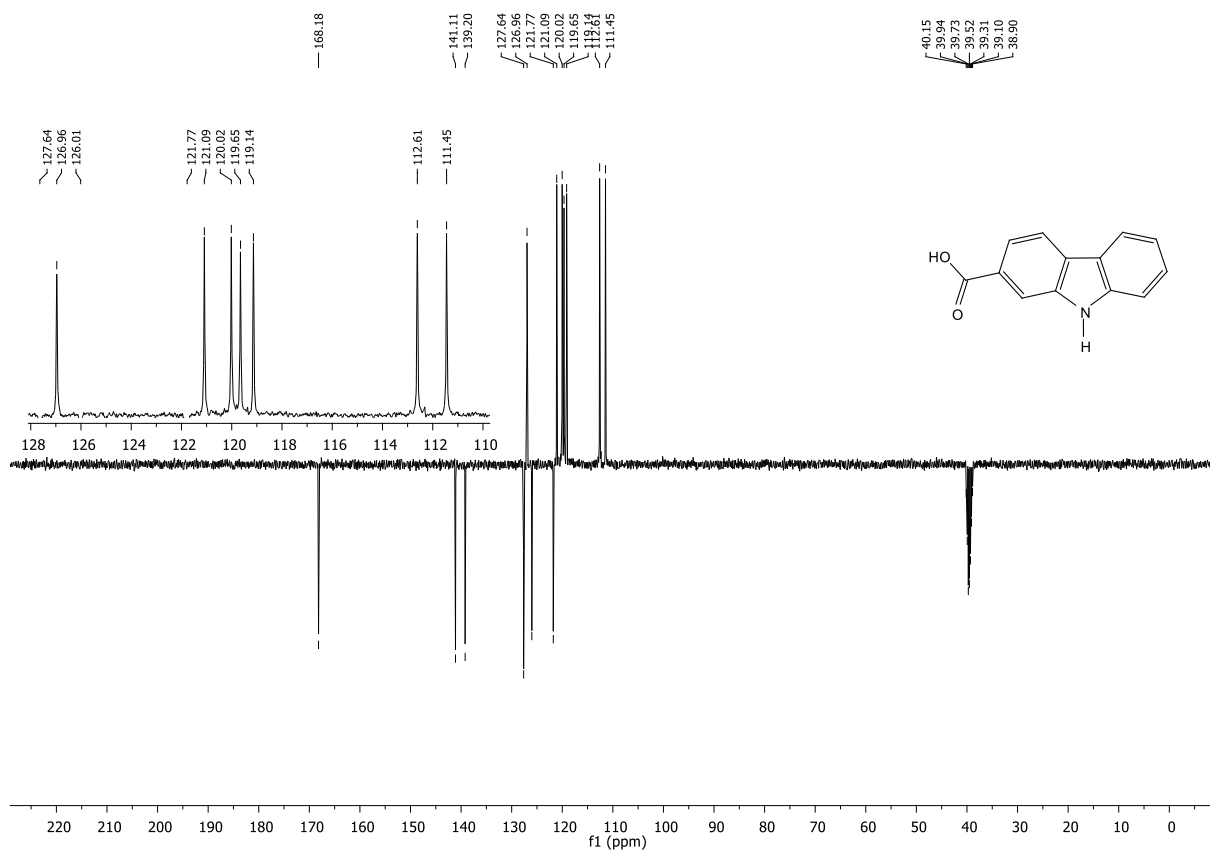


Figure 107: ^{13}C NMR of 9H-carbazole-2-carboxylic acid **94** spectrum in $\text{DMSO-}d_6$.

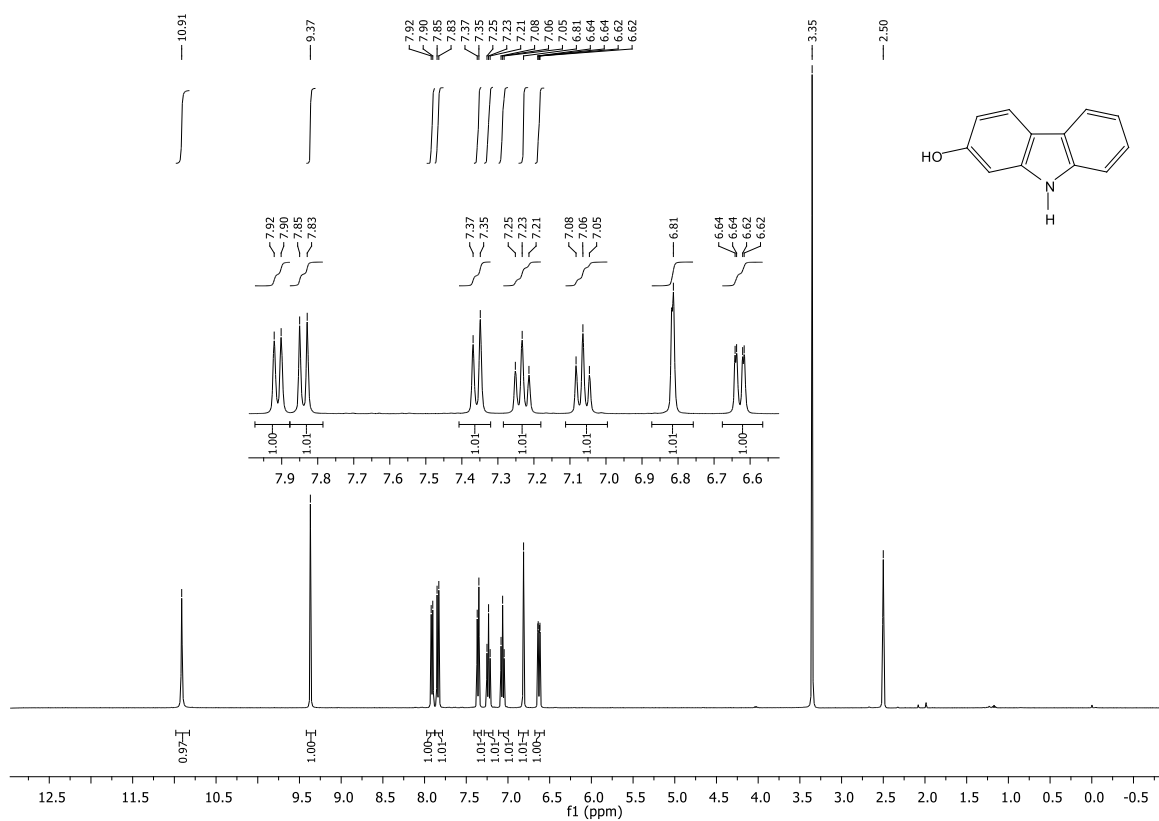


Figure 108: ^1H NMR of 2-hydroxy-9H-carbazole **95** spectrum in $\text{DMSO-}d_6$.

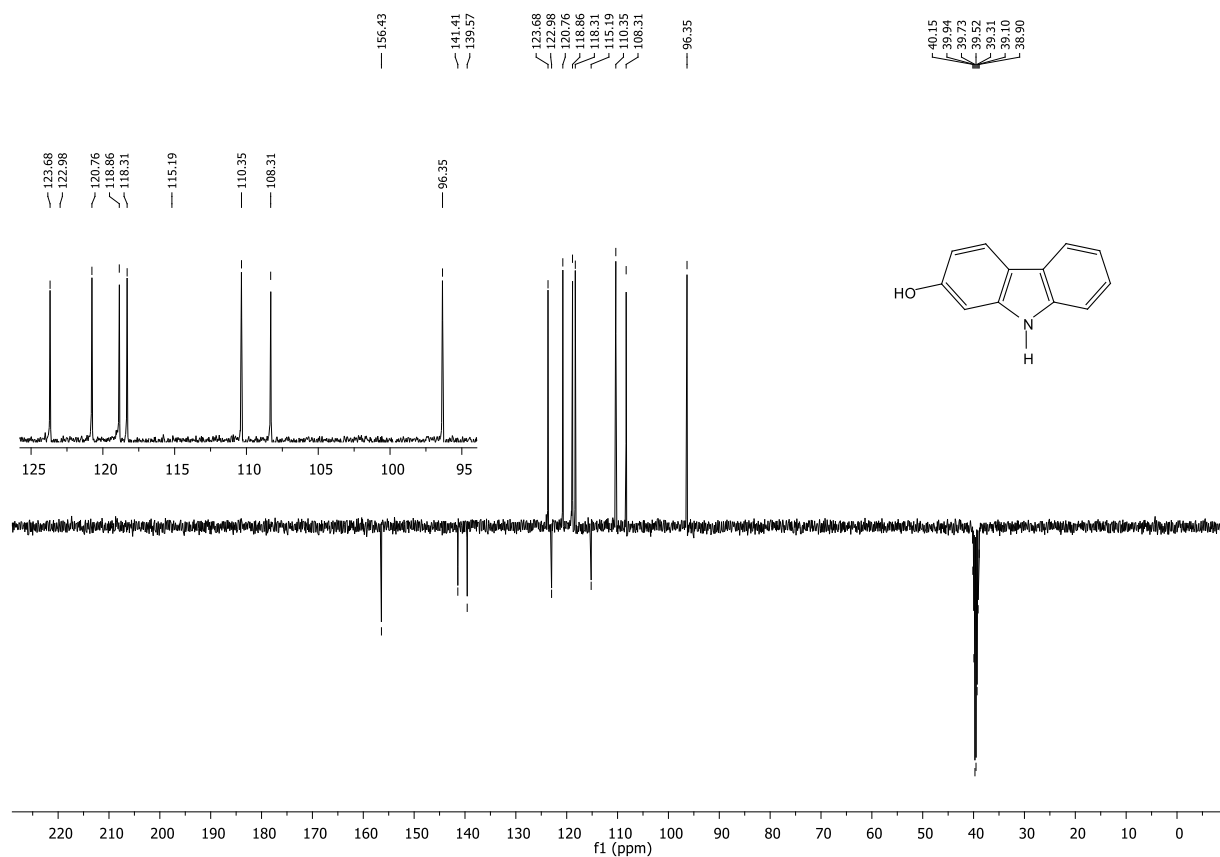


Figure 109: ^{13}C NMR of 2-hydroxy-9H-carbazole **95** spectrum in $\text{DMSO-}d_6$.

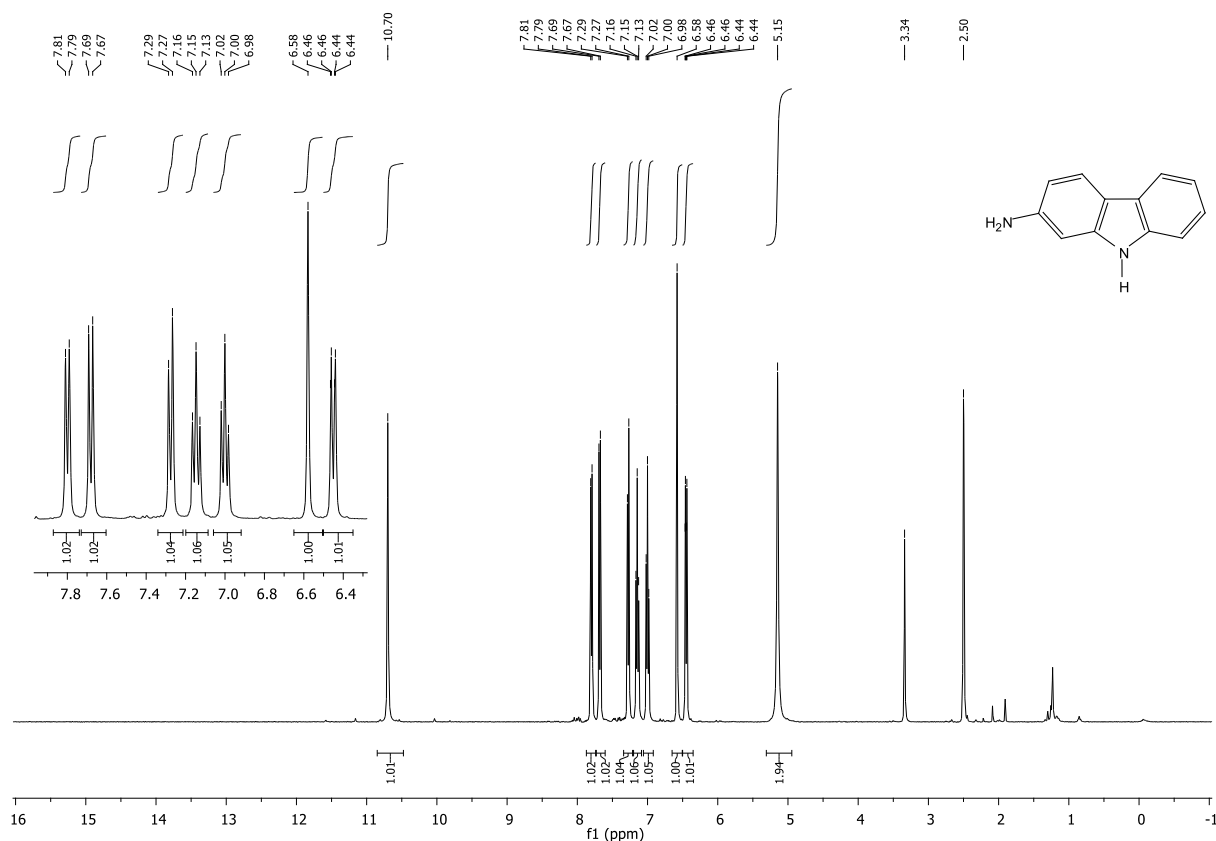


Figure 110: ^1H NMR of 2-amino-9H-carbazole **96** spectrum in $\text{DMSO-}d_6$.

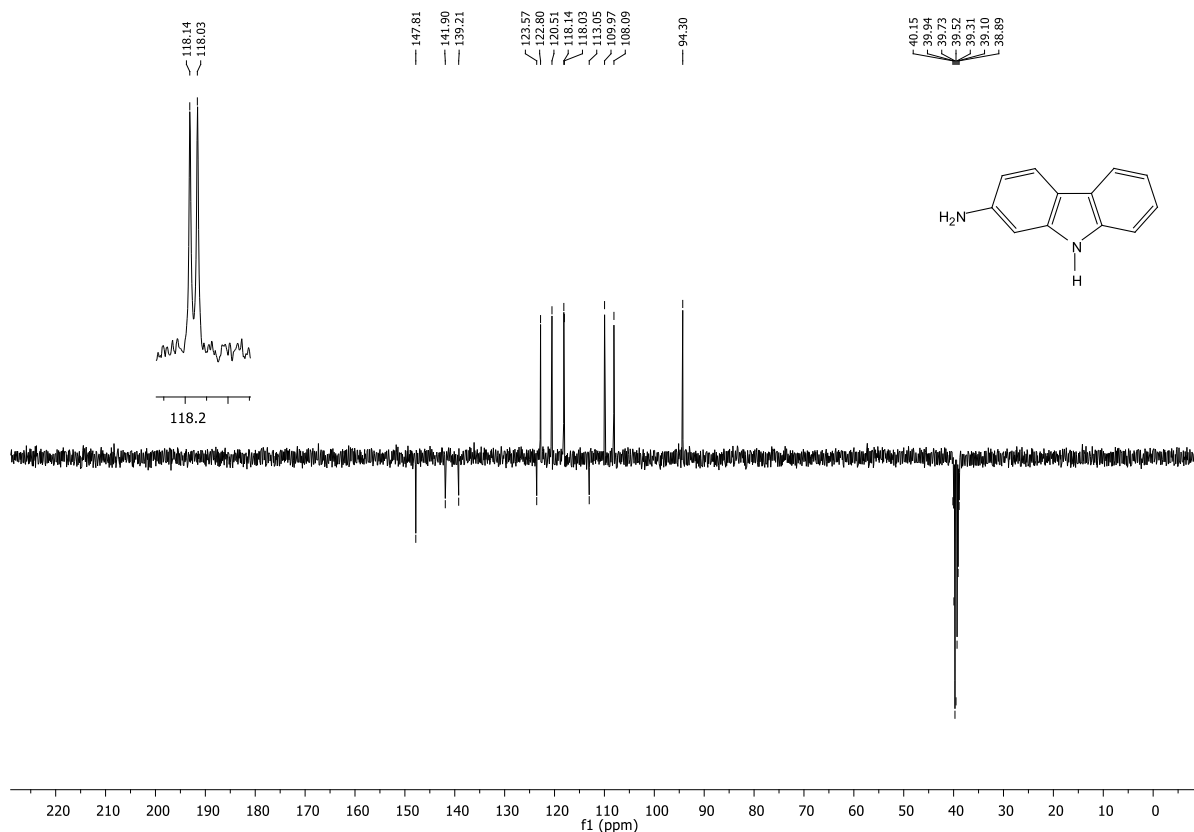


Figure 111: ^{13}C NMR of 2-hydroxy-9H-carbazole **96** spectrum in $\text{DMSO-}d_6$.

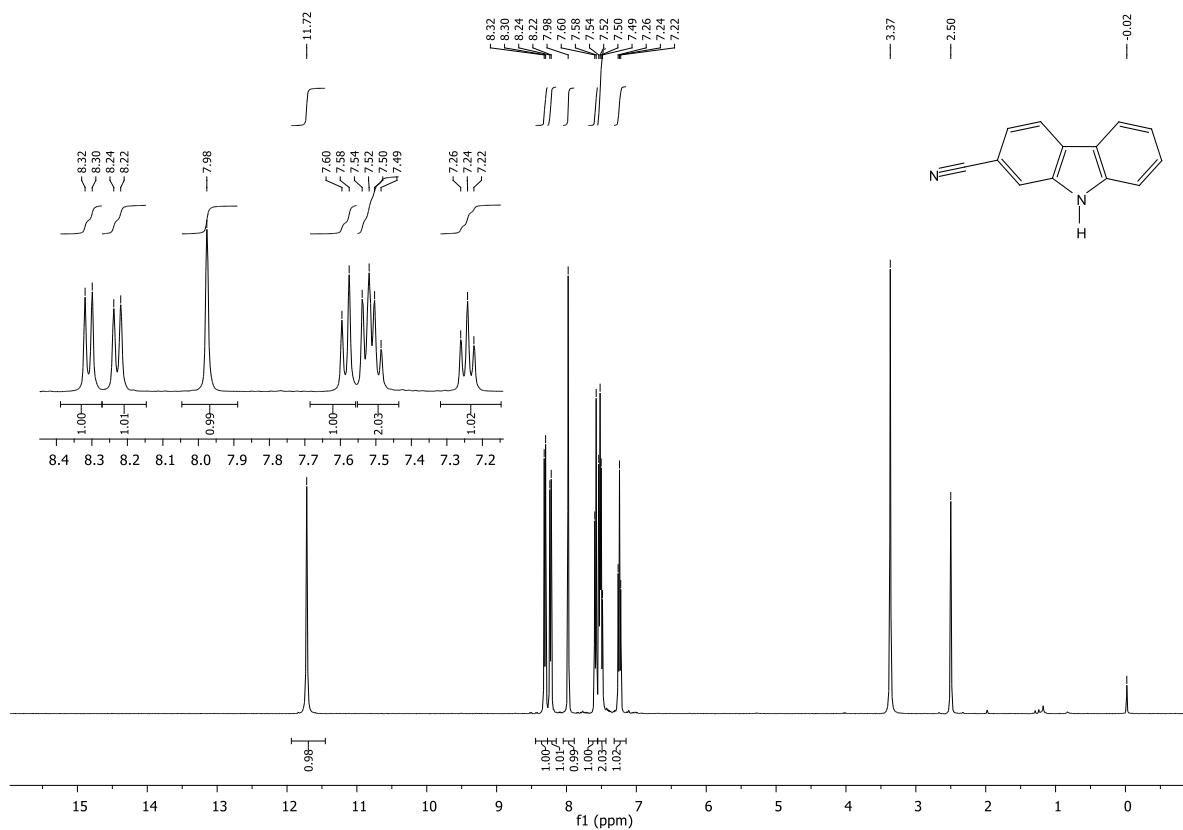


Figure 112: ^1H NMR of 2-cyano-9H-carbazole **97** spectrum in $\text{DMSO-}d_6$.

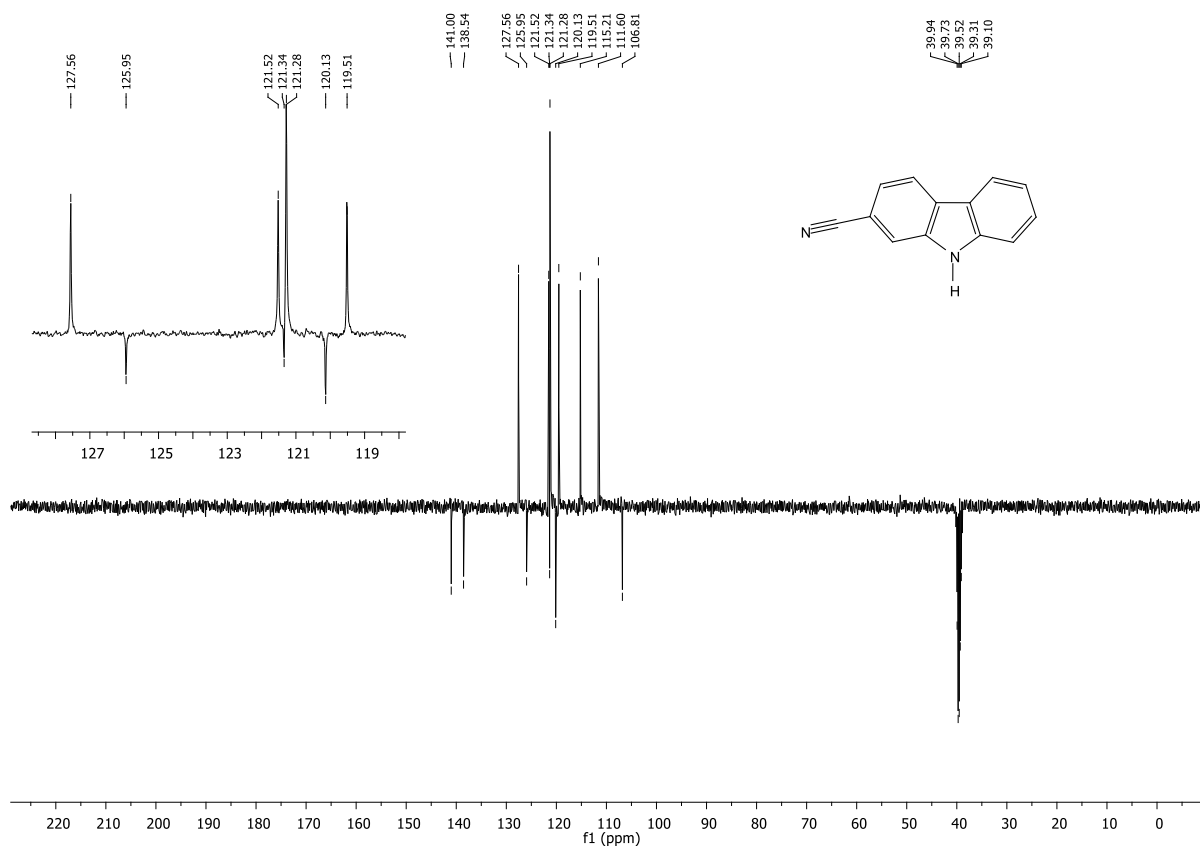


Figure 113: ^{13}C NMR of 2-cyano-9H-carbazole **97** spectrum in DMSO- d_6 .

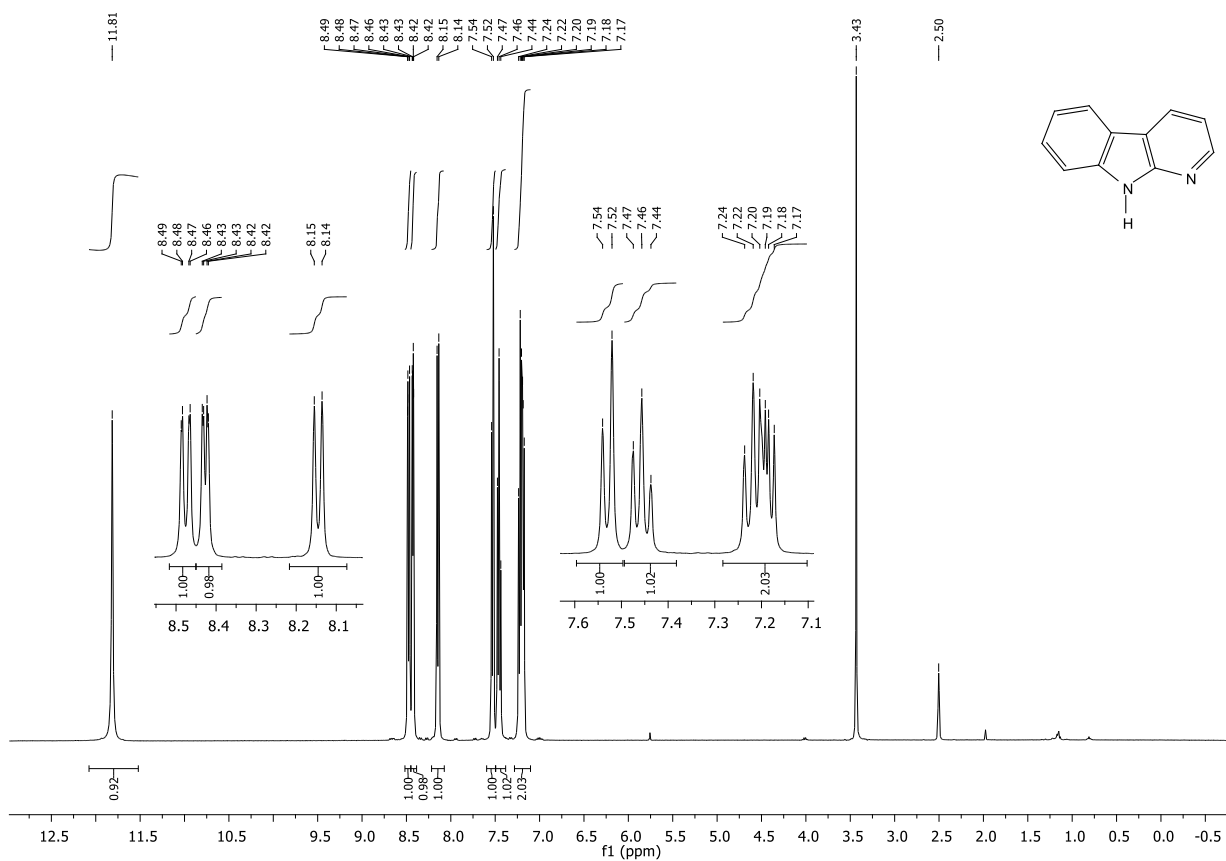


Figure 114: ^1H NMR of 9H-pyrido[2,3-b]indole **98** spectrum in DMSO- d_6 .

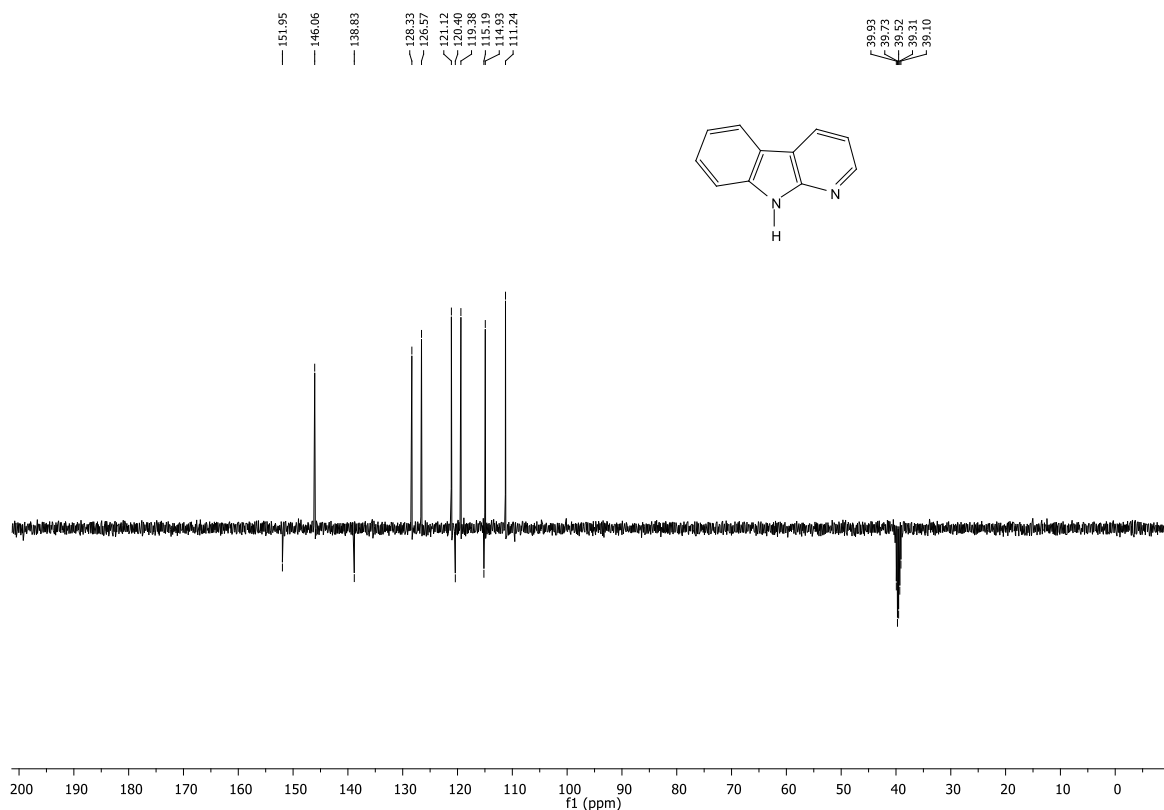


Figure 115: ^{13}C NMR of 9H-pyrido[2,3-b]indole **98** spectrum in DMSO- d_6 .

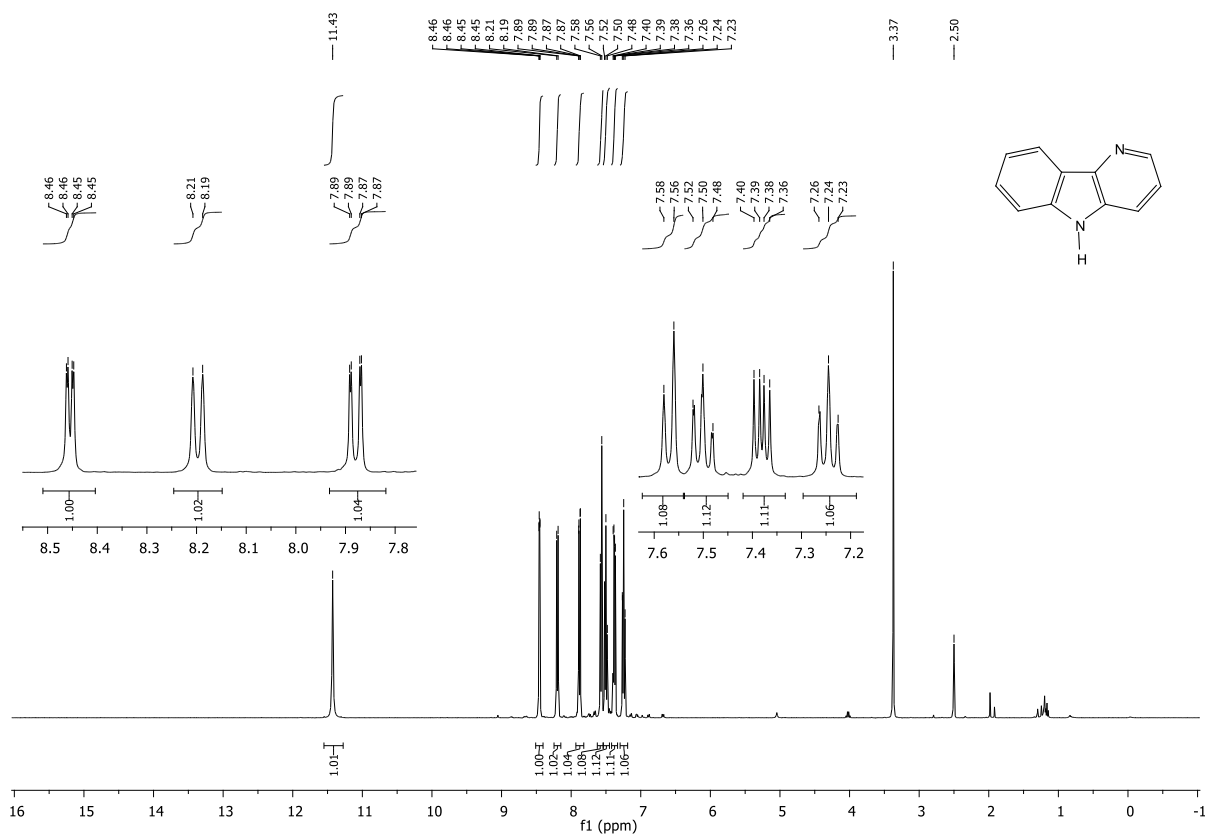


Figure 116: ^1H NMR of 5H-pyrido[3,2-b]indole **99** spectrum in DMSO- d_6 .

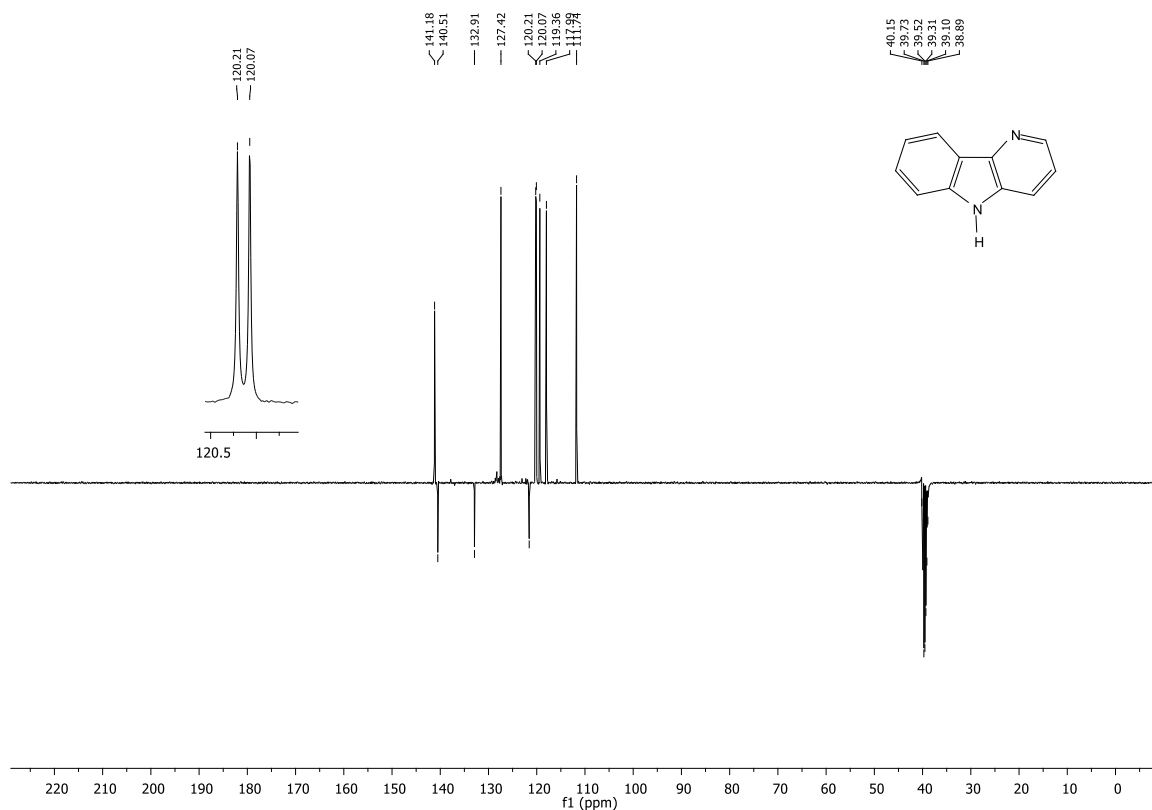


Figure 117: ^{13}C NMR of 5H-pyrido[3,2-b]indole **99** spectrum in DMSO- d_6 .

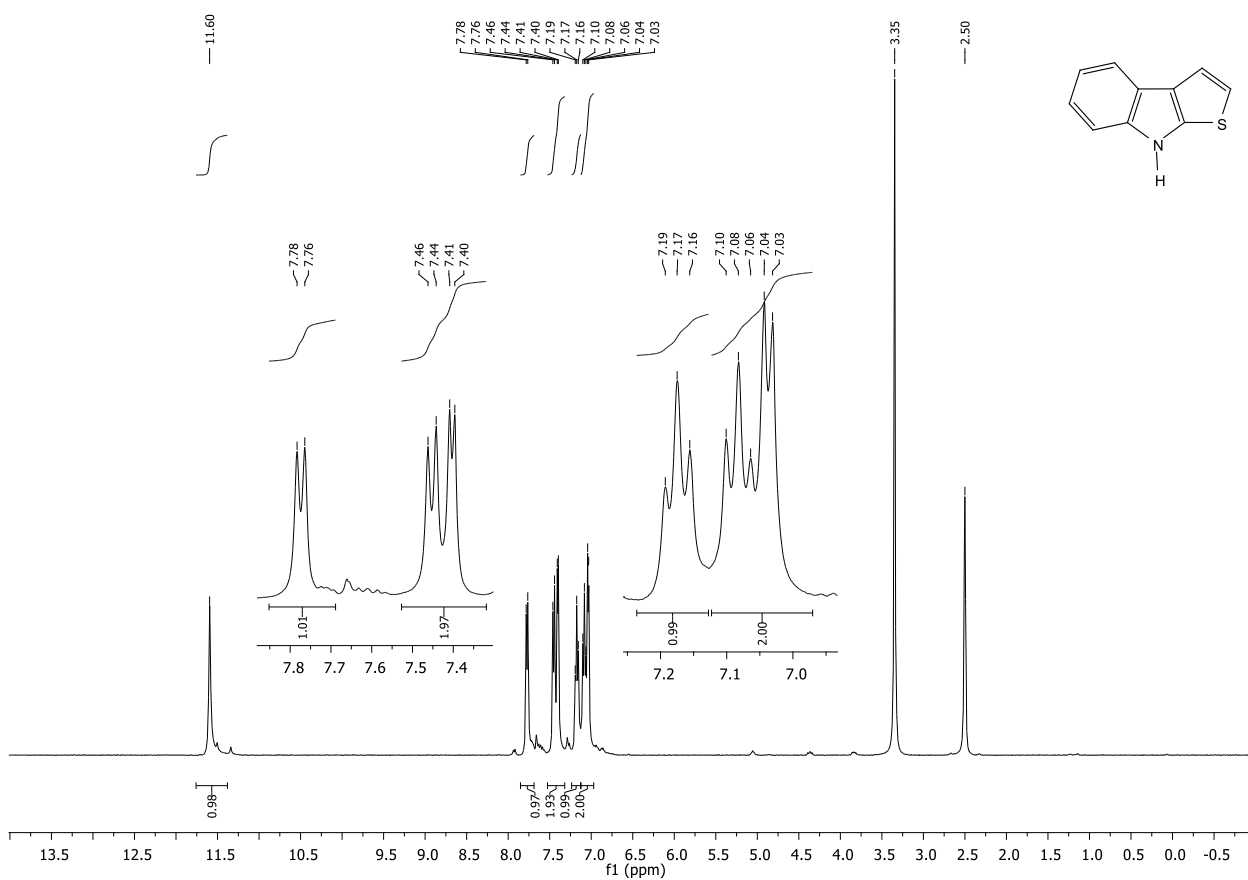


Figure 118: ^1H NMR of 8H-thieno[2,3-b]indole **100** spectrum in DMSO- d_6 .

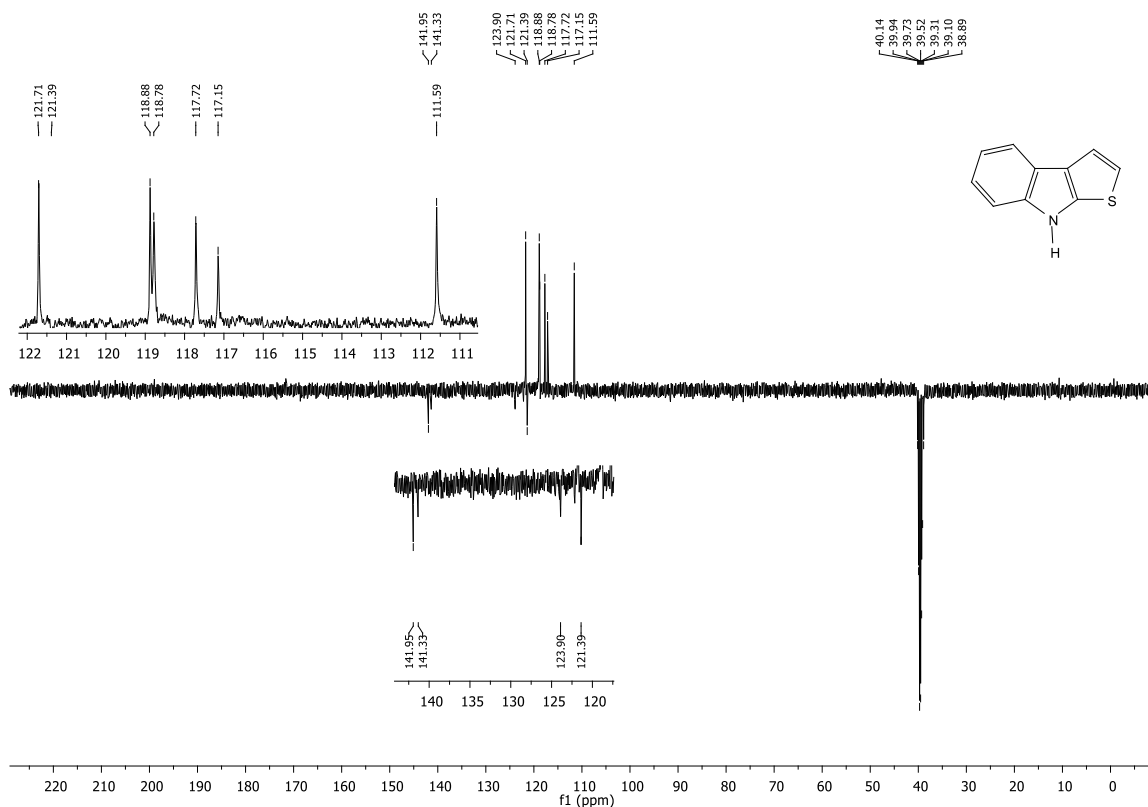


Figure 119: ^{13}C NMR of 8H-thieno[2,3-b]indole **100** spectrum in DMSO- d_6 .

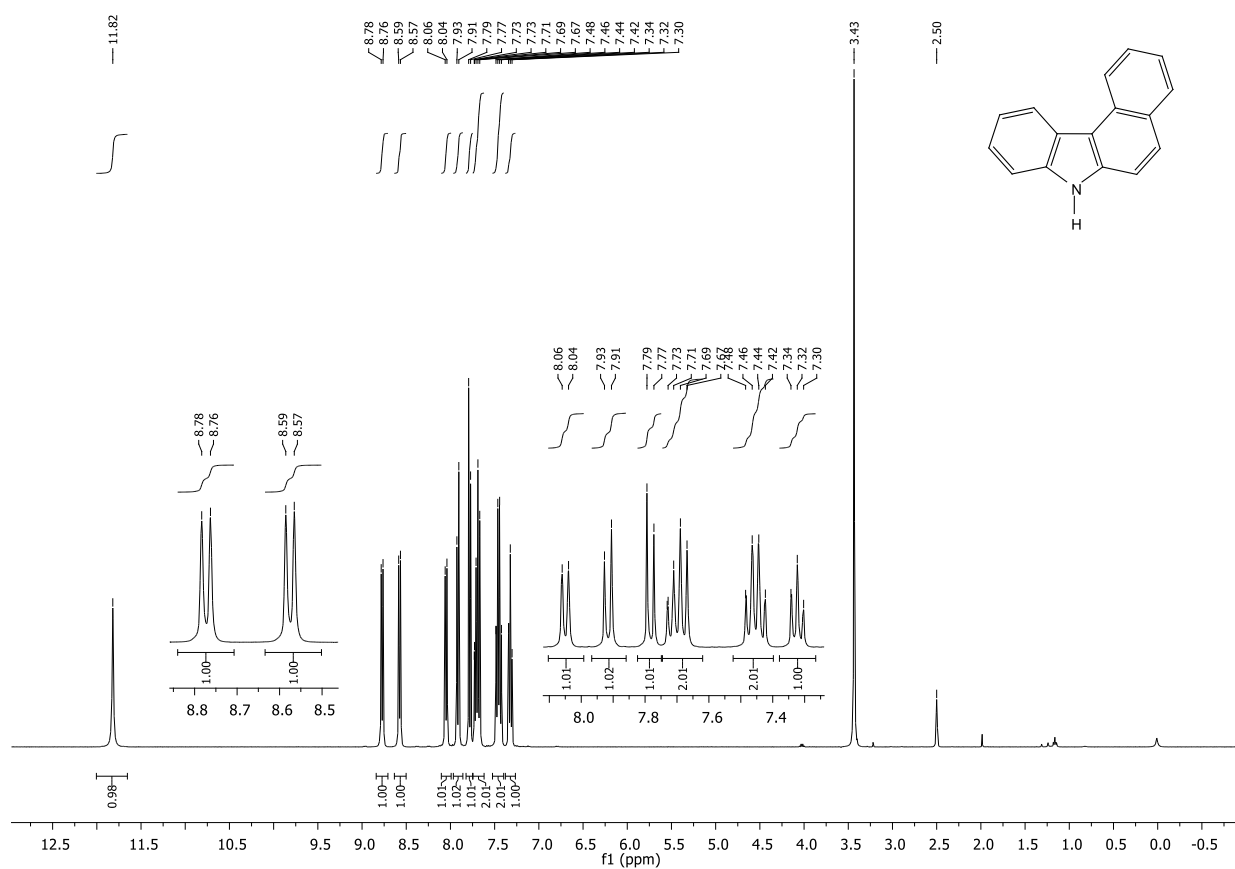


Figure 120: ^1H NMR of 7H-benzo[c]carbazole **101** spectrum in DMSO- d_6 .

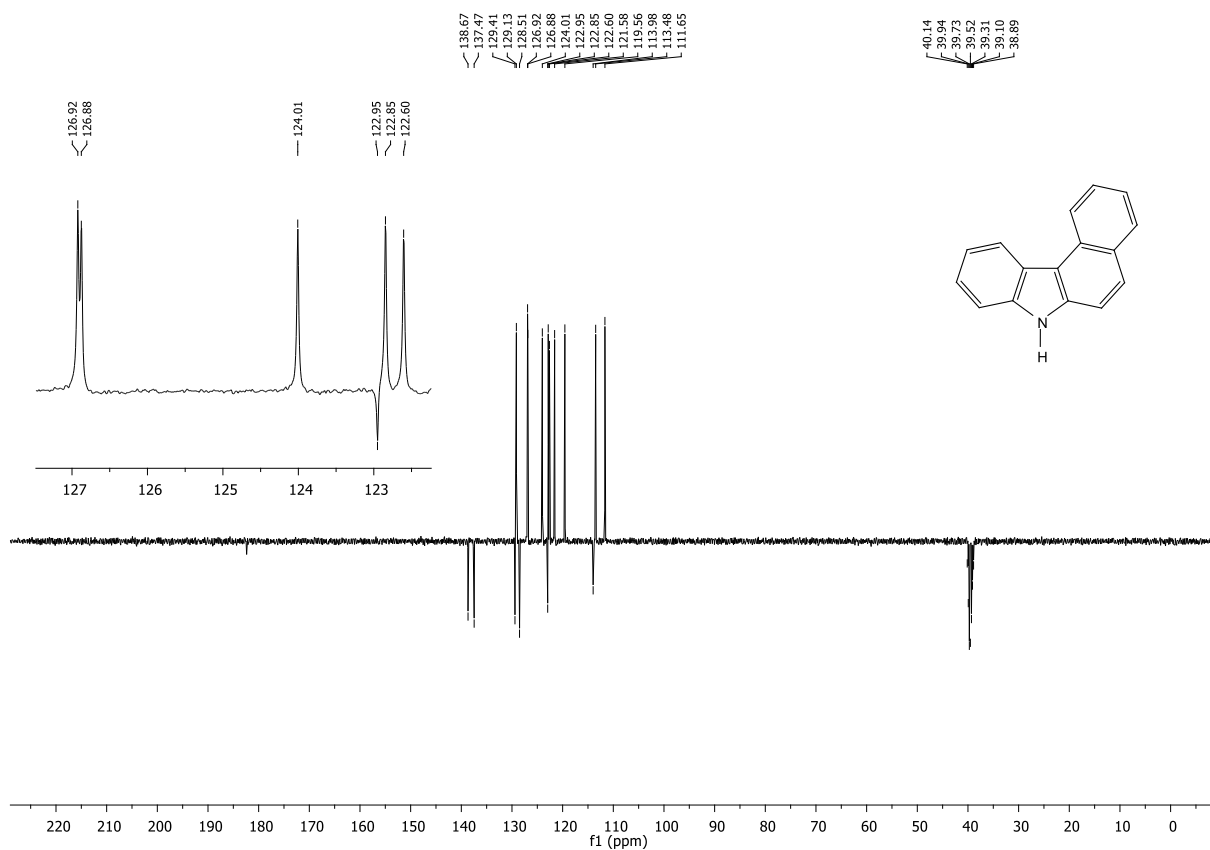


Figure 121: ^{13}C NMR of 7H-benzo[c]carbazole **101** spectrum in $\text{DMSO-}d_6$.

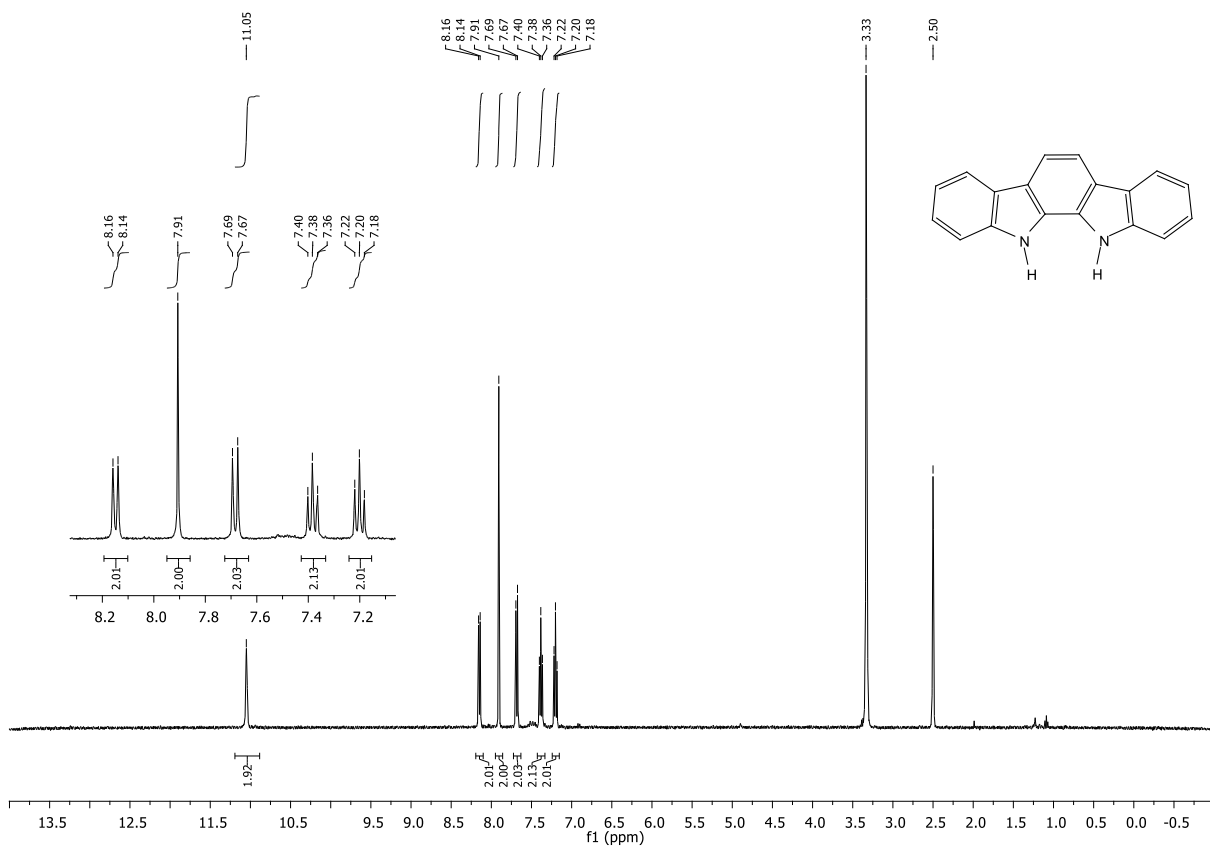


Figure 122: ^1H NMR of 11,12-dihydroindolo[2,3-a]carbazole **102** spectrum in $\text{DMSO-}d_6$.

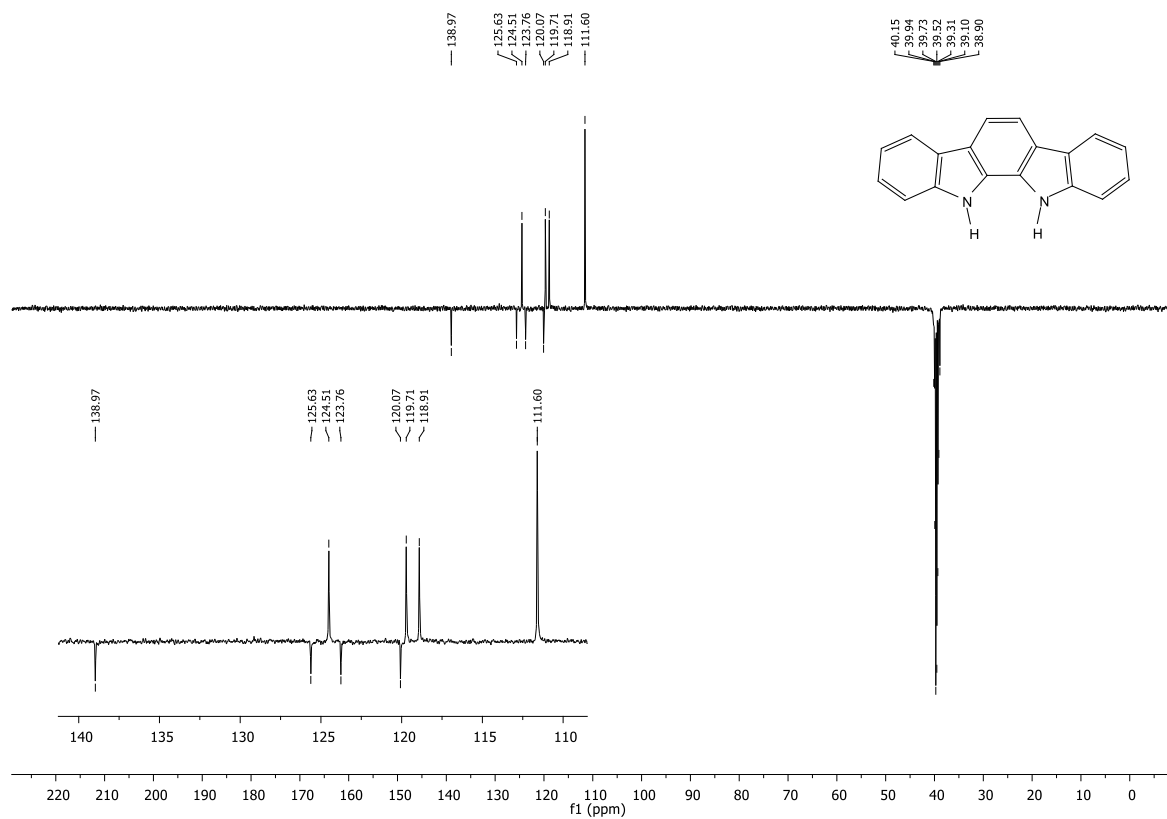


Figure 123: ^{13}C NMR of 11,12-dihydroindolo[2,3-a]carbazole **102** spectrum in $\text{DMSO-}d_6$.

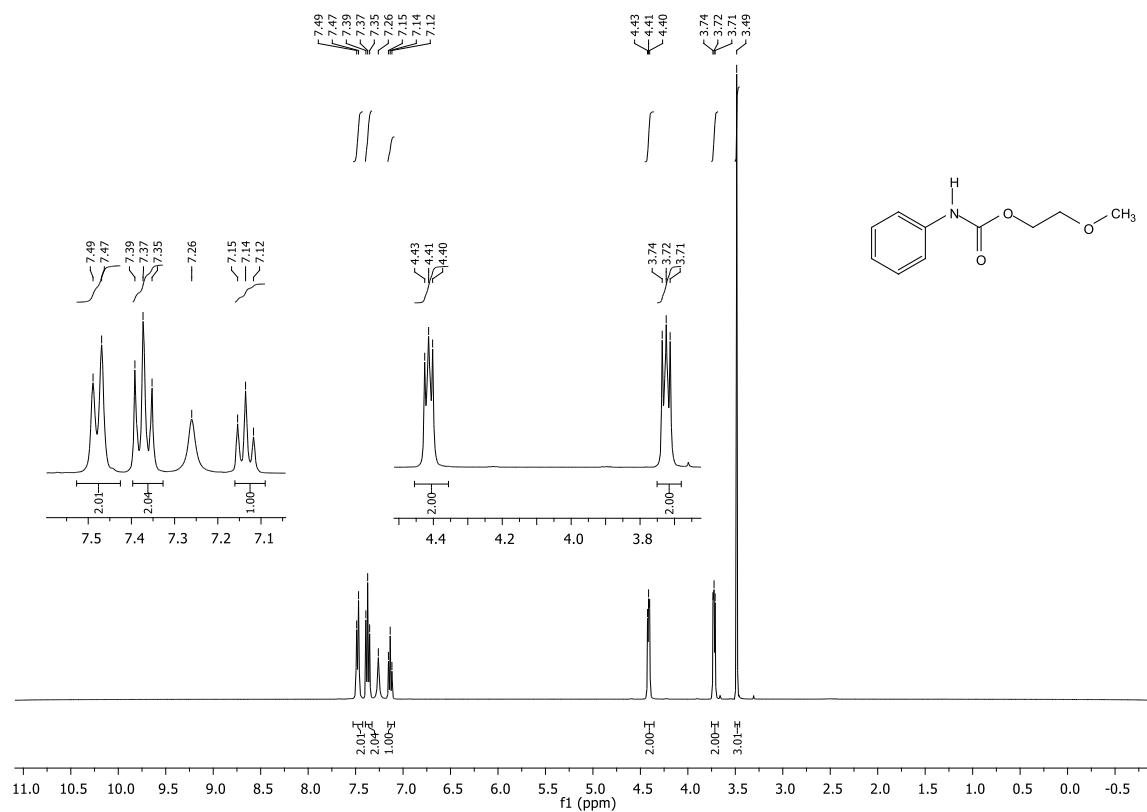


Figure 130: ^1H NMR spectrum of 2-methoxyethyl phenylcarbamate **105** in CDCl_3 .

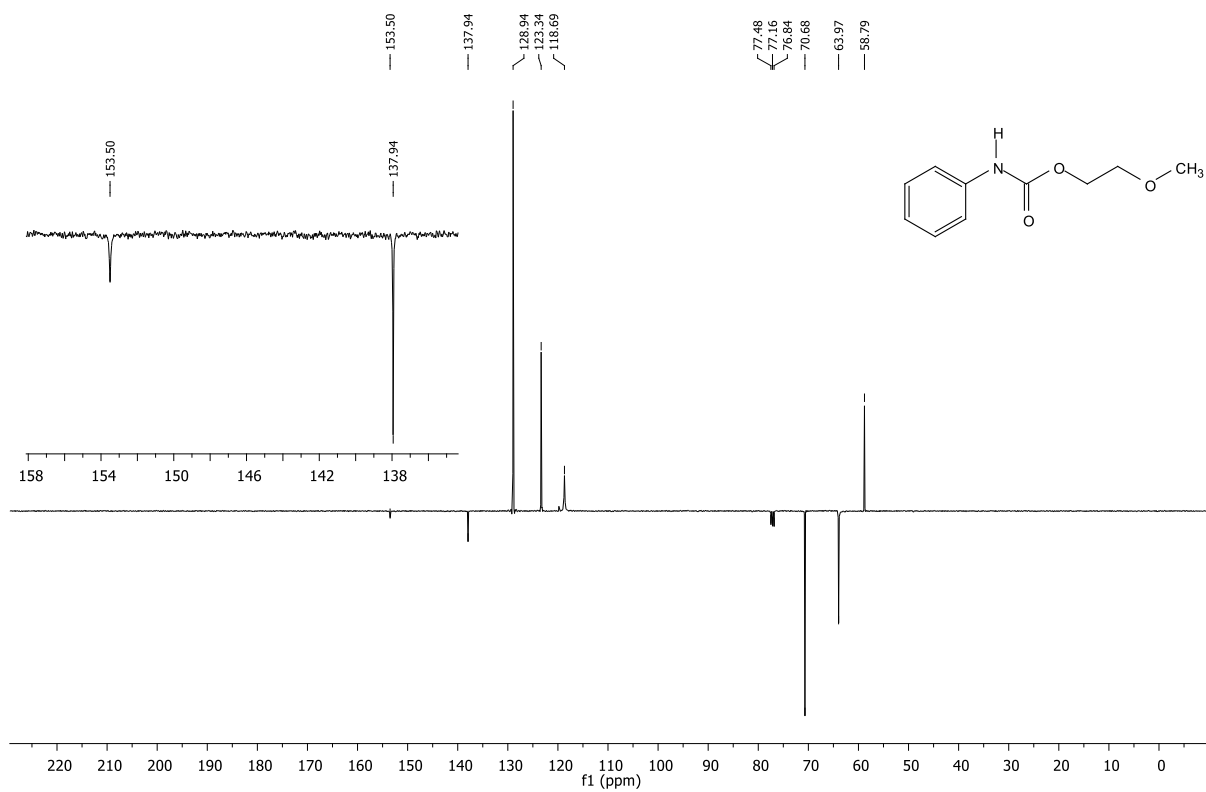


Figure 131: ^{13}C NMR spectrum of 2-methoxyethyl phenylcarbamate **105** in CDCl_3 .

2. Short resume of the PhD candidate.

Doaa R. Ramadan graduated in 2013 and received her master's degree in chemistry in 2017 from Alexandria University (Egypt). Currently, she is an assistant lecturer at Alexandria University. In 2017, she received a PhD grant from Milan University, and she performed her PhD research under the supervision of Prof. Fabio Ragaini in the field of homogenous catalysis by transition metal complexes.

Publications related to the PhD thesis.

- 1- Francesco Ferretti, Edoardo Barraco, Claudia Gatti, Doaa R. Ramadan and Fabio Ragaini: Palladium/Iodide Catalyzed Oxidative Carbonylation of Aniline to Diphenylurea: Effect of ppm Amounts of Iron Salts. *J. Catal.*, **2019**, 369, 257-266.
<https://doi.org/10.1016/j.jcat.2018.11.010>
- 2- Fabio Ragaini, Francesco Ferretti, Claudia Gatti and Doaa R. Ramadan: Rebuttal to polemic against conclusions drawn in "Palladium/Iodide Catalyzed Oxidative Carbonylation of Aniline to Diphenylurea: Effect of ppm Amounts of Iron Salts" (*J. Catal.*, **2019**, 369, 257–266). *J. Catal.*, **2019**, 380, 391-395.
<https://doi.org/10.1016/j.jcat.2019.03.030>
- 3- Francesco Ferretti, Doaa R. Ramadan and Fabio Ragaini: Transition Metal Catalyzed Reductive Cyclization Reactions of Nitroarenes and Nitroalkenes. *ChemcatChem*, **2019**, 11, 4450-4488.
<https://doi.org/10.1002/cctc.201901065>
- 4- Doaa R. Ramadan, Francesco Ferretti and Fabio Ragaini: Synthesis of Carbazoles from *o*-Nitrobiaryls, Catalyzed by Palladium/Phenanthroline Complexes and with Phenyl Formate as a CO Surrogate". **Manuscript in preparation.**

Other publications.

- 1- Doaa R. Ramadan, Aly A. Elbardan, Adnan A. Bekhit, Ayman El-Faham and Sherine N. Khattab: Synthesis and Characterization of Novel Dimeric *s*-Triazine Derivatives as Potential Anti-Bacterial Agents against MDR Clinical Isolates, *New J. Chem.*, **2018**, 42, 10676-10688.
<https://doi.org/10.1039/C8NJ01483C>
- 2- Nazly Hassan, Doaa R. Ramadan, Aly A. Elbardan, Asmaa Ebrahim and Sherine N. Khattab: Electrochemical Evaluation of Synthesized *s*-Triazine Derivatives for Improving 316L Stainless Steel for Biomedical Applications, *Monatsh Chem*, **2019**, 150, 1761–177.
<https://doi.org/10.1007/s00706-019-02499-z>

Communications to schools and congress.

- 1- Doaa R. Ramadan, Mohamed A. EL-Atawy, Fabio Ragaini: "Synthesis of Oxazines by Palladium Catalyzed Reductive Cyclization of Nitroarenes and Dienes Using Phenyl Formate as CO Surrogate".

The XIII Congress of the Interdivisional Group of Organometallic Chemistry of the Italian Chemical Society (**Co.GICO 2018**), Florence, Italy, July 18-20, **2018**.

- 2- Doaa Ramadan, Francesco Ferretti and Fabio Ragaini: "Palladium Catalyzed Reductive Cyclization of Nitrobiphenyls Using Formate Esters as CO Surrogates".

The 12th International School of Organometallic Chemistry (**ISOC 2019**), Camerino, Italy, August 31- September 04, **2019**.

- 3- Doaa Ramadan, Francesco Ferretti and Fabio Ragaini: "Pd/Phen Catalyzed synthesis of carbazoles by Reductive Cyclization of 2-Nitrobiaryls: Use of Formate Esters as CO Surrogates".

Chemistry for everyday life online school (**International School of Chemistry-Web Edition**) held online on September 1-6, **2020**.